Physiol Rev 90: 1195–1268, 2010;
doi:10.1152/physrev.00035.2008.

Neurophysiological and Computational Principles of Cortical Rhythms in Cognition

XIAO-JING WANG

Department of Neurobiology and Kavli Institute of Neuroscience, Yale University School of Medicine, New Haven, Connecticut

Wang X-J. Neurophysiological and Computational Principles of Cortical Rhythms in Cognition. *Physiol Rev* 90: 1195–1268, 2010; doi:10.1152/physrev.00035.2008.—Synchronous rhythms represent a core mechanism for sculpting temporal coordination of neural activity in the brain-wide network. This review focuses on oscillations in the cerebral cortex that occur during cognition, in alert behaving conditions. Over the last two decades, experimental and modeling work has made great strides in elucidating the detailed cellular and circuit basis of these rhythms, particularly gamma and theta rhythms. The underlying physiological mechanisms are diverse (ranging from resonance and pacemaker properties of single cells to multiple scenarios for population synchronization and wave

propagation), but also exhibit unifying principles. A major conceptual advance was the realization that synaptic inhibition plays a fundamental role in rhythmogenesis, either in an interneuronal network or in a reciprocal excitatory-inhibitory loop. Computational functions of synchronous oscillations in cognition are still a matter of debate among systems neuroscientists, in part because the notion of regular oscillation seems to contradict the common observation that spiking discharges of individual neurons in the cortex are highly stochastic and far from being clocklike. However, recent findings have led to a framework that goes beyond the conventional theory of coupled oscillators and reconciles the apparent dichotomy between irregular single neuron activity and field potential oscillations. From this perspective, a plethora of studies will be reviewed on the involvement of long-distance neuronal coherence in cognitive functions such as multisensory integration, working memory, and selective attention. Finally, implications of abnormal neural synchronization are discussed as they relate to mental disorders like schizophrenia and autism.

I. INTRODUCTION

A. Synchronization and Stochastic Neuronal Activity in the Cerebral Cortex

In 1958, Frédéric Bremer published a seminal review in this journal on "theoretical and experimental data pertaining to the nature, origin, synchrony and functional significance of brain waves" (110). Half a century later, the study of cortical rhythms has become an area of converging interests across many disciplines in neuroscience (143, 145). Network oscillations are attractive for cellular neurophysiologists interested in understanding network behavior in terms of the underlying biophysical mechanisms. Synchronous oscillations can be studied in detail using in vivo and in vitro preparations, and increasingly in combination with powerful genetic tools. Therefore, for neurophysiologists and theorists alike, the study of synchronous rhythms offers an excellent venue to investigate how collective network dynamics emerge from the interplay between cellular biophysics and synaptic circuits. On the other hand, for systems neurophysiologists working with alert animals, who have long recorded single neurons with tremendous success in uncovering neural correlates of behavior, understanding coordinated neural population patterns in a circuit represents a new challenge. Moreover, cognition involves a large network of brain structures; therefore, it is critical to elucidate neuronal interactions between different brain regions, increasingly with the help of multielectrode recordings and imaging techniques. Coherent oscillations, more generally neuronal synchrony, may play a role in well-timed coordination and communication between neural populations simultaneously engaged in a cognitive process.

There are many commonalities among network oscillations in various nervous systems. Indeed, it has been suggested that cortical circuits are similar to central pattern generators (1086). However, whereas central pattern generators are well described in terms of coupled oscillators (638), it is questionable that cortical rhythms can be conceptualized in that framework. Typically, brain rhythms of the waking brain are reflected by small-amplitude scalp electroencephalogram (EEG) signals. They occur intermittently by short episodes in time (378, 711), and synchronization is subtle and typically confined to restricted neural populations (238, 630). As a matter of fact, awake behaving states were traditionally characterized by "desynchronized EEG" in contrast to large-amplitude slow oscillations observed in quiet (non-rapid eye movement, non-REM) sleep (236, 908, 909, 913). It is an interesting and by no means obvious question as to how desynchronization or asynchrony is achieved in a neural network (2, 123, 126, 232, 241, 243, 345, 538, 997, 1016, 1029). Presumably, cortical networks in wakefulness are predominantly asynchronous at the same time weak oscillations and selective coherence are present. At the single-neuron level, spike discharges of cortical cells are highly irregular, characterized by some measures as approximate Poisson processes (862, 884), hence far from behaving as clocklike oscillators. Synaptic inputs to cortical neurons measured in vivo also display large stochastic fluctuations (236). Such irregular neural firing patterns may be computationally desirable to maximize information content of spike trains for neural coding of sensory information (36), generating stochastic choice behavior in decision making (226, 487, 1034) and other brain functions. At first sight, the strongly stochastic nature of neuronal spike discharges is at odds with the popular description of network rhythms in terms of synchronization of clocklike neural oscillators.

Unlike a well-defined function such as respiration or walking for a rhythmic motor pattern generation system (638), it has been elusive to conclusively demonstrate that specific brain processes causally depend on certain cortical oscillations (861, 876, 877). Instead of focusing on rhythmicity per se, the function of synchronous oscillations should be better appraised in the more general perspective of correlation between spike times of neurons. Neural correlation implies synchronization on some time scale, which can occur with or without oscillations. High variability of spike discharges itself depends on correlations in the inputs (420, 917), since the variability of inputs that converge onto a cortical neuron would be largely averaged out through summation over a large number of uncorrelated neurons (884). In the cortex, pairwise neural cor-

relation of trial-by-trial response fluctuations (noise correlation) is typically small (40, 187, 339, 568, 1097); recent work indicates that the population average of noise correlations is approximately zero in some dynamical states of the cortex (262, 433, 801). But even weak neural correlations can have strong impact on a network's state (851) and may be important for various computations ranging from sensory coding, to attentional gain modulation, to planning and goal choices (36, 221, 233, 294, 376, 642, 728, 771, 835, 838, 851, 890, 941, 979, 992, 1016). Perhaps no recent findings better highlighted the importance of correlated spike times than the discovery of spike-timing dependent plasticity (STDP) for synaptic learning (1, 81, 82, 151, 213, 344, 643, 879, 1093). STDP depends on the relative timing of the pre- and postsynaptic spikes as well as the firing rates (540, 643, 879, 880); if the spike discharges of a pair of neurons were uncorrelated Poisson processes, there would be no net modification of synaptic connections between the two (505, 826, 891). In the hippocampus, for instance, STDP represents an attractive mechanism for sequence learning in spatial navigation (1). As an animal moves along a linear track, location- and direction-selective place cells in the hippocampus are activated sequentially. If two neural pools fire one after another within tens of milliseconds, according to the STDP rule, synaptic connections from those firing earlier to those firing later should be strengthened, whereas synaptic connections in the opposite direction are weakened. An observable consequence is that the shape of the spatial tuning curve of hippocampal place cells becomes asymmetric (skewed) with experience, a prediction that was confirmed experimentally (673). This example illustrates how a learning mechanism specifically depends on temporal correlations of neural firing activity. Correlated activity (coherent rhythms in particular) also plays an important role in circuit pattern formation of the developing brain (88, 289, 1082).

Synchronous oscillations are a simple and appealing way to produce or enhance temporal correlations between neurons (419), which are critical for STDP. Conversely, STDP may be a driving force to determine neuronal synchronization patterns in a network (157, 319, 464, 731, 941), or to detect specific temporal patterns in the input (651). Interestingly, a recurrent network endowed with STDP at local synapses could self-organize into complex oscillatory patterns, perhaps at the border between synchronization and desychronization, with irregular yet correlated spatiotemporal dynamics (608). One of the main objectives of this review is to marshal experimental data and theoretical work that are beginning to resolve the apparent dichotomy between stochasticity and synchrony of cortical dynamics in cognition.

B. Cortical Oscillations Associated With Cognitive Behaviors

Bremer's 1958 review focused on the "alpha rhythm," large-amplitude EEG sinusoidal (~10 Hz) oscillations that spontaneously occur in an awake and relaxed state (20, 108, 110, 910). By that time, it was already known that other EEG rhythms could be observed in certain behavioral states (469), or be induced by sensory stimulus (9). However, these macroscopic EEG signals, when recorded from the scalp, have small amplitudes and are spatially poorly localized. Better measurements could be obtained invasively using subdural electrocorticogram (ECoG) with the scalp removed and electrodes directly placed on the cortical (pial) surface so that the signals are not smeared spatially by passing through the skull or mesoscopic local field potential (LFP) with electrodes inserted deep into the brain (732, 733). With the use of ECoG or LFP recordings in animals, a variety of brain rhythms have been found across various behavioral states during wakefulness, which are briefly described below.

1. Theta rhythm

Theta (4–8 Hz) rhythm is a prominent coherent oscillation observed in the hippocampus and its surrounding limbic structures during exploratory movements, e.g., when a rat navigates through a maze looking for food in a laboratory experiment (87, 141, 1002). During spatial navigation, hippocampal pyramidal neurons ("place cells") encode specific locations ("place field") of the rat during active exploration (738). The spike timing of a hippocampal neuron systematically shifts to an earlier phase of the theta cycle as the rat moves across the cell's place field, a phenomenon called "phase precession" (254, 456, 740, 881, 1080) (Fig. 1*A*). Theta phase precession has also been observed during navigation in two-dimensional arenas (457, 462, 881). While the frequency of theta oscillations is higher with a faster running speed of the animal, the linear relationship between the phase of spikes fired by a place cell and the distance traveled by the rat in the place field is independent of the running speed (343), suggesting that spatial information may be partly encoded by the precise timing of spikes. Hippocampal theta rhythm is believed to play a role in the formation and retrieval of episodic and spatial memory (425).

Theta rhythm has also been observed in the neocortex (150, 390, 474, 489, 516, 790). In humans, theta rhythm was found to be enhanced in various neocortical sites during working memory, for example, when a subject was required to remember a list of items across a delay of a few seconds (677, 790). Single-unit activity phase-locked to LFP theta rhythm was also observed in monkey's extrastriate cortex in a working memory task (569) and in the human brain (467). Theta rhythm appears to be par-

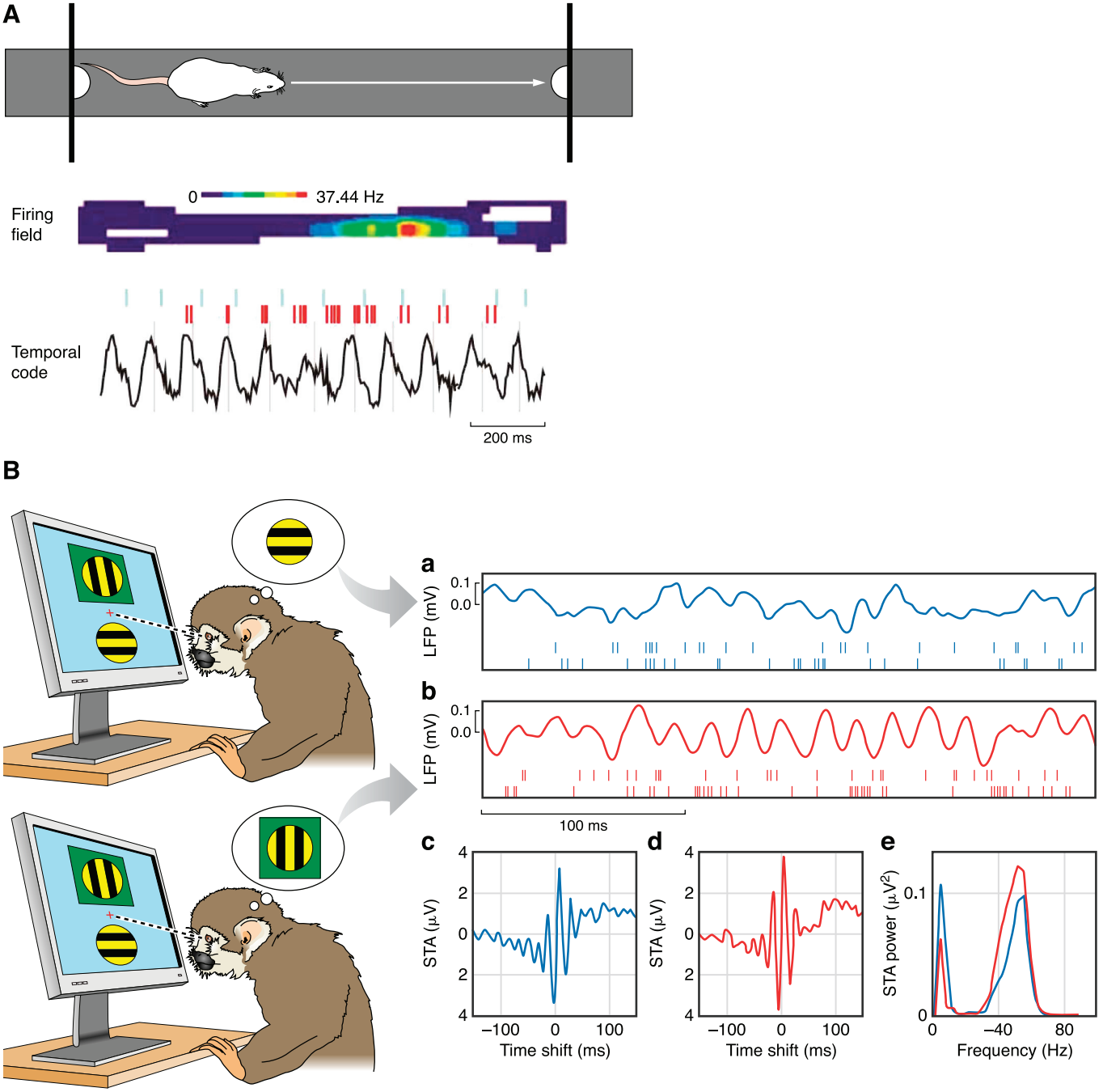

FIG. 1. Examples of synchronous oscillations in cognitive behaviors. *A*: theta rhythm in the hippocampus during spatial navigation. *Top*: in the task, rat shuttles back and forth along a linear track between food rewards contained in cups attached to movable walls. *Middle*: color-coded firing field of a place cell created from multiple runs in the eastward direction. *Bottom*: EEG theta rhythm and place cell firing (in red) for the same cell on a single eastward run. Ticks above the spikes indicate 0°/360° phase for each theta cycle. Bursts of spikes occur at higher than theta frequency causing each successive burst to move to an earlier phase of the theta cycle, despite initially rising then falling firing rate. *B*: attention induces changes in synchrony in the visual cortex. Data shown are from an experiment in which two visual stimuli were presented, one inside and one outside the receptive field of a neuron in area V4 of a behaving monkey. In the schematics (*left*), the green box represents the receptive field: this was not presented on the screen in the experiment. Red traces correspond to attention directed inside the receptive field of the recorded neuron; blue traces correspond to attention directed outside. Stimuli were the same in the two conditions. *a* and *b*: The continuous traces show the stimulus-driven local field potentials (LFPs). The spikes below were recorded simultaneously from different electrodes. *c* and *d*: Spike-triggered averages (STAs) computed during the stimulus presentation period. The STA corresponds to the average LFP waveform that is seen at the time of a spike. The *y*-axes indicate the mean LFP; the *x*-axes indicate time relative to the occurrence of a spike. *e*: Power spectra of the two STAs shown in *c* and *d*. When attention is focused inside the receptive field, the recorded neurons tend to fire more in phase with the frequency components around 50 Hz, and less so with respect to the frequencies around 10 Hz. [*A* from Huxter et al. (456); *B* from Salinas and Sejnowski (838) with the original experimental data reported in Fries et al. (312).]

ticularly prominent in the frontal midline (including the anterior cingulate cortex) (160, 348, 741, 980, 1022, 1069a), a subregion of the prefrontal cortex (PFC) implicated in behavioral monitoring (615), valuation of response outcomes (832), and other aspects of cognitive functions.

2. Ultrafast oscillations

Ultrafast oscillations (>100 Hz) were first reported in 1935 by Adrian in the cerebellum (7). In the hippocampus, EEG is characterized by transient sharp wave ripples (~100–200 Hz) that recur intermittently during awake immobility, consummatory behaviors and non-REM sleep, when theta rhythm is absent (146, 147). Similarly high-frequency transient oscillations have also been observed in the neocortex (150).

3. Beta rhythm

Beta (15–30 Hz) rhythm was initially observed in the primary motor cortex by Hans Berger in 1931. In a pioneering work with intracranial EEG (iEEG) recording from epileptic patients (469), Jasper and Penfield noted that beta rhythm occurred during "readiness" but ceased at the initiation of a movement. Electrophysiological studies on humans and monkeys generally confirmed the idea that beta rhythm is associated with preparation and inhibitory control in the motor system: the beta power is decreased at the onset of movement execution and increased when a response is withheld (41, 103, 711, 768, 822, 842, 925). Other studies indicate that beta oscillations are not limited to the motor system, but more generally are involved in sensorimotor integration and top-down signaling (see sect. VI).

4. Gamma rhythm

Gamma (30–80 Hz) rhythm was first shown to be induced by sensory stimulus in the olfactory bulb by Adrian (8, 9), and later studied extensively by Freeman (303). In the hippocampus, gamma rhythm often co-occurs and is temporally internested with theta rhythm (104, 694, 923). In the neocortex, Rougeul, Buser and their colleagues identified 40- to 50-Hz oscillations in the parietal and frontal areas, when cats appeared to be "in a class of 'attentive' behavioural states", for example, while watching a prey that just entered the room. These authors referred to this fast oscillation as "hypervigilance rhythm" (102). These observations presaged today's notion of enhanced gamma rhythm as a physiological fingerprint of attention (270, 311, 312) (Fig. 1*B*). The next major advance was the observation of gamma oscillations in spiking activity of neurons of the primary visual cortex by Gray and Singer and by Eckhorn and collaborators, first in anesthetized animals (263, 374, 376) and later in alert animals (307, 309, 375, 533, 630). Gamma-frequency synchronization between neural assemblies was suggested to play a role in integration of sensory information (372, 877), a hypothesis that has spurred an avalanche of experimental and theoretical studies on cortical rhythms and their possible functions.

5. Slow oscillations of up and down states

Slow (<1 Hz) oscillations of up and down states, discovered in 1993 by Steriade and collaborators (907, 911, 912), are the overriding EEG pattern during non-REM (slow-wave) sleep (4, 19, 207, 240). During large-amplitude EEG slow oscillations, virtually all cell types in the cerebral cortex repetitively switch between two membrane potential states: an up state (where neurons are depolarized at about −65 mV and fire at a low rate) and a down state (where neurons are hyperpolarized by 10–15 mV) (190, 679, 839, 912, 916), and the neocortex entrains other brain structures such as cerebellum (820) and amygdala (200). Recent work on human subjects and behaving animals indicates that non-REM sleep might play a role in memory consolidation (100, 449, 919, 920) and that this function might be related to the slow oscillation itself (449, 478, 565, 647).

This review focuses on these synchronous cortical oscillations directly associated with cognitive behavior.

C. Interplay Between Neuronal and Synaptic Dynamics

The last two decades have seen the accumulation of a wealth of our knowledge about brain rhythms during behavior, thanks to a confluence of experimental advances. First, in human studies, magnetoencephalogram (MEG) and iEEG recordings using as subjects epileptic patients (who are undergoing iEEG for localization of the seizure onset regions before surgery) provide measurements with a higher spatiotemporal resolution and much better signal-to-noise ratio than the scalp EEG. Second, an increasing number of physiologists record simultaneously LFP and single units from animals performing cognitive tasks; it is thus possible to examine the timing of spiking activity of individual cells relative to LFP oscillations during behavior. Third, new techniques make it possible to record in vivo from identified neuron types (pyramidal cells or different subclasses of GABAergic interneurons), yielding valuable information about how they relate to each other and to a population rhythm. Fourth, network oscillations similar to behaviorally relevant rhythms such as gamma and theta can be reproduced in cortical slices in vitro, where the circuit mechanisms underlying rhythm generation can be thoroughly analyzed. At the same time, it has been increasingly recognized that the membrane dynamics of single neurons are determined by a diverse

set of voltage-gated and calcium-gated ion channels. As a result, some subclass of cortical cells displays intrinsic oscillations and is potentially capable of serving as pacemakers of network rhythms. The history of research on synchronous neural oscillations is an excellent case of progressive advances from macroscopic (average) description of neural populations to a microscopic understanding of circuit dynamics of interconnected neurons endowed with all their glorious electrophysiological details. Fifth, with the new targeted optogenetic manipuation that allows one to rapidly and selectively activate or d-activate a subtype of nerve cells (227, 411, 613), it is now possible to establish causal links between an observed neural activity pattern and its underlying circuit mechanism(s). Sixth, and finally, mathematical theory and ever more sophisticated biophysically based neuronal network modeling provide valuable tools for exploring the dynamic behavior of such recurrent neural circuits, sometimes with surprising results.

What are the cellular mechanisms of synchronous cortical rhythms? In his 1958 review, Bremer articulated the idea that "the cortical waves are the synchronized pulsations of cortical neurons" and proposed that synchronization of large-amplitude alpha oscillations across the two hemispheres was produced by intracortical excitatory connections. The idea of synchronization by excitatory connections is intuitively appealing, as one would expect that mutual excitation between principal neurons should bring them into firing together. This idea gained support from experimental and computational studies on epilepsy, where blockade of synaptic inhibition in a cortical network led to extremely synchronous neural firing patterns, resembling epileptic discharges (968, 969). In the 1990s, however, modeling studies have begun to question the generality of this mechanism, with the finding that whether excitation synchronizes coupled neurons depends on the membrane properties of the constituent cells and the time courses of synaptic currents (415, 527, 1000). On the other hand, it has been known for a long time (21, 303, 318, 1060, 1061) that synchronous rhythms can be generated by an interplay between excitation and inhibition, as fast recurrent excitation followed by slower feedback inhibition readily gives rise to oscillations. In this scenario, inhibition plays an important role in rhythmogenesis. More surprisingly, in the early 1990s, Wang and Rinzel (1036, 1037) found, in modeling studies, that mutually inhibitory synaptic interactions can synchronize a population of GABAergic neurons; therefore, coherent oscillations can emerge in a purely inhibitory neuronal network. This "interneuronal network scenario" was initially revealed in a model of thalamic oscillations (1036, 1037) but has proven to be a general principle (275, 970, 1000, 1035). In particular, theoretical and experimental work found that this mechanism is capable of generating synchronous gamma (~40 Hz) oscillations in a hippocampal network of inhibitory neurons in vitro (970, 1035, 1053). Both the interneuronal network and the excitatory-inhibitory loop scenarios critically depend on synaptic inhibition, which thus does not merely control the overall network excitability but plays an essential role in temporally sculpting cortical network activity patterns during behavior.

D. Organization of This Review

In the first part of this review, I cover a rich variety of single neuron properties (see sect. II), basic synaptic circuit mechanisms and network architectures (see sects. III and IV) underlying the generation of cortical network oscillations associated with cognition. Then, I present the evidence showing that the theory of coupled oscillators is not adequate for capturing the salient characteristics of cortical dynamics of the waking brain. I present an alternative theoretical framework for describing weakly synchronous population rhythms in which single cells fire action potentials irregularly and intermittently in time (see sect. V). This is followed by section VI, which is devoted to recent work on behaving animals and humans that explore functional implications of synchrony and coherent rhythms, with an emphasis on long-distance neural communication and top-down signaling. In section VII, I briefly discuss possible implications for abnormal neural synchronization associated with mental disorders. Finally, I summarize some general insights that have been gained from experimental and theoretical studies (see sect. VIII).

II. SINGLE NEURONS AS BUILDING BLOCKS OF NETWORK OSCILLATIONS

Single neurons in the cortex are endowed with a rich repertoire of active ion channels that are distributed across the somatodendritic membrane (597, 623, 879, 899). As a result, diverse cell types display a variety of subthreshold membrane response dynamics and spike firing patterns. Synchronization of a circuit depends critically on the intrinsic membrane properties of its constituent cells. In a recurrent network, precisely how single neurons adjust the timing of action potentials in response to phasic synaptic inputs from other neurons greatly affects whether the network ultimately becomes synchronized or not. Moreover, the selection of a frequency band at which coherent oscillations occur is shaped by pacemaker or resonance properties of individual cells. Thanks to many studies over the last two decades, with close two-way interactions between experiments and theory, we now know a lot about the interplay between single neuron dynamics and network synchronization. In fact, this area represents an exam-

ple par excellence of why detailed single-cell properties do matter with regard to collective network dynamics. In this section, I review important aspects of cellular electroresponsiveness relevant to network oscillations.

A. Phase-Response Properties of Type I and Type II Neurons

All single neurons are oscillators, insofar as they respond to a constant input current I by repetitive firing of action potentials at a certain frequency f (period $T_0 = 1/f$). In the classic Hodgkin-Huxley model of action potential (437), this periodic behavior is mathematically described as a stable oscillatory state. Since action potentials are stereotypical events, it makes intuitive sense to focus on the timing of action potential, or the phase (between 0 to 360 degrees), relative to the oscillatory cycle. In this view, the issue of network synchronization can be formulated in terms of how synaptic interactions affect the phases of action potential among connected neurons. This "phase reduction theory," pioneered by Kopell, Ermentrout and others, is well founded under the "weak coupling condition," when synaptic interactions are not too strong to greatly alter the intrinsic frequency of neural oscillators (276, 280, 413, 524, 525, 539, 999, 1065). Even when synaptic interactions are not weak, the phase reduction theory still provides useful insights. For a sinusoidal oscillation, $\sin(2\pi ft)$, which arises from a linear system, phase shift induced by a brief pulse perturbation is the same regardless of when the pulse is applied. In contrast, neuronal oscillators are highly nonlinear, characterized by a stereotypical fast event (the action potential) followed by a slow refractory and recovery period. For such "relaxation type" oscillators (25, 922), the phase response highly depends on the timing of the input pulse. This is quantified by a "phase response curve" (PRC), where the induced phase shift of spike is plotted as a function of the phase at which a brief depolarizing current pulse is applied (210, 279, 359, 811, 1065).

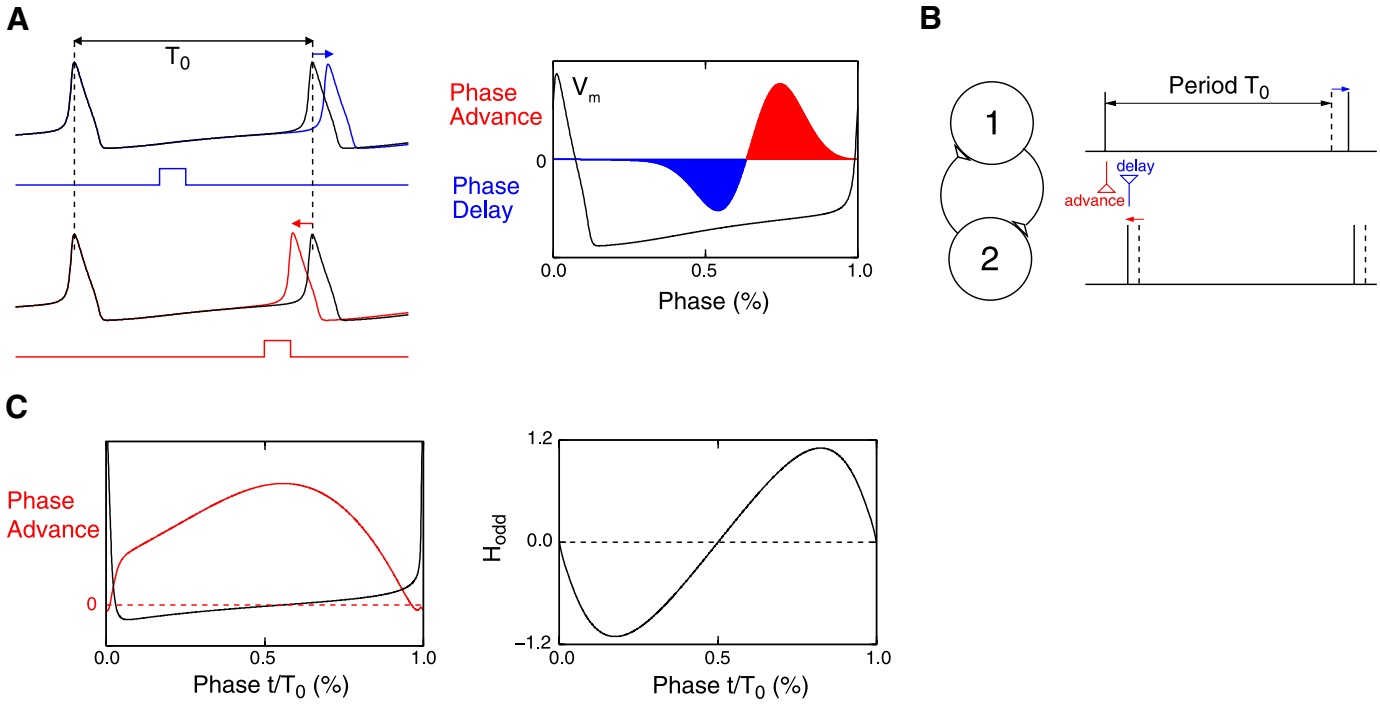

FIG. 2. Theory of coupled oscillators. *A*: phase response curve of the classical (type II) Hodgkin-Huxley model of action potential (437). *Left*: a small and brief depolarizing current pulse leads to either a phase delay (blue) or phase advance (red), depending on the timing of the pulse perturbation. T_0 is the oscillation period in the absence of perturbation. *Right*: induced phase change (positive for advance, negative for delay) as a function of the oscillatory phase at which the pulse perturbation is applied. Superimposed is the membrane potential for a full oscillation cycle (spike peak corresponds to zero phase). *B*: fast mutual excitation naturally gives rise to synchrony for two coupled Hodgkin-Huxley model neurons, as a cell firing slightly earlier advances the firing of the other cell, while the synaptic input back from the other cell delays its own firing, leading to reduced phase difference between the two in successive cycles. Dashed vertical lines, spike times for isolated neurons; solid lines, actual spike times in the presence of synaptic interaction. *C*: perfect synchronization by mutual inhibition. *Left*: phase response curve of a modified (type I) Hodgkin-Huxley model (1035), which does not exhibit significant phase delay (the negative lobe). *Right*: the phase reduction theory predicts the behavior of coupled neurons by the function $H_{odd}(\Phi)$, where Φ is the phase difference between the two neurons (*Eq. 4*). H_{odd} was computed using a synapse model with a reversal potential of −75 mV and a decay time constant of 10 ms. Steady-state behaviors correspond to Φ values such that $H_{odd}(\Phi) = 0$. In this example, zero-phase synchrony ($\Phi = 0$) is stable (where H_{odd} has a negative slope); 180 degree antiphase is unstable (where H_{odd} has a positive slope).

The classic Hodgkin-Huxley model exhibits a biphasic "type II" PRC (Fig. 2*A*) (119, 415): a depolarizing pulse induces a phase advance (making the spike to fire earlier), when it is applied some time before the next spike is expected to occur, but it actually delays the phase of the next spike when applied soon after the spike discharge. This is because during that time the neuron is recovering from afterhyperpolarization, as the delayed rectifier potassium current decays away and the fast sodium current deinactivates. Both decay processes are slowed momentarily by the brief depolarization; therefore, it takes longer for the next spike to be generated.

Intuitively, synaptic excitation is expected to synchronize coupled neurons, if neurons that happen to fire earlier in an oscillatory cycle advance the spike times of other ("later firing") neurons, which in turn delay the spike times of "earlier firing" neurons, so that all neurons will tend to fire more synchronously in the next oscillatory cycle and the network will be brought in phase. This is precisely what happens for type II neurons coupled by fast ("instantaneous") excitatory synapses (Fig. 2*B*). Assume that initially cell 1 fires ahead of cell 2. Then, synaptic excitation from cell 1 advances the next spike in cell 2. When cell 2 fires, cell 1 is still in the recovery phase, so synaptic excitation from cell 2 actually delays the next spike in cell 1. Therefore, interactions in both directions tend to reduce the phase difference between the two cells, eventually leading to spike-to-spike synchrony. However, this intuitive reasoning is no longer sufficient if synaptic interactions are not brief instantaneous perturbations, but have significant time courses of their own (see below).

Unlike the classic Hodgkin-Huxley model, a neuronal PRC may not display a significant "negative lobe" (119, 275, 658). That is, the spike phase is always advanced regardless of the stimulus timing, even though the amount of induced phase shift depends on the timing of the pulse perturbation. Such a "type I" PRC is shown in Figure 2*C*, *left panel*, using a model modified from the classic Hodgkin-Huxley model with some parameter variations (1035). The parameter changes reduce the potassium conductance and speed up the sodium and potassium current kinetics. As a result, the recovery from hyperpolarization is fast, and the delay portion of the PRC essentially disappears. Therefore, type I and type II PRCs can be produced by the same set of ion channels but with quantitatively different properties.

For type I neurons, a cell that fires earlier is phase-advanced by another cell that fires later, which acts against reducing the relative phase difference between the two. Hence, it is not straightforward to ascertain intuitively synchronization by mutual excitation between type I neurons. As it turns out, a mathematical analysis using the phase reduction theory, which will be discussed in section III, found that type I neurons tend to be much more easily synchronized by mutual inhibition than excitation (275, 415, 998). This theoretical finding shows that single cell properties can qualitatively alter network behavior in a completely counterintuitive way.

Phase response properties have been routinely characterized for neurons in central pattern generator systems (638, 772). More recently, in vitro slice studies have directly assessed PRCs of neurons in the mammalian cerebral cortex, using current perturbations that mimic excitatory or inhibitory postsynaptic potential (EPSP or IPSP) (719, 802, 936, 978). It was generally found that for a given cell, the classification of its PRC into type I or type II is consistent for a range of intrinsic oscillation frequencies, and not sensitive to the exact amplitude of postsynaptic potential perturbations (719, 936). Distinct neuron types exhibit differential preponderance for phase response properties. Nevertheless, neurons within a neural population are heterogeneous and exhibit both type I and type II PRCs (978), possibly as a result of quantitative differences in the expression of ion channels across neurons in a population.

The precise shape of PRC of a neuron depends on its repertoire and somatodendritic distribution of various ion channels. In general, regenerative currents (such as a persistent sodium current I_{NaP} that provides a positive feedback for membrane depolarization) tend to shift leftward a PRC and eradicate the negative lobe, thereby favoring type I behavior (362, 766). On the other hand, restorative currents (such as a voltage-activated M-type potassium current I_M that acts as a negative feedback for voltage changes) tend to accentuate the negative lobe (206, 277, 362, 1044). This is because a current like I_M is activated by depolarization during an action potential, and decays afterwards as the membrane recovers from afterhyperpolarization. A brief depolarization soon after a spike would counter this decay process, hence delaying the timing of the next spike. The hyperpolarization activated cation current I_H deactivates with depolarization, hence has a similar effect as a depolarization-activated outward current. I_H is thus expected to accentuate the negative lobe and favors type II PRC behavior, a prediction that was confirmed with pharmacological blockade of I_H in pyramidal neurons (362). Another important issue is how PRC depends on the location of synaptic inputs in a spatially complex neuron (362, 799). Goldberg et al. (362) addressed this question using both modeling and patch-clamp recording in vitro. They found that dendritic PRC (obtained using a current pulse applied onto the dendrite, 35–250 μm from the soma) is a linearly filtered version of somatic PRC (obtained using a current pulse applied onto the soma); the filter depends on the passive and active properties of the dendrite. As a result, somatic and dendritic PRCs can in principle show disparate behaviors. For example, because of an increasing gradient of expression of the H ion channel conductance from soma to distal dendrite (624), dendrites of a pyramidal

cell can display type II PRC, whereas its somatic PRC can be type I.

A calcium-activated potassium current (I_{KCa}) and, to a lesser degree, I_M and I_H, underlie spike-frequency adaptation, which is a common characteristic of pyramidal neurons (293, 619, 620, 650, 668, 793, 1027) and certain subclasses of inhibitory cells (499, 500). As it turns out, a large I_M (which has a low voltage threshold and is significant at resting membrane potential), but not I_{KCa} (which depends on calcium influx through the opening of high-threshold calcium channels during action potentials), can switch a neuron from type I to type II (277, 782). Conversely, a reduction of I_M (e.g., by cholinergic modulation) can transform a pyramidal cell from type II to type I (921). Hence, type I versus type II PRC behavior depends on low-threshold potassium currents, but is not necessarily correlated with a neuron's (primarily I_{KCa} dependent) spike-frequency adaptation. Indeed, in vitro pyramidal cells display strong spike-frequency adaptation, yet show mostly type I behavior; when they do display type II PRCs, the negative lobe is fairly shallow (362, 395, 802, 978). Also, "low-threshold spiking" (LTS) interneurons display spike-frequency adaptation, whereas fast spiking (FS) interneurons do not (499, 500, 645, 668). At the same time, the observed tendency appears to be type I behavior for LTS cells and type II behavior for FS cells (936). Such differential PRC properties of different neural types have important implications for their distinct roles in generating network rhythms (see sect. III).

B. Resonance

Resonance refers to the phenomenon of band-passed neuronal response, with maximal response at a preferred input frequency. In studies using sinusoidal input currents of varying frequencies, or the "impedance amplitude profile" protocol that sweeps through many frequencies in a single stimulus (453–455, 784), many neuron types were found to display resonance, namely, a peak in their impedance (the ratio of the subthreshold membrane potential response and the input current intensity) at a particular (resonance) stimulus frequency. Resonance is intuitively expected when single neurons are damped oscillators, hence display an intrinsic preferred frequency (552, 1025). However, resonance does not necessarily require damped oscillation of single neurons (453, 805). It readily takes place when there are two opposing processes; one counteracts membrane potential V_m changes at low frequencies (with a time constant τ_1), and the other does the same at high frequencies (with a time constant τ_2). The combination of the two gives rise to a peaked response at a frequency f_R intermediate between $1/(2\pi\tau_1)$ and $1/(2\pi\tau_2)$ (453).

Membrane passive properties (e.g., the leak conductance) naturally act as a low-pass filter ($\tau_2 = \tau_m \sim 10$ ms), whereas voltage-gated active channels give rise to high-pass filtering. For example, an I_H opposes voltage changes in a subthreshold voltage range: a hyperpolarization of V_m is counteracted by an increased inward I_H, whereas when V_m is depolarized I_H inactivation has the same effect as activation of an outward current. I_H has a time constant on the order of 100 ms, thus behaves as a high-pass filter. The interplay with the leak conductance as a low-pass filter results in a resonance at $f_R \sim 5$–10 Hz. An H-current dependent mechanism underlies resonance observed in layer II stellate cells of entorhinal cortex, and combined with membrane noise gives rise to subthreshold oscillations in these cells (242, 298, 356, 396, 397, 519). Interestingly, I_H-dependent resonance is most prominent when the inputs are located at distal dendrites (191, 192, 637, 991), consistent with an increasing gradient of I_H expression from soma to distal dendrite of pyramidal neurons (624). Another example is a voltage-gated potassium current, like I_M or a low-threshold slowly inactivating potassium current I_{KS}, which counteracts membrane potential changes in a depolarized range. Together with suppressed responses at high frequencies by the leak conductance, such a current produces resonance when neurons are excited to significantly above the resting membrane potential but below firing threshold (445, 453). A single neuron may display more than one resonance (bandpass) filter that is spatially segregated, for instance, an I_H-dependent mechanism in the dendrite and an I_M-dependent mechanism in the soma (446).

Typically, resonance by a depolarization-activated K^+ current is greatly amplified by the presence of a persistent sodium current I_{NaP}, which is a positive feedback operating in the same voltage range as I_M or I_{KS} (394, 445, 453–455, 463, 601, 705, 1025, 1047). The resonance frequency f_R critically depends on the activation time constant of the slow potassium current (1025), often in the theta (4–8 Hz) (394, 445, 1025, 1046) or gamma (~40 Hz) frequency range (1025).

How does subthreshold resonance relate to neuronal firing of action potentials? It has been shown that, in hippocampus, neurons display similar frequency preference for membrane potential responses and spike discharges at low firing rates (when V_m stays below firing threshold most of the time) (769). Moreover, resonance frequency is in the theta frequency range for pyramidal cells, and in the gamma frequency range for fast spiking interneurons, suggesting differential roles of these two major cell types in theta- versus gamma-frequency network oscillations (769). In a systematical modeling study of neuronal resonance, Richardson et al. (805) considered two model neurons with resonance frequency at f_R, one based on I_H and the other on I_{KS} and I_{NaP}. They used input currents composed of three components: a baseline that controls the overall average spike rate r_0 of the model neuron, a weak sinusoidal wave at frequency f, and a

background noise term mimicking stochastic synaptic bombardments in vivo (236). They found that, interestingly, subthreshold resonance may or may not be reflected in the spike firing activity, depending on the degree of neural firing variability. When noise is weak and firing is regular, the maximal modulation by the sinusoidal input occurs at $f = r_0$, so the preferred frequency is the firing rate itself. In contrast, when noise is strong and firing is irregular, the firing response is best modulated by the subthreshold resonance frequency at $f = f_R$. This is true even when the mean firing rate r_0 is much higher than f_R, e.g., $r_0 = 20$ Hz and $f_R = 5$ Hz (Fig. 3). Although somewhat surprising, this result may be explained by observing that, with a stronger noise, a lower mean input is needed to produce the same mean firing rate r_0, because spikes are more often triggered by stochastic input fluctuations. Therefore, on average, the membrane potential is lower where subthreshold resonance plays a more important role. In other words, noise is important for unmasking a subthreshold resonance in the spike firing patterns. This insight is likely to have implications for understanding the relationship between highly irregular neural discharges and coherent network rhythms (see sect. V).

C. Subthreshold and Mixed-Mode Membrane Oscillations

Strong resonance is usually a manifestation of membrane potential oscillations, because even a transient ("damped") oscillation endows a neuron with an intrinsic preferred frequency, and a sinusoidal input with matched frequency evokes maximal responses (453, 805). A neuron becomes a pacemaker if it displays sustained intrinsic oscillations (15, 106, 599, 600, 1038). In the neocortex, membrane potential oscillations below spike threshold were first reported at theta frequency in layer II entorhinal cortical neurons by Alonso and Llinás in 1989 (15) and at gamma frequency in neocortical neurons by Llinás et al. in 1991 (600). In both cases, the intrinsic rhythmicity was shown to be TTX sensitive, suggesting that a low-threshold Na^+ current plays a critical role. These findings motivated a computational model, published in 1993, proposing that the observed intrinsic membrane potential oscillations arise from the interplay between a low-threshold persistent Na^+ current I_{NaP} and a slow low-threshold K^+ current (I_{KS}) (1025). Oscillation naturally occurs as a result of the interaction between a positive feedback (between V_m depolarization and I_{NaP} activation) and a slower negative feedback (depolarization induced I_{KS} activation). The activation time constant of I_{KS} controls the recovery phase of the oscillation cycle, hence largely determines the rhythmic frequency which can be in the gamma or theta frequency range (1025).

Notably, the model predicts a different relationship between the oscillation frequency and the input drive in these two cases. In the gamma frequency regime, subthreshold oscillation frequency increases with the input drive. In the theta frequency regime, the frequency remains roughly constant (exhibiting a plateau), as long as the oscillation is subthreshold, and starts to increase with

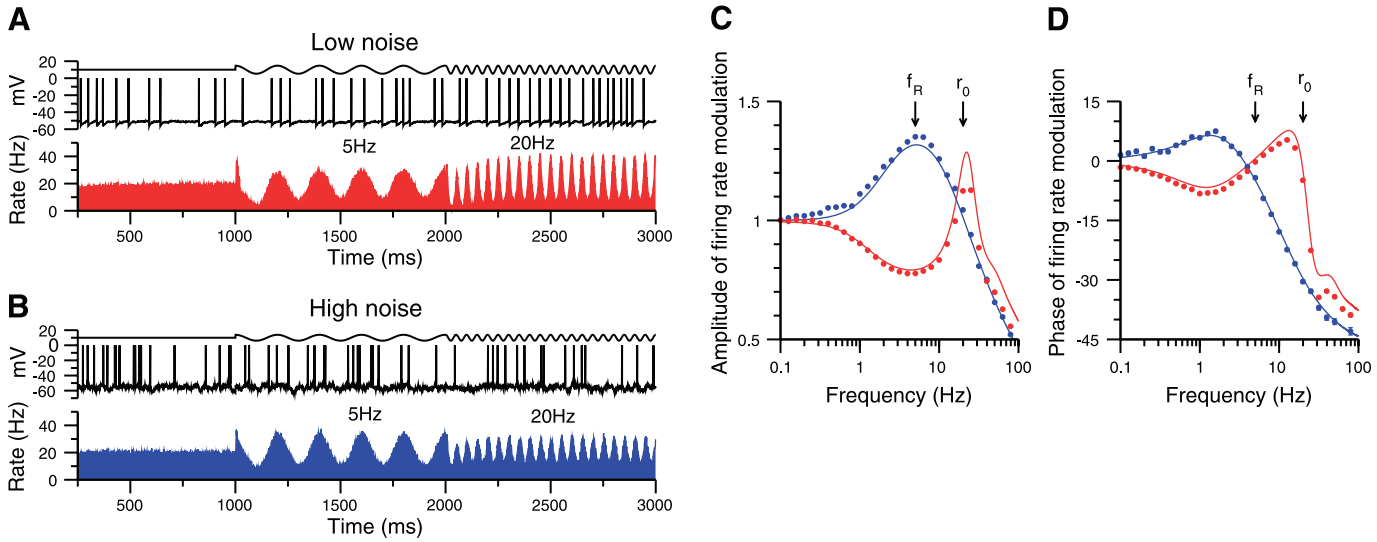

FIG. 3. Subthreshold and spiking resonance of a model neuron in the presence of noise. The model neuron exhibits subthreshold membrane resonance at frequency f_R of 5 Hz. *A*: response with low noise. *Top*: input current with three (tonic, 5-Hz and 20-Hz sinusoidal current injection) epochs. The mean output firing rate remains constant ($r_0 = 20$ Hz) throughout. *Middle*: a sample membrane trace. *Bottom*: poststimulus histogram. *B*: response with high noise. Same format as in *A*. *C*: signal gain amplitude versus input frequency f (normalized to be one at $f = 0$). Firing rate resonance occurs at the subthreshold resonance frequency ($f = f_R$) with high noise (blue), but at the mean firing frequency ($f = r_0$) with low noise (red). *D*: phase shift of the firing response relative to the sinusoidal input (positive, phase advance; negative, phase delay). [Adapted from Richardson et al. (805).]

the applied current intensity when spike firing becomes significant. The predicted plateau phenomenon was observed in stellate cells of entorhinal cortex (Fig. 5*F* in Ref. 13).

Among neural types that exhibit subthreshold membrane oscillations, of special interest are GABAergic neurons in the nucleus basalis (16) and medial septum (858) (Fig. 4*A*). The nucleus basalis and medial septum are the major parts of the basal forebrain that provide the neuromodulatory transmitter acetylcholine to the neocortex and hippocampus, respectively (669, 833, 909, 910). In addition to cholinergic cells, these structures also contain GABAergic cells with axonal projections to the cortical mantle. GABAergic cells in the medial septum are believed to act as a pacemaker for theta rhythm in the hippocampus, and those in the nucleus basalis may play a similar role for theta rhythm in the neocortex. As shown in Figure 4*A*, medial septum noncholinergic (putative GABAergic) cells display "mixed-mode oscillations" in which periodic repetition of clusters of spikes are interspersed in time with epochs of subthreshold oscillations. The intercluster oscillation is in the theta frequency range, whereas both subthreshold membrane potential oscillations and intracluster spike firing rate are in the gamma frequency range. Such mixed-mode oscillations are especially interesting because in the entorhinal cortex and hippocampus theta rhythm is often temporally nested with faster gamma-frequency oscillations (104, 146, 148, 176, 181, 358, 472, 888, 923). Cluster firing was first reported experimentally in 1939 by Arvanitaki (34); it was modeled and analyzed mathematically in the 1980s by Rinzel (810). A biophysical basis of such internested gamma and theta mixed-mode oscillation was described by the aforementioned ionic channel model (1025, 1031) (Fig. 4*B*). The mechanism relies on two assumptions. First, a low-threshold K^+ current, like a slow A-type current, should be transient and inactivates slowly. Second, the neuronal spike afterhyperpolarization is strong so that the average membrane potential is lower during spike discharges than during subthreshold epochs. Thus, when the neuron fires a cluster of spikes, the deinactivation of I_{KS} slowly builds up during spike afterhyperpolarizations,

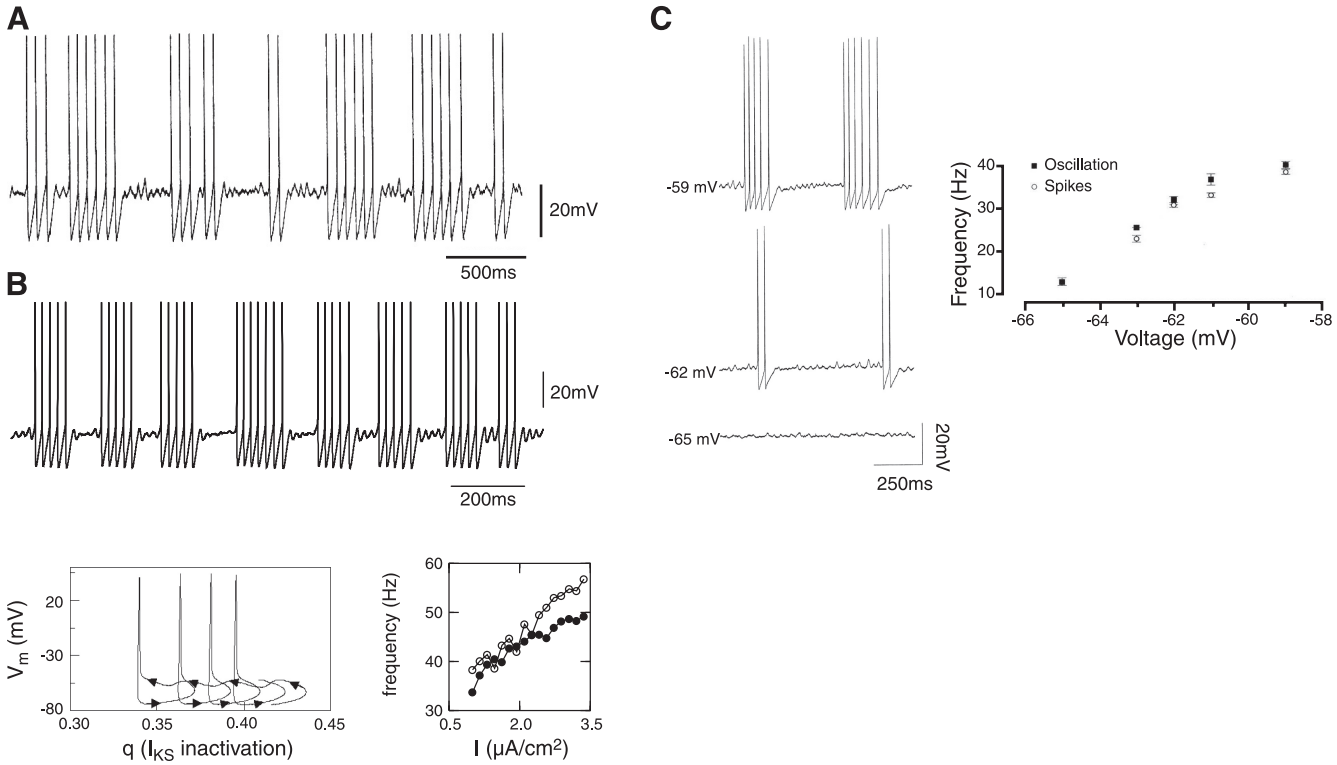

FIG. 4. Mixed-mode membrane oscillations in a single neuron. *A*: a noncholinergic (putative GABAergic) cell in the rat medial septum displays rhythmic alternations at theta frequency between "clusters" of spikes and epochs of subthreshold membrane potential oscillations. *B*: a model of GABAergic neurons in the medial septum. *Top*: a membrane trace. The simulated oscillation is faster than the experimental data (see the different time scales), because the model simulation was done at body temperature (37°C), whereas the in vitro trace was recorded at 32°. *Bottom left*: membrane potential versus the inactivation gating variable q for a low-threshold potassium channel (I_{KS}). I_{KS} gradually deinactivates (increase of q, hence I_{KS}) during the hyperpolarizing phases of spikes (arrows to the *right*), whereas it inactivates (decreasing q) during subthreshold membrane oscillations (arrows to the *left*). *Bottom right*: the frequency of subthreshold oscillations (open circle) and intracluster spike firing rate (filled circle) covary as a function of the input current intensity. *C*: similar behavior of principal (mitral) cells of the rat olfactory bulb. *Left*: mixed subthreshold oscillation and clustered spike firing of a mitral cell in response to three current intensities. *Right*: frequencies of subthreshold oscillation and intracluster spike firing versus the mean membrane potential which was varied by current injection. [*A* from Serafin et al. (858); *B* from Wang (1031); *C* from Desmaisons et al. (231).]

so the amplitude of I_{KS} increases gradually and eventually becomes large enough to terminate a spiking episode. When the cell does not fire spikes in a subsequent subthreshold epoch, the membrane potential is relatively depolarized and I_{KS} slowly decreases due to inactivation, until the cell is sufficiently recovered and can start to fire again. The subthreshold oscillations are produced by the interplay between a Na^+ current and the low-threshold activation of I_{KS}; the same oscillatory wave modulates repetitive action potentials during clustered spike firing, hence the frequency is similar for the two. In this scenario, the theta frequency of intrinsic oscillations in septal GABAergic cells is largely controlled by a single current (I_{KS}). This model prediction has not yet been tested experimentally.

Interestingly, in recent years such subthreshold oscillations have been observed in many cell types, including neocortical neurons (394), mitral cells in the olfactory bulb (48, 231), magnocellular neuron in hypothalamus (90), mesencephalic trigeminal neurons (755), dorsal column nuclei neurons in culture (798), and hippocampal interneurons in the lacunosum-moleculare layer (101). Figure 4*C* shows an example of olfactory mitral cell. Similar to the model (Fig. 4*B*, *bottom right*), in this cell the frequency of subthreshold oscillation and the rate of intracluster spike discharges remain similar, when they both vary with increased input current drive (hence mean V_m depolarization). In all these diverse cell types, V_m oscillations were shown to be blocked by TTX but not by calcium channel blockers, confirming the model prediction that subthreshold oscillations are independent of calcium channels. Moreover, in some studies, voltage-gated K^+ currents have been shown to play a critical role. Membrane potential oscillations were abolished by TEA (15 mM) in neocortical cells (3–15 Hz at 34°) (394) and hypothalamic magnocellular neurons (10–70 Hz at 32°) (90), and by 4-aminopyridine (4-AP) in mitral cells of the olfactory bulb (20–40 Hz at 30°) (48) and hippocampal lacunosum moleculare interneurons (7 Hz at 32°) (101).

If a K^+ current that opposes I_{NaP} does not inactivate, for example, of an M type, clustered spiking interspersed with subthreshold oscillatory episodes is still possible, but no longer displays regular periodicity (6, 271, 394). In this case, spikes are triggered by noise, on top of the membrane potential oscillatory wave (1047). Also, whereas some cell types are able to exhibit purely subthreshold oscillations (13, 231, 519, 798), in other neurons subthreshold membrane oscillations always occur interspersed with spike clusters (16, 101, 755, 858). This difference presumably reflects whether the spike threshold is significantly above, or overlaps with, the voltage range for activation of the low-threshold ion channels responsible for generating membrane potential oscillations (1031). In either case, with increasing amplitude of input current, the number of spikes per cluster increases and spike firing become dominant over subthreshold oscillatory episodes.

Taken together, there is a convergence of evidence in support of a general ion channel mechanism for subthreshold rhythmogenesis. This mechanism involves a voltage-gated Na^+ current, and the oscillation frequency is controlled by the activation kinetics of K^+ currents. There exist a wide diversity of voltage-gated K^+ currents with disparate kinetic properties and operating in different voltage ranges (178, 859, 893). This offers a powerful means for generating membrane oscillations at distinct frequencies, by a selective expression of a subset of these currents in distinct cell types.

D. Rhythmic Bursting

Like pacemaker neurons in central pattern generators (638), subtypes of cortical cells fire bursts of spikes (brief clusters of spikes) rhythmically at preferred frequencies (597). Bursting neurons have the potential to serve as pacemakers for synchronous network oscillations (193), and bursts of spikes may underlie or enhance neuronal resonance (435, 956). In the cortex, two types of rhythmic bursting neurons have been observed. Hippocampal pyramidal cells (968) and layer 5 neocortical pyramidal neurons (875) show a preponderance for slow rhythmic bursting at 4–15 Hz. High-frequency (>300 Hz) action potential burst firing depends on rapid regenerative processes mediated by voltage-gated calcium and sodium channels (494, 506, 875, 968, 1058, 1072). Calcium-activated potassium currents (with time constants ~100 ms) terminate the burst and control the time course of after-burst recovery, hence helping to set the oscillation frequency (~10 Hz) (10, 159, 369, 875, 968). Interestingly, bursting occurs more readily, when its underlying inward and outward channels are located in the dendrite, separated from the perisomatic region where action potentials are produced (506, 629, 773, 968). Furthermore, phasic burst firing in layer 5 pyramidal neurons (292) (and in dopaminergic neurons, Refs. 228, 481, 583) depends on the voltage-gated NMDA receptors for glutamate-mediated synaptic transmission.

In the neocortex, another class of pyramidal neurons (called "chattering cells") exhibit fast rhythmic bursting in the gamma frequency range, with intraburst spike rates of 300–500 Hz (Fig. 5*A*) (122, 154, 211, 220, 307, 373, 730, 904). Because the gamma cycle is only tens of milliseconds, potassium currents such as I_M and I_{KCa} are likely to be too slow to set the periodicity of fast bursting in chattering cells. A compartmental model (1028) suggests that the fast rhythmic bursting in chattering neurons can be generated by a Ca^{2+}-independent ionic mechanism (Fig. 5*B*). Instead, it relies on a voltage-gated persistent Na^+ current (I_{NaP}) that is electrotonically separated from

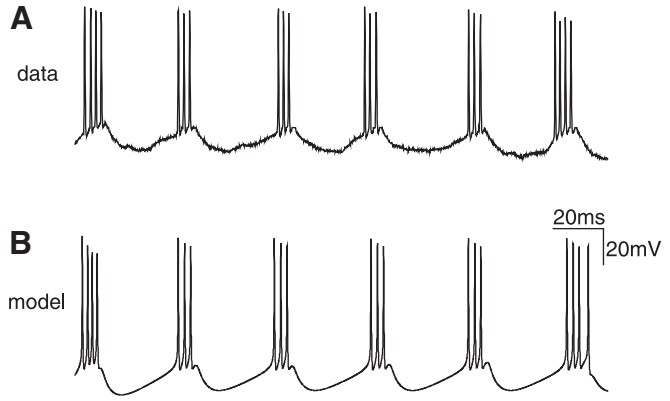

FIG. 5. Rhythmic bursting of cortical neurons. *A*: a chattering neuron recorded in vivo from the cat visual cortex shows rhythmic bursting in the gamma frequency range. *B*: a model chattering neuron endowed with a ping-pong interplay between two electrotonic compartments. [*A* from Gray and McCormick (373); *B* from Wang (1028).]

the action potential initiation zone. In one scenario, perisomatic action potentials propagate back to the dendritic sites, where a Na^+-dependent afterdepolarization is produced, which in turn triggers more spikes in the perisomatic region. Alternatively, the Na^+ channels underlying afterdepolarization may be near the soma, whereas the spike generation zone is in the initial segment of the axon. In either case, the "ping-pong" iterative interplay between spikes and afterdepolarization underlies a burst of spikes, which is terminated by the activation of a K^+ current. The deactivation of the K^+ current during hyperpolarization leads to the recovery and eventually to the start of a new burst (1028). It has also been proposed that afterdepolarization depends on a calcium-activated cation current (27). The sodium-dependent and calcium-independent model was supported by an in vitro experiment which showed that the spike afterdepolarization and the generation of spike bursts were suppressed by phenytoin which blocked persistent Na^+ channels, but not sensitive to blocking calcium transmembrane influx or intracellular chelation of free Ca^{2+} (122, 211). Interestingly, a TTX-sensitive sodium channel in interplay with a Kv3 channel in the dendrites was also found to underlie oscillatory bursting in a sensory neuron in electric fish (247, 574, 984, 985), suggesting that this mechanism may be versatile in vertebrates. Moreover, calcium-dependent processes can modulate, rather than generate, chattering behavior. In chattering neuron models, slow K^+ currents like I_M and I_{KCa} tend to suppress burst firing by virtue of reduced cellular excitability, and a reduction of these currents by neuromodulators like acetylcholine can transform a cell from tonic spiking to fast rhythmic bursting (972, 1028). Since arousal and attention are associated with cholinergic activation of the cortical system (669, 908, 909, 913), this result suggests a cholinergic mechanism for promoting neocortical gamma oscillations in attentive states.

To summarize, putative pacemaker neurons for the gamma and theta rhythms of the waking brain seem to critically rely on Na^+ and K^+ currents, which give rise to either subthreshold membrane oscillations or rhythmic bursting. Subthreshold oscillations and repetitive bursting may have different implications for synchronization of coupled neurons. Subthreshold oscillations could subserve a signal carrier for phase-locking and resonance, by virtue of the cell's sensitivity to small but precisely timed inputs (13, 106, 177, 217, 1048). On the other hand, bursts may provide a reliable signal for the rhythmicity to be transmitted across probabilistic and unreliable synapses between neurons (590, 659, 1028).

III. BASIC MECHANISMS FOR NETWORK SYNCHRONIZATION

A generic cortical circuit consists of two major cell types: excitatory principal neurons and inhibitory interneurons. It follows that three types of synchronization mechanisms by chemical synapses are conceivable: recurrent excitation between principal neurons, mutual inhibition between interneurons, and feedback inhibition through the excitatory-inhibitory loop. More recently, electrical synapses by gap junctions have also been proposed to contribute to neural synchrony. Here I describe each of these mechanisms in turn.

A. Mutual Excitation Between Pyramidal Neurons

For any type of synaptic coupling, a general mathematical approach for studying synchrony of neural oscillators is provided by the theory of phase-coupled oscillators (276, 415, 524, 539). The idea is that, if synaptic interactions are relatively weak, their effect is the synaptic current from the presynaptic neuron into the postsynaptic neuron, averaged over the oscillation period. Specifically, consider two oscillatory neurons with an intrinsic period of T_0 (frequency $f = 1/T_0$), described by their respective phases ϕ_1 and ϕ_2 (defined between 0 and 2π, with the spike time defined at zero phase by convention). The synaptic current from cell 2 to cell 1 is $I_{syn}(\phi_1,\phi_2) = g_{syn}s_2(\phi_2)[V_I(\phi_1) - V_{syn}]$, where V_1 is the voltage of cell 1, s_2 is a "gating variable" for the synaptic current and activated by spike firing of cell 2, g_{syn} is the maximum synaptic conductance, and V_{syn} is the synaptic reversal potential. The interaction function $H(\phi_1,\phi_2)$ is given by the average of the product of $I_{syn}(\phi_1,\phi_2)$ and $Z(\phi_1)$ (a single neuron's phase response curve, see sect. IIA) over an oscillatory period. Mathematically, we have (276, 279, 415, 1000)

$$H(\phi_1 - \phi_2) = \frac{1}{2\pi}\int_{-\pi}^{\pi} Z(\phi + \phi_1 - \phi_2)[-I_{syn}(\phi + \phi_1 - \phi_2, \phi)/C_m]d\phi \quad (1)$$

where C_m is the membrane capacitance.

The dynamical equations for describing the two interacting neurons are given by

$$\frac{d\phi_1}{dt} = 2\pi f + H(\phi_1 - \phi_2) \quad (2)$$

$$\frac{d\phi_2}{dt} = 2\pi f + H(\phi_2 - \phi_1) \quad (3)$$

Subtracting these two equations yields the following equation for the phase difference $\Phi = \phi_1 - \phi_2$

$$\frac{d\phi}{dt} = H(\Phi) - H(-\Phi) = H_{odd}(\Phi) \quad (4)$$

where $H_{odd}(\Phi)$ is the odd part of the H function, which determines the phase relationship. Any steady-state phase locking at Φ_{ss} is given by solving $H_{odd}(\Phi) = 0$, which means that at $\Phi = \Phi_{ss}$, $d\Phi/dt$ is zero; hence, the relative phase no longer changes over time. The stability of a steady-state phase locking is determined by the slope of H_{odd} through the steady state. Consider a steady-state Φ_{ss} at which point the slope of H_{odd} is negative. Combined with the fact that H_{odd} is zero at Φ_{ss}, we know that $d\Phi/dt = H_{odd}$ is positive for Φ slightly smaller than Φ_{ss}, and negative otherwise. As a result, if Φ is perturbed to be below (respectively, above) Φ_{ss}, then it is predicted to increase (respectively, decrease) over time; in either case, the system evolves back to Φ_{ss}. In other words, coupling acts to attenuate any small perturbation away from the steady state, and Φ_{ss} is stable. Conversely, a steady state is dynamically unstable if the slope of H_{odd} at Φ_{ss} is positive.

The phase reduction theory thus provides a general framework for predicting the synchronization properties of neurons that behave as oscillators and are coupled by relatively weak synaptic interactions. In general, type II neurons are synchronized by sufficiently fast synapses (as illustrated in sect. II*A*, Fig. 2*B*), relative to the oscillation period (415, 1000). For a higher frequency rhythm, the period is shorter, and faster synaptic kinetics are required to produce synchrony. Moreover, the stronger the "negative lobe" of the type II PRC, the higher the likelihood for synchrony by mutual excitation. This is why the presence of voltage-gated K^+ currents encourages synchrony by excitatory connections between pyramidal neurons (206). The same qualitative explanation applies to synchronization of slow rhythmic firing of epileptic discharges (characterized by large after-hyperpolarizations) in a disinhibited pyramidal cell population (964, 968, 773).

As shown above, a key insight from theoretical analysis is that to determine network synchrony, interactions between spiking neurons cannot be treated as instantaneous; quantitative synaptic time courses matter a great deal. Furthermore, the required synaptic kinetics is different for different oscillation frequencies. Thus AMPA receptor-mediated glutamatergic transmission, with a decay time constant τ_{syn} in the millisecond range, may be suited for synchronizing slow rhythms at a few Hertz (415, 718). For example, in hippocampal slices, activation of cholinergic muscarinic receptors by carbachol can induce theta frequency oscillation that is independent of synaptic inhibition (965). Experiments and modeling showed that AMPA receptor-mediated excitatory synapses (time constant of a few milliseconds) are sufficient for synchronizing 5- to 10-Hz rhythmic bursting (with a period ~100 ms) in the carbachol induced rhythm in vitro (965). This rhythm, however, is quite different from theta oscillations in behaving animals during spatial navigation, as discussed in section IV*F*.

On the other hand, an excitatory-excitatory mechanism does not seem to be suitable for robustly synchronizing faster rhythms (with a much shorter period of tens of milliseconds), such as gamma (~40 Hz) oscillations. This is the case even when single neurons display intrinsic rhythmic bursting, as shown in a model of coupled chattering cells (28). Thus synaptic excitation mediated by ionotropic glutamate receptors, alone, is likely to be insufficient for generating coherent network oscillations at high frequencies.

B. Inhibitory Interneuronal Network

With slow synapses (comparable to an oscillation period), inhibition rather than excitation generates neural synchrony (415, 1000, 1036, 1037). For type I neurons, even fast excitation does not lead to zero-phase synchrony (415, 275). Indeed, it was found that type I neurons typically show antiphase behavior with excitatory coupling (415, 275, 1035). On the other hand, reciprocal inhibition turned out to be an effective mechanism for neuronal synchrony. This is illustrated in Fig. 2*C*, *right panel*, where the function $H_{odd}(\Phi)$ is shown for a pair of type I model neurons characterized by the PRC given in Fig. 2*C*, *left panel*. With kinetics of $GABA_A$ receptor-mediated synaptic currents (τ_{syn} ~10 ms), the antiphase state is unstable while the zero-phase state is stable; hence, the pair of neurons are perfectly synchronized.

Wang and Buzsaki (1035) found that, in this network model of GABAergic interneurons, spike firing (oscillation) frequency of individual neurons can be varied in a broad range, e.g., by changing the mean external drive or the strength of synaptic interactions among neurons in the network, yet the synchrony is high only in the gamma frequency band (1035). Therefore, networks of inhibitory interneurons provide a mechanism for coherent brain oscillations, particularly gamma rhythm. Whittington, Traub, and collaborators (970, 1053) were the first to report experimentally synchronous ~40 Hz oscillations in rat hippocampus in vitro, when fast excitatory glutamate

synaptic transmissions mediated by AMPA and NMDA receptors were blocked (1053). In the experiment, when metabotropic glutamate receptors were activated pharmacologically, hippocampal slices exhibited oscillatory activity patterns. Oscillatory IPSPs in the 40-Hz frequency range were observed in simultaneously recorded pyramidal cells. These IPSPs presumably originated from the firing activities of GABAergic interneurons. Drugs that slowed down the kinetics of GABA*A* receptor-mediated synaptic currents led to lower oscillation frequency, confirming a model prediction and lending support of an interneuronal network mechanism for gamma oscillations (970, 1035, 1053).

At first sight it seems paradoxical that reciprocal inhibition can bring coupled neurons to fire spikes synchronously, since spiking in one neuron triggers a synaptic current that hyperpolarizes the membrane potentials of target neurons. In fact, "half-center" oscillators consisting of two reciprocally inhibitory neurons (or neural pools) in antiphase represent a standard circuit mechanism for central pattern generators that, by innervating antagonistic sets of muscles, produce rhythmic motor patterns such as walking and swimming (347, 638, 856). As depicted in a classic model (757), consider a pair of neurons endowed with some slow fatigue process and coupled reciprocally by fast synaptic inhibition. At any moment one (neuron 1) is active and effectively suppresses the other (neuron 2). When this inhibition wanes over time and eventually falls below a critical level, for example, due to spike rate adaptation of neuron 1 or short-term depression of synapses, neuron 2 is "released" from inhibition, becomes active, and suppresses neuron 1 in turn. In the "release scenario," coupled inhibitory neurons tend to fire out-of-phase with each other. There is, however, a fundamentally different mode of behavior for coupled inhibitory neurons, called the "escape scenario" (1036). In this scenario, coupled by slower synapses, GABAergic neurons can simultaneously fire action potentials, undergo inhibition together, and "escape" from it synchronously. Whether an inhibitory neural network displays release or escape type behavior depends on the details of active neural properties and synaptic kinetics (638, 882), and a dynamic clamp experiment suggests that the same circuit can be switched from one to the other mode by neuromodulation (866).

It is worth emphasizing again that different synaptic subtypes are suitable for synchronizing circuit rhythms at different frequency ranges. Thus, whereas $GABA_B$ receptor-mediated inhibitory synapses (τ_{syn} ~100 ms) may play a role in synchronizing slow rhythms at a few Hertz, $GABA_A$ receptor-dependent inhibition (τ_{syn} ~5–10 ms) may be adequate for synchronizing fast rhythms in the gamma frequency band. Of course, synaptic currents cannot be too slow relative to the oscillation cycle; otherwise, interactions between neurons would become roughly tonic and phasic information critical for synchronization would be lost (1035, 1049). For type I neurons, synchrony can be realized even with relatively fast inhibitory synapses (275). Synaptic latency (including axonal delay) (123, 621) and rise time (33, 1000, 1049), as well as the decay time, contribute to determining the synchronous firing patterns. These theoretical results are supported by the observation that, during development of the rodent brain, the frequency and synchrony of gamma oscillations reach adult levels in a time course that parallels with that of cellular properties of basket cells and kinetic time constants of their synaptic connections (250, 547).

Just as it is difficult to synchronize an array of clocks with a wide range of intrinsic periods, neural synchrony is more difficult to achieve in the presence of heterogeneity, which introduces a variety of intrinsic oscillation frequencies among individual neurons (539, 1035). This is an important issue because the oscillation frequency of a neuron varies considerably with the input current intensity, with type I neurons typically showing a much wider range of firing frequencies than type II neurons (811, 937). For example, the frequency-current relationship of a fast-spiking interneuron has a slope of ~400 Hz/nA (542, 668, 730). In a "regular spiking" pyramidal cell that displays spike-frequency adaptation, the *f-I* slope is similar (~350 Hz/nA) for the initial spike firing and ~150 Hz/nA in the adapted steady state (650, 730). This implies that a small variation in the net input current leads to a large change in the oscillation frequency. In vivo, excitatory synaptic currents evoked by sensory stimulation were estimated to be in the range of 0.5–1.0 nA in cortical neurons (11, 23, 405). Given such input variations, and the high heterogeneity of both cellular and synaptic properties in interneurons (887), how can synchronous oscillations be maintained robustly? Modeling studies suggest that synchrony can be more robustly realized in spite of heterogeneity when $GABA_A$ receptor-mediated synaptic inhibition is strong (53, 54, 947, 1008). Furthermore, network oscillations may be enhanced by subclasses of specialized neurons with distinct frequency preference due to their resonance or pacemaker biophysical properties (see sect. II). Finally, as we shall see in section V, sparsely synchronized oscillations, characterized by irregular firing of individual cells, are more robust in the presence of heterogeneities.

C. Excitatory-Inhibitory Feedback Loop

Back in the early 1970s, Wilson and Cowan (1060) showed that, in a population firing rate model, network oscillation emerges naturally from reciprocal interactions between excitatory and inhibitory neural pools, under the condition that recurrent connections are strong and inhibition is slower or delayed relative to excitation. Such a model was proposed for gamma oscillations in the olfac-

tory bulb (300, 303) and in the hippocampus (443, 578). The mechanism is easy to understand as follows. An oscillatory cycle begins when fast excitation drives up neural firing in a positive feedback, until slower inhibition is recruited to eventually bring down population activity. As the excitatory drive to interneurons wanes, the network recovers from inhibition and the next cycle starts anew, leading to rhythmic behavior (318, 414, 747, 976, 1028).

In contrast to "rate synchrony" at the level of population activities, "spike-to-spike synchrony" refers to precise phase-locking of spike times among neurons in a network oscillation. In the scenario in which a coherent oscillation is generated among a population of GABAergic cells, pyramidal neurons are presumably synchronized by inhibitory inputs to produce a population rhythm. Consistent with this scenario, an early modeling study by Lytton and Sejnowski found that IPSPs impinging on the somatic region were more effective than EPSPs on dendrites at rhythmically entraining the spike discharges of a pyramidal cell in the gamma frequency band, suggesting that perisoma-targeting basket cells play a role in phase locking pyramidal neurons (616). This idea was supported experimentally by Cobb et al. (177), who showed that in hippocampal slices, spiking activity of pyramidal cells could be entrained with a high temporal precision by a single basket cell. This is demonstrated again recently using optogenetic method to activate a subtype of genetically targeted neurons in the intact brain. Two groups reported that activating channorodopsin-2 (a cation channel) in fast spiking interneurons led to entrainment of pyramidal cells preferentially at gamma frequencies in mouse frontal (885) and somatosensory (155) cortex. When photoactivation was administrated at different frequencies in fast spiking interneurons but not pyramidal cells, the LFP power at the stimulus frequency exhibited a pronounced peak in the gamma frequency band (Fig. 6) (155).

Entrainment involves unidirectional inhibitory-to-excitatory coupling, whereas in the hippocampus (305) and neocortex (85), interneurons and pyramidal cells are reciprocally connected. An alternative to the interneuronal network model is that spike-to-spike synchrony emerges from the interplay between excitatory principal neurons and inhibitory interneurons. In models of interacting excitatory and inhibitory neural oscillators, two regimes were identified (62, 96, 414, 1062). In the first regime, interneurons are sufficiently driven by external inputs and show a phase advance relative to excitatory neurons. The oscillation frequency is comparable to single neuron firing rates. In the other, recurrent excitatory inputs provide a major drive to interneurons, which lag behind excitatory cells but the phase delay is never larger than a quarter of the oscillation cycle ($\pi/2$ radians, or 90 degrees). Although mutual excitation between principal neurons can-

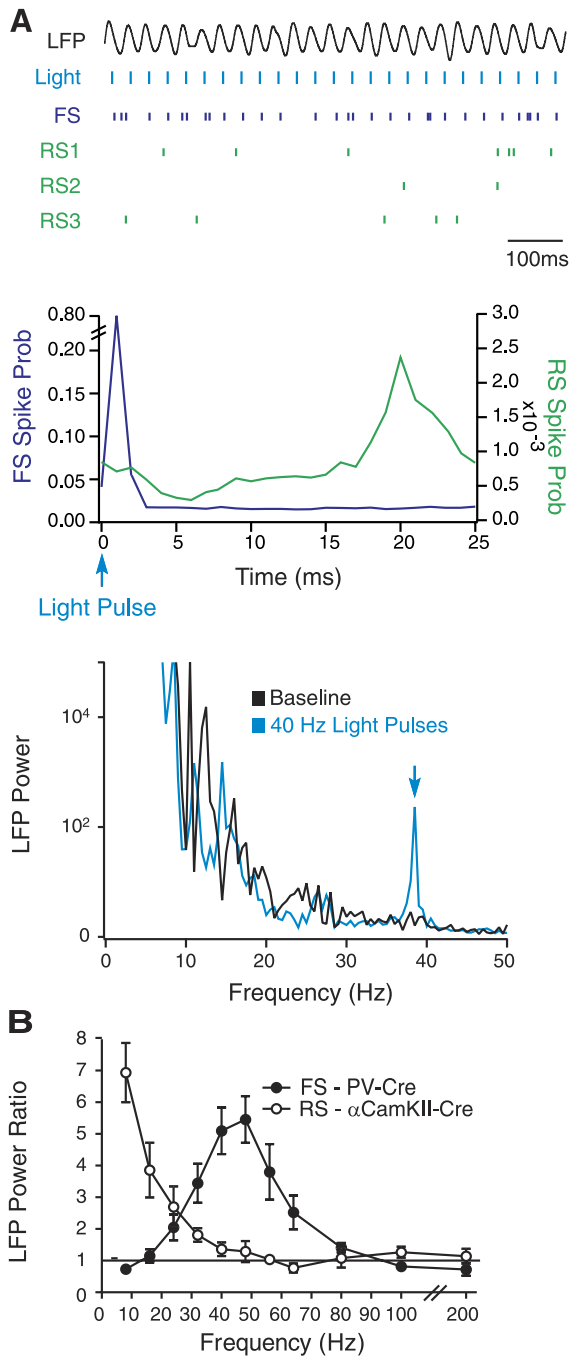

FIG. 6. Entrainment of a cortical network in vivo by optogenetically activating fast spiking interneurons. *A*: spiking activity of neurons in mouse somatosensory cortex in response to channorodopsin-2 activation of FS interneurons by repetitive light pulses at 40 Hz. *Top*: LFP and raster plots of an FS cell (blue) and nearby regular spiking pyramidal cells recorded simultaneously (RS1–3, green). *Middle*: overlay of the FS (blue) and RS (green) spike probability profiles, computed from 17 RS cells and 9 FS cells. Light pulses at 0 ms evoked FS spikes with a delay of 1–2 ms, followed by an increase in RS spiking at 17–24 ms. *Bottom*: power spectrum of LFP in control (black, with a broad profile) and with activation of FS cells by 40-Hz light pulses (blue, with a sharp peak at 40 Hz). *B*: mean LFP power ratio in each frequency band in response to light activation of FS (filled circles) and RS (open circles) cells at those stimulus frequencies. [*A*, *top* and *middle panels*, kindly provided by Jessica Cardin; *A*, *bottom panel*, and *B* from Cardin et al. (155).]

not by itself produce synchrony, it enhances oscillation generated by the feedback inhibition through amplifying excitatory neural population activity. A mathematical analysis found that the second regime is less sensitive to heterogeneity, hence more robust than the first regime (414).

In a local cortical circuit of the intact brain, both the interneuronal network mechanism and the excitatory-inhibitory feedback loop mechanism are present, and one or the other may be more predominant depending on the relative strengths of the two (96, 127, 414, 949). To some extent, these two mechanisms may be redundant to ensure the robustness of a synchronous rhythm. However, they are not likely to behave exactly the same way. For example, synchrony by the excitatory-inhibitory feedback loop mechanism is actually less prominent in the presence, than in the absence, of the inhibitory-to-inhibitory coupling between GABAergic neurons (413, 414, 939). This is because I-to-I coupling reduces the effective time constant of the inhibitory neural population, an accelerated dynamics of interneurons runs counter to a significant delay of feedback inhibition that is required in the excitatory-inhibitory loop scenario for rhythmogenesis (939). More importantly, in cortical circuits where neuronal activity is highly irregular, the interneuronal network and the excitatory-inhibitory loop give rise to synchronous oscillations in different frequency bands, which potentially are predominant in different brain states or serving different functions (see sect. v).

D. Synaptic Filtering

Short-term synaptic plasticity induces temporal filtering of presynaptic inputs, with the characteristic frequency dependence determined by the relative strength and time constants of facilitation and depression (942, 944, 1098). At a synaptic connection exhibiting both facilitation and depression, the release probability of transmitters (hence the synaptic response per presynaptic spike) could be a nonmonotonic function of the presynaptic firing frequency: an increased firing rate induces facilitation leading to a larger release probability; this release probability reaches a maximum at a preferred input frequency, then decreases at higher frequencies where depression becomes dominant (644, 659). This by itself does not constitute a "synaptic resonance," because the synaptic response per unit time, which is the product of the release probability and the presynaptic firing rate, is still a monotonic function of the firing rate. Some synapses in cortical neurons also display a "notch" (a dip) of synaptic response in a narrow range of presynaptic firing frequencies (942). Synaptic filtering may contribute to frequency-dependent neural responses, often in interplay with presynaptic burst firing (296, 466, 659, 696). Its role in synchronous oscillations awaits to be fully elucidated in the future.

E. Slow Negative Feedback

As indicated above, combining fast positive feedback and slow negative feedback offers a general recipe for rhythmogenesis. Delayed negative feedback (359) is a versatile mechanism that can be realized, in diverse forms and on multiple time scales, in neural circuits without synaptic inhibition. A common negative-feedback process at the single-cell level is spike-rate adaptation of pyramidal neurons, originating from depolarization-induced activations of voltage-gated and calcium-gated potassium currents (I_M and I_{KCa}), which in turn reduce the neuronal excitability. In a population of interacting pyramidal cells, such a negative feedback (with a kinetic time constant of ~100 ms) in interplay with fast recurrent synaptic excitation can give rise to network oscillations at ~10 Hz (321, 929, 999, 1029). Another slow negative feedback for generating rhythmic patterns is short-term synaptic depression of recurrent synapses onto excitatory neurons (508, 603, 827, 928, 929, 1029), or short-term facilitation of excitatory synapses onto inhibitory interneurons (675). In these cases, the biophysical time constants of facilitation and depression, ranging from several hundreds of milliseconds to a few seconds, set the scale of network oscillation periodicity.

The ~10-Hz oscillations observed in layer 5 of the neocortex appears to be generated by such a mechanism, in which the positive feedback relies on intrinsic voltage-gated inward currents as well as synaptic excitation, and the negative feedback is independent of the $GABA_A$ receptor-mediated synaptic inhibition (292, 875). The independence from synaptic inhibition was recently confirmed by an in vivo study with anesthetized rats, in which patch-clamp intracellular recording revealed that 10- to 15-Hz membrane oscillations were prominent in layer 5 but not layer 2/3 neurons of the primary visual cortex and that these oscillations disappeared when the voltage of the recorded cell was near 0 mV (the reversal potential of excitatory postsynaptic currents) (924).

A qualitatively similar scenario underlies the generation of slow (<1 Hz) oscillations observed in quiet sleep (190, 195, 553, 610, 679, 776, 779, 839, 905, 912, 915, 916). In this case, negative feedbacks operate on longer time scales (a few seconds) that are mediated by activity-dependent K^+ conductances in single neurons (183, 752, 839) and synaptic depression (68, 190, 440). According to this scenario, the up state is maintained through synaptic interactions between pyramidal cells; this excitation wanes over time due to synaptic depression and/or reduced neural spike discharges, and when it falls below a threshold level, the network undergoes a transition to the

down state, which is quasi-stable with the help of an inwardly rectifying K^+ channel (916). In the down state, neurons are hyperpolarized and largely silent, the activity-dependent negative feedback processes decay away, and the network recovers leading to the onset of the next up state (183). The dynamics of up and down states vary greatly: the up states can be longer than down states (190, 198, 916, 954) or otherwise (911, 912); transitions between up and down states are sometimes nearly periodic (751, 912) but often highly stochastic (198, 225, 553, 916). In an in vitro preparation, slow (<1 Hz) oscillations spontaneously occur in ferret cortical slices that resemble slow oscillations observed in vivo, offering an opportunity to identify its underlying cellular and circuit mechanisms (839). Experiments (841) and computational modeling (183) suggest that the transition from the up state to the down state is induced, at least in part, by the opening of a Na^+-activated K^+ current (I_{KNa}), known to exist in these neurons. Here, the negative feedback is activated by the buildup of the intracelluar Na^+ concentration through sodium spikes, and the recovery is due to the extrusion of Na^+ ions by a Na^+/K^+ pump (operating on a time scale of ~10 s) (1041). A network model (183) of interconnected pyramidal and interneuron populations, endowed with this cellular mechanism, reproduced salient in vivo and in vitro observations, including a gradual increase in the input resistance of pyramidal cells over the course of an up state (190) and a maintained balance between synaptic excitation and inhibition in spite of changes in the firing rate (240, 268, 405, 869). A more recent study showed that the same model exhibits beta and gamma frequency oscillations in the up state similar to those observed in vivo in awake animals. This result is in line with the increasing evidence that up states of slow oscillations during non-REM sleep resemble closely to the activated state of wakefulness in characteristics ranging from EEG or LFP patterns and spatial correlation length, to membrane fluctuations of single cells (234, 239, 830, 831, 914; reviewed in Refs. 240, 404).

F. Electrical Coupling

Electrical synapses are gap junction-mediated connections between neurons. In the mammalian brain, neuronal gap junctions are prevalent during postnatal development and remain present in adulthood at least in certain classes of neurons, such as parvalbumin-expressing GABAergic cells (322, 333, 680). A direct demonstration of gap junctions requires intracellular recording simultaneously from two neurons, by depolarizing or hyperpolarizing one neuron with current injection and measuring the resulting change in the membrane potential of another neuron. Such experiments became possible only recently with the advance of new techniques, like infrared-differential interference contrast optics that allows the experimenter to visually identify recorded neurons. Remarkably, it was found that gap junctions almost exclusively connect GABAergic interneurons within the same class. For example, perisomatic-targeting, parvalbumin-expressing FS cells are connected among themselves by gap junctions; so are dendrite-targeting, somatostatin-expressing LTS cells, but electrical synapses are rare between mixed-type (FS-LTS) cell pairs (331, 350). So far, at least five such distinct networks of electrically coupled GABAergic interneurons have been identified (for a review, see Ref. 434).

Compared with chemical synapses, electrical coupling has properties that seem especially desirable for subserving neural synchronization: it is fast and usually bidirectional (at least between neurons of the same type) and acts to equalize the membrane potentials of the connected neurons. This mechanism of intrapopulation coordination may be especially important for some cell types, such as LTS interneurons which exhibit a paucity of inhibitory synapses among themselves (350). Electrical synapses have been suggested to promote oscillatory activity (331, 350) and contribute to coincidence detection in inhibitory neurons (332). Computational modeling studies generally found that sufficiently strong electrical synapses encourage synchrony (175, 351, 631, 767, 927, 966, 971), but can also have desynchronizing effects depending on the interplay with inhibitory synapses and the intrinsic membrane properties of the constituent cells (729, 767, 867). A pair of FS interneurons or LTS neurons coupled by gap junctions showed similar phase-locking behavior, despite their differences in the biophysical properties. Interestingly, FS and LTS neurons are synchronized preferentially in the gamma and beta frequency bands, respectively (631). It should be noted that in the cortex gap junctions are restricted to neighboring neurons, within 50 μm (351). Therefore, electrical coupling is spatially very localized, like diffusion in physical and chemical systems.

To experimentally assess the role of electrical synapses in brain rhythms, one must be able to induce a disruption of gap junction communications and examine its impact on a network oscillation. Presently, there are no drugs that block gap junctions with a high degree of selectivity, but genetic manipulations have proven a powerful tool. Connexin 36 is the predominant gap junction protein expressed in neurons of the mammalian brain (186). Both in vitro (442) and in vivo (131) studies showed that in mice, connexin 36 knockout only produced a reduction of the field potential gamma power (or the degree of network synchronization), without affecting the oscillation frequency. Given that electrical synapses are much faster than chemical synapses, they may be especially important for synchronizing the ultrafast (100–200 Hz) sharp wave ripples. An in vitro experiment supports a critical involvement of gap junctions in the generation of sharp wave ripples (256). Electrical coupling between

Purkinje cells, provided that it is sufficiently strong, has also been proposed as a mechanism for sustaining ultrafast oscillations in the cerebellum (622, 681). On the other hand, connexin 36 knockout had no effect on ultrafast (>100 Hz) field ripple oscillations in mice in vitro (442) or in vivo (131). Traub and colleagues (211, 409, 849, 967, 971) proposed that other connexin subtypes, forming electrical synapses between the axons of excitatory cells, underlie fast oscillations in the hippocampus. This idea arose from a network model in which single neurons were described with elaborated dendritic and axonal arbors (971), which is rarely done in theoretical studies of large-scale cortical networks. Unlike gap junctions at the dendrite, those located between axons make it possible for a spike in one neuron to directly trigger a spike in another neuron, which was found to be necessary to generate ultrafast oscillations in a sparsely connected model network (971). Other modeling studies suggest that chemical synapses may be sufficient to generate >100 Hz fast oscillations in an interneuronal network (125, 127, 222, 342) (see sect. V).

G. Correlation-Induced Stochastic Synchrony

Mechanisms for synchronizing neurons discussed above rely on oscillatory synaptic inputs, which are produced in a recurrent network. Synchronization between neural oscillators can also be realized by shared but random inputs in a network where neurons do not directly interact with each other (329, 330, 714, 770, 898, 940). In this scenario, common (correlated) noise gives rise to phase synchronization of otherwise uncoupled oscillators, when two conditions are satisfied (329). First, single neurons are intrinsic oscillators with roughly the same frequency. For this to be realized in spite of input heterogeneity, this scenario is better suited and more robust for type II cells (which display a relatively flat current-frequency curve, Refs. 811, 937) than for type I cells (which display a steep current-frequency curve, Refs. 639, 658, 1035). Second, neurons receive partially correlated fluctuating synaptic inputs that can be broad-band (i.e., they do not have to be rhythmic) but should be fast relative to the period of the intrinsic neuronal oscillation. Under these conditions, brief (compared with the intrinsic oscillation period) and correlated fluctuations in the inputs act as a common pulse to reset the oscillation phases of neurons in a network. This can be understood by considering a population of uncoupled neural oscillators, which is initially asynchronous. This means that spike times of neurons are uniformly distributed on the oscillation cycle. The response of each neuron to a common pulse is given by the phase response curve (which may be type I or type II) (see sect. II*A*). This brief input would speed up those that fire later than the others, and would either slow down (for type II cells) or not significantly alter (for type I cells) the spiking phase of those cells that are "ahead," thereby leading to population synchrony (281). As expected intuitively, an intermediate level of noise is optimal: too little noise would not be sufficient to induce phase synchronization, whereas too much noise would overwhelm and destroy intrinsic neuronal oscillations.

Synchronous fast oscillations are prominent in the olfactory system and play a major role in odor stimulus processing (79, 117, 161, 303, 308, 441, 461, 501, 503, 555, 556, 584, 847, 1043). Numerous studies have shown that coherent rhythmicity in the rat olfactory bulb depends on the reciprocal, dendrodendritic synaptic interactions between excitatory principal mitral cells and inhibitory granule interneurons (218, 544, 545, 700, 734, 791), with possibly additional contribution of electrical coupling (306, 683). Many models for gamma oscillations in the olfactory bulb are based on a feedback inhibition mechanism (61, 66, 67, 109, 303, 584). Galán et al. (329) noted, however, that so far there is no direct proof that inhibitory synaptic potentials are synchronized in mitral cells. They proposed to apply the scenario of correlation-induced stochastic synchrony to the olfactory bulb, where shared noisy synaptic inputs could synchronize mitral neurons endowed with subthreshold oscillations (their membrane oscillation frequency as well as spiking rate are in the gamma band and relatively insensitive to input strength; Fig. 4*C*) (48, 231, 640). What are the sources of common synaptic noise and, more generally, whether this scenario or the excitatory-inhibitory loop scenario is responsible for the rhythmogenesis in the olfactory bulb, remain to be determined in future experiments.

In summary, two-way interactions between theory and experimentation have proven extremely fruitful in uncovering fundamental processes through which neural networks (cortical circuits in particular) are synchronized. Mutual excitation between principal cells, in conjunction with some negative feedback process other than synaptic inhibition, is suitable for generating certain forms of slow oscillations. On the other hand, mutual inhibition between interneurons and reciprocal loop between excitatory and inhibitory cells provide two general mechanisms for rhythmogenesis, especially fast cortical oscillations. In addition, gap junctions contribute to population synchrony. Finally, correlated noise may also lead to spike-to-spike synchrony of otherwise uncoupled neural oscillators. These diverse core mechanisms may be deployed differentially, or in any combinations, in different cortical circuits.

IV. NETWORK ARCHITECTURE

Studies of a couple of neurons have yielded valuable information about the synchronization mechanisms (see

sect. III). To go beyond neural pairs toward predicting the behavior of large populations of neurons, a key step is to have a firm grasp of how network connectivity properties sculpt activity patterns. Recent advances in neural anatomy and imaging have opened a new era of experimental studies of detailed "wiring diagrams" of a functional circuit (173, 586, 860). In computational studies of synchronous oscillations, different types of network architectures have been considered, which will be reviewed below.

A. All-to-All Networks: Synchrony, Asynchrony, and Clustering

Some basic insights into neural synchronization were obtained in studies of models where neurons are coupled globally (every neuron is connected to every other neuron). When perfect (zero phase) synchrony is predicted for a pair of neurons, the same often holds true for an all-to-tall network. For example, Figure 7*A* shows synchronous gamma oscillations of a population of type I neurons coupled globally by synaptic inhibition, with the behavior of a pair of the same neurons described in Figure 2*C*. On the other hand, when a pair of neurons display phase shift relative to each other, the activity pattern of an all-to-all coupled population of such neurons could be totally asynchronous or exhibit a variety of complex patterns. Perhaps the most commonly observed pattern is clustering, where a network breaks into a small number of fixed clusters of neurons (5, 53, 366, 367, 413, 526, 1035, 1040, 1049). Neurons within a cluster fire together, and different clusters take turns to fire over time; hence, single neurons fire intermittently (only once in a few oscillation cycle). The network frequency is equal to the number of clusters times the firing frequency of single cells. In a clustering state, single cells still discharge spikes in a fairly regular fashion. Moreover, clustering states usually occur in a restricted range of noise (126).

B. Sparse Random Networks

In local cortical circuits, synaptic connections are sparse (892, 902); the probability for a pair of pyramidal cells to be connected in either direction is ~0.1–0.2 (573, 892). Coherent oscillations require a minimum connectedness. Consider a network in which any neuron makes synaptic contacts on average with M_{syn} neurons. Modeling work revealed that, in a randomly connected interneuronal network model, synchrony depends on M_{syn} in a highly nonlinear fashion. Obviously, if M_{syn} is zero, then neurons are not connected to each other and fire independently. It turns out that if M_{syn} is below a threshold M_{thr}, the network remains completely asynchronous. Coherent oscillation emerges as a qualitatively new type of collective network behavior when M_{syn} is above M_{thr} (Fig. 7B). Importantly, this threshold does not depend on the network size; thus small and very large networks can have the same threshold connectedness for synchrony. Intuitively, synchronization requires a sufficient amount of network connectedness, e.g., there should be a large connected neural cluster of rougly the same size as the entire network. For random graphs, this only requires that the number of links per node be larger than a threshold value, independent of the network size (12, 273). Interestingly, synchronization of a neural rhythm also depends on the biophysics of synaptic interactions and intrinsic cellular dynamics. This is strikingly demonstrated in a network model of mutually inhibitory neurons where, given similar synaptic coupling time constants, the threshold connectedness M_{thr} is ~50 with conductance-based Hodgkin-Huxley type (type I) model interneurons (1035), but is several thousands with "leaky integrate-and-fire" (LIF) model neurons (366). By comparison, In the hippocampus CA1, the axon arbor of a single basket cell contacts, on average, ~60 other basket neurons within a spatial span of ~500 μm (874). Hence, a model with Hodgkin-Huxley type neurons but not LIF neurons would predict that gamma synchrony can be realized with realistic sparse connectivity in a population of fast spiking interneurons. These findings underscored the importance of detailed physiological properties of single neurons in determining collective network behavior. The conclusion about the small minimum number of synapses per neuron required for synchrony in a random network also holds for two population models of excitatory and inhibitory neurons (96, 1040).

C. Complex Networks

Connectivity in a local cortical network is not completely random (149, 554, 699, 892). In particular, synaptic connections depend on the spatial distance between connected neurons, which can greatly affect global synchrony (63), or generate propagating waves (see sect. IV*D*).

Consider, again, a population of mutually inhibitory interneurons. Even if interneurons and their connections are distributed homogeneously, high-density local connectivity alone may not give rise to global coherence in large networks. The reason is that with an increasing network size, the average "path length" (the minimum distance between two neurons through intermediate connected neurons) and the associated synaptic delays become excessively high. As suggested by Watts and Strogatz (1042), however, the path length can be dramatically decreased by a few randomly placed "short-cuts" that connect distant parts of the network. Can a small number of "long-range" interneurons serve this exact role? To assess this possibility, we simulated

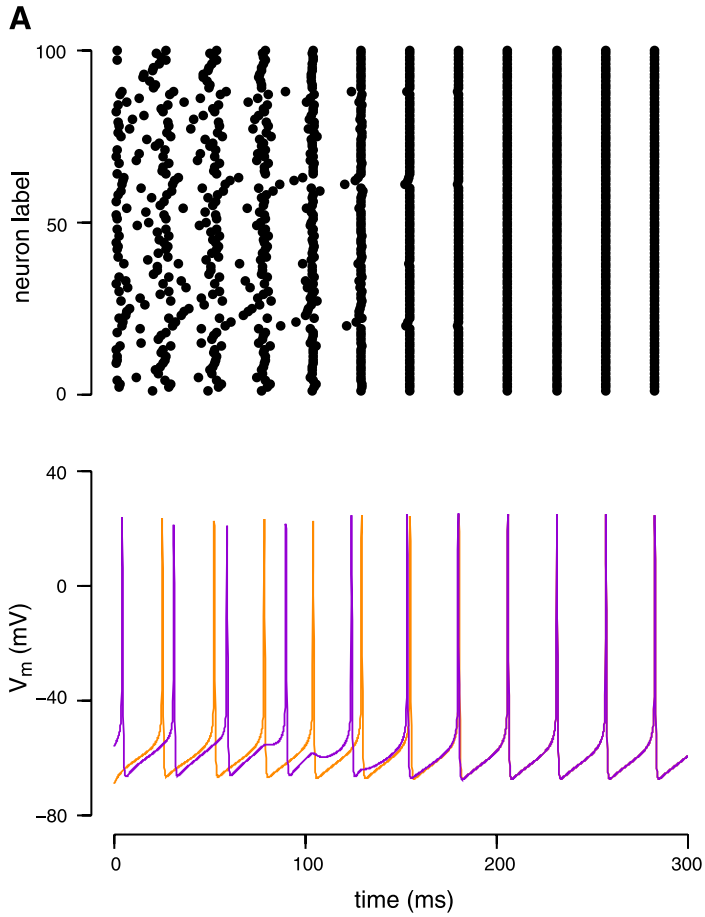

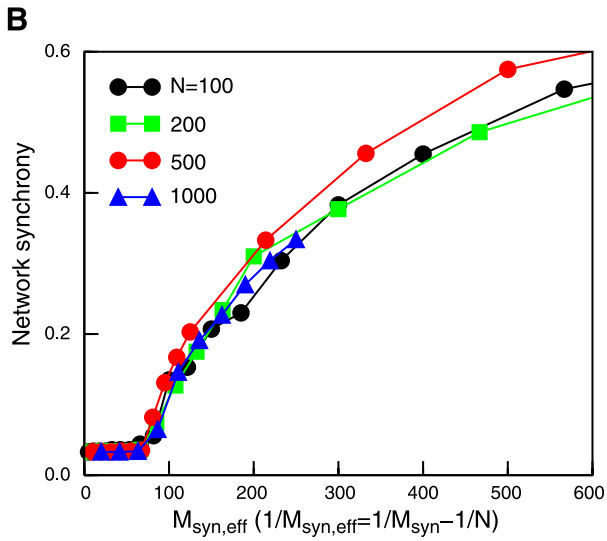

FIG. 7. Synchronization in an inhibitory interneuronal network. *A*: an example of network synchronization in a fully connected network of type I conductance-based neurons. *Top*: rastergram where each row of dots represents spikes discharged by one of the neurons in the network. *Bottom*: membrane potentials of two neurons. Neurons initially fire asynchronized, but quickly become perfectly synchronized by mutual inhibition. *B*: in a random network, the network coherence is plotted versus the mean number of recurrent synapses per cell M_{syn}. [The correction term ($\sim 1/N$) takes into account the finite network size effect.] Different curves correspond to different network size (N = 100, 200, 500, 1,000). There is a critical threshold for the connectedness above which network synchrony occurs. This threshold connectivity is independent of the network size. [Adapted from Buzsáki (142) and Wang and Buzsáki (1035).]

a network model of 4,000 inhibitory cells (149), which corresponds to approximately all basket cells in the dorsal hippocampus of the rat (304). We considered how rewiring from local to long-range connections affects the synchronization behavior of the network. With a local architecture, the connection probability between two neurons decreases with their distance, according to a Gaussian distribution. When the Gaussian distribution is narrow (characteristic range ~20 neurons), the network is asynchronous and the population firing rate is essentially constant in time (Fig. 8*A*). Next, while fixing the average number of connections per neuron, a fraction p of the existing connections are rewired according to a probability that falls off as an

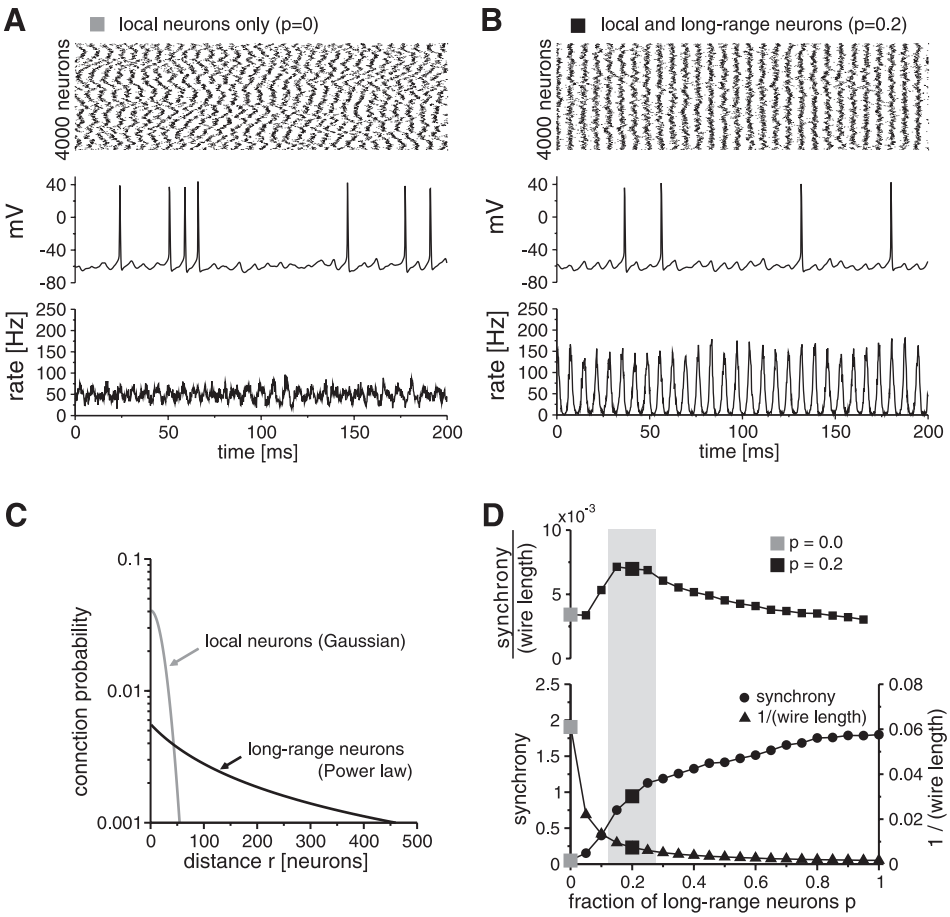

FIG. 8. Trade-off between synchronization by long-range connections and minimization of the network wire cost. *A*: oscillations in a network of interneurons coupled by inhibitory synapses, with local (Gaussian) connectivity (spatial length is 20 neurons, in a network of 4,000 neurons). The network is essentially asynchronous. *Top panel*: spike raster of sample neurons. *Middle panel*: the voltage trace of a representative neuron. *Bottom panel*: population firing rate. *B*: oscillations in a network with local and long-range connections. Neurons are connected with Gaussian distributed synapses (as in *A*), but $p = 25\%$ of the synapses are reconnected with a power law distribution. Note strong oscillatory rhythm. *C*: illustration of the connectivity probability functions: the Gaussian distributed connections are local (gray line), whereas long-range connections are described by a power distribution (black line). *D*: with increasing reconnection probability p from the local Gaussian distribution to the power distribution, the network synchrony increases while the inverse of the wire length of connections decreases. High synchrony at a low wire cost corresponds to an optimal range of p values (a small ratio of long-range and short-range connections, shaded region). [From Buzsáki (142).]

inverse power law with the distance. The power distribution makes it much more likely to have long-range connections than a Gaussian or exponential distribution (Fig. 8*C*). The network synchrony becomes significant with $p > 0.1$ (Fig. 8*D*). As illustrated in Figure 8*B*, the network with $p = 0.25$ exhibits highly synchronous network oscillations at 150 Hz, in the frequency range of sharp wave ripples (100–200 Hz). Therefore, wide-range network synchrony could be achieved with a small fraction of the local connectivity removed and replaced by long-range connections. In fact, increasing p above 0.4 only enhances the network synchrony modestly. On the other hand, the "wire length" of the network (the total length of interneuronal connections) obviously increases with p (Fig. 8*D*). Therefore, there is a trade-off between the need of long-range connections for network synchronization, and minimizing the cost for these long-range wires (Fig. 8*D*). Hence, an optimal design for network synchronization with a minimal wire-cost can be achieved by a division of labor between a large subpopulation of short-range interneurons and a small subpopulation of long-range interneuron cells in the hippocampus. Another modeling study also found that spiking coherence between neural pairs could be maximal with such small-world network topology (510).

Complex networks have been the subject of active research in recent years (12, 1042), and various types of network connectivity schemes have begun to be applied to neuroscience: small-world networks (with predominantly local connections and rare long-distance connections) (149, 546, 806, 823, 1085), networks endowed with "hubs" (a few nodes with an unusually large number of connections with the rest of the network) (699) or a community structure (721), and networks with dynamic motifs (elementary building blocks from which more complex dynamic behavior can be assembled) (464, 1095). For example, even a few percent of neurons with an exceptionally large number of connections ("hubs") can dramatically alter a circuit's dynamical behavior (699).

The proposal of GABAergic "hub neurons" has gained some empirical support from a recent work (94). Monitoring multiple neurons by calcium imaging of spontaneous activity and assessing functional connectivity by pairwise correlation analysis of the observed calcium activity, Bonifazi et al. (94) found that hippocampal CA3 networks in the developing rats and

mice exhibit a scale-free topology. The distribution of the number of output links per neuron decays as a power law, with an exponent of ~1.2, and "hub neurons" (defined as the top 40% highest connected) are a subpopulation of GABAergic cells with widespread axonal arbors. Stimulation of hub neurons, but not those with low connectivity, affected synchronous network dynamics, demonstrating the functional importance of these hub neurons (94).

The simple models discussed above were designed for a local area; in a large-scale cortical network, the spatial structure of coherent oscillations is likely to be much more complex. In awake states, the correlation between LFPs decays with the distance between the recording electrodes, with a characteristic spatial length of ~3–5 mm within a cortical area (134, 238). On the other hand, long-distance synchronization among selective neural populations in disparate cortical regions has been reported during cognitive tasks (see sect. VI). A future challenge is to elucidate the wiring topology and statistics that underlie brain-wide synchronization.

D. Spatially Structured Networks: Propagating Waves

Sensory processing, decision making, and motor action all engage selective neural populations. Localized neural activity either remains spatially confined in time or propagates as a wave among neural pools that are spatially separated but engaged in the same computation or behavioral state. Wave propagation has been observed on multiple spatial scales. MEG studies of human subjects revealed gamma oscillatory episodes that started in the frontal cortex and propagated front-to-back across the cortical surface (Fig. 9*A*) (598, 804). Slow sleep oscillations measured with high-density EEG recordings also appear to start in the frontal cortex and travel in an antero-posterior direction (652, 654); slow waves primarily involve areas in the prefrontal cortex (214, 709) that overlap with the default network in the human resting state (393). In alert monkeys performing an instructed delayed reaching task, LFP beta oscillations, evoked by the instruction cue in the motor and premotor cortical areas, are not synchronous globally but propagate as waves whose latencies and amplitudes provide information about the visual target to be reached (828). In vivo multielectrode EEG recording or voltage-sensitive dye imaging has also revealed stimulus-induced waves in the olfactory bulb (264, 301, 743), turtle visual cortex (781), and rat somatosensory cortex (761). Numerous studies have also demonstrated wave propagation of evoked responses in cortical slices in vitro (189, 935, 1076, 1079) (for movie demos, see http://www9.georgetown.edu/faculty/wuj/propagationwave.html). Wave propagation naturally occurs because connections between neurons are spatially confined. Within a cortical area, the probability of synaptic contact decreases with the physical distance between a pair of neurons for both excitatory pyramidal cells and inhibitory interneurons (353, 874, 902). Therefore, spiking activity spreads from a group of neurons to its neighbors and onto the rest of the network as a propagating wave. Wave propagation can also take place in an electrically coupled neural network, when the distance dependence of electrical coupling is taken into account (581), just as expected for "excitable media," diffusion-coupled spatially extended chemical or biological systems (710).

A key characteristic of brain waves is propagation speed (282). A "wavefront" is an activity packet that sweeps across a network, such as a brief burst of spikes, a response evoked by sensory stimulus, or the event of switching from an inactive (down) state to an active (up) state. For a wavefront, the propagation speed is determined by cellular and synaptic properties that control the surge of activity, but not what happens afterwards such as the slow afterhyperpolarization (278, 282, 459, 815). In vivo (using anesthetized animals) (115, 383, 410, 762) and in vitro (839, 1075) studies estimated propagation speeds to be on the order of ~10 mm/s in the rodent cortex. A similar wave speed was observed in a human study of binocular rivalry. As a subject experienced an alternation from one to another perceived pattern, functional brain imaging showed that the dominance of the new pattern emerged locally and propagated like a wave as it rendered the old pattern invisible (572). Much faster propagating waves, at ~100 mm/s, have been reported in ferret piriform cortex (840), in rodent cortex (using voltage-sensitive dye imaging) in vivo (Fig. 9*B*) (1079) and in vitro (74, 189), and in the motor cortex of behaving monkeys (828). Wave speed appears to be sensitive to modest changes of synaptic inhibition that sculpts cortical local circuits, as it is known that ~10–20% suppression of $GABA_A$ receptor-mediated inhibition can increase wave speed by 10-fold (162, 172, 183, 448, 839). Moreover, the inclusion of a small amount of long-distance connections, in addition to predominantly local connections, reminiscent of "small-world" type architecture with a mixture of mostly local and sparsely long-distance connections (see sect. IV*C*), significantly increases the signal propagation speed (183).

In contrast to smooth wavefront propagation, another "lurching" type of wave propagates in a discontinuous manner (170, 368, 812). Imagine a spatially structured inhibitory circuit of GABAergic neurons that are endowed with a "postinhibitory rebound" property (spike discharges triggered by a long-lasting hyperpolarization) (47, 196, 597, 908, 1026, 1039). A group of cells fire a burst of spikes, inhibiting for a period of time their neighboring cells. The latter, when synaptic inhibition has waned,

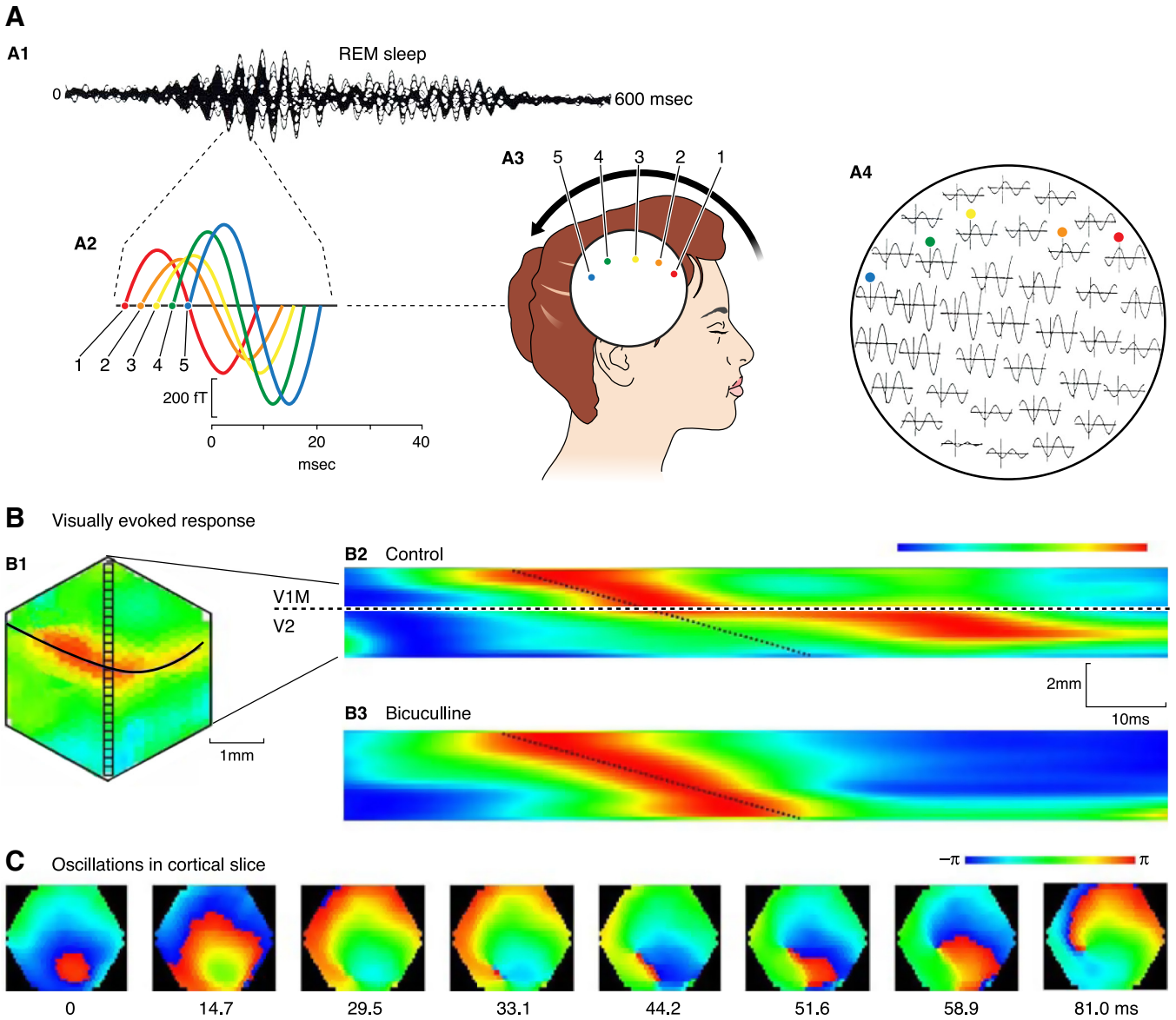

FIG. 9. Propagating waves. *A*: rostrocaudal phase shift of 40-Hz oscillation during rapid eye movement (REM) sleep as measured using MEG. *A1* shows synchronous activation in 37 channels during a 600-ms period. The oscillation in the left part of *trace A1* has been expanded in *trace A2* to show five different recording sites over the head. The five recording sites of *trace A2* are displayed in *diagram A3* for a single epoch, to illustrate the phase shift for the different 40-Hz waves during REM sleep. The direction of the phase shift is illustrated by an arrow above *diagram A3*. The actual traces and their sites of recordings for a single epoch are shown in *diagram A4* for all 37 channels (ft, femtotesla). *B*: voltage-sensitive dye imaging of propagating waves in rat visual cortex in vivo. A rat visual cortex was imaged through a cranial window. *B1*: a snapshot of visually evoked cortical activity propagating through the border of V1 and V2 areas. *B2*: a spatial-temporal map made from one row of optical detectors (small boxes in *B1*) showing the time course of wave propagation. A visual stimulation to the eye evoked an activity in area V1 and propagated to V2. The map starts at 108 ms post stimulus. The propagating velocity in both V1 and V2 is ~100 mm/s (the oblique broken line marks the velocity of 100 mm/s). Propagating velocity is greatly reduced at the border between V1-V2 areas (marked by a horizontal broken line). *B3*: when the cortical inhibition is slightly suppressed by GABAergic antagonist bicuculline, the slowing down at the V1/V2 border is completely eliminated. *C*: propagating waves during carbachol induced ~10 Hz oscillations in a brain slice cut from rat visual cortex (tangential section). Images are the phase map during the oscillation. From *left*: at the beginning of an oscillation cycle, a propagating wave is started from a small region (red area at image of 0 ms) and propagating outward as a ring wave. The ring wave breaks and generates two phase singularities (at 33.1 ms). One of them further develops into a rotating spiral (after 58.9 ms). The spiral wave further sustains for ~1,000 ms (~10 more rotations, images not shown). [*A* modified from Llinás and Ribary (598); *B* from Xu et al. (1079); *C* from Huang et al. (448).]

escape from it and discharge in turn, leading to another episode of activity that lurches forward across the neural population. Because the network is silent during periods when synaptic inhibition is strong, the activity pattern is discontinuous in a lurching wave. Lurching waves may also take place in an excitatory network, provided that synaptic transmission has a sufficiently long latency (113, 365).

Wave fronts should be distinguished from traveling waves, in which neurons fire rhythmically and the oscillation phase ϕ varies as a function of time and spatial location (279). For a plane wave, the phase is linear with the spatial position x and time t, like $\phi = 2\pi[ft - (f/v)x]$, where f is the oscillation frequency, v is the propagation velocity, and $\lambda = v/f$ is the wavelength. In two- or three-dimensional nerve tissues, more complex waves such as spiral wave (Fig. 9*C*) can take place (448, 508, 686). Traveling waves have been observed in a number of studies (reviewed in Refs. 279, 1076), including MEG gamma oscillations (804), EEG slow sleep oscillations (652), evoked responses in the cortex (32, 302, 781), and hippocampal theta oscillations (609). Traveling waves during theta oscillations in CA1 propagate along the septotemporal axis of the hippocampus, with $v \sim 80–100$ mm/s and $\lambda \sim 10–15$ mm. Given that the length of the septotemporal axis of CA1 is $L \sim 10$ mm, the total phase difference is L/λ, between 240 and 360 degrees, i.e., two-thirds to a full theta cycle (609). Interestingly, in all existing studies, the total phase shift is often $\sim\pi/2$, never larger than 2π. In other words, the observed spatial variation in peak amplitude is less than the full oscillation cycle, regardless of oscillation frequency (e.g., theta or gamma), the physical size of the neural system, or species examined (279). Modeling studies showed that a phase wave depends on the spatial extent and connectivity delay (including the axonal delay and synaptic latency). In the same model, a gradual increase in the connection delay can lead to an abrupt transition from global synchronous oscillation (when delays are short) to phase waves (when delays are long) (205).

E. Interaction Between Diverse Cell Types

So far I have discussed networks consisting of either one neural population or two (excitatory and inhibitory) neural populations. However, neural circuits in the cerebral cortex are more complex. In particular, given the wide diversity of inhibitory cell subtypes (305, 645), what are their relative roles in rhythmogenesis? In this regard, the best studied case is theta and gamma rhythms in the hippocampus. Early pioneering in vivo studies found that, in the rat hippocampus, putative pyramidal cells (p) show overall maximal firing rate close to the trough of the LFP theta (recorded in the pyramidal layer of CA1), and fast-spiking interneurons in the pyramidal layer [int(p)] preceded pyramidal cells by $\sim 60°$ (208, 209). In vitro and modeling studies suggested that different interneurons play differential roles in theta oscillations (89, 354, 821). More recently, using juxtacellular recording that allowed investigators to identify the cell type of the recorded neuron, Somogyi, Klausberger, and collaborators were able to characterize theta phase preferences of diverse hippocampal interneurons in vivo of rats under urethane anesthesia (Fig. 10*A*) (511–514, 889). Interestingly, two types of phase relationships were observed. Basket and axon-axonic interneurons, which control the spiking output of pyramidal cells, are roughly out of phase with the pyramidal cells, whereas bistratified and oriens-lacunosum-moleculare (O-LM) interneurons, which gate synaptic inputs to pyramidal dendrites, are approximately in phase with the pyramidal cells. More precisely, maximal firing occurred at 20° for pyramidal cells, 271° for parvalbumin basket cells, 185° for axo-axonic cells, 1° for bistratified cells, and 19° for O-LM cells (0° is at the trough). Phase relationships between several cell types during hippocampal theta have been analyzed in modeling studies (341, 406, 744) but remain only partially understood. Note that the phase difference between fast spiking neurons and pyramidal cells appears to be much smaller in the awake than anesthetized condition; therefore, the phase relationships between different cell types depend on the animal's behavioral state.

The juxtacellular recording technique applied to gamma rhythm revealed that, in CA1, dendrite-targeting bistratified cells (rather than perisoma-targeting basket cells) exhibited the strongest modulation by field oscillations (511, 982). This does not necessarily imply, however, that bistratified cells play a more important role than basket cells in the rhythmogenesis. One reason is that neural activity in CA1 might reflect oscillatory inputs from CA3 as a "source area" for gamma rhythm (209, 291). In cholinergically induced gamma oscillations in CA3 slices, basket and axo-axonal cells were found to display the largest rhythmic modulation among diverse interneurons (408). Moreover, spike firing of these interneuron subtypes and pyramidal cells displayed different preferred phases of the gamma cycle (407, 408) (Fig. 10*B*). These phase relationships provide clues with unprecedented detail about the organization and temporal dynamics of the underlying complex circuit.

F. Interaction Across Multiple Network Modules

Whereas local circuits are capable of generating gamma oscillations (35, 53, 104, 209, 291, 632), the mechanism of the hippocampal theta rhythm appears to involve larger systems. Lesioning the fornix-fimbria abolished hippocampal theta, while rhythmic firings persisted in septal cells (22, 763, 1012), leading to the hypothesis that the hippocampal theta rhythm depends on the afferent inputs from the medial septum (87, 918, 1006). The medial septum supplies acetylcholine to the hippocampus; this modulation of excitability is believed to be important for

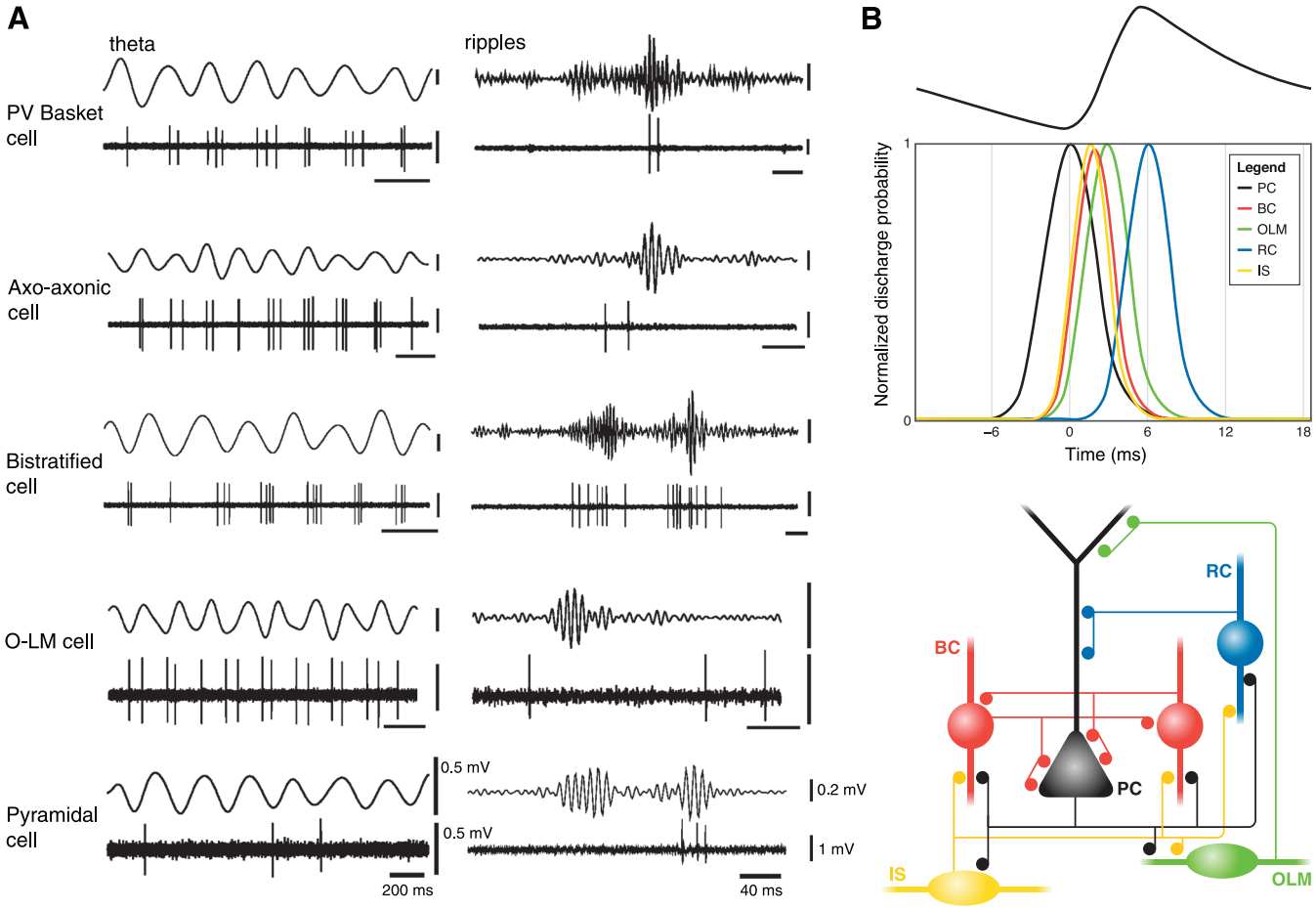

FIG. 10. Complex circuit dynamics in multiple neuron types during synchronous oscillations. *A*: behavior of four (basket, axo-axonic, bistratified, oriens-lacunosum-moleculare) subclasses of inhibitory interneurons and pyramidal cells during theta rhythm (*left*) and sharp-wave ripples (*right*) recorded in vivo from the hippocampus of anesthetized rats. In each panel are plotted LFP (*top*) and juxtacellularly recorded spike train of an identified cell (*bottom*). During theta oscillations, while basket and axo-axonic cells (which control the output of pyramidal neurons) tend to fire at the peak, bistratified and O-LM cells (which control the inputs to pyramidal cells) as well as pyramidal cells tend to fire at the trough, of field theta. Note also intermittent firing characteristic of pyramidal neurons in both theta rhythm and fast ripples. *B*: behavior of several subtypes of interneurons [basket/axo-axonal cells, interneurons targeting proximate dendrites in the stratium radiatum (RC), interneuron-targeting cells (IS), interneurons in the stratum oriens projecting to the distal dendrites in the stratum lacunosum-moleculare (OLM)] and pyramidal cells during gamma oscillations induced by cholinergic activation in rat hippocampal slices in vitro. Note that pyramidal cells fire maximally at the trough of the local field oscillation, and ahead of interneurons (*left*). [*A* modified from Somogyi and Klausberger (889), kindly provided by Drs. Thomas Klausberger and Peter Somogyi; *B* from Hájos et al. (408).]

promoting theta rhythm in the hippocampus (141). In in vitro hippocampal slices, cholinergic activation alone, e.g., by the muscarinic receptor agonist carbachol, can induce oscillations at theta frequency (290, 618, 965). This rhythmic phenomenon in vitro differs from theta rhythm in vivo in that it is independent of GABAergic synaptic transmission (618, 965) and becomes similar to epileptic discharges with a high dose of carbachol (1057). Pyramidal cells fire bursts of spikes regularly in carbachol induced theta in vitro (965), whereas they fire sparsely in behaving animals (208). Interestingly, a recent study (370) found that the intact isolated hippocampus in toto (but not 500-μm-thick slices) displayed spontaneous, atropine (a muscarinic receptor antagonist)-resistant, theta (~5 Hz) oscillations, while pyramidal cells fired spikes sparsely (<0.5 Hz). This self-generated theta appeared to originate in CA1; there are multiple theta oscillators along the septotemporal axis in CA1, with faster oscillators entraining slower ones. The circuit mechanism of this in vitro theta rhythm, possibly involving specific type(s) of GABAergic cells (1050), remains to be elucidated in future experiments. Thus, under certain conditions, theta frequency oscillations could emerge within the hippocampal circuit. The fact remains, however, that in vivo the medial septum is necessary for generating theta oscillations in the hippocampus and entorhinal cortex. Perhaps the propensity of hippocampal networks to oscillate at theta frequency reflects a resonance mechanism (see sect. II*B*) rather than theta rhythmogenesis itself. Indeed, hippocampal pyramidal cells show maximal subthreshold membrane potential changes (resonance) as well as firing preference to sinusoidal inputs in the theta frequency range (577, 769).

Interestingly, theta oscillation observed in anesthetized animals is blocked by atropine, but theta oscillation associated with free movements in behaving animals is insensitive to atropine (hence independent of muscarinic activation) (531, 918, 1002). If movement-related theta is atropine resistant, precisely how does it depend on the medial septum? As mentioned in section II*C*, medial septum contains two major types of neurons (105, 384), which are thought to play distinct roles in theta rhythm generation: cholinergic cells acting via muscarinic receptors modulate slowly the excitability of hippocampal neurons (180, 326), whereas GABAergic cells play a role of pacemakers via fast $GABA_A$ receptor-mediated synaptic transmission (918), by selectively innervating GABAergic interneurons but not pyramidal cells in the hippocampus (304). Septal GABAergic cells display rhythmic firing at theta frequency in vivo (99, 255, 340, 509, 1005), are endowed with a significant H-current thus likely to display resonance in the theta frequency range (635, 1005), and display a temporal lead over the hippocampal local field theta oscillation (412). It has therefore been hypothesized that septal GABAergic afferents impose theta rhythmicity upon GABAergic cells in the hippocampus (304), that in turn phasically pace spike firing of pyramidal neurons (963, 1083). This scenario was supported by several lines of evidence. First, when cholinergic neurons (but not GABAergic neurons) in the medial septum were chemically damaged, the frequency of hippocampal theta was found to remain unchanged, but the power was dramatically reduced (29, 571), consistent with the view that cholinergic cells contribute to theta rhythm by providing a tonic drive to the hippocampus. Second, $GABA_A$ receptors in septal GABAergic cells but not cholinergic cells contain α_1-subunit (334), and zolpidem (a preferential $GABA_A$ α_1-subunit modulator) suppressed theta oscillation both in the hippocampus and septum (990). Third, local injection of $GABA_A$ receptor antagonist in the medial septum eliminated theta rhythmicity in the putative cholinergic cells, but not that in the putative GABAergic cells (as differentiated by broad versus brief spikes, respectively) (107). This last result could be interpreted as evidence that oscillations in cholinergic cells depend on the inhibitory synaptic inputs from GABAergic neurons, which may behave as pacemakers for the hippocampal theta (141, 918) (see sect. II*C*). There is also evidence that noncholinergic (putative GABAergic) cells in the nucleus basalis promote LFP oscillations in the neocortex (588).

Somewhat surprisingly, a modeling study found that synaptic interactions could not synchronize a medial septum network of interconnected GABAergic cells endowed with intrinsic mixed-mode oscillations (as in Fig. 4*B*), but synchronization was realized in a reciprocal loop between these septal GABAergic cells and a subtype of GABAergic cells in the hippocampus (1031). This result suggests a critical role in theta synchrony of backprojections from the hippocampus to the medial septum. The latter do not originate from pyramidal cells, but a subpopulation of GABAergic, calbindin- and somatostatin-containing cells with horizontally oriented dendrites located in stratum oriens (14, 479, 962). Septally projecting hippocampal cells fire at the trough of the theta cycle (479) (like O-LM cell in Fig. 10*A*). A reciprocal GABA-GABA septohippocampal loop is well established anatomically: septally projecting hippocampal GABAergic cells receive a large proportion (up to 54% on somata and 27% on dendrites) of GABAergic inputs from the medial septum (930), and hippocamposeptal fibers innervate hippocampally projecting GABAergic, but not cholinergic, neurons in the medial septum (962). Inhibitory feedback projection from the hippocampus onto GABAergic cells in the medial septum was also physiologically confirmed in an in vitro septo-hippocampal preparation containing the intact interconnecting fornix/fimbria pathway (635). Whether the reciprocal loop is critical for theta synchronization can be directly tested by selectively disabling the hippocamposeptal pathway with pharmacological, transgenic or optogenetic manipulations.

One of the open issues is the synaptic mechanism that can account for the observed relationship between theta oscillations in the entorhinal cortex and hippocampus. The atropine-resistant form of theta oscillation in the hippocampus depends on the integrity of afferent inputs from the entorhinal cortex (141, 492); therefore, movement-related hippocampal theta involves the entorhinal cortex, hippocampus, and the medial septum in a interconnected large circuitry. There are multiple generators for field theta oscillations in the entorhinal cortex and hippocampus (522, 691, 695, 702). CA1 pyramidal neurons fire with the lowest probability at a phase of the theta cycle where the direct synaptic excitation from the entorhinal cortex into their distal dendrites is maximal (141, 208, 492). Simultaneous recording from the two structures in awake behaving rats revealed that the peak of the population activity in the entorhinal cortex is aligned with the timing of dendritic excitation of hippocampal target neurons, but the firing of the latter is typically offset by a half theta cycle (691). Note that, in anesthetized animals, perisoma-targeting interneurons show maximal firing ~100–180° out of phase with pyramidal cells (889) (Fig. 10*A*), hence at the same preferred theta phase as the entorhinal inputs onto the CA1 distal dendrites. This output-controlling inhibition could veto direct entorhinal excitation, thereby rendering the activities of the hippocampus and entorhinal cortex relatively independent on some time scale. However, in nonanesthetized animals, putative perisoma-targeting interneurons fire roughly 60° ahead of pyramidal cells, not 180° out of phase (208). Furthermore, even if the activity of perisomsa-targeting interneurons is phasically aligned with the synaptic excitation from the entorhinal cortex, it should delay firing of pyramidal cells

by a few milliseconds, but not a half theta cycle (~60 ms). It will be a challenge to understand, using both experiments and modeling, how perisoma-targeting and dendrite-targeting inhibitory neural types in interplay with pyramidal cells give rise to the observed theta phase relationships, as well as their computational implications.

In summary, network architecture is a predominant determinant of spatiotemporal neural activity patterns, the richness and complexity of which are only beginning to be revealed and promise to be a fertile ground in the coming years with the accelerated pace of knowledge accumulation about neural circuit wiring properties. Yet, connectivity alone does not predict behavior. As illustrated by examples above, synchrony depends on a combination of the required network properties (such as the minimal connectedness) and the dynamics of constituent single neurons and synapses.

V. SYNCHRONOUS RHYTHMS WITH IRREGULAR NEURAL ACTIVITY

Do concepts and insights summarized in sections II-IV provide a suitable framework for understanding brain rhythms observed in cognitive behavior? The answer depends in part on our ability to account for the following seeming paradox. In the cortex, especially in awake behaving conditions, even when a synchronous oscillation is detected in LFP, it is often not readily discernable in highly irregular spike trains of single units (468, 706). To resolve this puzzle, a necessary step is to understand the physical basis of EEG and LFP signals and how they relate to the electrical activity of single cells. There is a reasonable consensus that LFP is a weighted spatial average of the flow of currents along the dendrosomatic axis of pyramidal neurons (144, 201, 202, 690). The spatial extent over which neural signals are integrated by LFP has been estimated to be ~500 μm (75, 532, 595), based on a model of the columnar structure for some stimulus selectivity. Recent work used more direct analysis. Optical imaging from the cat visual cortex revealed that LFP could be quantitatively accounted for by membrane potentials, filtered by a Gaussian kernel with a width of σ ~100 μm. It follows that >95% of the LFP signals originated within a radius of 250 μm (2.5σ) of the recording electrode tip (498). Another study, using LFP and MUA recordings, obtained similar estimates in the monkey visual cortex: LFP sums signals spatially with a radius of ~120 μm in layer 4B and 200 μm in superficial and deep layers (1078). Therefore, LFP appears to reflect neural signals within a narrower spatial extent than previously thought.

The relationship between LFP and spiking activity remains a topic of active research. A recent monkey physiological study found that a linear filter operation on the activity of a few neurons can account for a significant fraction of the LFP time course (792), and a study combining LFP and single-unit recording from epileptic human subjects found that broad-band (2–150 Hz) LFP power is positively correlated with the single-unit firing rate (634). Yet, it is generally held that LFP primarily reflects synaptic inputs rather than spiking outputs (37, 164, 690). For example, in anesthetized monkeys, LFP in the visual cortex was not significantly affected when spike activity was reduced by pharmacologically induced hyperpolarization (794). There is also evidence that LFP in a visual cortical area shows similar stimulus-feature selectivity as the spiking output of upstream neurons that project to the recorded site (507). However, this does not mean that LFP exclusively reflects afferent inputs from outside of the recorded brain area, because cortical networks are endowed with an abundance of intrinsic connections; therefore, a large fraction of synaptic connections onto a cortical neuron originate within the local circuit (85, 253). A recent study showed that a recurrent cortical network model can reproduce many features of LFP observed in a monkey experiment, suggesting precisely how spike rates relate to EEG power in different frequency bands (663). Furthermore, voltage-dependent membrane changes other than synaptic events, including spike afterhyperpolarization, also contribute to the generation of LFP signals (144, 492).

A. Local Field Oscillations Versus Stochastic Spike Discharges of Single Cells

Isolated cortical neurons fire regularly under certain conditions, e.g., when driven by a constant current injection in vitro. In the intact brain, however, cortical cells are bombarded by highly fluctuating synaptic inputs, and typically fire seemingly random spike trains. A simple statistic of variability is Fano factor, defined as the ratio of the variance over the mean of spike count (in a proper time window). Another measure is the coefficient of variation (CV) of interspike intervals (ISIs). Fano factor and CV are both zero for periodic responses and one for Poisson processes. Variability of spiking responses is higher in the cortex than in the periphery (495). In cat and monkey primary visual cortex, Fano factor is ~1 for neurons recorded from anesthetized (153, 884, 957, 958) and awake (430, 742, 883, 1014) animals (but see Refs. 392, 495). Fano factor or CV is also close to 1 for spiking activity of single-units recorded in extrastriate cortical areas of alert behaving monkeys, including the middle temporal area MT (39, 116, 863, 883), V4 (664, 688), prefrontal cortex (184, 864), and motor cortex (716). A recent study compared CV of neural activity in several cortical

areas and found that the average CV of single units is ~1.0 for MT, ~0.96 for the lateral intraparietal association area (LIP), and ~0.87 for motorlike area 5 in the parietal cortex (628). In all three areas examined, ISI histograms are well fitted by gamma distributions without repetitive peaks; hence, neural activity is typically far from being clocklike. However, a high (~1) Fano factor or CV is not necessarily inconsistent with the presence of synchronous oscillations. Although these are useful measures of neural variability, they do not probe temporal structures and are not sufficient to determine whether a spike train is consistent with a Poisson process (17, 497). In particular, importantly, a significant fraction of measured variability is likely due to the variability of neural firing rates (rather than Poissonian spiking with a fixed firing rate) (863).

Nevertheless, it is notable that, even when simultaneously recorded LFP exhibits coherent fast oscillations, spike trains of cortical neurons are still highly irregular (Fig. 11). In the neocortex and hippocampus, gamma oscillations observed in vivo are typically associated with stochastic and sparse spiking activity of individual cells (104, 181, 185, 208, 209, 238, 263, 312, 377, 759). Csicsvari et al. (208) examined spiking activity of hippocampal pyramidal neurons and interneurons that were associated with field oscillations. During sharp-wave ripples, CA1 cells fire at much lower rates (~5 Hz for pyramidal cells; ~30 Hz for interneurons) than LFP oscillations (100–200 Hz). Similarly, during internested theta (3–7 Hz) and gamma (30–70 Hz) rhythms, pyramidal cells and interneurons fire stochastically at lower rates compared with gamma (~1.5 Hz for pyramidal cells, 15 Hz for interneurons) (208). During both sharp-wave ripples and theta oscillations, the interspike intervals are broadly distributed with CV ~1 for pyramidal cells and ~0.7 for interneurons (208). Caution is warranted in interpreting the reported CV values, since a high CV might, at least partly, be due to the burstiness of spike discharges (1056). Moreover, distinct cell types display different degrees of modulation by a field rhythm (Fig. 10); a minority of neurons might conceivably behave as a pacemaker (559) but are not clearly reflected in the population averages. Also, the aforementioned statistics are global averages and may be different for any neuron at specific times, for example, when a hippocampal cell fires at a high rate and may display prominent oscillations as the rat traverses across its place field (Fig. 1*A*). On the other hand, it is also true that theta rhythm in the rat hippocampus represents perhaps the most prominent rhythm observed in

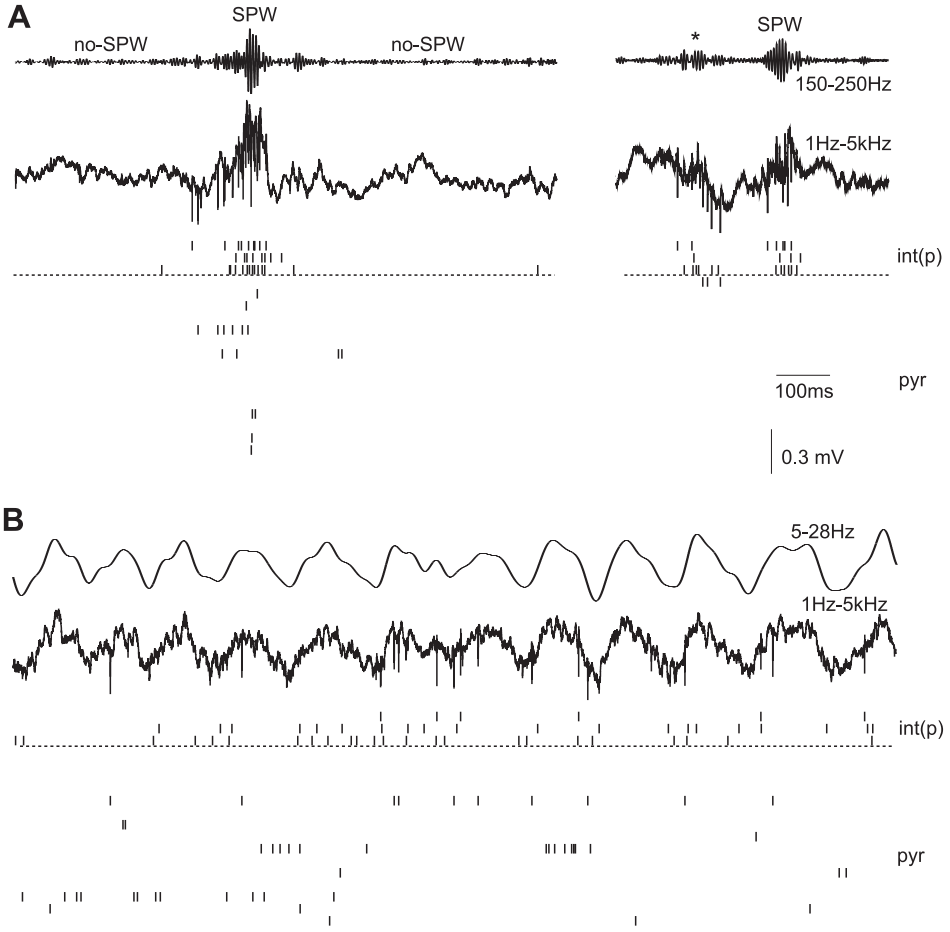

FIG. 11. Field oscillation and spiking activity of interneurons and pyramidal cells in the hippocampus of behaving rats. *A*: episodes of sharp-wave ripples during slow-wave sleep. *B*: theta rhythm during rapid-eye-movement sleep. Filtered (top) and wide-band (bottom) local field traces recorded from one of the tetrodes. Below LFP traces are shown action potentials of isolated neurons (vertical ticks) for three interneurons [int(p)] in the CA1 pyramidal layer and 15 pyramidal (pyr) cells recorded by four tetrodes. [From Csicsvari et al. (208).]

the mammalian cortex during behavior. In the neocortex, field oscillations associated with cognitive tasks are generally much weaker. There is a dearth of work in which the variability of single-unit spike trains and field oscillations are analyzed at the same time. Such studies in the future would be highly desirable, particularly in behaving animals.

Assuming that LFP monitors subthreshold membrane changes, can LFP oscillations in a cortical circuit coexist with predominantly random spiking output of constituent single cells?

B. Sparsely Synchronized Oscillations

To reconcile irregular neural firing with a LFP rhythm, one possibility is that the majority of neurons in a network fire irregularly and asynchronously so that they are largely averaged out in LFP, and field oscillations are generated by a small subset of neurons endowed with pacemaker properties (like chattering cells in the neocortex). This is unlikely. In a study with in vivo intracellular recordings (154), fast rhythmic bursting (chattering) neurons were identified by their responses to constant current injection. Interestingly, it was found that, when these cells responded to visual stimuli, hyperpolarization of the membrane potential did not reduce the relative power of visually evoked gamma oscillations in the voltage response, suggesting that gamma oscillations triggered by visual stimulation are predominantly produced by synaptic inputs, not intrinsic rhythmic bursting of single cells.

In an alternative scenario, most neurons participate in the generation of field oscillations, but the rhythmic modulation of neural firing probability is small, as illustrated in Figure 12*B* for hippocampal pyramidal cells during gamma oscillations. A framework to describe such network oscillatory dynamics has been developed, taking a diametrically opposite view from that of coupled oscillators. The idea is to start with a network in which neurons predominantly behave as "Geiger counters" and examine how a coherent rhythm might emerge from a dynamical destabilization of the asynchronous network state (123–127, 342). Brunel and Hakim (124) and Brunel (123) assumed that isolated neurons are driven by a large amount of background synaptic noise and generate Poisson-like spike trains, and considered populations of such neurons randomly connected by delayed synaptic interactions (while neglecting synaptic current time courses). It is intuitive to see why oscillations occur in such a network of inhibitory cells: neurons fire spikes together, generating IPSPs that occur only after a delay τ. The shared feedback inhibition hyperpolarizes neurons synchronously. When this inhibition wanes over time, another collective firing episode can occur again, leading to a population oscillation with the period roughly equals to 2τ (124). Given that monosynaptic transmission latency is typically only a few milliseconds, the frequency of oscillations based on synaptic delay in a local circuit is typically very high (e.g., 200 Hz with $\tau = 2.5$ ms). This conceptual framework has been generalized by taking into account realistic synaptic kinetics and applied to physiologically realistic rhythms (127, 342). In addition, delays are longer for long-distance synaptic interactions, and delayed inhibitory feedback has been proposed as a mechanism of rhythmogenesis in systems ranging from the electric fish (248, 249, 589, 641) to the basal ganglia-thalamo-cortical system of the mammalian brain (563).

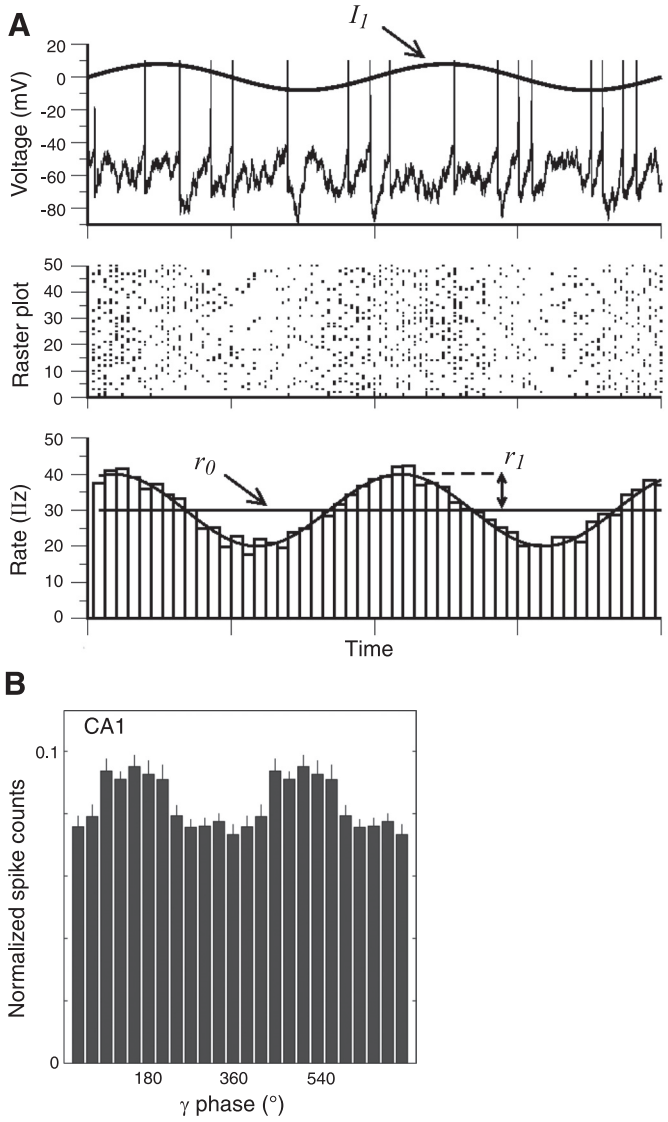

FIG. 12. Population rhythmicity with irregular spike activity of single neurons. *A*: network dynamics is schematically illustrated here in the form of single neuron activity in response to network inputs composed of a large amount of noise and a weak sinusoidal wave (*top*). The raster plot (*middle*) reveals the modulation of the instantaneous firing rate, which has a large tonic component (r_0) and a small sinusoidal component (of amplitude r_1) (*bottom*). *B*: distributions of spike times across phases of 25–50 Hz gamma oscillations for CA1 place cells in freely moving rats, showing a small rhythmic modulation on top of a tonic baseline. [*A* adapted from Richardson et al. (805); *B* from Colgin et al. (181).]

It is instructive to consider the network behavior as a function of the synaptic coupling strength. When the coupling strength is zero, neurons do not interact with each other; the completely asynchronous network is characterized by a constant (r_0) population firing rate over time. When the coupling strength is gradually increased beyond a certain threshold level, the asynchronous state is no longer stable because small perturbations are amplified by strong synaptic interactions, and a network rhythm emerges. The transition from asynchrony to collective rhythmicity can be described mathematically by the theory of bifurcations in nonlinear dynamical systems (922). Biologically, this illustrates how graded changes in network property (like the coupling strength) can yield qualitatively different behavior in a recurrent neural circuit. Because the oscillatory component is significantly smaller than the tonic component and noise, spike output of single cells remains highly irregular, and the mean firing rate of neurons (r_0) can be essentially uncorrelated with the network oscillation frequency (f). Therefore, a measure of LFP (based on an averaged synaptic current) displays small oscillations superimposed on a large baseline component, and the presence of field oscillation coexists with Poisson-like spike discharges of single cells.

If single neurons discharge spikes irregularly with no intrinsic periodicity, what determines the frequency f of a network rhythm? Under the condition that the oscillatory component is small, a systematic answer is provided by a linear analysis (127). Consider a population of mutually inhibitory neurons. Assume that an oscillatory population firing rate is given by $r(t) = r_0 + r_1 \sin(2\pi ft)$, where f is the oscillation frequency and the oscillation amplitude r_1 is small compared with r_0 (Fig. 12*A*). The recurrent network synaptic current produced by this neural firing is given by $I_{syn}(t) = I_0 + I_1 \sin[2\pi ft + \Phi_{syn}(f)]$, where the synaptic phase shift $\Phi_{syn}(f)$ is determined by the synaptic filtering properties such as the latency, rise time, and decay time. On the other hand, given a sinusoidal input current [the sum of noisy background drive and $-I_{syn}(t)$, where the minus sign originates from the inhibitory nature of the inputs and yields an additional phase shift of π], the spiking response of a neuron is determined by its intrinsic membrane properties. The rate of spiking output $r(t)$ is a tonic component plus a sinusoidal wave, characterized by an amplitude $r_1(f)$ and a phase shift $\Phi_{cell}(f)$ with respect to the input current, or $r(t) = r_0 + r_1 \sin[2\pi ft + \Phi_{syn}(f) + \Phi_{cell}(f) + \pi]$. Because this $r(t)$ is the same as the one that gives rise to $I_{syn}(t)$, self-consistency implies that (127)

$$\Phi_{syn}(f) + \Phi_{cell}(f) = \pi(\mathrm{mod}[2\pi]) \quad (5)$$

Solving this equation determines the frequency f. It is remarkable that this equation (hence the network oscillation frequency f) is independent of the neuronal firing rate r_0, demonstrating a salient characteristic of such sparsely synchronized rhythms. The analytically predicted network oscillation frequency has been checked and shown to be fairly accurate in direct simulations of spiking neural network models (127, 342). This theoretical framework can be extended to two populations of pyramidal cells and inhibitory interneurons (123, 127, 342). An example is shown in Figure 13, where the model network displays gamma oscillations while single cells fire sparsely with wide distributions of firing rates across neural populations.

This analysis shows that even though single-neuron activity is highly irregular, the frequency of a collective network rhythm is determined by both the synaptic properties [$\Phi_{syn}(f)$] and single cell's membrane properties [$\Phi_{cell}(f)$]. The amplitude factor $r_1(f)$ and the phase shift $\Phi_{cell}(f)$ can be analyzed by studying a single neuron in response to an injected current with three components (a baseline I_0, a small sinusoidal wave, and a noise filtered by a synaptic time constant τ_{syn}). This insight inspired a number of studies using different types of single neuron models. It turns out that, with realistic synaptic filtering time constants, for a leaky integrate-and-fire (LIF) neuron model, both r_1 and Φ_{cell} are approximately insensitive to the frequency f (128). On the other hand, for a Hodgkin-Huxley type I neuron (1035), $r_1(f)$ decays like $1/f$, and Φ_{cell} shows an increased lag with larger f, independent of τ_{syn} (297, 342). This is captured by a simpler, "exponential LIF" model (taking into account the nonlinear action potential upstroke) (297, 342).

Motivated by these theoretical predictions, an in vitro experiment has been carried out, where single cortical pyramidal cells were driven by the same type of noisy current as in modeling studies (523). It was found that, as predicted theoretically, in pyramidal cells the phase delay $\Phi_{cell}(f)$ increases with f, and the phase shift curve is insensitive to the noise-filtering time constant. Moreover, at low frequency $f \sim 10$ Hz, pyramidal neurons actually show a phase advance with respect to the current drive (523). This phase advance may result from a potassium current (293, 650, 668, 1027) or an H-type hyperpolarization activated cation current (715), which produces a preferred spike timing at the upstroke (phase-advanced relative to the peak) of a sinusoidal input current (95, 321, 338, 492, 506, 623, 625, 715). At high input frequencies, such slow ionic currents are less effective, and the cellular phase shift becomes a lag due to the passive membrane RC property (125, 297, 342). These results highlight the point that single neuron properties do matter with regard to determining collective network synchrony, even in the cases where single neuron behavior is highly irregular. Since different single neuron models (e.g., the linear LIF or a Hodgkin-Huxley type neuron) are characterized by different $\Phi_{cell}(f)$, different choices of single cell models can lead to divergent conclusions about a network oscillation's frequency.

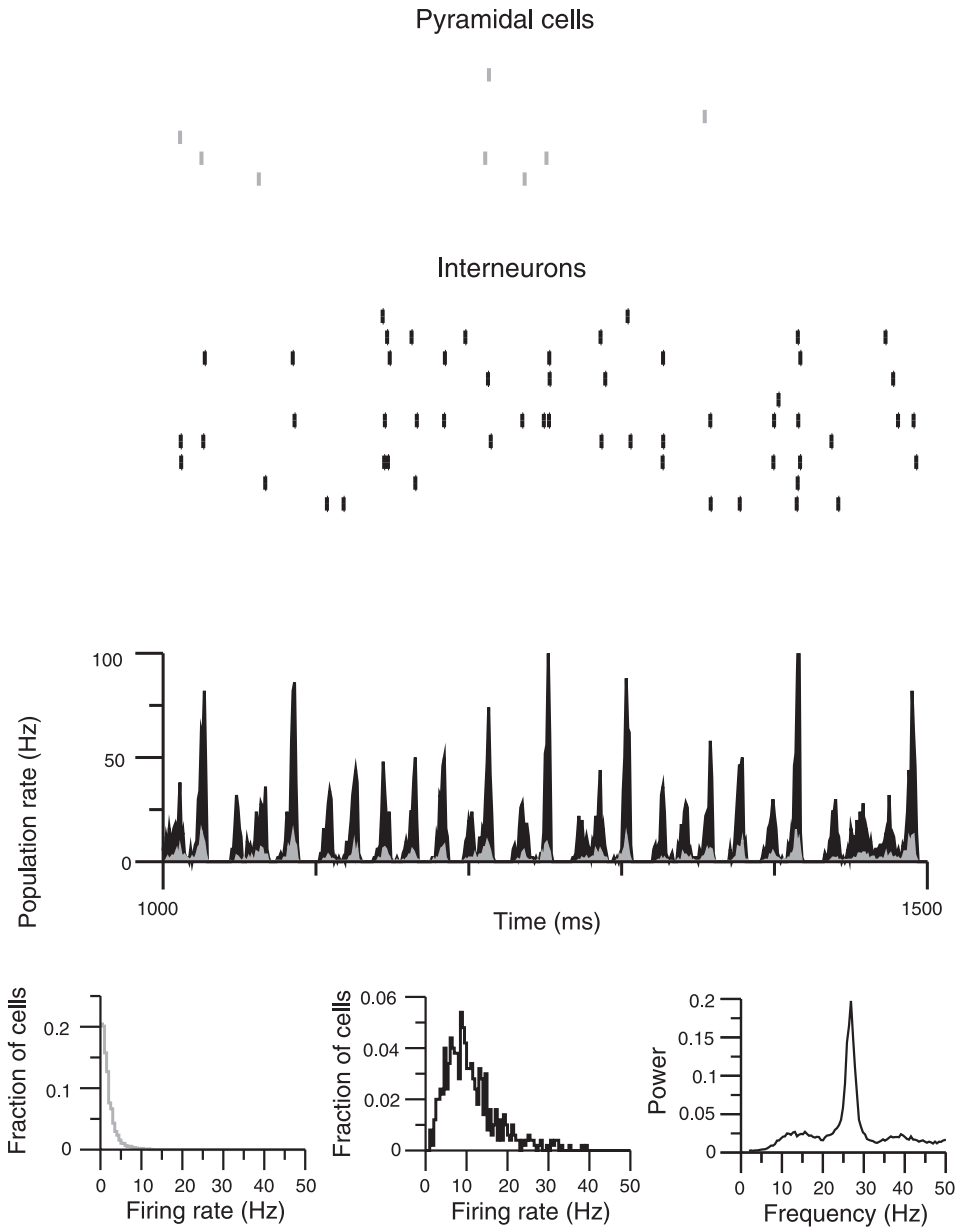

FIG. 13. Excitatory-inhibitory feedback loop for synchronous gamma oscillations with irregularly firing neurons. Computer simulation of a model with two neural populations (pyramidal cells and interneurons) in a sparsely connected random network. The network shows a collective oscillation at 55 Hz (see population rates and the power spectrum), whereas single neurons fire spikes intermittently in time at low rates (2 Hz for pyramidal cells, 10 Hz for interneurons; see rastergrams). [From Brunel and Wang (127).]

In a network of interconnected pyramidal cells and interneurons, a synchronous rhythm can predominantly arise from an interneuronal (I-I loop) mechanism or an excitatory-inhibitory (E-I) loop mechanism (Fig. 14*A*). The latter is akin to that proposed in previous firing-rate models (303, 318, 578, 976, 1060); what is new is a framework for quantitatively predicting the oscillation frequency and the phase relationships in terms of cellular and synaptic properties. Interestingly, it can be shown that the oscillation frequency produced by the E-I loop is generally slower than that by the I-I loop (127, 342). Thus, given typical synaptic time constants of AMPA receptor-mediated excitation and $GABA_A$ receptor-mediated inhibition, it is expected that 100- to 200-Hz ultrafast rhythms could arise from an I-I scenario, with the frequency largely controlled by the synaptic transmission latency and rise time, and the ~40 Hz gamma rhythm primarily depends on an E-I scenario, which is more sensitive to synaptic decay times (Fig. 14*B*). This is in stark contrast to networks of coupled oscillators for which the interneuronal circuit mechanism preferentially synchronizes in the gamma frequency range (Fig. 7).

Generally, the network dynamics involve a mixture of both the I-I loop and E-I loop scenarios. One such situation is when the synaptic excitation and inhibition balance is the same in pyramidal cells and interneurons. In a model, when the excitation/inhibition ratio is gradually increased (for both E and I neural populations at the same time), the network oscillation frequency can either

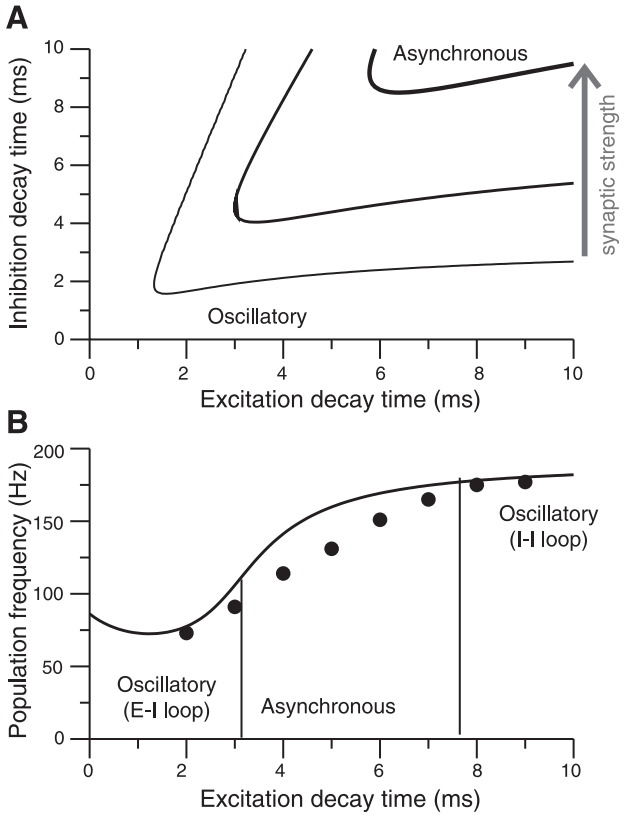

FIG. 14. Dependence of sparsely synchronized oscillations on the strength and relative speeds of synaptic excitation and inhibition. *A*: network dynamical behavior as a function of the excitatory (τ_E) and inhibitory (τ_I) synaptic time constants. A line separates the asynchronous state (top right region) from the synchronous oscillation state (bottom left region). This is shown with three levels of recurrent connection strength; coherent oscillations become more prevalent with stronger recurrence of the network. *B*: population frequency as a function of the excitatory synaptic decay time constant τ_E, with fixed $\tau_I = 5$ ms. Qualitatively, there are two kinds of instability from the asynchronous state to coherent oscillation. On one hand, when τ_E is much smaller than τ_I, the asynchronous dynamics is destabilized and oscillation develops through delayed inhibition in an excitatory-inhibitory loop scenario. On the other hand, when τ_E is sufficiently large, the excitatory drive is roughly tonic and the interneuronal network by itself generates synchronous oscillation. The oscillation frequency is much lower with shorter τ_E (gamma rhythm by the pyramid-interneuron loop mechanism) than with longer τ_E (ultrafast rhythm by the interneuronal network mechanism). [Adapted from Brunel and Wang (127).]

decrease or first increase then show an abrupt drop and then decrease continuously (342), illustrating complex behaviors that can occur even in a rather simple system of two randomly connected neural populations.

As a rule, stronger recurrent synaptic interactions greatly enhance the network's propensity to exhibit synchronous oscillations (Fig. 14*A*). This result sheds insight onto why gamma-band oscillations naturally occur in CA3 (291, 632), which is endowed with more excitatory local collaterals than CA1 in the hippocampus (671), or superficial layers 2/3 of the necortex (132), which are endowed with a higher abundance of local horizontal connections than in deep layers 5/6 (in the cat V1, 21.6, 0.9, and 4.6% of all excitatory-excitatory synapses are horizontal synaptic connections between pyramidal cells in layer 2/3, layer 5, and layer 6, respectively; Ref. 85). Furthermore, as we shall discuss in section VI, cognitive functions such as selective attention involve highly recurrent areas like the prefrontal cortex prone to fast oscillations, which may explain why beta and gamma rhythms are often enhanced throughout the brain with the engagement of "cognitive-type" cortical circuitry.

C. Specific Cases: Fast Cortical Rhythms

There is increasing experimental evidence that fast rhythms in the cerebral cortex display salient characteristics of sparsely synchronized oscillations.

1. Ultrafast (100–200 Hz) rhythm

As mentioned earlier, data from Csicsvari et al. (208) and others showed that sharp-wave ripples appear to represent an example of sparsely synchronized oscillation, with both pyramidal cells and interneurons showing a high degree of irregularity and firing intermittently at much lower firing rates than field oscillations (100–200 Hz), and pyramidal cells typically firing ahead of fast spiking interneurons during the oscillation cycle (140, 147, 148, 208, 561).

Fast (~200 Hz) rhythm has also been observed, first by Adrian and co-workers (7, 171, 460), in the cerebellum. The cerebellum is a structure critical for fine motor coordination, and it has been hypothesized (460) that precise timing required for motor control involves millisecond-scale synchrony between Purkinje cells (73, 261, 868). A recent study, using tetrode recordings from multiple single units in vivo, found that precise synchrony between Purkinje neurons is directly related to fast field oscillations of the rat cerebellum in vivo (222). This cerebellar rhythm shared characteristics of a sparsely synchronized oscillation. The field oscillation frequency was ~150–250 Hz, whereas an average firing rate of individual Purkinje cells was ~38 Hz. Neuronal spike discharges did not occur at multiple intervals of the field oscillatory period. Cross-correlation of neighboring Purkinje cells displayed a peak at ~1–5 ms, but quickly (within 2 cycles) decayed to a large baseline, as expected from highly stochastic neural dynamics.

Current-source density analysis suggested that the fast oscillations were generated in the layers containing soma and proximal dendrites of Purkinje cells. The precise synchrony did not appear to be caused by common excitation from parallel fiber inputs, because the spatial extent of coherence was similar in the direction "on beam" (along the parallel fibers) or "off beam" (parasagittally). Moreover, blocking AMPA receptor-mediated excitation by GYKI 52466 actually enhanced the oscillation

power. On the other hand, blocking $GABA_A$ receptors by picrotoxin reduced the oscillation power by ~40%, suggesting that synaptic inhibition contributes to in vivo ~200 Hz cerebellar oscillations. This conclusion was in contrast to another study reporting that gap junctions played a critical role in ~100 Hz oscillations induced by nicotine receptor activation in in vitro cerebellar slices (681). De Solages et al. (222) replicated salient in vivo experimental observations in an inhibitory neural network model, and *Equation 5* predicted approximately the network oscillation frequency. Interestingly, the generation of ~200 Hz oscillations requires fast time constants of inhibitory postsynaptic currents, consistent with the measurements in vitro from the mature cerebellum (<3-fold quicker compared with those in the developing cerebellum). Moreover, using a two-compartment neuron model for Purkinje cells, with recurrent synaptic inhibition near the soma relatively isolated from a large dendrite, produced significantly higher oscillation frequencies than when Purkinje cells were described by a one-compartment model. These results illustrate, again, how detailed synaptic and cellular properties together determine the frequency of a collective network oscillation with irregular neuronal discharges.

2. Gamma and beta rhythms

In vivo gamma rhythms in the olfactory bulb (264, 496, 816), hippocampus (104, 208, 209), and neocortex (914, 238, 423, 783) all display features of a sparsely synchronized oscillation, with single neurons firing irregularly at lower rates than LFP oscillations. In in vitro neocortical or hippocampal slices, when gamma rhythm is induced by muscarinic acetylcholine receptor activation, pyramidal neurons fire sparsely in <5% of the cycles (132, 291). Intracellular voltage measurements and voltage-clamp recordings of synaptic currents provided a wealth of evidence that strongly support the excitatory-inhibitory loop mechanism for beta and gamma oscillations. First, spiking probability of single neurons displays a peaked distribution of phases with respect to the field gamma cycle, with pyramidal cells leading perisomatic-targeting interneurons by a few (ranging from 2 to 8) milliseconds (209, 408, 423, 632, 746). This means that inhibitory neurons lag pyramidal cells by a significant phase difference [in vivo, ~60° (209); in vitro, ~55° (632) or ~23° (408, 746)]. This phase lag is qualitatively consistent with the feedback inhibition model proposed by Freeman (300) and Leung (578).

Second, synaptic excitation is not tonic, unlike a predominantly interneuronal network mechanism. During spontaneous gamma oscillations in the hippocampus (35) and odor-evoked beta oscillations in the piriform cortex (775), in vivo whole cell voltage-clamp measurements from neurons revealed that EPSCs precede IPSCs by a few milliseconds. Both in vivo and in vitro, excitatory and inhibitory synaptic conductances in a single neuron fluctuate together on a rapid time scale, leading to considerable cycle-by-cycle variations of the gamma cycle duration (35).

Third, in vitro carbachol-induced fast oscillations were abolished by blockade of either fast excitatory AMPA receptors or inhibitory $GABA_A$ receptors in the hippocampus (291, 632) and neocortex (132, 155). A reduction by genetic manipulation of glutamatergic synaptic transmission in parvalbumin-expressing fast spiking interneurons led to a reduced gamma oscillations (320). It might be argued that, in these experiments, blocking AMPA receptors deprived a cortical network of its main excitatory drive (which was not compensated by other means) necessary to induce synchronous activity in an interneuronal network. Nevertheless, these studies lend strong support of a feedback loop mechanism for self-sustained gamma rhythm in hippocampus and neocortex. In recent optogenetic studies, gamma oscillations were induced by light stimulation of fast spiking interneurons, but they were largely eliminated by blocking AMPA and NMDA receptors (155), and optically stimulating pyramidal cells enhanced gamma oscillations (885), suggesting that gamma rhythmogenesis depended on excitatory drive of interneurons by pyramidal cells, in a feedback loop.

LFP beta (~15–30 Hz) rhythm is also consistent with the sparsely synchronized oscillation behavior, as evident in single neuron activity recorded from the motor cortex in behaving monkeys (see, for example. Fig. 3 in Ref. 713). The mechanisms of beta-band oscillations have been much less studied but may be generated by a similar circuit mechanism as gamma rhythm. For example, Hodgkin-Huxley type models of interacting pyramidal neurons and interneurons, with a number of commonalities but also some differences, exhibit network oscillations either in the gamma band (342) or beta band (183, 185). The time scale of beta rhythmicity is comparable to the spike afterhyperpolarization lasting for 30–100 ms that has been revealed by intracellular recording of motor cortex neurons in awake monkeys (169). The slower frequency may be determined by a mixture of cellular and synaptic properties, including voltage- and calcium-gated potassium currents in pyramidal cells and the strength of recurrent excitatory connections (817, 1052, 1054), perhaps also involving specific subtypes of interneurons (667, 682, 758).

It is presently not fully understood what are the circuit properties required to quantitatively explain the observed relative phase lag between excitatory and inhibitory cells during gamma and beta rhythms (342). A critical step forward is to not just look at the phase relationship of spike firing of different neural populations, but also the phase relationship between the spiking activity of

a neural population and the synaptic current produced in target neural populations. In a remarkable paper, again studying in vitro cholinergically induced gamma oscillations, Oren et al. (746) measured phase distributions of excitatory and inhibitory synaptic currents in the pyramidal cells and three different types of interneurons. It will be interesting to see, in future work, whether the observed phase relationships of firing activity and synaptic currents can be quantitatively accounted for by the theory of sparsely synchronized oscillations (124, 127, 342, 662).

Even when fast oscillations are generated by reciprocal interactions between pyramidal cells and interneurons, inhibitory synaptic inputs may be especially suited for mediating precise synchrony in a cortical circuit (177, 616, 666, 701, 756, 778, 934), and subclasses of interneurons that target soma or dendrites of pyramidal cells produce entrainment in a frequency- and phase-specific manner (934). This is consistent with the finding in vivo that inhibitory synaptic potentials contained more power in the gamma frequency range than excitatory synaptic potentials (Fig. 15*C*), and barrages of IPSPs but not EPSPs showed marked synchrony between simultaneously recorded pyramidal neurons (35, 404, 405, 423). In this view, high-frequency LFP fluctuations are likely to reflect more synaptic inhibition than excitation.

To conclude, the theory of sparsely synchronized oscillations provides a promising new framework, which goes beyond the idea of coupled oscillators, for describing fast rhythms in the cerebral cortex. These two theories make distinct predictions. In particular, according to the model of coupled oscillators, the interneuronal mechanism generates synchrony preferentially in the gamma frequency range; in contrast, the theory of sparsely synchronized oscillations predicts that gamma rhythms primarily arise from interactions between excitatory and inhibitory neurons, whereas mutual inhibition between interneurons naturally gives rise to ultrafast (>100 Hz) oscillations. Importantly, the theory of sparsely synchronized oscillations makes it possible to reconcile population oscillations with highly stochastic firing of single neurons.

VI. FUNCTIONAL IMPLICATIONS: SYNCHRONIZATION AND LONG-DISTANCE COMMUNICATION

The previous sections covered the basic physiological mechanisms of brain oscillations observed in behaving conditions and a framework for describing cortical rhythms with irregular firing of single neurons as commonly seen in alert behaving states. We are thus in a position to discuss how cortical synchronization may contribute to cognitive functions. Most of the work summarized here involves descending top-down signaling in the neocortex of monkeys and humans.

A. Methodological Considerations

Recent years have seen a surge of research on oscillations and their synchronization across cortical areas during a variety of cognitive tasks. While these studies hold great promises, they also brought into the fore many methodological issues that remain to be resolved. As pointed out by Uhlhaas et al. (987): "In contrast to conventional analyses of ERP (evoked response potential), e.g., there are currently no general guidances and standards regarding the analyses of task-related oscillations and their synchronization. Analyses of oscillations are dependent upon several parameters, such as the choice of size of the width of the analysis window, the assessment of pretask baseline activity, the methods to assess spectral densities, phase locking, and coherence. Last but not least, even details such as the definition of reference electrodes in EEG recordings need to be standardized to guarantee replicability and comparison of results."

Without diverting into technical details, it is worth briefly pointing out here a number of issues, some of which are not only about measurement or analysis but fundamentally depend on our understanding of the nature of neural dynamics (e.g., neurons are viewed as regular oscillators or irregularly firing devices) in the cerebral cortex.

First, caution must be exercised with interpreting scalp EEGs (314, 1088). For example, certain forms of induced gamma band responses from scalp EEG, characterized by transient enhancement of broad band (30–100 Hz) power ~200–300 ms after stimulus onset (932), may actually be an artifact related to eye muscles that produce miniature saccades (1088; see Refs. 676, 1089 for a debate; among the contentious issues is the choice of the reference point for EEG data). MEG, intracranial EEG, and LFP are less prone to such artifacts.

Second, unlike clocklike rhythm (with a narrowly peaked power spectrum) observed in vitro under certain conditions (Fig. 15*A*), the power spectrum of LFP recorded in vivo is typically dominated by a power-law ($\sim 1/f^{\alpha}$) over a wide range of frequencies (148, 185, 431, 576). A rhythm, if present, is manifested by the existence of a small peak superimposed on this broad power spectrum (Fig. 15*B*). A common practice is to filter out this power decay ("normalizing the power spectrum") prior to spectral analysis (689, 873, 878), often assuming $\alpha = 1$ ("1/*f* noise"). This, however, could lead to artifacts. For example, frequency scaling of LFP power spectrum may depend on the behavioral state, with α varying between 1 and 2 (69, 70).

The power law of LFP spectrum is partly due to low-pass filtering by the extracellular medium (70, 71), but also reflects fluctuations of neuronal signals on multiple time scales. Indeed, during episodes of spontaneous

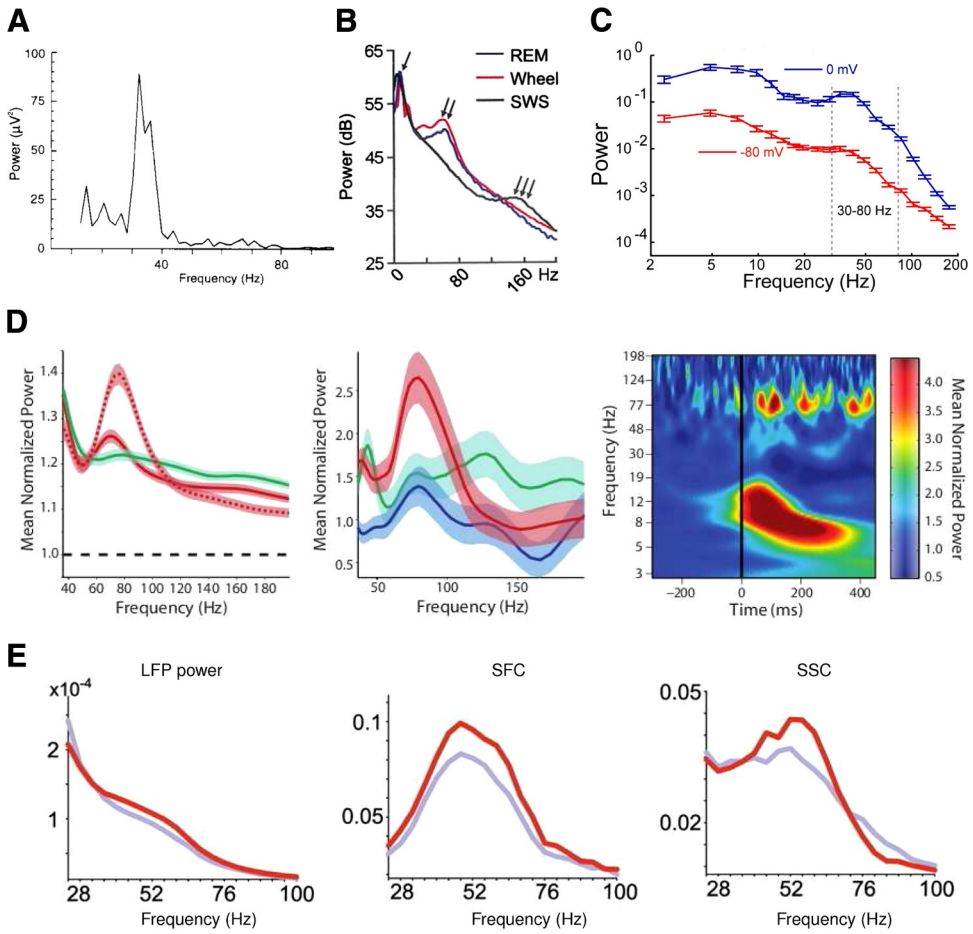

FIG. 15. Local and long-distance synchronization in the gamma frequency range. *A*: under certain conditions in vitro, LFP gamma may exhibit a sharp peak in the power spectrum. In this case, gamma rhythm was induced pharmacologically by metabotropic gluatamte receptor activation in a rat hippocampal slice where fast synaptic excitations mediated by AMPA and NMDA receptors were blocked. *B*: in contrast, in vivo LFP oscillations are typically manifested by small peaks superimposed on high powers at low frequencies (reflecting slow fluctuations or drifts over time). Data were obtained in a single mouse during wheel running (red), REM sleep (blue), and slow-wave sleep (SWS, black). *C*: power spectra of intracellularly recorded synaptic potentials recorded from a pyramidal neuron of ferret in vivo. Membrane fluctuations are dominated by inhibitory postsynaptic potentials near 0 mV (blue) and by excitatory synaptic potentials near −80 mV (red). The peak in the gamma band is more significant at 0 mV, suggesting a prominent role for synaptic inhibition in rhythmic fluctuations. *D*: coherence between two cortical areas of alert monkeys in cross-modal information processing. LFPs were measured from the auditory cortex and the superior temporal sulcus (STS), an association area involved with face processing and cross-modal integration. Voice: trials when a naturalistic sound (monkey's vocalization) was played; face: trials when the corresponding mouth movement was shown visually; face+voice: trials when both stimuli were presented concurrently. *Left*: LFP power spectrum displays a peak in the gamma frequency range for both the auditory cortex and STS (red) in the face+voice condition, but there is no significant gamma-band peak in the auditory cortex with voice alone (green). *Middle*: inter-areal coherence displays a maximum in the gamma-band correlated with cross-modal integration (red), but not when face (blue) or voice (green) was presented alone. *Right*: time-frequency cross-areal coherence as a function of time in the face+voice condition, showing coherence at gamma interspersed with theta transiently (for ~300 ms). *E*: coherence in V4 during sustained stimulation from behaving monkeys in an attention task. Red: attended condition; gray: nonattended condition. *Left*: LFP power spectrum from area V4. *Middle*: spike-to-field coherence (between multiunit activity and LFP). *Right*: spike-to-spike coherence between two simultaneously recorded multiunit spike trains. SSC (defined between 0 and 1) is <5%. [*A* from Whittington et al. (1053); *B* from Buzsáki et al. (148); *C* from Hasenstaub et al. (423); *D* from Ghazanfar et al. (349) (with left panel kindly produced by Dr. A Ghazanfar); *E* from Fries et al. (315).]

network activity ("up state") (240, 404) or sensory responses (269), excitatory and inhibitory synaptic potentials in a single neuron display fluctuations on a range of time scales (Fig. 15*C*), and such synaptic currents across the dendrosomatic membrane are a major component of the physiological substrate of LFP. Furthermore, it has been suggested that, in some cases, an enhanced high-frequency power might not reflect synchronous rhythms but a decrease in the low frequency power and a concomitant broadband power increase (684). Therefore, to assess synchronous oscillations, it is important to understand better LFP broadband power structure and its dependence on behavioral conditions.

Third, since the voltage produced by volume-conducting currents decays inversely with distance from the point sources, LFPs in neighboring structures might be synchronous merely as a result of volume conduction (732, 955; but see Ref. 906). Current source density (CSD)

analysis (266, 299, 690, 722, 764) avoids this problem. On the other hand, rhythms are often not detectable in the spike trains of individual cells. For these reasons, spike-field coherence has become a measure of choice for assessing relative timing of neural activity to a population rhythm, or synchronization between brain regions (with LFP recorded in one area and spiking activity in another). Statistically reliable estimation of spike-field coherence, however, remains a difficult problem. For example, results of multitaper spectral analysis are sensitive to the number of tapers used and to a suitable smoothing frequency window. The values of these parameters are often chosen ad hoc; a disciplined approach is lacking (314). Observed coherence (defined between 0 and 1) is usually quite small: in attention studies, with LFP and spiking activity recorded from the same area, spike-field coherence is typically on the order of 0.1 for multiunit spike trains (1070) and single-unit spike trains (84), whereas spike-spike coherence of multiunits is ~0.05 (314). This underscores the notion that oscillatory synchrony, if present, is weak between neurons.

Fourth, a peak in the coherence spectrum of two neural signals is readily interpretable when both signals are rhythmic (each with a peaked power spectrum) (Fig. 15*D*). However, it can happen that one of the signals is rhythmic while the other is not. This is illustrated by a study with awake cats (64). It was found that LFP coherence between the basolateral amygdala and the rhinal cortical areas was peaked in the gamma (35–45 Hz) frequency range; the LFP of the amygdala showed a peak in the same gamma band, but those from the perihinal and entorhinal cortices did not.

Moreover, in principle, it is conceivable that a coherence spectrum exhibits a peak, in the absence of a rhythm. Figure 15*E* shows an example in which, while the LFP power spectrum is devoid of a clear peak, spike-field (between LFP and a multiunit spike train) and spike-spike (between spike trains of two multiunits recorded from different electrodes) coherence spectra display a peak in the gamma band (314). Thus a peaked coherence spectrum does not necessarily imply the presence of a rhythm.

Fifth, LFP signals may be distorted because the circuit of a metal microelectrode operates as a voltage divider with a frequency-dependent gain (814). This results in frequency-dependent phase shifts and amplitude attenuation when the electrode impedance is not negligible relative to the effective input impedance of the head-stage amplifier (717). Consequently, caution is warranted in the analysis of frequency-dependent phase shifts (such as the relative phase between LFP and spike discharges) and interpreting them as evidence of a "phase code."

Sixth, synchronous events occur episodically, typically lasting only for ~200–500 ms (285, 349, 378, 678, 711, 760) (Fig. 15*D*). Several methods have been developed, including multitapering (560, 759, 1069, 1091), wavelet transforms (549, 550, 561, 566, 932), empirical mode decomposition using short-term Hilbert transform (585), and "matching pursuit" using Gabor functions (796). But the relative advantages and shortcomings of these methods are not fully understood. At the very least, it should be insisted that reported oscillatory/synchronous episodes must last much longer than the time window used in such analyses.

In response to long-lasting inputs, short oscillation episodes may reoccur intermittently in a slow temporal pattern (67, 378, 557, 711, 788, 1043). Modeling studies discussed above are not adequate to account for recurrence of transient episodes of neural activity, which remain to be better understood theoretically (but see Ref. 789).

Seventh, coherence spectrum reflects both correlation of power amplitudes and phase synchronization. To avoid this confound, elaborated methods such as phase-locking statistics (543, 1004) and power correlation as a function of the relative phase (1070) have been developed to more directly assess phase coherence of two neural signals. However, such methods are justified if the two signals are strongly oscillatory with a nearly identical rhythmic frequency (so the phase is well defined in the same way for both signals). In contrast, the applicability of such methods is not entirely clear if the two signals have broad-band power spectra, as is generally the case. At a minimum, such studies need to ensure that each of the two signals does display a peaked power spectrum (hence a rhythm is present) and that the peaks of the two spectra have a considerable overlapping frequency range. Lack of such information would render it difficult to evaluate the meaning and implications of reported phase coherence.

Eighth, as there are often two or more internested rhythms (143, 548, 819, 907), analysis techniques have been proposed to describe cross-frequency coupling (e.g., to examine how the gamma amplitude depends on the theta phase). A common practice is to compute band-passed signals at two different frequencies f_1 and f_2 (e.g., theta and gamma) and assess the statistical dependence between the two-amplitude time series, the two-phase time series, or one amplitude and the other phase time series (37a, 150, 216, 229, 748, 1084). Clearly, many of the aforementioned concerns also apply to the analysis of cross-frequency coupling.

Ninth, long-distance communication involves interactions between multiple cortical areas. Analysis methods have been developed to interrogate the directionality of the flow of signals between two or multiple recorded areas, such as the Granger causality analysis (93, 118, 244, 371, 381, 560) and its frequency-domain representation (38, 244). It is currently unclear how directionality in-

ferred from such methods can be mapped onto the actual anatomical and functional connectivity in the brain (288, 402). A fusion of several techniques may help make progress on this important issue.

Tenth, even when there is no rhythm (in the sense that an LFP power spectrum does not exhibit a well-defined peak), it is a common practice to divide an LFP power spectrum into different frequency bands (57, 80, 112, 204, 704, 1017, 1018). This is often done with an arbitrary choice of passbands, but methods such as the empirical mode decomposition (447, 585) have been developed that decompose a time series into narrow-band components by identifying the physical time scales intrinsic to the data. This approach has been used, for instance, in investigations of the physiological basis of functional magnetic resonance imaging, by examining the correlation between blood oxygenation level-dependent (BOLD) responses and LFP power in different frequency bands. Correlations were found especially strong between BOLD and LFP gamma power in the neocortex (361, 604–606, 636, 704, 725, 727, 1013, 1090) and theta power in the hippocampus (267).

Similarly, a coherence spectrum may not show a peak at all, but one can still consider the coherence in different frequency bands and seek whether the coherence at a particular frequency is enhanced or decreased in a comparison between two stimulation or behavioral conditions. For example, a recent study (138) examined LFP coherence between the lateral intraparietal area (LIP) in the parietal cortex and the frontal eye field (FEF) in the frontal cortex of behaving monkeys, during visual search which is either based on bottom-up attention (when a salient target "pops up") or top-down attention (looking for a target that is similar to distractors). The coherence spectrum did not display a clear peak under either of the two conditions. The difference between the two coherence spectra, however, showed that top-down attention was associated with a differential enhancement in the beta frequency range and a suppression in the gamma frequency range.

It stands to reason that LFP powers or coherence powers in different frequency bands provide different information about the recorded signals and its neuronal underpinning. Nevertheless, confusion often arises if band-passed powers are identified with various rhythms, whereas there is no explicit assessment as to whether a well-defined rhythm or peaked coherence spectrum actually exists. Conceptually, will we be able to achieve a fundamental understanding of the cortical dynamics, by dividing a broad power spectrum into frequency bands and theorizing the band-passed powers in terms of oscillations? Probably not. An adequate framework is presently lacking to explain these diverse types of network coherence.

For the sake of clarity, below I will review studies of neural synchronization in cognitive behaviors without dwelling on methodological issues. However, it is worth keeping in mind the potential pitfalls discussed above, which call forth a concerted effort to set the standards for the field.

B. Phase Coding

Phase coding is a key, yet still controversial, concept in studies of the role of neural oscillations in local circuit functions and in long-distance communication between brain areas (143, 144, 313, 786, 850, 951, 955) as well as in memory functions (425, 488, 591, 592, 594). In general, the phase coding hypothesis posits that neurons represent information in terms of spike times with respect to the phases of ongoing network fluctuations, rather than only by spike rates. In a simple situation, network fluctuations (e.g., measured by LFP) are rhythmic with a well-defined periodicity T. If neuronal spike times [defined in the phase variable $\phi = 2\pi t/T \bmod(2\pi)$] are not uniformly distributed between 0 and 2π, but narrowly concentrated around a preferred phase of the LFP oscillation, then spike phases may convey information (e.g., about a sensory stimulus or behavioral metrics), above and beyond average spike counts.

An extensively studied example of phase coding is the neural representation of space in the hippocampus and entorhinal cortex. As introduced at the beginning of this article, during exploration in a familiar environment, a pyramidal "place cell" in the hippocampus is activated when the animal passes through its "place field" (739); hence, it shows a bell-shaped activity profile in space and (given a constant velocity) over time (Fig. 16*A*). Furthermore, spike firing exhibits phase precession, shifting to earlier phases of the theta cycle as the animal moves across the place field (Fig. 1*A*). Pooled-trial phase precession ranges over 360° (a full theta cycle) (418, 456, 660, 661, 740, 881, 1081, 1099); there is a large trial-to-trial variability, and single-trial phase precession range is limited to ~180° (848). The firing rate of a place cell is a bell-shaped function of spatial location, hence is roughly the same for the animal to be at different locations of equal distance to the center of the place field. In contrast, because of the phase precession phenomenon, the preferred phase of neural firing relative to the theta cycle is a linear function of the animal's location across the place field, thus can potentially disambiguate locations that spike counts alone cannot. Indeed, analyses suggest that position reconstruction from activity of hippocampal place cells can be improved by taking into account the contributions of phase coding (456, 473, 865, 881).

Phase precession of hippocampal place cells has been proposed to result from recurrent network dynam-

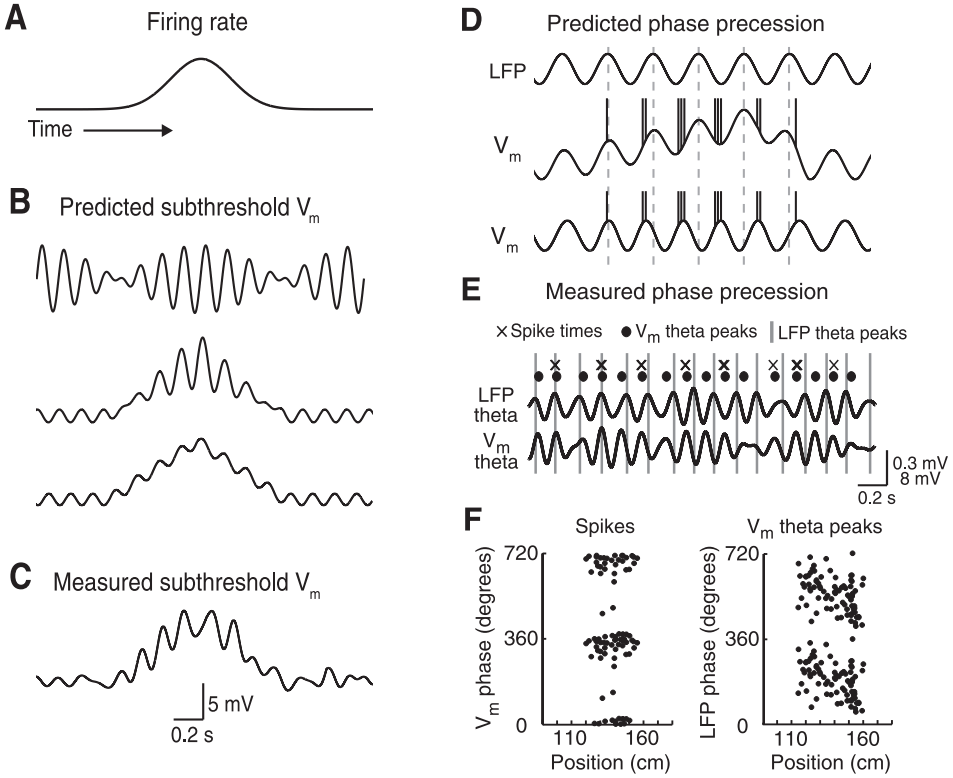

FIG. 16. Phase coding by place cells in the hippocampus of mouse performing a virtual navigation task. *A*: schematic of a place cell firing rate. *B*: schematics of predicted subthreshold membrane potentials (aligned to *A*) from three different models. *Top*: in a dual oscillator interference model, two sets of theta-modulated inputs at different frequencies interfere to create a beatlike pattern of membrane potential fluctuations. *Middle*: in a soma-dendritic interference model, the cell receives theta-modulated inhibitory and excitatory inputs. In the place field, the excitatory drive increases, resulting in a ramplike depolarization and an increase in the amplitude of excitatory theta oscillations. *Bottom*: in a network model, a ramp of excitatory drive interacts with theta-modulated inhibitory inputs. *C*: example of a subthreshold membrane potential (filtered from DC-10 Hz) recorded intracellularly from a place cell. Note the simultaneous ramp of depolarization and increase in theta oscillation amplitude. Scale bars refer to the experimentally measured trace only. *D*: schematics of the LFP theta rhythm (*top*) and predicted relationships between intracellular and LFP theta to account for phase precession (*middle* and *bottom*). *Middle*: intracellular and LFP theta have the same frequency. Phase precession of spikes occurs relative to both intracellular and LFP theta owing to a ramp of depolarization. An asymmetric ramp is shown. *Bottom*: intracellular theta in the place field has a higher frequency than LFP theta. Spikes precess relative to LFP theta but not intracellular theta. *E*: filtered (610 Hz) membrane potential and LFP traces in the place field from a simultaneous LFP and whole cell recording. The times of LFP theta peaks (gray lines), intracellular theta peaks (circles), and spikes (crosses) are shown to illustrate the phase precession of spikes and intracellular theta relative to LFP theta oscillations, and the absence of phase precession of spikes relative to intracellular theta oscillations. *F*: phase precession of spike times relative to intracellular theta (*left*) and phase precession of intracellular theta peak times relative to LFP theta (*right*) from a simultaneous LFP and whole cell recording. [Adapted from Harvey et al. (422).]

ics (674, 945, 977, 1021). However, neurons in the medial entorhinal cortex layer II, which provide the main inputs to the hippocampus, also display hippocampus-independent phase precession (401). Another, "soma-dendritic interference model" for phase precession (338, 492, 625) assumes the interplay of two oscillatory inputs onto pyramidal cells: a pacemaker input (e.g., somatic inhibition driven by the medial septum) and a dendritic excitation (e.g., from the entorhinal cortex) that is spatially dependent, hence increases as the animal moves toward the center of the place field. A somewhat different "dual oscillator interference model" assumes the linear addition of two independent oscillatory influences onto pyramidal cells (740, 575). Consider a place cell that receives the sum of two sinusoidal inputs $I = A[\sin(2\pi f_0 t) + \sin(2\pi f_i t)]$, where f_0 represents an external input (and reflected by LFP) and f_i is determined by some intrinsic mechanism and is higher than f_0. If the difference between f_i and f_0 is small, the two waves move in and out of phase in an interference pattern, with the beating frequency f_i^b proportional to $(f_i - f_0)$. Assume further that the neuron fires spikes when the total input exceeds a threshold, then spike timing naturally displays phase precession with respect to the LFP theta wave at f_0. Since the change in the firing phase $\Delta\phi \sim f^b t$, and the location of the rat in the place field $\Delta x = vt$ (where v is the running speed), $\Delta\phi = (f^b/v)\Delta x$ grows linearly with the spatial location. Moreover, if the intrinsic frequency f_i increases with v, such that $f^b = \kappa v$, then $\Delta\phi = \kappa\Delta x$, i.e., the linear relationship between the spike phase and the spatial location does not depend on the running speed. This prediction has been confirmed experimentally (343).

The membrane potential oscillation during phase precession is differentially predicted by the three models: it exhibits a beating pattern in the dual oscillator interference model, a ramplike depolarization with increasing theta oscillation amplitudes in the soma-dendritic interference model, and a ramplike depolarization with a constant theta oscillation amplitude in the recurrent network model (Fig. 16*B*). In a tour de force, Harvey et al. (422) tested these models by intracellular recording from hippocampal cells in mice performing virtual navigation. It was revealed that the membrane potential of pyramidal neurons exhibits the time course predicted by the "soma-dendrite interference model" but not other models (Fig. 16*C*). Furthermore, the membrane potential undergoes phase precession with respect to LFP, whereas spiking always occurs at the peak of the transmembrane voltage oscillations (Fig. 16, *D–F*), in agreement with the "soma-dendritic interference model" or "dual oscillator interference model." It remains to be seen whether the recurrent network model can be modified to account for these data.

The dual oscillator interference model has also been applied to the entorhinal cortex, where layer II pyramidal cells display multiple firing fields as predicted by the model (Fig. 16*B*, *top trace*). Indeed, these "grid cells" fire whenever the rat is on any vertex of a triangular lattice spanning the whole surface of the environment (400, 703, 843). In recent years, the dual oscillator interference model has been proposed to account for phase precession as well as the spatial pattern itself of grid cell activity (135, 136, 426, 737). The basic insight is that given animal's running speed v, a temporal interference pattern is converted into a spatial interference pattern (a grid) of firing activity, with the characteristic spatial length $L = v/f_i^b$ (86, 135, 136). The model predicts that the grid scale decreases with the frequency of theta modulation of grid cells, but does not depend on the animal's running speed, which was supported by experimental measurements from behaving rats (471). Furthermore, the grid scale increases from dorsal to ventral medial entorhinal cortex (400). Assuming that the frequency f_i reflects intrinsic membrane oscillations of stellate cells in layer II of the entorhinal cortex (13, 272, 1047), the oscillatory interference model predicts a decreasing gradient of the oscillation frequency along the dorsoventral axis. Consistent with this prediction, an in vitro study found that stellate cells near the dorsal border have slightly higher frequencies (by ~2 Hz) of subthreshold membrane oscillations than those near the ventral border of entorhinal cortex (357, 426). It remains to be seen whether this modest variation in the oscillation frequency is sufficient to account for the observed grid scale gradient from dorsal to ventral medial entorhinal cortex. One potential weakness of this scenario is its extreme sensitivity to noise: computer model simulations found that the grid structure is completely lost when a noise as small as 0.003 Hz was added to the intrinsic frequency f_i (355), and it was estimated that a biologically constrained oscillatory interference scenario predicts a stable grid pattern only for <1 s, far less than what is observed experimentally (1096). Understanding whether the model can be rendered robustly in spite of neural variability will critically test the oscillatory interference model.

In the neocortex, the idea of phase coding at <10 Hz is supported by evidence from a number of physiological work on rats, monkeys, and humans. In a study of visual responses to natural visual stimuli (movies) in anesthetized monkeys, phase coding was examined in different frequency bands of LFP fluctuations. It was found that spike phases of low-band [1–4 Hz (693, 1051) or 8–12 Hz (504, 750)] passed LFP conveyed a significant amount of additional information about movie stimuli beyond that conveyed by spike counts alone. Such a phase dependence may come about through a conversion from phase-modulated strength of afferent input into a particular phase of neuronal firing (the "rate-to-phase transform"). Mclelland and Paulsen (670) examined the "rate-to-phase transform" of single pyramidal cells in rat neocortex in vitro and found that, in the presence of a theta-band membrane oscillation, the level of a tonic excitation could be linearly converted onto a preferred firing phase (670). In human studies, it was reported that detection of a near-threshold stimulus depends on the stimulus onset time relative to the phase of ongoing 5–10 Hz oscillations in the frontal cortex (137) or parietal cortex (657). The likelihood of perception of a faint stimulus depends on neural excitability, which covaries with EEG fluctuations on a fine time scale. As a result, the threshold of conscious perception varies with the phase of theta/alpha band EEG oscillations (137, 274, 657, 995, 1077).

Phase coding has also been proposed for fast gamma-band oscillations (313, 591). A recent study reported that, in a task when monkeys must remember two stimulus items during the mnemonic delay period, spikes of neurons in the prefrontal cortex carried information about the individual memorized objects at different gamma oscillatory phases according to their order of presentation (873). In addition, it has been reported that, in visual cortex of awake monkeys, gamma-band phase of neural spiking (in response to visual stimulation) displayed a systematical relationship with the firing rate (1011). Other studies raised questions about the robustness of phase coding at gamma frequencies. Gamma oscillations are very variable in the neocortex; the oscillation frequencies range widely, and the moment-to-moment LFP cycle duration and phases fluctuate greatly over time. For instance, in an in vivo rat experiment, the gamma cycle duration was found to vary considerably (12–40 ms), whereas the timing of maximum neural firing relative to

the gamma peak remained fixed, implying that the preferred oscillatory phase of neural activity is not reliable (35). In the aforementioned monkey experiment using movie stimuli, at higher frequencies (>12 Hz), the phases of band-passed LFP were highly unrepeatable across different trials at fixed sensory input (Fig. 17) (693); hence, phase coding at higher frequencies (including the gamma band) was unreliable (see also Ref. 797). Search for stimulus coding by EEG gamma phase in human studies has yielded mixed results (518, 975). Finally, in their in vitro work, Mclelland and Paulsen (670) did not observe the "rate-to-phase transform" of single pyramidal cells (the firing phase was independent of the tonic input intensity), if the ongoing rhythm was at gamma rather than theta frequency, in discord with the idea that the input intensity could be encoded by the gamma phase of spiking discharges.

In general, phase noise represents a hindrance for phase modulation as a communication scheme (325). Quite unlike sinusoidal waves typically analyzed in artificial communication systems, neural circuit oscillations are nonlinear. Nevertheless, whereas stable nonlinear oscillators are resistant to amplitude perturbations, they are sensitive to phase perturbations (359, 465, 710, 922). Therefore, noise is a considerable concern for the phase coding concept, more so for higher frequency rhythms (e.g., gamma- versus theta-band). Quantifying the variability of LFP phases, the variability and the fraction of spikes phase-locked to LFP fluctuations, will help clarify the concept of phase coding in studies of local processing as well as synchronization between cortical areas discussed below.

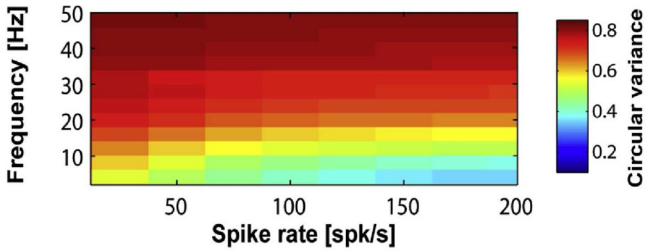

FIG. 17. Phase reliability of LFPs strongly depends on the frequency bands. Under natural visual stimulation (movies) in anesthetized monkeys, for band-passed LFPs in a given frequency range (*y*-axis, in 4-Hz-wide nonoverlapping intervals), the LFP phase at any fixed time during the movie fluctuates from trial to trial, and this phase (un)reliability of V1 LFPs was assessed by the circular variance across trials [defined between 0 (total reliability) and 1 (total unreliability)]. It is plotted as function of the spike rate in the corresponding window, since the reliable phase values must be observed during periods of firing to be useful for phase-of-spiking stimulus coding. Phase coding is reliable if the circular variance is small; this is the case only at low frequencies (a few Hertz). [From Montemurro et al. (693).]

C. Learning and Memory

Insofar as spike synchrony represents a versatile mechanism for sculpting neural temporal correlations, it is a significant factor in determining synaptic learning by virtue of STDP. In line with the facts that theta phase coding of information is reliable (see sect. VI*B*), and activity-induced synaptic plasticity depends on spike timing relative to theta phase (450, 753), numerous studies on behaving humans and animals have implicated theta phase modulation in memory formation and retrieval (24, 60, 156, 424, 425, 432, 488, 515, 518, 832a). A focus of recent research is the interaction between the hippocampus and neocortex, which is functionally important for memory consolidation (931). Simultaneous recordings from the hippocampus and medial frontal cortex in freely behaving rats found that many frontal neurons discharge spikes that are phase-locked to the hippocampal theta rhythm (260, 458, 484, 870, 878), presumably driven by monosynaptic connections from the the ventral CA1 (421, 470), and gamma oscillations generated locally in the neocortex are entrained by the hippocampal theta rhythm (878). Correlated neural firing and LFP coherence between the hippocampus and frontal cortex were enhanced at the theta frequency during a spatial memory task (484); correlation analysis of simultaneously recorded single hippocampal and frontal neurons revealed a hippocampo-frontal directionality (870). This theta-entrained communication may play a role in inducing spike-timing-dependent plastic changes across these networks. Furthermore, intracranial EEG recording in epilepsy patients (287, 854) as well as rat (961, 1045) and monkey physiology (486) indicate that gamma-band oscillations and gamma-theta coupling may also contribute to learning and memory processes. In particular, the dialog between hippocampus and neocortex is mediated through the perirhinal and entorhinal cortices. The rhinal cortices are also strongly and reciprocally connected with amygdala; this connection is thought to be important to facilitate learning in emotionally arousing situations. In awake and behaving rats, coherence of gamma oscillations is prominent in LFPs simultaneously recorded from the rhinal cortices and amygdala, and single-unit spiking activity in both structures was modulated by field oscillations, suggesting a role of gamma-band coherence in effective communication between the amygdala and rhinal cortices (64). There is also evidence for gamma band coupling between the frontal cortex and striatum (76) and theta-band coupling between the hippocampus and striatum (960) during action selection, and gamma-band coupling between the amygdala and striatum during learning (777).

Sleep has long been thought to aid consolidation of newly acquired information in the memory system, and there is accumulating evidence for a beneficial effect of sleep on memory consolidation (100, 919, 920, 1020). In-

terestingly, while dreams during REM sleep are often thought of as reactivated memories, recent work suggests that non-REM, slow-wave sleep is also involved with memory consolidation. In a spatial task where rats repeatedly ran through a sequence of place fields of several simultaneously recorded hippocampal place cells, it was found that immediately following the experience, these cells repeatedly fired in the precisely same sequential order during slow-wave sleep (565). Furthermore, during slow-wave sleep, hippocampal neurons are phase locked to neocortical up and down states (403). Frontal neurons consistently fire within 100 ms after hippocampal neurons, and this coupling is much stronger during sharp wave sleep than REM sleep (1055). Coordinated activity in hippocampal and neocortical neurons displayed replay of temporal patterns observed in the previous awake experience, suggesting that slow-wave sleep may facilitate simultaneous reactivation of coherent memory traces in the hippocampus and neocortex (478). In human studies, motor learning increased slow-wave activity during subsequent sleep, locally in specific brain regions, and this local increase after learning correlated with improved performance of the task after sleep (449). In another study, boosting slow oscillations artificially by transcranial electrical field stimulation enhanced hippocampus-dependent memory (647).

Precisely how slow-wave sleep might contribute to memory consolidation remains unclear presently. Compared with wakefulness, slow-wave sleep is characterized by a breakdown of effective connectivity in the cortex, as assessed by how the activation of one cortical area (evoked by transcranial magnetic stimulation) is transmitted to the rest of the brain (653, 284). At the same time, during slow-wave sleep, the cortex undergoes synchronous up and down states, which might be particularly suited for inducing some form of spike-timing-dependent plasticity across brain regions. The sign (potentiation versus depression), however, depends on precise timing relationship between neurons (81, 213). In fact, there is evidence that excitatory synaptic connections in the cortex are overall depressed in sleep and potentiated in wakefulness (1019), suggesting that a primary function of slow-wave sleep is homeostatic regulation of synaptic circuitry (283, 655, 959).

A correlation between neural coherence and memory behavior, whenever observed, is typically weak. For example, Jutras et al. (486) recorded from single units and LFP in hippocampus of monkeys on a recognition memory task. In the experiment, each visual stimulus was presented twice, randomly interleaved with other stimuli. Although the monkeys were not required to produce a behavioral response, memory recall was assessed by monkey's looking time on a stimulus which is shorter with a repeated item compared with its first presentation. It was found that spike-field coherence increased by ~10% from a baseline of ~0.1 in the gamma frequency range during encoding of stimuli (at their first presentations) that were subsequently well recognized relative to those stimuli that were poorly recognized (at their repeat presentations). The increased coherence may aid STDP, hence learning (486, 1067). One may reasonably ask: Why does this 10% of 10% coherence matter, and how about the majority of spikes that are not correlated with field gamma? Stable computation may require that spiking activity of neurons is predominantly asynchronous, and learning through STDP relies on a small fraction of synchronous spikes, but at the present we do not know if that is the case. It will be a challenge, in future research, to develop a quantitative, biophysical, model that can account for memory behavior (good versus poor recognition) based on the observed small change in spike-field coherence.

D. Multisensory Integration

While wakefulness is not associated with large-amplitude EEG synchronization, subtle synchronous coordination is thought to be important for the integrative brain functions in behaving states. A general computation of this kind is to combine information from different sensory modalities, such as binding of vocalized sounds with vocalizing faces in speech perception (257). The traditional hierarchical model posits that crossmodal integration is instantiated by convergence of input pathways from different senses to higher-level multisensory areas. Recent experimental evidence, however, points to the possibility that multisensory interplay involves coherent oscillations across cortical areas (349, 490, 549, 551, 627, 687, 857, 1087).

Ghazanfar et al. (349) investigated binding of a vocalized sound and its associated mouth movement in monkeys. They recorded LFP and single units from the auditory cortex and the superior temporal sulcus (STS, an association area involved with integrating audiovisual biological motion). While the power spectrum of LFP displays a peak in the gamma band in the auditory cortex when a voice stimulus was presented, and in STS when a face was presented, the inter-areal coherence shows a peak only when both stimuli were presented simultaneously (Fig. 15*D*); hence, gamma band coherence across areas is correlated with multisensory integration. Another study by the same group used visual and auditory inputs that were either looming or receding. It was found that coincident looming visual and auditory stimuli to be particularly salient behaviorally (presumably mimicking an approaching object, potentially a predator) (626). Gamma power in an auditory cortical area or STS was no different in the unisensory versus multisensory condition. On the other hand,

gamma-band coherence between the two areas was significantly larger with congruent visual and auditory looming stimuli, compared with a looming visual or auditory stimulus alone, or to incongruent visual and auditory stimuli (one was looming, the other was receding) (627). This finding suggests that synchronization may act as a mechanism for rapidly and transiently enhancing functional connections between selective neural populations that encode stimuli of different modalities. The resulting correlated activity of the two cortical areas may impact more effectively on downstream neurons (287, 310, 549, 838, 1068), as a potential mechanism for integration of sensory information across modalities.

E. Selective Attention and Working Memory

As noted at the beginning of this review, gamma oscillation was initially called a "hypervigilance rhythm" because of its correlate with highly alert brain states (102). Over the years, this idea has received increasing supporting evidence. EEG or MEG recordings in human studies have shown that attention is associated with a reduced EEG alpha rhythm (152, 452, 780, 845, 946, 983, 1073) and increased gamma rhythm (224, 311, 852). A recent study using "dynamic causal models" of MEG data found that forward and backward functional connections between cortical areas are asymmetric and frequency dependent; high (gamma) frequencies in higher cortical areas suppressed low (alpha) frequencies in lower areas (168). Enhanced gamma power associated with attention has been documented for various sensory modalities: audition (203, 223, 285, 328, 388, 482, 785, 886, 952), vision (245, 270, 754, 797, 872, 938), somatosensation (65, 427, 521, 797, 824), and pain (386, 427). For example, Ray et al. (797) recorded subdural electrocorticography (ECoG) in epileptic patients, when they were asked to pay attention to either auditory stimuli or vibrotactile stimuli. ECoG in the auditory and somatosensory cortical areas showed an early and a late component of event-related gamma-band activity. The early component was localized in modality specific cortical areas, and not modulated by attention. In contrast, the late component (400 ms after the target stimulus onset) is larger in the somatosensory (respectively auditory) cortex when subjects attended vibrotactile (respectively sound) stimuli. Moreover, at electrode sites in the prefrontal cortex, ECoG gamma activity was negligible when a stimulus was presented in an unattended modality, but large in response to the presentation of an attended stimulus regardless of whether it was auditory or vibrotactile. These observations suggest that gamma-band oscillations in a sensory area are enhanced by selective attention, involving top-down signals from the prefrontal cortex.

In a ground-breaking study, Fries et al. (312) combined neuronal recording with LFP measurements in monkeys performing a task that depended on location-specific visual attention. In this task, monkeys were required to direct attention to one of two visual (moving grating) stimuli that were inside and outside, respectively, the receptive field (RF) of recorded neurons (multiunit activity) and LFP in the cortical area V4 (an important area for visual object processing) (312). It was found that attention into the RF, compared with attention outside the RF, reduced LFP power at low frequencies (<15 Hz) and enhanced gamma power (at 30–90 Hz) (Fig. 1*B*). Local synchronization was assessed using spike-triggered averaging of LFPs, which was enhanced by attention while multiunit spike activity remains seemingly stochastic (Fig. 1*B*). This observation was confirmed with spike-field coherence, which measures phase synchronization between spikes and LFP as a function of frequency. Subsequently, with the use of the same task paradigm. it was reported that large spike-field coherence immediately before the onset of a test stimulus was correlated with faster response times, demonstrating an effect at the behavioral level (1069). In a separate study using a visual search paradigm (where the subject looks for a target stimulus surrounded by distractor stimuli) while recording from monkey's V4, spike-field coherence displayed a peak in the gamma band when a preferred stimulus was presented in the RF of a recorded neuron, and it matched a feature of the target (84). Because it occurred even when the preferred stimulus is a distractor and the target itself is not in the RF, the finding suggests a role of gamma band coherence in parallel processing of all objects in a cluttered scene. Finally, the same group recently carried out simultaneous recording from neurons in V4 and in FEF (a putative "source area" for top-down attention signal) and found that attention to a stimulus in their joint RFs increased inter-areal coherence especially in the gamma band, with a time shift consistent with the idea that FEF initiates attention induced enhancement of gamma oscillations (381).

How enhanced synchrony might contribute to selective attention has been investigated in modeling work. In an early study, Niebur and co-workers (723, 724) proposed that an attentional signal increases synchrony among sensory neurons, and this enhanced temporal correlation is detected by interneurons, which in turn suppress other neurons selective for nonattended stimuli, thereby implementing biased competition (230, 698, 803). Other work argued that competitive advantage by attention is amplified if an attentional signal directly targets interneurons engaged in gamma oscillations (97, 98, 133, 948–950, 1092). Assuming that oscillations are generated by an interneuronal mechanism, Tiesinga and collaborators (948, 950) examined the impact of random jitters among (otherwise perfectly clocklike)

inhibitory inputs to a pyramidal cell and showed that less jitter (higher synchrony) leads to a larger slope of the pyramidal cell's input-output relationship, suggesting that synchrony contributes to gain modulation (665, 973, 974). This scenario for the multiplicative gain modulation requires that jitters of spike times be small (<5 ms); thus interneurons must behave almost like regular oscillators. A related but more general mechanism for gain modulation is mediated by correlated excitatory and inhibitory inputs (837, 838). A fairly consistent observation that has not been taken into account in these models is that the variability of spike trains, measured by the Fano factor, is typically high (~1 or larger) and is either unaffected (664, 900) or only slightly decreased (688) by selective attention. Note that both competition and gain modulation can be realized by mechanisms solely based on rate modulation, e.g., competition through feedback inhibition (30, 803) and gain modulation by balanced inputs (163) or by a noise-induced input-output power law (708). Nevertheless, rate modulation may be enhanced by the presence of gamma oscillations (129), which might lead to improved sensory processing such as signal discrimination (656).

These modeling studies focused on how a tonic attentional input modulates oscillations intrinsically generated in a sensory circuit. On the other hand, top-down attentional signals may themselves be endowed with rhythmicity. The parietal and prefrontal cortical areas are "source areas" for top-down attentional signals to sensory systems (179, 194, 230, 697), and coherence between these areas and early visual areas is modulated by attention (872). The parieto-prefrontal circuit is also important for working memory, brain's ability to temporally hold information "online" (324). In monkey experiments where subjects were required to remember the location of a stimulus cue across a delay period (a few seconds), neurons in the parietal cortex (360) and prefrontal cortex (323) exhibited location-selective persistent activity during the delay (see Ref. 188 for a review). Such persistent neural activity could also serve spatial attention by providing a location-specific and internally sustained top-down attention signal to bias sensory processing. Therefore, working memory and attention control may share a common cortical circuit substrate. There is also evidence that, whereas fast gamma oscillations are involved in the maintenance of relevant information, the slow alpha rhythm is implicated in suppressing irrelevant information in memory (475, 517, 748, 749, 846) and attention (246, 845, 946) tasks. Hence, at a given cortical site, alpha rhythm may be reduced when attention is focused on external stimuli processed by that brain area, but enhanced when sensory information flow to that area is behaviorally irrelevant and should be ignored.

Does activation of the parieto-prefrontal circuit induce similar synchronous oscillations during working memory tasks as in attention tasks? Indeed, MEG, EEG, and intracranial EEG recordings in human studies have revealed gamma oscillations in parietal, frontal, and other cortical areas during working memory tasks (444, 476, 477, 614, 994). Moreover, in a monkey experiment using a spatial working memory task, LFP and spike-field coherence in the lateral intraparietal (LIP) area showed enhanced gamma oscillations during a mnemonic delay period (759). A small number of single units in LIP also displayed a peaked power spectrum in the gamma frequency range. In contrast, other studies using the same spatial working memory task did not find gamma oscillations in the majority of single units recorded from the posterior parietal cortex area 7a (480) or dorsolateral prefrontal cortex (184). These results highlighted the need for simultaneous recording of LFP as well as single-unit activity, to resolve the discrepancy between studies and better assess coherent oscillations in an activated parieto-prefrontal network.

Self-sustained persistent activity has been hypothesized to be generated by reverberatory local circuit dynamics (18, 364, 1030). Interestingly, in biophysically realistic models of working memory (182, 939, 1029), highly recurrent networks naturally give rise to fast coherent oscillations. The amplitude of network gamma oscillations is controlled not only by the strength of recurrent connections, but also the ratio of NMDA and AMPA receptors at the horizontal excitatory connections (129, 182, 939, 1029). This is because, as discussed in sections III*C* and V*C*, oscillations readily occur in an excitatory-inhibitory loop, when synaptic excitation is mediated by AMPA receptors and faster than inhibition.

If the working memory/attention circuit is prone to fast oscillations, attention-induced enhancement of gamma oscillations in sensory circuits may simply be a signature of the engagement of such a "source area" for top-down biasing signals. To test this idea, Ardid et al. (31) considered a two-module model of spiking neurons that consists of a reciprocal loop between a sensory (e.g., MT) network and a working memory (e.g., PFC) network. In this model, feature-selective attentional signal, originating in the working memory circuit, projects top-down to bias stimulus processing in the sensory circuit (Fig. 18*A*). The model captures biased competition and provides a circuit implementation of the "feature-similarity gain principle," namely, the attentional effect on a neuron's firing rate is a graded "gain modulation function" of the difference between the neuron's preferred feature and the attended feature (649, 973). The sensory circuit (in response to a stimulus) and the working memory circuit (when activated during sustained attention) both display sparsely synchronized gamma-band oscillations (Fig. 18, *B* and *D*) while spiking of sensory neurons is highly

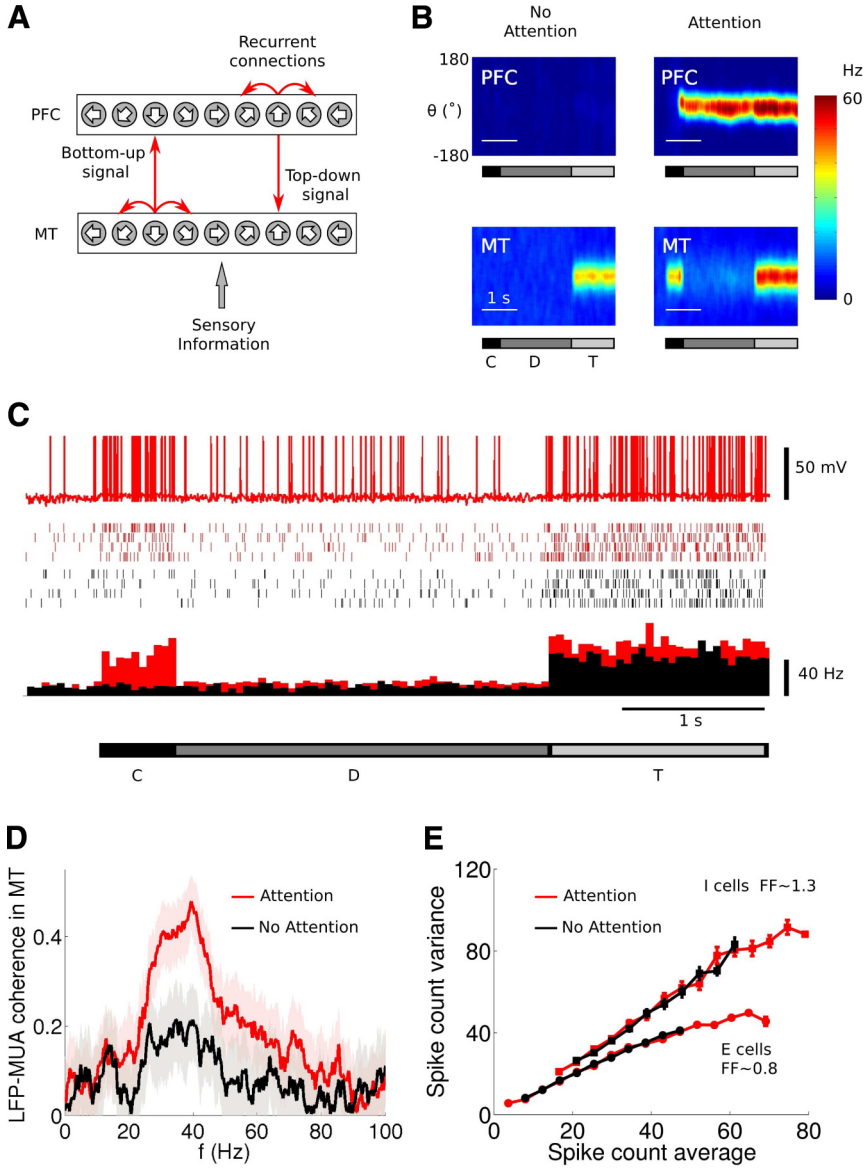

FIG. 18. Synchronous field gamma oscillation with irregular neural firing in a spiking network model of selective attention. *A*: schematic model architecture of a reciprocal loop between a sensory (MT) circuit and a working memory (PFC) circuit ("source area" for top-down attention signals). Each of the two circuits includes excitatory pyramidal neurons (E cells) and inhibitory interneurons (I cells) that are selective for a stimulus feature. Local connections within each circuit and cross-areal connections between excitatory cells depend on their respective preferred stimulus features. Top-down projection from the working memory circuit targets both excitatory and inhibitory cells in the sensory circuit. *B*: network activity for an unattended (*left*) and an attended trial (*right*). *x*-Axis, time; *y*-axis, neurons labeled by preferred feature. Activity is color coded. C, cue period when an attentional cue is presented; D, delay period; T, test period when a sensory stimulus is presented. Note that in the attended trial (*right*), the attention cue triggers a self-sustained activity pattern in PFC, and enhanced sensory response in MT during tested period. Also note striplike structure in the spatiotemporal activity pattern, indicating synchronous oscillations. *C*: activity of a neuron in response to a preferred stimulus. *Top*, sample membrane potential; *middle*, spike trains in several trials; *bottom*, trial-averaged activity (red, attended; black, unattended trials). *D*: average coherence between the LFP and MUA in the sensory circuit increases in the gamma-frequency range for attention (red) relative to non-attention (black) trials during test stimulus presentation. *E*: the variance versus mean of spike counts (Fano factor is given by the slope) for E cells and I cells in attended (red) and unattended (black) trials. [*A–C* from Ardid et al. (30); *D* and *E* from Ardid et al. (31).]

irregular (with the Fano factor close to 1) (Fig. 18, *C* and *E*). Thus the model reproduces the common observation from monkey experiments that weak network rhythmicity coexists with highly irregular neuronal spike discharges, which is important since how synchrony affects attention depends on the dynamical state of the network. In this model, the activation of the "source area" (which itself is oscillatory) during selective attention results in an enhancement of oscillations in the sensory circuit (Fig. 18*D*) and inter-areal coherence in the gamma frequency band. In this model, a manipulation that abolishes inter-areal coherence reduced attentional gain modulation by ~10% (31). Therefore, in a dynamic state where single neurons fire stochastically rather than behaving like oscillators, gamma-band coherence across areas may play a modest but significant role in boosting sensory processing during selective attention.

F. Top-Down Signaling in a Cortical Circuit Loop With Layered Structure

Curiously, while gamma oscillations are commonly enhanced under conditions that involve cognitive control, top-down signaling itself may be particularly associated with beta-band neural activity. As mentioned in section I, numerous studies have documented beta oscillations associated with movement behavior (26, 41–46, 103, 197, 252, 286, 562, 567, 617, 711–713, 735, 765, 836, 842, 1001) and response inhibition (520, 536, 537, 774, 925, 1094). But beta power has also been implicated in broader cognitive processes. Descending control in cognitive tasks was examined in several recent monkey physiological experiments, used LFP and single-unit recordings from two cortical areas. In a delayed match-to-sample task, when the subjects had to retain in working memory the identity

and spatial location of a visual sample stimulus, to decide whether it matches a second stimulus presented a delay later, there was an enhanced coherence at ~20 Hz between MT (a sensory area) and LIP (a cognitive area), in LFP or neural spikes, in a way that is specific to the preferred location and feature of the recording sites (834). A second study used a visual search task and found that the LFP coherence between LIP and FEF is enhanced at ~20 Hz in guided search (which involves top-down signaling from FEF) when distractors resemble the target in some feature (color or orientation of a visual stimulus), compared with "pop-up" (which is a feedforward process) when the target is dissimilar to the distractors (138). In a third experiment, subjects performed a reach movement either freely or according to an instructed cue, and spike-field coherence at ~15 Hz was enhanced between a parietal ("reach") area and a frontal (premotor) area in free choices compared with forced choices (760). It is noteworthy that in all three experiments, the enhanced coherence was observed in the beta, not gamma, frequency range.

Why would beta oscillations play a special role in top-down signaling? To answer this question, it is essential to consider in more detail reciprocal interactions between cortical areas with laminar structures (167, 611, 612, 787, 943). In the neocortex, gamma-band oscillations is prominent in superficial layers 2/3 (132), which is endowed with abundant horizontal connections (85). In contrast, deep layers 5/6 seem to have a propensity to display lower-frequency beta-band oscillations. In an experiment with monkeys performing an attention task, lamina-localized recording revealed gamma oscillations in superficial layers and beta oscillations in deep layers (130). In consonance with this observation is the finding from an in vitro somatosensory rat cortical slice preparation with application of kainate (817). When the superficial and deep layers were separated by a cut through layer 4, they were found to exhibit oscillations in the gamma versus beta frequency ranges, respectively (817; see Ref. 530 for a detailed model with multiple cortical layers). Consider two reciprocally connected cortical areas, as schematically illustrated in Figure 19. Feedforward projections from a "lower" cortical area to a "higher" area originate in the superficial layers, whereas the deep layers of the higher area mediate feedback projections to the lower area as well as to subcortical brain structures (50, 253, 352). A recent model of the thalamocortical system also proposes that beta rhythm primarily emerges in the deep layers of the cortex (387). Thus beta oscillations produced in the deep layers may be especially involved in long-distance signaling along feedback pathways. Top-down signals may encode expectation that guides learning; consistent with this idea was the finding that, in the hippocampus, beta oscillations were prominent especially in the early phase of learning in a novel environment (77).

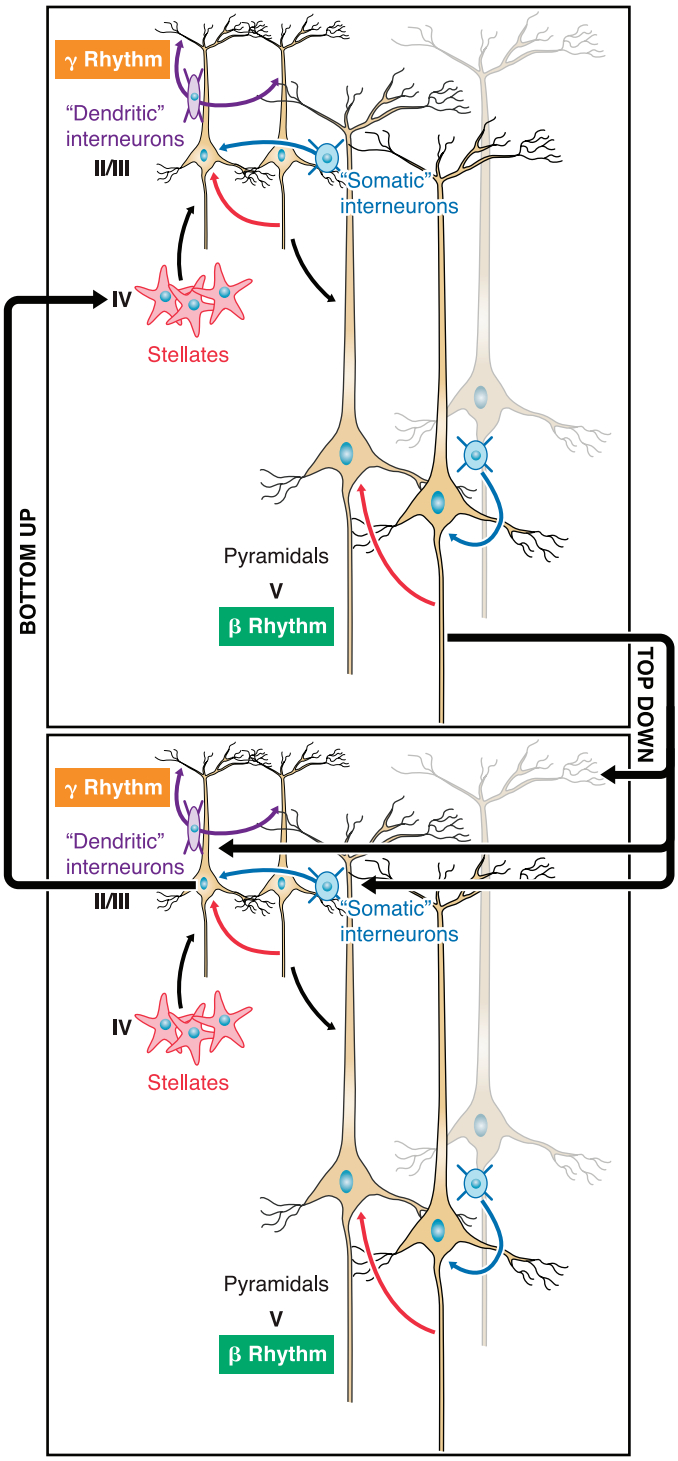

FIG. 19. Schematic circuit for the interplay between beta- and gamma-band oscillations in top-down signaling. Shown is a reciprocally connected loop between a sensory-type area and a cognitive-type area. In each area, the superficial layers are endowed with strong intrinsic synaptic connections and generate synchronous oscillations in the gamma frequency range, whereas the deep layers have a propensity to display oscillations in the beta frequency range. Top-down projections originate in the deep layers and predominantly target the superficial layers, where they innervate pyramidal cells (brown), as well as dendrite-targeting (purple) and perisoma-targeting (blue) inhibitory interneurons. In this scenario, beta oscillations are directly involved in top-down signaling, which interacts with locally generated gamma oscillations.

Beta oscillations in top-down signaling are especially well documented in the rat olfactory system. Field oscillations occur in both gamma and beta frequency bands in the olfactory bulb (91, 111, 607, 648, 795, 1003) and the piriform cortex (111, 720, 775). Simultaneous field potential recordings in behaving rats indicated that beta band oscillations originate in the cortex (502). This is reinforced by a study with urethane-anesthetized rat showing that beta, but not gamma, rhythm was abolished by lesion of the cortifugal pathway (the lateral olfactory tract); hence, beta oscillations may be produced within the piriform cortex and (from the deep layers) projected back to the olfactory bulb (720). Recent two-photon guided minimal stimulation experiments (49) demonstrated that feedback projections from the piriform cortex target inhibitory granule cells in the olfactory bulb, with synapses that exhibited short-term facilitation when tested at ~20 Hz, suggesting a specific pathway for beta frequency top-down signaling in the olfactory system.

A prominent role of beta-band oscillations in top-down projections would explain why inter-areal coherence associated with selective attention (385, 834), working memory (933), guided search (138, 139, 726), object recognition (855), perception (251, 327), or sensorimotor integration (57, 118, 121, 1066) is especially conspicuous in the beta frequency range. It may also account for beta rhythm observed during attention in the basal ganglia (197) or in the thalamus (1074), as a result of inputs from deep layers of cortical areas upstream. Interestingly, modeling studies showed that synchronization can tolerate longer synaptic delays for beta than gamma oscillation (83, 282, 528), suggesting that long-distance oscillatory synchronization may be more robustly realized at beta frequencies.

Theta band oscillations may also play a role in top-down processing (871, 1017, 1018). Just as gamma rhythm is commonly associated with working memory and attention, so are field theta oscillations (489, 569, 677, 790, 981) and theta-band inter-areal synchronization (844). In anesthetized rats, theta frequency oscillations are especially prominent in deep layers of the neocortex (924). In a study with behaving cats performing a visual discrimination task (stimulus 1, go; stimulus 2, no go) (1018), it was found that cross-correlation of field potentials from the primary visual cortex and the association area 7 was enhanced on go stimulus trials, in the theta- but not gamma-band. This increased coherence is selective between the infragranular layer of area 7 and supragranular layer of V1 (with area 7 leading V1 by a time lag), suggesting a top-down influence. This and other studies (reviewed in Ref. 1017) are consistent with the view that long-distance neural synchronization might primarily occur in slower (beta and theta) frequency bands.

If the top-down signaling carries beta-band rhythms, how does this fit with the idea of enhanced gamma-band oscillations during attention and working memory, as discussed above? Feedback projections from a cognitive-type area to a sensory area preferentially synapses onto neurons in the superficial layers 2/3, including pyramidal cells, perisoma-targeting, and dendrite-targeting interneurons (Fig. 19) (51, 672). Therefore, such top-down signals are well suited to modulate gamma oscillations, locally generated in the superficial layers in a context-dependent manner.

Synchronization also involves interactions between the neocortex and the thalamus (235, 391, 451, 483, 451, 601, 907, 1007). In particular, the widespread cortical projections of matrix cells in the dorsal thalamic nuclei (483) and the intralaminar nonspecific thalamic nuclei (601) appear to be well suited for synchronizing disparate cortical areas. The relative importance of cortico-cortical versus cortico-thalamic connections remains to be elucidated in the future.

VII. SYNCHRONIZATION DYSFUNCTION ASSOCIATED WITH MENTAL DISORDERS

Data reviewed above begin to reveal specific roles of cortical oscillations in integrative brain processes and executive control. To demonstrate that these contributions are critical, one way would be to disrupt oscillations (e.g., by optogenetic methods) and assess the consequences in cognitive behaviors. Another direction is to examine how neural synchronization may be impaired in patients known to exhibit deficits in information integration, working memory, and selective attention. Insights gained along this line would not only clarify whether, or in what specific ways, cortical oscillations are truly important for cognition, but also might help us understand the neural circuit basis of cognitive impairments associated with brain disorders. Summarized here briefly, this area of research is still new, but with potentially significant implications in Psychiatry and Neurology (428, 564, 986, 989).

A. Schizophrenia

Cognitive deficits are at the core of a wide range of mental pathologies in schizophrenia (379). Friston (316) argued that key cognitive functions that are impaired in schizophrenia, such as distractibility of attention and loosening of association in thought, could be caused by abnormal functional connections in the brain. A number of theoretical, behavioral, and fMRI studies reported impaired connectivity in the schizophrenic brain (212, 336, 438, 439, 558, 596, 1059, 1063). In physiological studies, there have been an avalanche of recent publications reporting impaired beta- and gamma-band synchronization in schizophrenic patients in a variety of behavioral tasks

(55, 174, 295, 398, 534, 541, 570, 587, 894, 895, 926, 986, 987; reviewed in Ref. 988). Some of these studies are not free from confounds discussed in section VI*A*, but taken together, these studies indicate that EEG fluctuations in the beta and gamma bands are abnormal in schizophrenia. For example, while subjects viewed a Gestalt stimulus, phase coherence between distributed cortical areas was reduced in schizophrenic subjects compared with control, in either gamma (894) or beta (986) frequency range. A few studies attempted to directly assess the correlation between synchrony and behavior. Spencer and collaborators (895) found that in response to a Gestalt stimulus, there was a brief (~100 ms) burst of gamma-band EEG power phase-locked to the reaction time in the occipital cortex of healthy subjects, but the peaked power was weaker and at lower frequencies in schizophrenic patients. In another study, schizophrenic patients were found to perform worse than the control group in a perception task (detection of human faces in degraded pictures); at the same time, MEG over parietal cortical sites displayed sensory responses concentrated in the beta/gamma frequency range, that was smaller in schizophrenia than in healthy subjects (953, 989). Recent studies found abnormal gamma-band EEG signals (399) and abnormal brain network connectivity as assessed by correlations of beta-band MEG signals recorded in the prefrontal and parietal cortices (59), during working memory in schizophrenia.

Inter-areal connections may well be aberrant in schizophrenia, but physiologically measured alternation in inter-areal coherence may also arise from impaired dynamics in circumscribed brain structures leading to abnormal brain-wide neural signals. For example, a computational study suggests that the lower frequency of EEG oscillations seen in schizophrenic subjects (895) could be explained by some observed deficits in the inhibitory GABA system of schizophrenic patients in the prefrontal cortex. Specifically, decreased GABA transporter 1 (GAT1) and the 67-kDa isoform of glutamate decarboxylase (GAD67, an enzyme that synthesizes GABA) (579, 580) may lead to a slower $GABA_A$ receptor-mediated IPSCs, hence lower-frequency oscillations (1009). Moreover, in a rat model of schizophrenia, a reduction of parvalbumin-expressing interneurons in the medial frontal cortex and ventral subiculum gave rise to a reduced gamma-band response to a conditioned tone during a latent inhibition paradigm and an impaired behavioral expression of latent inhibition (602).

On the other hand, schizophrenia is associated with NMDA hypofunction (especially in the prefrontal cortex) (199, 535), which may cause cognitive dysfunctions in multiple ways. First, NMDA receptors are important for synaptic plasticity; hence, abnormal NMDA signaling is detrimental to learning and memory (903). Second, working memory may be impaired because persistent activity cannot be stably maintained by fast AMPA receptor-mediated excitation alone (182, 259, 800, 939, 1023, 1029, 1030). Third, NMDA receptor-mediated excitatory reverberation may be critical for slow time integration of information underlying decision making computations (1032, 1034, 1071). Fourth, NMDA hypofunction leads to a selective reduction of the excitatory drive for a subpopulation of interneurons (72, 389, 582, 1024); one of the consequences could be abnormal inhibition-dependent synchronous oscillations (593, 633, 818). The precise mechanism remains controversial, in part because in the adult rodent frontal cortex, the majority of parvalbumin-expressing fast spiking interneurons, which should play a critical role in gamma oscillations, are devoid of the NMDA receptors (1024). Abnormal changes could occur throughout the cortex, or more selectively in certain cortical regions like the PFC. Since strongly recurrent working memory circuits are particularly prone to fast oscillations, as we discussed in section VI*E*, abnormal gamma or beta rhythm observed in schizophrenia could be a sign of an impaired working memory circuitry (1033), in line with the well-documented working memory and selective attention deficits associated with schizophrenia (52, 258, 363, 379). In addition, cortical oscillations are strongly influenced by the activation of neuromodulators, and an early lesion study (692) showed that cortical gamma rhythm in the parietal and frontal cortices depended on dopamine signaling which, as is well known, is severely impaired in the PFC associated with schizophrenia (265, 363, 853).

In summary, extant empirical evidence points to two candidate explanations for reduced beta- and gamma-band synchronization associated with schizophrenia: *1*) dysfunctional operations in the prefronto-parietal circuit of critical importance to working memory, attention, and decision making and *2*) impairments in long-range connections throughout the brainweb. Obviously, these two are not mutually exclusive and may both be affected by the disease. Future experiments designed to differentially elucidate these two scenarios would shed important insights onto the brain circuit basis of integration dysfunctions in schizophrenia.

B. Autism Spectrum Disorders

Patients with autism spectrum disorders (ASD) have impaired sociability, communication deficits, and unusual patterns of restricted activities. Individuals with ASD commonly show "persistent preoccupation with parts of objects"; they are superior at certain tasks that require attention to local details, but poor at performing tasks based on global meaning. Therefore, a characteristic of ASD appears to be a relative inability to integrate pieces of information into coherent wholes (317, 346, 416, 417).

The "weak coherence account" has recently been examined using fMRI and EEG/MEG techniques. fMRI experiments consistently reported a reduced functional connectivity in ASD subjects (158, 485, 493, 529, 1010). Of particular interest were the observations of a reduced connectivity in the cortical language system during sentence comprehension (485), and in the prefronto-parietal system of "theory of mind" when patients were asked to attribute a mental state to animated geometric figures with implied intentions (e.g., coaxing, tricking) (493). More recently, EEG/MEG studies, with much better time resolution (but poor spatial resolution) than fMRI, have been carried out to assess neural synchronization in ASD subjects (78, 120, 382, 685, 707, 745, 1064; reviewed in Refs. 813, 986, 989). The results so far are inconclusive, and reported abnormality of gamma-band EEG power in ASD patients was not correlated to behavioral difference with the healthy control group. Among possible reasons are that most published work looked at band-passed EEG powers in different locations rather than inter-areal coherence, and that in these studies subjects were either in the resting state or viewing visual stimuli, but not engaged in processes (such as mentalizing or communicative intent) that are dysfunctional in ASD. Future studies will undoubtedly address these issues. It will also be interesting, in future work, to combine fMRI with simultaneous EEG/MEG recording to investigate whether and how abnormal neural synchrony in the brain system directly correlates with atypical functional connectivity measured by fMRI in ASD subjects.

Interestingly, whereas schizophrenia is associated with NMDA hypofunction, the autistic brain appears to exhibit NMDA hyperfunction. Studies using a rat model of autism (with prenatal exposure to valproic acid) suggest that ASD is associated with an abnormal increase in the NMDA receptor expression, leading to hyperplasticity and hyperconnectivity between pyramidal cells in local cortical circuits (646, 807–809). This would provide an explanation for dysfunctional brain connectivity. In addition, as discussed in sections III and V (Fig. 14), a tightly maintained balance between synaptic excitation and inhibition is critical to normal neural synchronization. Hence, an abnormal excitation-to-inhibition ratio (in part due to excessive NMDA receptor expression) associated with heterogeneous subtypes of autism (215, 825) could give rise to aberrant neural synchronization (and potentially the resulting behavioral symptoms) associated with autism spectrum disorders. Therefore, in principle, the same molecular alternation (impaired NMDA signaling) can cause abnormal connectivity assessed by fMRI and abnormal synchrony measured by EEG/MEG; hence, the two must be correlated, but they occur through separate processes (synaptic plasticity and "online" excitation/inhibition dynamics, respectively).

Brain dysfunctional connectivity has drawn increasing attention not only in schizophrenia and autism research, but also in the fields of neurodegenerative diseases (429) and neurological disorders (428). This in part arose from a growing appreciation that inasmuch as cognitive functions are carried out through coordinated action of multiple interacting brain structures (112a), cognitive deficits associated with brain disorders cannot be fully understood in terms of focal abnormalities confined to certain brain regions. To make progress, we need to know a lot more about the brain connectome (92, 586, 860, 897, 996). What are the defining features of the brain-wide architecture? Can it be described by the small-world network or other types of complex networks (3, 56, 436, 491, 896, 993)? Can we use graph theoretical analysis to assess circuit properties [such as the path length (a measure of effective communication), the clustering coefficient (the degree of clustering of connections), cost efficiency, hub structures (nodes with an exceptionally large number of connections and low clustering)], as a tool to quantify the network basis of mental illness? For example, the brains of both Alzheimer's disease (219, 901) and schizophrenia (58, 829) show shorter path lengths (indicative of network randomization), but what are the differences in their connectivity properties that can account for the entirely different behavioral symptoms of these two brain diseases? Likewise, abnormal gamma and beta oscillations have been observed in patients with schizophrenia, ASD, and other brain disorders, but are these deficits specific in each disorder to serve as a biomaker and phenotype for diagnostic purpose? Future research along these lines is needed to identify distinct types of network dysfunctional connectivity associated with different disorders.

VIII. CONCLUDING REMARKS

Remarkable progress has been made over the last two decades in our understanding of the physiological basis of synchronous oscillations such as gamma and theta rhythms, which occur in the cerebral cortex of awake behaving mammals. We have learned that there is a wide diversity of cellular and circuit mechanisms underlying the generation of such rhythms; at the same time some unifying themes and general principles have begun to emerge. Impact of single neuron properties on network oscillations can be systematically characterized according to whether they display type I or type II phase response dynamics, resonance, or pacemaker properties. Intrinsic gamma or theta (subthreshold or bursting) oscillations in individual neurons appear to critically depend on voltage-gated sodium and potassium channels. This is in contrast to, for example, spindle waves during quiet sleep or epileptic discharges where rhythmogenesis

of pacemaker neurons relies on calcium channels (236, 237, 908, 964, 968).

As a general rule, for cortical rhythms observed in awake states, circuit synchronization depends on synaptic inhibition, either through mutual inhibition in an interneuronal network or feedback inhibition in a reciprocal loop between excitatory and inhibitory neural populations. Subclasses of GABAergic cells contribute differentially to different rhythms, and to the timing of pyramidal neuronal activity at different phases of an oscillation cycle. Cortical rhythms can arise from synchronization of coupled oscillators when noise is absent or small, which are well described in the framework of coupled oscillators. Alternatively, they can emerge from strong feedback synaptic interactions in a predominantly asynchronous circuit with highly stochastic spiking activity of individual cells, which are captured by the theory of sparsely synchronized oscillations. These two scenarios should be readily distinguishable when the level of population rhythmicity or coherence is quantitatively assessed at the same time as the variability of single neuron spike activity. Furthermore, importantly, they have contrasting predictions about the circuit mechanisms of different fast cortical rhythms. As we have seen, rhythms produced by an interneuronal mechanism in cortical circuits are ultrafast (>100 Hz) when single neurons fire irregularly in a sparsely synchronized oscillation, but at ~40 Hz when single neurons behave like regular oscillators. With highly irregular firing of single neurons, the excitatory-inhibitory loop mechanism naturally gives rise to gamma- and beta-band oscillations. The propensity is especially high when recurrent connections are strong, a characteristic of "cognitive-type" (working memory and decision making) cortical areas like the prefrontal or posterior parietal cortex. Therefore, gamma and beta oscillations are expected to be naturally enhanced in any behavioral task that engages top-down control signals from these areas. In a laminar cortical circuit, descending signals originate in the deep layers (which are prone to beta rhythm) of a "source area" and project to the superficial layers (where gamma oscillations are prevalent) of a recipient area. This model remains to be tested experimentally, and computational implications of the proposed dynamic interplay between beta and gamma oscillations deserve to be explored in the future.

An increasing number of recent studies have documented long-distance coherence in specific cognitive processes. Under the premise that stochasticity predominates in the cortex, in the sense that single neuron firing is irregular and population activity is prevalently asynchronous, functional implications of weak synchrony embedded in highly stochastic neural activity patterns can be more appropriately appraised in the framework of sparsely synchronized oscillations rather than coupled regular oscillators. Two possible views are conceivable with regard to the role of weak synchrony in long-distance neuronal communication. In the first scenario, the bulk of (asynchronous) spike firing might be somehow blocked, e.g., due to a strict balance between excitation and inhibition (1015). Consequently, as a "default mode," interareal communication channel is closed in the absence of synchronization, and transient coherence provides a temporal window of opportunity for effective communication. In an alternative scenario, spike firing (synchronous or not) carries the main flow of information among cortical areas. Some types of computation and synaptic plasticity critically depend on correlations in fluctuating neural activity, and synchronous oscillations provide an appealing means for modulating spatiotemporal neural correlations. This modulation may be modest but important, in the same vein as gain modulation of sensory neurons by selective attention which is typically weak yet functionally significant (e.g., leading to our ability to filter out unattended sensory objects at the behavioral level). While neural firing rates and correlations may covary under some conditions (165, 166, 221), they may be independent from each other under other circumstances (114, 312). If so, enhanced neuronal correlation by weak synchrony could be a viable mechanism to implement flexible and guided communications across the complex brain-wide neural network in cognition.

Looking forward, we must be cognizant that weak oscillations are only partial clues of spatiotemporal spiking activity patterns in the cortex that are far from being well understood. The advance of techniques such as high-density multielectrode recording (142, 560, 771) and two-photon imaging with bulk loading of calcium sensitive dyes (335, 380, 736) has opened up the possibility to monitor simultaneously many single cells; such data will give rise to insights into, and inspire novel mathematical models of, neural circuit dynamics. The challenge is not only technical but also conceptual. Cortical neural circuits are extraordinarily complex, and complex dynamical systems (such as turbulent fluids with a hierarchy of coherent structures embedded in stochastic spatiotemporal processes) cannot be described solely in terms of oscillations or even low-dimensional aperiodic (chaotic) dynamics (337). New developments lay ahead in our quest for understanding the nature of the coordinated and gated brain dynamic operations underlying flexible cognitive behavior.

ACKNOWLEDGMENTS

I thank Angel Alonso, Nicolas Brunel, Gyuri Buzsáki, Albert Compte, Robert Desimone, Bard Ermentrout, Walter Freeman, Caroline Geisler, Rodolfo Llinás, Eve Marder, David McCormick, John Rinzel, Mavi Sanchez-Vives, and Roger Traub for many discussions over the years as well as Salvador Ardid, Jessica Cardin, Tatiana Engel, Asif Ghazanfar, Chris Harvey, Bilal Hei-

der, Thomas Klausberger, May-Britt Moser, and Jian-young Wu for their kind help with figures.

Address for reprint requests and other correspondence: X.-J. Wang, Dept. of Neurobiology, Yale University School of Medicine, 333 Cedar St., New Haven, CT 06520 (e-mail: xjwang@yale.edu).

GRANTS

This work was supported by National Institute of Mental Health Grant 2-R01-MH-62349, the Kavli Foundation, and the Swartz Foundation.

REFERENCES

1. **Abbott LF, Blum KI.** Functional significance of long-term potentiation for sequence learning and prediction. *Cereb Cortex* 6: 406–416, 1996.
2. **Abbott LF, van Vreeswijk C.** Asynchronous states in a network of pulse-coupled oscillators. *Phys Rev E* 48: 1483–1490, 1993.
3. **Achard S, Salvador R, Whitcher B, Suckling J, Bullmore E.** A resilient, low-frequency, small-world human brain functional network with highly connected association cortical hubs. *J Neurosci* 26: 63–72, 2006.
4. **Achermann P, Borbély AA.** Low-frequency (>1 Hz) oscillations in the human sleep electroencephalogram. *Neuroscience* 81: 213–222, 1997.
5. **Achuthan S, Canavier CC.** Phase-resetting curves determine synchronization, phase locking, and clustering in networks of neural oscillators. *J Neurosci* 29: 5218–5233, 2009.
6. **Acker CD, Kopell N, White JA.** Synchronization of strongly coupled excitatory neurons: relating network behavior to biophysics. *J Comput Neurosci* 15: 71–90, 2003.
7. **Adrian E.** Discharge frequencies in the cerebral and cerebellar cortex. *Proc Phys Soc* 83: 32–33, 1935.
8. **Adrian E.** Olfactory reactions in the brain of the hedgehog. *J Physiol* 100: 459–473, 1942.
9. **Adrian E.** The electrical activity of the mammalian olfactory bulb. *Electroencephalogr Clin Neurophysiol* 2: 377–388, 1950.
10. **Agmon A, Connors BW.** Repetitive burst-firing neurons in the deep layers of mouse somatosensory cortex. *Neurosci Lett* 99: 137–141, 1989.
11. **Ahmed B, Anderson J, Douglas R, Martin K, Whitteridge D.** Estimates of the net excitatory currents evoked by visual stimulation of identified neurons in cat visual cortex. *Cereb Cortex* 8: 462–476, 1998.
12. **Albert R, Barabási AL.** Statistical mechanics of complex networks. *Rev Mod Phys* 74: 47–97, 2002.
13. **Alonso A, Klink R.** Differential electroresponsiveness of stellate and pyramidal-like cells of medial entorhinal cortex layer II. *J Neurophysiol* 70: 128–143, 1993.
14. **Alonso A, Köhler C.** Evidence for separate projections of hippocampal pyramidal and non-pyramidal neurons to different parts of the septum in the rat brain. *Neurosci Lett* 31: 209–214, 1982.
15. **Alonso A, Llins R.** Subthreshold Na^+-dependent theta-like rhythmicity in stellate cells of entorhinal cortex layer II. Nature 342: 175–177, 1989.
16. **Alonso A, Khateb A, Fort P, Jones B, Mhlethaler M.** Differential oscillatory properties of cholinergic and noncholinergic nucleus basalis neurons in guinea pig brain slice. *Eur J Neurosci* 8: 169–182, 1996.
17. **Amarasingham A, Chen T, Geman S, Harrison M, Sheinberg D.** Spike count reliability and the Poisson hypothesis. *J Neurosci* 26: 801–809, 2006.
18. **Amit DJ.** The Hebbian paradigm reintegrated: local reverberations as internal representations. *Behav Brain Sci* 18: 617–626, 1995.
19. **Amzica F, Steriade M.** The K-complex: its low (>1 Hz) rhythmicity and relation to delta waves. *Neurology* 49: 952–959, 1997.
20. **Andersen P, Andersson SA.** *Physiological Basis of the Alpha-Rhythm*. New York: Appleton-Century-Crofts, 1968.
21. **Andersen P, Eccles J.** Inhibitory phasing of neuronal discharge. *Nature* 196: 645–647, 1962.
22. **Andersen P, Bland H, Myhrer T, Schwartzkroin P.** Septohippocampal pathway necessary for dentate theta production. *Brain Res* 165: 13–22, 1979.
23. **Anderson JS, Carandini M, Ferster D.** Orientation tuning of input conductance, excitation, and inhibition in cat primary visual cortex. *J Neurophysiol* 84: 909–926, 2000.
24. **Anderson KL, Rajagovindan R, Ghacibeh GA, Meador KJ, Ding M.** Theta oscillations mediate interaction between prefrontal cortex and medial temporal lobe in human memory. *Cereb Cortex* 2010.
25. **Andronov AA, Vitt AA, Khaikin SE.** *Theory of Oscillators*. New York: Dover, 1987.
26. **Aoki F, Fetz EE, Shupe L, Lettich E, Ojemann GA.** Increased gamma-range activity in human sensorimotor cortex during performance of visuomotor tasks. *Clin Neurophysiol* 110: 524–537, 1999.
27. **Aoyagi T, Kang Y, Terada N, Kaneko T, Fukai T.** The role of Ca^{2+}-dependent cationic current in generating gamma frequency rhythmic bursts: modeling study. *Neuroscience* 115: 1127–1138, 2002.
28. **Aoyagi T, Takekawa T, Fukai T.** Gamma rhythmic bursts: coherence control in networks of cortical pyramidal neurons. *Neural Comput* 15: 1035–1061, 2003.
29. **Apartis E, Poindessous-Jazat F, Lamour Y, Bassant M.** Loss of rhythmically bursting neurons in rat medial septum following selective lesion of septohippocampal cholinergic system. *J Neurophysiol* 79: 1633–1642, 1998.
30. **Ardid S, Wang XJ, Compte A.** An integrated microcircuit model of attentional processing in the neocortex. *J Neurosci* 27: 8486–8495, 2007.
31. **Ardid S, Wang XJ, Compte A.** Reconciling coherent oscillation with modulation of irregular spiking activity in selective attention: gamma-range synchronization between sensory and executive cortical areas. *J Neurosci* 30: 2856–2870, 2010.
32. **Arieli A, Shoham D, Hildesheim R, Grinvald A.** Coherent spatiotemporal patterns of ongoing activity revealed by real-time optical imaging coupled with single-unit recording in the cat visual cortex. *J Neurophysiol* 73: 2072–2093, 1995.
33. **Arthur J, Boahen K.** Synchrony in silicon: the gamma rhythm. *IEEE Trans Neural Netw* 18: 1815–1825, 2007.
34. **Arvanitaki A.** Recherches sur la réponse oscillatoire locale de l'axone géant isolé de sepia. *Arch Int Physiol* 49: 209–256, 1939.
35. **Atallah BV, Scanziani M.** Instantaneous modulation of gamma oscillation frequency by balancing excitation with inhibition. *Neuron* 62: 566–577, 2009.
36. **Averbeck BB, Latham P, Pouget A.** Neural correlations, population coding and computation. *Nature Rev Neurosci* 7: 358–366, 2006.
37. **Avitan L, Teicher M, Abeles M.** EEG generator-a model of potentials in a volume conductor. *J Neurophysiol* 102: 3046–3059, 2009.

37a. **Axmacher N, Henseler MM, Jensen O, Weinreich I, Elger CE, Fell J.** Cross-frequency coupling supports multi-item working memory in the human hippocampus. *Proc Natl Acad Sci USA* 107: 3228–3233, 2010.

38. **Baccalá L, Sameshima K.** Partial directed coherence: a new concept in neural structure determination. *Biol Cybern* 84: 463–474, 2001.
39. **Bair W, O'Keefe L.** The influence of fixational eye movements on the response of neurons in area MT of the macaque. *Vis Neurosci* 15: 779–786, 1998.
40. **Bair W, Zohary E, Newsome WT.** Correlated firing in macaque visual area MT: time scales and relationship to behavior. *J Neurosci* 21: 1676–1697, 2001.
41. **Baker S, Olivier E, Lemon R.** Coherent oscillations in monkey motor cortex and hand muscle EMG show task-dependent modulation. *J Physiol* 501: 225–241, 1997.
42. **Baker S, Spinks R, Jackson A, Lemon R.** Synchronization in monkey motor cortex during a precision grip task. I. Task-dependent modulation in single-unit synchrony. *J Neurophysiol* 85: 869–885, 2001.

43. **Baker S, Pinches E, Lemon R.** Synchronization in monkey motor cortex during a precision grip task. II. Effect of oscillatory activity on corticospinal output. *J Neurophysiol* 89: 1941–1953, 2003.
44. **Baker SN.** Oscillatory interactions between sensorimotor cortex and the periphery. *Curr Opin Neurobiol* 17: 649–655, 2007.
45. **Baker SN, Kilner JM, Pinches EM, Lemon RN.** The role of synchrony and oscillations in the motor output. *Exp Brain Res* 128: 109–117, 1999.
46. **Baker SN, Chiu M, Fetz EE.** Afferent encoding of central oscillations in the monkey arm. *J Neurophysiol* 95: 3904–3910, 2006.
47. **Bal T, McCormick D.** Mechanisms of oscillatory activity in guinea-pig nucleus reticularis thalami in vitro: a mammalian pacemaker. *J Physiol* 468: 669–691, 1993.
48. **Balu R, Larimer P, Strowbridge BW.** Phasic stimuli evoke precisely timed spikes in intermittently discharging mitral cells. *J Neurophysiol* 92: 743–753, 2004.
49. **Balu R, Pressler RT, Strowbridge BW.** Multiple modes of synaptic excitation of olfactory bulb granule cells. *J Neurosci* 27: 5621–5632, 2007.
50. **Barbas H, Rempel-Clower N.** Cortical structure predicts the pattern of corticocortical connections. *Cereb Cortex* 7: 635–646, 1997.
51. **Barbas H, Medalla M, Alade O, Suski J, Zikopoulos B, Lera P.** Relationship of prefrontal connections to inhibitory systems in superior temporal areas in the rhesus monkey. *Cereb Cortex* 15: 1356–1370, 2005.
52. **Barch D.** The cognitive neuroscience of schizophrenia. *Annu RevClin Psychol* 1: 321–353, 2005.
53. **Bartos M, Vida I, Frotscher M, Meyer A, Monyer H, Geiger JRP, Jonas P.** Fast synaptic inhibition promotes synchronized gamma oscillations in hippocampal interneuron networks. *Proc Natl Acad Sci USA* 99: 13222–13227, 2002.
54. **Bartos M, Vida I, Jonas P.** Synaptic mechanisms of synchronized gamma oscillations in inhibitory interneuron networks. *Nat Rev Neurosci* 8: 45–56, 2007.
55. **Basar-Eroglu C, Schmiedt-Fehr C, Mathes B, Zimmermann J, Brand A.** Are oscillatory brain responses generally reduced in schizophrenia during long sustained attentional processing? *Int J Psychophysiol* 71: 75–83, 2009.
56. **Bassett DS, Bullmore E.** Small-world brain networks. *Neuroscientist* 12: 512–523, 2006.
57. **Bassett DS, Meyer-Lindenberg A, Achard S, Duke T, Bullmore E.** Adaptive reconfiguration of fractal small-world human brain functional networks. *Proc Natl Acad Sci USA* 103: 19518–19523, 2006.
58. **Bassett DS, Bullmore E, Verchinski BA, Mattay VS, Weinberger DR, Meyer-Lindenberg A.** Hierarchical organization of human cortical networks in health and schizophrenia. *J Neurosci* 28: 9239–9248, 2008.
59. **Bassett DS, Bullmore ET, Meyer-Lindenberg A, Apud JA, Weinberger DR, Coppola R.** Cognitive fitness of cost-efficient brain functional networks. *Proc Natl Acad Sci USA* 106: 11747–11752, 2009.
60. **Bastiaansen M, Hagoort P.** Event-induced theta responses as a window on the dynamics of memory. *Cortex* 39: 967–992, 2003.
61. **Bathellier B, Lagier S, Faure P, Lledo P.** Circuit properties generating gamma oscillations in a network model of the olfactory bulb. *J Neurophysiol* 95: 2678–2691, 2006.
62. **Bathellier B, Carleton A, Gerstner W.** Gamma oscillations in a nonlinear regime: a minimal model approach using heterogeneous integrate-and-fire networks. *Neural Comput* 20: 2973–3002, 2008.
63. **Battaglia D, Brunel N, Hansel D.** Temporal decorrelation of collective oscillations in neural networks with local inhibition and long-range excitation. *Phys Rev Lett* 99: 238106, 2007.
64. **Bauer E, Paz R, Paré D.** Gamma oscillations coordinate amygdalo-rhinal interactions during learning. *J Neurosci* 27: 9369–9379, 2007.
65. **Bauer M, Oostenveld R, Peeters M, Fries P.** Tactile spatial attention enhances gamma-band activity in somatosensory cortex and reduces low-frequency activity in parieto-occipital areas. *J Neurosci* 26: 490–501, 2006.
66. **Bazhenov M, Stopfer M, Rabinovich M, Abarbanel H, Sejnowski T, Laurent G.** Model of cellular and network mechanisms for odor-evoked temporal patterning in the locust antennal lobe. *Neuron* 30: 569–581, 2001.
67. **Bazhenov M, Stopfer M, Rabinovich M, Huerta R, Abarbanel H, Sejnowski T, Laurent G.** Model of transient oscillatory synchronization in the locust antennal lobe. *Neuron* 30: 553–567, 2001.
68. **Bazhenov M, Timofeev I, Steriade M, Sejnowski TJ.** Model of thalamocortical slow-wave sleep oscillations and transitions to activated States. *J Neurosci* 22: 8691–8704, 2002.
69. **Bédard C, Destexhe A.** Macroscopic models of local field potentials and the apparent 1/f noise in brain activity. *Biophys J* 96: 2589–2603, 2009.
70. **Bédard C, Kröger H, Destexhe A.** Does the 1/f frequency scaling of brain signals reflect self-organized critical states? *Phys Rev Lett*, 97: 118–120, 2006.
71. **Bédard C, Kröger H, Destexhe A.** Model of low-pass filtering of local field potentials in brain tissue. *Phys Rev E Stat Nonlin Soft Matter Phys* 73: 51–91, 2006.
72. **Belforte JE, Zsiros V, Sklar ER, Jiang Z, Yu G, Li Y, Quinlan EM, Nakazawa K.** Postnatal NMDA receptor ablation in corticolimbic interneurons confers schizophrenia-like phenotypes. *Nat Neurosci* 13: 76–83, 2010.
73. **Bell C, Grimm R.** Discharge properties of Purkinje cells recorded on single and double microelectrodes. *J Neurophysiol* 32: 1044–1055, 1969.
74. **Benucci A, Frazor R, Carandini M.** Standing waves and traveling waves distinguish two circuits in visual cortex. *Neuron* 55: 103–117, 2007.
75. **Berens P, Keliris GA, Ecker AS, Logothetis NK, Tolias AS.** Feature selectivity of the gamma-band of the local field potential in primate primary visual cortex. *Front Neurosci* 2: 199–207, 2008.
76. **Berke JD.** Fast oscillations in cortical-striatal networks switch frequency following rewarding events and stimulant drugs. *Eur J Neurosci* 30: 848–859, 2009.
77. **Berke JD, Hetrick V, Breck J, Greene RW.** Transient 23–30 Hz oscillations in mouse hippocampus during exploration of novel environments. *Hippocampus* 18: 519–529, 2008.
78. **Bernier R, Dawson G, Webb S, Murias M.** EEG mu rhythm and imitation impairments in individuals with autism spectrum disorder. *Brain Cogn* 64: 228–237, 2007.
79. **Beshel J, Kopell N, Kay LM.** Olfactory bulb gamma oscillations are enhanced with task demands. *J Neurosci* 27: 8358–8365, 2007.
80. **Betti V, Zappasodi F, Rossini PM, Aglioti SM, Tecchio F.** Synchronous with your feelings: sensorimotor γ band and empathy for pain. *J Neurosci* 29: 12384–12392, 2009.
81. **Bi G, Poo M.** Synaptic modification by correlated activity: Hebb's postulate revisited. *Annu Rev Neurosci* 24: 139–166, 2001.
82. **Bi GQ, Poo MM.** Synaptic modifications in cultured hippocampal neurons: dependence on spike timing, synaptic strength, and postsynaptic cell type. *J Neurosci* 18: 10464–10472, 1998.
83. **Bibbig A, Traub R, Whittington M.** Long-range synchronization of gamma and beta oscillations and the plasticity of excitatory and inhibitory synapses: a network model. *J Neurophysiol* 88: 1634–1654, 2002.
84. **Bichot NP, Rossi AF, Desimone R.** Parallel and serial neural mechanisms for visual search in macaque area V4. *Science* 308: 529–534, 2005.
85. **Binzegger T, Douglas R, Martin K.** A quantitative map of the circuit of cat primary visual cortex. *J Neurosci* 24: 8441–8453, 2004.
86. **Blair HT, Gupta K, Zhang K.** Conversion of a phase- to a rate-coded position signal by a three-stage model of theta cells, grid cells, and place cells. *Hippocampus* 18: 1239–1255, 2008.
87. **Bland B.** The physiology and pharmacology of hippocampal formation theta rhythms. *Prog Neurobiol* 26: 1–54, 1986.
88. **Blankenship AG, Feller MB.** Mechanisms underlying spontaneous patterned activity in developing neural circuits. *Nat Rev Neurosci* 11: 18–29, 2010.
89. **Blatow M, Rozov A, Katona I, Hormuzdi SG, Meyer AH, Whittington MA, Caputi A, Monyer H.** A novel network of

multipolar bursting interneurons generates theta frequency oscillations in neocortex. *Neuron* 38: 805–817, 2003.
90. **Boehmer G, Greffrath W, Martin E, Hermann S.** Subthreshold oscillation of the membrane potential in magnocellular neurones of the rat supraoptic nucleus. *J Physiol* 526: 115–128, 2000.
91. **Boeijinga P, Lopes da Silva F.** Modulations of EEG activity in the entorhinal cortex and forebrain olfactory areas during odour sampling. *Brain Res* 478: 257–268, 1989.
92. **Bohland JW, Wu C, Barbas H, Bokil H, Bota M, Breiter HC, Cline HT, Doyle JC, Freed PJ, Greenspan RJ, Haber SN, Hawrylycz M, Herrera DG, Hilgetag CC, Huang ZJ, Jones A, Jones EG, Karten HJ, Kleinfeld D, Ktter R, Lester HA, Lin JM, Mensh BD, Mikula S, Panksepp J, Price JL, Safdieh J, Saper CB, Schiff ND, Schmahmann JD, Stillman BW, Svoboda K, Swanson LW, Toga AW, Van Essen DC, Watson JD, Mitra PP.** A proposal for a coordinated effort for the determination of brainwide neuroanatomical connectivity in model organisms at a mesoscopic scale. *PLoS Comput Biol* 5: e1000334, 2009.
93. **Bollimunta A, Chen Y, Schroeder C, Ding M.** Neuronal mechanisms of cortical alpha oscillations in awake-behaving macaques. *J Neurosci* 28: 9976–9988, 2008.
94. **Bonifazi P, Goldin M, Picardo MA, Jorquera I, Cattani A, Bianconi G, Represa A, Ben-Ari Y, Cossart R.** GABAergic hub neurons orchestrate synchrony in developing hippocampal networks. *Science* 326: 1419–1424, 2009.
95. **Booth V, Bose A.** Neural mechanisms for generating rate and temporal codes in model CA3 pyramidal cells. *J Neurophysiol* 85: 2432–2445, 2001.
96. **Börgers C, Kopell N.** Synchronization in networks of excitatory and inhibitory neurons with sparse, random connectivity. *Neural Comput* 15: 509–538, 2003.
97. **Börgers C, Kopell N.** Gamma oscillations and stimulus selection. *Neural Comput* 20: 383–414, 2008.
98. **Börgers C, Epstein S, Kopell NJ.** Gamma oscillations mediate stimulus competition and attentional selection in a cortical network model. *Proc Natl Acad Sci USA* 105: 18023–18028, 2008.
99. **Borhegyi Z, Varga V, Szilgyi N, Fabo D, Freund T.** Phase segregation of medial septal GABAergic neurons during hippocampal theta activity. *J Neurosci* 24: 8470–8479, 2004.
100. **Born J, Rasch B, Gais S.** Sleep to remember. *Neuroscientist* 12: 410–424, 2006.
101. **Bourdeau M, Morin F, Laurent C, Azzi M, Lacaille J.** Kv4.3-mediated A-type K^+ currents underlie rhythmic activity in hippocampal interneurons. *J Neurosci* 27: 1942–1953, 2007.
102. **Bouyer J, Montaron M, Rougeul A.** Fast fronto-parietal rhythms during combined focused attentive behaviour and immobility in cat: cortical and thalamic localizations. *Electroencephalogr Clin Neurophysiol* 51: 244–252, 1981.
103. **Bouyer JJ, Montaron MF, Vahnée JM, Albert MP, Rougeul A.** Anatomical localization of cortical beta rhythms in cat. *Neuroscience* 22: 863–869, 1987.
104. **Bragin A, Jando G, Nadasdy Z, Hetke J, Wise K, Buzsáki G.** Gamma (40–100 Hz) oscillation in the hippocampus of the behaving rat. *J Neurosci* 15: 47–60, 1995.
105. **Brashear H, Zaborszky L, Heimer L.** Distribution of GABAergic and cholinergic neurons in the rat diagonal band. *Neuroscience* 17: 439–451, 1986.
106. **Braun H, Wissing H, Schäfer K, Hirsch M.** Oscillation and noise determine signal transduction in shark multimodal sensory cells. *Nature* 367: 270–273, 1994.
107. **Brazhnik E, Fox S.** Action potentials and relations to the theta rhythm of medial septal neurons in vivo. *Exp Brain Res* 127: 244–258, 1999.
108. **Brazier MAB.** *A History of the Electrical Activity of the Brain: The First Half-Century.* New York: Macmillan, 1961.
109. **Brea JN, Kay LM, Kopell NJ.** Biophysical model for gamma rhythms in the olfactory bulb via subthreshold oscillations. *Proc Natl Acad Sci USA* 106: 21954–21959, 2009.
110. **Bremer F.** Cerebral and cerebellar potentials. *Physiol Rev* 38: 357–388, 1958.
111. **Bressler S, Freeman W.** Frequency analysis of olfactory system EEG in cat, rabbit, and rat. *Electroencephalogr Clin Neurophysiol* 50: 19–24, 1980.
112. **Bressler SL, Coppola R, Nakamura R.** Episodic multiregional cortical coherence at multiple frequencies during visual task performance. *Nature* 366: 153–156, 1993.
112a. **Bressler SL, Menon V.** Large-scale brain networks in cognition: emerging methods and principles. *Trends Cogn Sci* 14: 277–290, 2010.
113. **Bressloff PC.** Synaptically generated wave propagation in excitable neural media. *Phys Rev Lett* 82: 2979–2982, 1999.
114. **Bringuier V, Frgnac Y, Baranyi A, Debanne D, Shulz D.** Synaptic origin and stimulus dependency of neuronal oscillatory activity in the primary visual cortex of the cat. *J Physiol* 500: 751–774, 1997.
115. **Bringuier V, Chavane F, Glaeser L, Frgnac Y.** Horizontal propagation of visual activity in the synaptic integration field of area 17 neurons. *Science* 283: 695–699, 1999.
116. **Britten KH, Shadlen MN, Newsome WT, Movshon JA.** Responses of neurons in macaque MT to stochastic motion signals. *Visual Neurosci* 10: 1157–1169, 1993.
117. **Brody C, Hopfield J.** Simple networks for spike-timing-based computation, with application to olfactory processing. *Neuron* 37: 843–852, 2003.
118. **Brovelli A, Ding M, Ledberg A, Chen Y, Nakamura R, Bressler S.** Beta oscillations in a large-scale sensorimotor cortical network: directional influences revealed by Granger causality. *Proc Natl Acad Sci USA* 101: 9849–9854, 2004.
119. **Brown E, Moehlis J, Holmes P.** On the phase reduction and response dynamics of neural oscillator populations. *Neural Comput* 16: 673–715, 2004.
120. **Brown E, Gao J, Holmes P, Bogacz R, Gilzenrat M, Cohen JD.** Simple neural networks that optimize decisions. *Int J Bifurcationand Chaos* 15: 803–826, 2005.
121. **Brown P, Marsden J.** Cortical network resonance and motor activity in humans. *Neuroscientist* 7: 518–527, 2001.
122. **Brumberg JC, Nowak LG, McCormick DA.** Ionic mechanisms underlying repetitive high-frequency burst firing in supragranular cortical neurons. *J Neurosci* 20: 4829–4843, 2000.
123. **Brunel N.** Dynamics of sparsely connected networks of excitatory and inhibitory spiking neurons. *J Comput Neurosci* 8: 183–208, 2000.
124. **Brunel N, Hakim V.** Fast global oscillations in networks of integrate-and-fire neurons with low firing rates. *Neural Computation* 11: 1621–1671, 1999.
125. **Brunel N, Hakim V.** Sparsely synchronized neuronal oscillations. *Chaos* 18: 15–113, 2008.
126. **Brunel N, Hansel D.** How noise affects the synchronization properties of recurrent networks of inhibitory neurons. *Neural Comput* 18: 1066–1110, 2006.
127. **Brunel N, Wang XJ.** What determines the frequency of fast network oscillations with irregular neural discharges? I. Synaptic dynamics and excitation-inhibition balance. *J Neurophysiol* 90: 415–430, 2003.
128. **Brunel N, Chance FS, Fourcaud N, Abbott LF.** Effects of synaptic noise and filtering on the frequency response of spiking neurons. *Phys Rev Lett* 86: 2186–2189, 2001.
129. **Buehlmann A, Deco G.** The neuronal basis of attention: rate versus synchronization modulation. *J Neurosci* 28: 7679–7686, 2008.
130. **Buffalo EA, Desimone PFR.** Layer-specific attentional modulation in early visual areas. *Soc Neurosci Abstr* 30: 717.7679–716, 2004.
131. **Buhl D, Harris K, Hormuzdi S, Monyer H, Buzski G.** Selective impairment of hippocampal gamma oscillations in connexin-36 knock-out mouse in vivo. *J Neurosci* 23: 1013–1018, 2003.
132. **Buhl EH, Tamas G, Fisahn A.** Cholinergic activation and tonic excitation induce persistent gamma oscillations in mouse somatosensory cortex in vitro. *J Physiol* 513: 117–126, 1998.
133. **Buia C, Tiesinga P.** Role of interneuron diversity in the cortical microcircuit for attention. *J Neurophysiol* 99: 2158–2182, 2008.
134. **Bullock TH, McClune MC.** Lateral coherence of the electrocorticogram: a new measure of brain synchrony. *Electroencephalogr Clin Neurophysiol* 73: 479–498, 1989.
135. **Burgess N.** Grid cells and theta as oscillatory interference: theory and predictions. *Hippocampus* 18: 1157–1174, 2008.

136. **Burgess N, Barry C, O'Keefe J.** An oscillatory interference model of grid cell firing. *Hippocampus* 17: 801–812, 2007.
137. **Busch NA, Dubois J, VanRullen R.** The phase of ongoing EEG oscillations predicts visual perception. *J Neurosci* 29: 7869–7876, 2009.
138. **Buschman T, Miller E.** Top-down versus bottom-up control of attention in the prefrontal and posterior parietal cortices. *Science* 315: 1860–1862, 2007.
139. **Buschman TJ, Miller EK.** Serial, covert shifts of attention during visual search are reflected by the frontal eye fields and correlated with population oscillations. *Neuron* 63: 386–396, 2009.
140. **Buzsáki G.** Hippocampal sharp waves: their origin and significance. *Brain Res* 398: 242–252, 1986.
141. **Buzsáki G.** Theta oscillations in the hippocampus. *Neuron* 33: 325–340, 2002.
142. **Buzsáki G.** Large-scale recording of neuronal ensembles. *Nat Neurosci* 7: 446–451, 2004.
143. **Buzsáki G.** *Rhythms of the Brain*. New York: Oxford Univ. Press, 2006.
144. **Buzsáki G, Chrobak J.** Temporal structure in spatially organized neuronal ensembles: a role for interneuronal networks. *Curr Opin Neurobiol* 5: 504–510, 1995.
145. **Buzsáki G, Draguhn A.** Neuronal oscillations in cortical networks. *Science* 304: 1926–1929, 2004.
146. **Buzsáki G, Leung LW, Vanderwolf CH.** Cellular bases of hippocampal EEG in the behaving rat. *Brain Res* 287: 139–171, 1983.
147. **Buzsáki G, Urioste R, Hetke J, Wise K.** High frequency network oscillation in the hippocampus. *Science* 256: 1025–1027, 1992.
148. **Buzsáki G, Buhl D, Harris K, Csicsvari J, Czh B, Morozov A.** Hippocampal network patterns of activity in the mouse. *Neuroscience* 116: 201–211, 2003.
149. **Buzsáki G, Geisler C, Henze DA, Wang XJ.** Interneuron diversity series: circuit complexity and axon wiring economy of cortical interneurons. *Trends Neurosci* 27: 186–193, 2004.
150. **Canolty R, Edwards E, Dalal S, Soltani M, Nagarajan S, Kirsch H, Berger M, Barbaro N, Knight R.** High gamma power is phase-locked to theta oscillations in human neocortex. *Science* 313: 1626–1628, 2006.
151. **Caporale N, Dan Y.** Spike timing-dependent plasticity: a hebbian learning rule. *Annu Rev Neurosci* 31: 25–46, 2008.
152. **Capotosto P, Babiloni C, Romani GL, Corbetta M.** Frontoparietal cortex controls spatial attention through modulation of anticipatory alpha rhythms. *J Neurosci* 29: 5863–5872, 2009.
153. **Carandini M.** Amplification of trial-to-trial response variability by neurons in visual cortex. *PLoS Biol* 2: E264, 2004.
154. **Cardin J, Palmer L, Contreras D.** Stimulus-dependent gamma (30–50 Hz) oscillations in simple and complex fast rhythmic bursting cells in primary visual cortex. *J Neurosci* 25: 5339–5350, 2005.
155. **Cardin JA, Carlén M, Meletis K, Knoblich U, Zhang F, Deisseroth K, Tsai LH, Moore CI.** Driving fast-spiking cells induces gamma rhythm and controls sensory responses. *Nature* 459: 663–667, 2009.
156. **Cashdollar N, Malecki U, Rugg-Gunn FJ, Duncan JS, Lavie N, Duzel E.** Hippocampus-dependent and -independent theta-networks of active maintenance. *Proc Natl Acad Sci USA* 106: 20493–20498, 2009.
157. **Cassenaer S, Laurent G.** Hebbian STDP in mushroom bodies facilitates the synchronous flow of olfactory information in locusts. *Nature* 448: 709–713, 2007.
158. **Castelli F, Frith C, Happé F, Frith U.** Autism, Asperger syndrome and brain mechanisms for the attribution of mental states to animated shapes. *Brain* 125: 1839–1849, 2002.
159. **Castro-Alamancos MA, Rigas P, Tawara-Hirata Y.** Resonance (approximately 10 Hz) of excitatory networks in motor cortex: effects of voltage-dependent ion channel blockers. *J Physiol* 578: 173–191, 2007.
160. **Cavanagh JF, Cohen MX, Allen JJ.** Prelude to and resolution of an error: EEG phase synchrony reveals cognitive control dynamics during action monitoring. *J Neurosci* 29: 98–105, 2009.
161. **Cenier T, Amat C, Litaudon P, Garcia S, Lafaye de Micheaux P, Liquet B, Roux S, Buonviso N.** Odor vapor pressure and quality modulate local field potential oscillatory patterns in the olfactory bulb of the anesthetized rat. *Eur. J Neurosci* 27: 1432–1440, 2008.
162. **Chagnac-Amitai Y, Connors B.** Horizontal spread of synchronized activity in neocortex and its control by GABA-mediated inhibition. *J Neurophysiol* 61: 747–758, 1989.
163. **Chance FS, Abbott LF, Reyes AD.** Gain modulation from background synaptic input. *Neuron* 35: 773–782, 2002.
164. **Chang HT.** Dendritic potential of cortical neurons produced by direct electrical stimulation of the cerebral cortex. *J Neurophysiol* 14: 1–21, 1951.
165. **Chawla D, Lumer E, Friston K.** The relationship between synchronization among neuronal populations and their mean activity levels. *Neural Comput* 11: 1389–1411, 1999.
166. **Chawla D, Lumer E, Friston K.** Relating macroscopic measures of brain activity to fast, dynamic neuronal interactions. *Neural Comput* 12: 2805–2821, 2000.
167. **Chawla D, Friston K, Lumer E.** Zero-lag synchronous dynamics in triplets of interconnected cortical areas. *Neural Netw* 14: 727–735, 2001.
168. **Chen CC, Henson RN, Stephan KE, Kilner JM, Friston KJ.** Forward and backward connections in the brain: a DCM study of functional asymmetries. *Neuroimage* 45: 453–462, 2009.
169. **Chen D, Fetz EE.** Characteristic membrane potential trajectories in primate sensorimotor cortex neurons recorded in vivo. *J Neurophysiol* 94: 2713–2725, 2005.
170. **Chen Z, Ermentrout B, Wang XJ.** Wave propagation mediated by $GABA_B$ synapse and rebound excitation in an inhibitory network: a reduced model approach. *J Comput Neurosci* 5: 53–69, 1998.
171. **Cheron G, Servais L, Dan B.** Cerebellar network plasticity: from genes to fast oscillation. *Neuroscience* 153: 1–19, 2008.
172. **Chervin R, Pierce P, Connors B.** Periodicity and directionality in the propagation of epileptiform discharges across neocortex. *J Neurophysiol* 60: 1695–1713, 1988.
173. **Chklovskii DB, Mel BW, Svoboda K.** Cortical rewiring and information storage. *Nature* 431: 782–788, 2004.
174. **Cho R, Konecky R, Carter C.** Impairments in frontal cortical gamma synchrony and cognitive control in schizophrenia. *Proc Natl Acad Sci USA* 103: 19878–19883, 2006.
175. **Chow C and Kopell N.** Dynamics of spiking neurons with electrical coupling. *Neural Comput* 12: 1643–1678, 2000.
176. **Chrobak JJ, Buzsáki G.** Gamma oscillations in the entorhinal cortex of the freely behaving rat. *J Neurosci* 18: 388–398, 1998.
177. **Cobb S, Buhl E, Halasy K, Paulsen O, Somogyi P.** Synchronization of neuronal activity in hippocampus by individual GABAergic interneurons. *Nature* 378: 75–78, 1995.
178. **Coetzee W, Amarillo Y, Chiu J, Chow A, Lau D, McCormack T, Moreno H, Nadal M, Ozaita A, Pountney D, Saganich M, Vega-Saenz de Miera E, Rudy B.** Molecular diversity of K^+ channels. *Ann NY Acad Sci* 868: 233–285, 1999.
179. **Colby CL, Godberg ME.** Space and attention in parietal cortex. *Annu Rev Neurosci* 22: 319–349, 1999.
180. **Cole A, Nicoll R.** Characterization of a slow cholinergic postsynaptic potential recorded in vitro from rat hippocampal pyramidal cells. *J Physiol* 352: 173–188, 1984.
181. **Colgin LL, Denninger T, Fyhn M, Hafting T, Bonnevie T, Jensen O, Moser MB, Moser EI.** Frequency of gamma oscillations routes flow of information in the hippocampus. *Nature* 462: 353–357, 2009.
182. **Compte A, Brunel N, Goldman-Rakic PS, Wang XJ.** Synaptic mechanisms and network dynamics underlying spatial working memory in a cortical network model. *Cereb Cortex* 10: 910–923, 2000.
183. **Compte A, Sanchez-Vives MV, McCormick DA, Wang XJ.** Cellular and network mechanisms of slow oscillatory activity (>1 Hz) and wave propagations in a cortical network model. *J Neurophysiol* 89: 2707–2725, 2003.
184. **Compte A, Constantinidis C, Tegner J, Raghavachari S, Chafee MV, Goldman-Rakic PS, Wang XJ.** Temporally irregular mnemonic persistent activity in prefrontal neurons of monkeys during a delayed response task. *J Neurophysiol* 90: 3441–3454, 2003.

185. **Compte A, Reig R, Descalzo VF, Harvey MA, Puccini GD, Sanchez-Vives MV.** Spontaneous high-frequency (10–80 Hz) oscillations during up states in the cerebral cortex in vitro. *J Neurosci* 28: 13828–13844, 2008.
186. **Connors B, Long M.** Electrical synapses in the mammalian brain. *Annu Rev Neurosci* 27: 393–418, 2004.
187. **Constantinidis C, Goldman-Rakic PS.** Correlated discharges among putative pyramidal neurons and interneurons in the primate prefrontal cortex. *J Neurophysiol* 88: 3487–3497, 2002.
188. **Constantinidis C, Wang XJ.** A neural circuit basis for spatial working memory. *Neuroscientist* 10: 553–565, 2004.
189. **Contreras D, Llinas R.** Voltage-sensitive dye imaging of neocortical spatiotemporal dynamics to afferent activation frequency. *J Neurosci* 21: 9403–9413, 2001.
190. **Contreras D, Timofeev I, Steriade M.** Mechanisms of long-lasting hyperpolarizations underlying slow sleep oscillations in cat corticothalamic networks. *J Physiol* 494: 251–264, 1996.
191. **Cook E, Guest J, Liang Y, Masse N, Colbert C.** Dendrite-to-soma input/output function of continuous time-varying signals in hippocampal CA1 pyramidal neurons. *J Neurophysiol* 98: 2943–2955, 2007.
192. **Cook E, Wilhelm A, Guest J, Liang Y, Masse N, Colbert C.** The neuronal transfer function: contributions from voltage- and time-dependent mechanisms. *Prog Brain Res* 165: 1–12, 2007.
193. **Coombes S, Bressloff PC.** *Bursting: The Genesis of Rhythm in the Nervous System*. Singapore: World Scientific, 2005.
194. **Corbetta M, Shulman G.** Control of goal-directed and stimulus-driven attention in the brain. *Nat Rev Neurosci* 3: 201–215, 2002.
195. **Cossart R, Aronov D, Yuste R.** Attractor dynamics of network UP states in the neocortex. *Nature* 423: 283–288, 2003.
196. **Coulter D, Huguenard J, Prince D.** Calcium currents in rat thalamocortical relay neurones: kinetic properties of the transient, low-threshold current. *J Physiol* 414: 587–604, 1989.
197. **Courtemanche R, Fujii N, Graybiel A.** Synchronous, focally modulated beta-band oscillations characterize local field potential activity in the striatum of awake behaving monkeys. *J Neurosci* 23: 11741–11752, 2003.
198. **Cowan RL, Wilson CJ.** Spontaneous firing patterns and axonal projections of single corticostriatal neurons in the rat medial agranular cortex. *J Neurophysiol* 71: 17–32, 1994.
199. **Coyle JT, Tsai G, Goff D.** Converging evidence of NMDA receptor hypofunction in the pathophysiology of schizophrenia. *Ann NY Acad Sci* 1003: 318–327, 2003.
200. **Crane JW, Windels F, Sah P.** Oscillations in the basolateral amygdala: aversive stimulation is state dependent and resets the oscillatory phase. *J Neurophysiol* 102: 1379–1387, 2009.
201. **Creutzfeldt OD, Watanabe S, Lux HD.** Relations between EEG phenomena and potentials of single cortical cells. I. Evoked responses after thalamic and erpicortical stimulation. *Electroencephalogr Clin Neurophysiol* 20: 1–18, 1966.
202. **Creutzfeldt OD, Watanabe S, Lux HD.** Relations between EEG phenomena and potentials of single cortical cells. II. Spontaneous and convulsoid activity. *Electroencephalogr Clin Neurophysiol* 20: 19–37, 1966.
203. **Crone N, Boatman D, Gordon B, Hao L.** Induced electrocorticographic gamma activity during auditory perception. Brazier Award-winning article, 2001. *Clin Neurophysiol* 112: 565–582, 2001.
204. **Crone N, Sinai A, Korzeniewska A.** High-frequency gamma oscillations and human brain mapping with electrocorticography. *Prog Brain Res* 159: 275–295, 2006.
205. **Crook S, Ermentrout G, Vanier M, Bower J.** The role of axonal delay in the synchronization of networks of coupled cortical oscillators. *J Comput Neurosci* 4: 161–172, 1997.
206. **Crook S, Ermentrout G, Bower J.** Spike frequency adaptation affects the synchronization properties of networks of cortical oscillations. *Neural Comput* 10: 837–854, 1998.
207. **Crunelli V, Hughes SW.** The (1 Hz) rhythm of non-REM sleep: a dialogue between three cardinal oscillators. *Nat Neurosci* 2009.
208. **Csicsvari J, Hirase H, Czurko A, Mamiya A, Buzsáki G.** Oscillatory coupling of hippocampal pyramidal cells and interneurons in the behaving rat. *J Neurosci* 19: 274–287, 1999.
209. **Csicsvari J, Jamieson B, Wise K, Buzski G.** Mechanisms of gamma oscillations in the hippocampus of the behaving rat. *Neuron* 37: 311–322, 2003.
210. **Cui J, Canavier CC, Butera RJ.** Functional phase response curves: a method for understanding synchronization of adapting neurons. *J Neurophysiol* 102: 387–398, 2009.
211. **Cunningham M, Whittington M, Bibbig A, Roopun A, LeBeau F, Vogt A, Monyer H, Buhl E, Traub R.** A role for fast rhythmic bursting neurons in cortical gamma oscillations in vitro. *Proc Natl Acad Sci USA* 101: 7152–7157, 2004.
212. **Damoiseaux J, Beckmann C, Arigita E, Barkhof F, Scheltens P, Stam C, Smith S, Rombouts S.** Reduced resting-state brain activity in the "default network" in normal aging. *Cereb Cortex* 18: 1856–1864, 2008.
213. **Dan Y, Poo MM.** Spike timing-dependent plasticity: from synapse to perception. *Physiol Rev* 86: 1033–1048, 2006.
214. **Dang-Vu TT, Schabus M, Desseilles M, Albouy G, Boly M, Darsaud A, Gais S, Rauchs G, Sterpenich V, Vandewalle G, Carrier J, Moonen G, Balteau E, Degueldre C, Luxen A, Phillips C, Maquet P.** Spontaneous neural activity during human slow wave sleep. *Proc Natl Acad Sci USA* 105: 15160–15165, 2008.
215. **Dani VS, Chang Q, Maffei A, Turrigiano GG, Jaenisch R, Nelson SB.** Reduced cortical activity due to a shift in the balance between excitation and inhibition in a mouse model of Rett syndrome. *Proc Natl Acad Sci USA* 102: 12560–12565, 2005.
216. **Darvas F, Miller KJ, Rao RP, Ojemann JG.** Nonlinear phase-phase cross-frequency coupling mediates communication between distant sites in human neocortex. *J Neurosci* 29: 426–435, 2009.
217. **David FO, Hugues E, Cenier T, Fourcaud-Trocm N, Buonviso N.** Specific entrainment of mitral cells during gamma oscillation in the rat olfactory bulb. *PLoS Comput Biol* 5: e1000551, 2009.
218. **Davison AP, Feng J, Brown D.** Dendrodendritic inhibition and simulated odor responses in a detailed olfactory bulb network model. *J Neurophysiol* 90: 1921–1935, 2003.
219. **De Haan W, Pijnenburg YA, Strijers RL, van der Made Y, van der Flier WM, Scheltens P, Stam CJ.** Functional neural network analysis in frontotemporal dementia and Alzheimer's disease using EEG and graph theory. *BMC Neurosci* 10: 101, 2009.
220. **De Kock C, Sakmann B.** High frequency action potential bursts (≤100 Hz) in L2/3 and L5B thick tufted neurons in anaesthetized and awake rat primary somatosensory cortex. *J Physiol* 586: 3353–3364, 2008.
221. **De la Rocha J, Doiron B, Shea-Brown E, Josic´ K, Reyes A.** Correlation between neural spike trains increases with firing rate. *Nature* 448: 802–806, 2007.
222. **De Solages C, Szapiro G, Brunel N, Hakim V, Isope P, Buisseret P, Rousseau C, Barbour B, Lna C.** High-frequency organization and synchrony of activity in the Purkinje cell layer of the cerebellum. *Neuron* 58: 775–788, 2008.
223. **Debener S, Herrmann CS, Kranczioch C, Gembris D, Engel AK.** Top-down attentional processing enhances auditory evoked gamma band activity. *Neuroreport* 14: 683–686, 2003.
224. **Deco G, Thiele A.** Attention: oscillations and neuropharmacology. *Eur J Neurosci* 30: 347–354, 2009.
225. **Deco G, Mart D, Ledberg A, Reig R, Sanchez Vives MV.** Effective reduced diffusion-models: a data driven approach to the analysis of neuronal dynamics. *PLoS Comput Biol* 5: e1000587, 2009.
226. **Deco G, Rolls ET, Romo R.** Stochastic dynamics as a principle of brain function. *Prog Neurobiol* 88: 1–16, 2009.
227. **Deisseroth K, Feng G, Majewska A, Miesenbck G, Ting A, Schnitzer M.** Next-generation optical technologies for illuminating genetically targeted brain circuits. *J Neurosci* 26: 10380–10386, 2006.
228. **Deister CA, Teagarden MA, Wilson CJ, Paladini CA.** An intrinsic neuronal oscillator underlies dopaminergic neuron bursting. *J Neurosci* 29: 15888–15897, 2009.
229. **Demiralp T, Bayraktaroglu Z, Lenz D, Junge S, Busch NA, Maess B, Ergen M, Herrmann CS.** Gamma amplitudes are coupled to theta phase in human EEG during visual perception. *Int J Psychophysiol* 64: 24–30, 2007.

230. **Desimone R, Duncan J.** Neural mechanisms of selective visual attention. *Annu Rev Neurosci* 18: 193–222, 1995.
231. **Desmaisons D, Vincent JD, Lledo PM.** Control of action potential timing by intrinsic subthreshold oscillations in olfactory bulb output neurons. *J Neurosci* 19: 10727–10737, 1999.
232. **Destexhe A.** Self-sustained asynchronous irregular states and Up-Down states in thalamic, cortical and thalamocortical networks of nonlinear integrate-and-fire neurons. *J Comput Neurosci* 27: 493–506, 2009.
233. **Destexhe A, Contreras D.** Neuronal computations with stochastic network states. *Science* 314: 85–90, 2006.
234. **Destexhe A, Paré D.** Impact of network activity on the integrative properties of neocortical pyramidal neurons in vivo. *J Neurophysiol* 81: 1531–1547, 1999.
235. **Destexhe A, Sejnowski TJ.** *Thalamocortical Assemblies: How Ion Channels, Single Neurons and Large-Scale Networks Organize Sleep Oscillations*. New York: Oxford Univ. Press, 2001.
236. **Destexhe A, Sejnowski TJ.** Interactions between membrane conductances underlying thalamocortical slow-wave oscillations. *Physiol Rev* 83: 1401–1453, 2003.
237. **Destexhe A, Contreras D, Steriade M, Sejnowski T, Huguenard J.** In vivo, in vitro, and computational analysis of dendritic calcium currents in thalamic reticular neurons. *J Neurosci* 16: 169–185, 1996.
238. **Destexhe A, Contreras D, Steriade M.** Spatiotemporal analysis of local field potentials and unit discharges in cat cerebral cortex during natural wake and sleep states. *J Neurosci* 19: 4595–4608, 1999.
239. **Destexhe A, Rudolph M, Paré D.** The high-conductance state of neocortical neurons in vivo. *Nat Rev Neurosci* 4: 739–751, 2003.
240. **Destexhe A, Hughes SW, Rudolph M, Crunelli V.** Are corticothalamic "up" states fragments of wakefulness? *Trends Neurosci* 30: 334–342, 2007.
241. **DeVille R, Peskin C.** Synchrony and asynchrony in a fully stochastic neural network. *Bull Math Biol* 70: 1608–1633, 2008.
242. **Dickson CT, Magistretti J, Shalinsky MH, Fransn E, Hasselmo ME, Alonso A.** Properties and role of I_h in the pacing of subthreshold oscillations in entorhinal cortex layer II neurons. *J Neurophysiol* 83: 2562–2579, 2000.
243. **Diesmann M, Gewaltig M, Aertsen A.** Stable propagation of synchronous spiking in cortical neural networks. *Nature* 402: 529–533, 1999.
244. **Ding M, Chen Y, Bressler SLR.** Granger causality: basic theory and application to neuroscience. In: *Handbook of Time Series Analysis*, edited by B. Schelter, M. Winterhalder, J. Timmer. Weinhein, Germany: Wiley-VCH Verlag, 2006, p. .437–460
245. **Doesburg S, Roggeveen A, Kitajo K, Ward L.** Large-scale gamma-band phase synchronization and selective attention. *Cereb Cortex* 18: 386–396, 2008.
246. **Doesburg SM, Green JJ, McDonald JJ, Ward LM.** From local inhibition to long-range integration: a functional dissociation of alpha-band synchronization across cortical scales in visuospatial attention. *Brain Res* 1303: 97–110, 2009.
247. **Doiron B, Longtin A, Turner R, Maler L.** Model of gamma frequency burst discharge generated by conditional backpropagation. *J Neurophysiol* 86: 1523–1545, 2001.
248. **Doiron B, Chacron M, Maler L, Longtin A, Bastian J.** Inhibitory feedback required for network oscillatory responses to communication but not prey stimuli. *Nature* 421: 539–543, 2003.
249. **Doiron B, Lindner B, Longtin A, Maler L, Bastian J.** Oscillatory activity in electrosensory neurons increases with the spatial correlation of the stochastic input stimulus. *Phys Rev Lett* 93: 048101, 2004.
250. **Doischer D, Hosp JA, Yanagawa Y, Obata K, Jonas P, Vida I, Bartos M.** Postnatal differentiation of basket cells from slow to fast signaling devices. *J Neurosci* 28: 12956–12968, 2008.
251. **Donner TH, Siegel M, Oostenveld R, Fries P, Bauer M, Engel AK.** Population activity in the human dorsal pathway predicts the accuracy of visual motion detection. *J Neurophysiol* 98: 345–359, 2007.
252. **Donoghue J, Sanes J, Hatsopoulos N, Gal G.** Neural discharge and local field potential oscillations in primate motor cortex during voluntary movements. *J Neurophysiol* 79: 159–173, 1998.
253. **Douglas RJ, Martin KAC.** Neuronal circuits of the neocortex. *Annu Rev Neurosci* 27: 419–451, 2004.
254. **Dragoi G, Buzsáki G.** Temporal encoding of place sequences by hippocampal cell assemblies. *Neuron* 50: 145–157, 2006.
255. **Dragoi G, Carpi D, Recce M, Csicsvari J, Buzsáki G.** Interactions between hippocampus and medial septum during sharp waves and theta oscillation in the behaving rat. *J Neurosci* 19: 6191–6199, 1999.
256. **Draguhn A, Traub RD, Schmitz D, Jefferys JGR.** Electrical coupling underlies high-frequency oscillations in the hippocampus *invitro*. *Nature* 394: 189–193, 1998.
257. **Driver J, Noesselt T.** Multisensory interplay reveals crossmodal influences on "sensory-specific" brain regions, neural responses, and judgments. *Neuron* 57: 11–23, 2008.
258. **Durstewitz D, Seamans J.** The dual-state theory of prefrontal cortex dopamine function with relevance to catechol-O-methyltransferase genotypes and schizophrenia. *Biol Psychiatry* doi:10.1016/j.biopsych.2008.05.015.
259. **Durstewitz D, Seamans JK, Sejnowski TJ.** Dopamine-mediated stabilization of delay-period activity in a network model of prefrontal cortex. *J Neurophysiol* 83: 1733–1750, 2000.
260. **Dzirasa K, Ramsey AJ, Takahashi DY, Stapleton J, Potes JM, Williams JK, Gainetdinov RR, Sameshima K, Caron MG, Nicolelis MA.** Hyperdopaminergia and NMDA receptor hypofunction disrupt neural phase signaling. *J Neurosci* 29: 8215–8224, 2009.
261. **Ebner T, Bloedel J.** Correlation between activity of Purkinje cells and its modification by natural peripheral stimuli. *J Neurophysiol* 45: 948–961, 1981.
262. **Ecker AS, Berens P, Keliris GA, Bethge M, Logothetis NK, Tolias AS.** Decorrelated neuronal firing in cortical microcircuits. *Science* 327: 584–587, 2010.
263. **Eckhorn R, Bauer R, Jordan W, Brosch M, Kruse W, Munk M, Reitboeck H.** Coherent oscillations: a mechanism of feature linking in the visual cortex? Multiple electrode and correlation analyses in the cat. *Biol Cybern* 60: 121–130, 1988.
264. **Eeckman FH, Freeman WJ.** Correlations between unit firing and EEG in the rat olfactory system. *Brain Res* 528: 238–244, 1990.
265. **Egan M, Goldberg T, Kolachana B, Callicott J, Mazzanti C, Straub R, Goldman D, Weinberger D.** Effect of COMT Val108/158 Met genotype on frontal lobe function and risk for schizophrenia. *Proc Natl Acad Sci USA* 98: 6917–6922, 2001.
266. **Einevoll GT, Pettersen KH, Devor A, Ulbert I, Halgren E, Dale AM.** Laminar population analysis: estimating firing rates and evoked synaptic activity from multielectrode recordings in rat barrel cortex. *J Neurophysiol* 97: 2174–2190, 2007.
267. **Ekstrom A, Suthana N, Millett D, Fried I, Bookheimer S.** Correlation between BOLD fMRI and theta-band local field potentials in the human hippocampal area. *J Neurophysiol* 101: 2668–2678, 2009.
268. **El Boustani S, Pospischil M, Rudolph-Lilith M, Destexhe A.** Activated cortical states: experiments, analyses and models. *J Physiol* 101: 99–109, 2007.
269. **El Boustani S, Marre O, Bhuret S, Baudot P, Yger P, Bal T, Destexhe A, Frgnac Y.** Network-state modulation of power-law frequency-scaling in visual cortical neurons. *PLoS Comput. Biol.* 5: e1000519, 2009.
270. **Engel A, Fries P, Singer W.** Dynamic predictions: oscillations and synchrony in top-down processing. *Nat Rev Neurosci* 2: 704–716, 2001.
271. **Engel T, Schimansky-Geier L, Herz A, Schreiber S, Erchova I.** Subthreshold membrane-potential resonances shape spike-train patterns in the entorhinal cortex. *J Neurophysiol* 100: 1576–1589, 2008.
272. **Erchova I, Kreck G, Heinemann U, Herz AV.** Dynamics of rat entorhinal cortex layer II and III cells: characteristics of membrane potential resonance at rest predict oscillation properties near threshold. *J Physiol* 560: 89–110, 2004.
273. **Erdos P, Renyi A.** On the evolution of random graphs. *Publ Math Inst Hung Acad Sci* 5: 17–61, 1960.
274. **Ergenoglu T, Demiralp T, Bayraktaroglu Z, Ergen M, Beydagi H, Uresin Y.** Alpha rhythm of the EEG modulates visual

detection performance in humans. *Brain Res Cogn Brain Res* 20: 376–383, 2004.
275. **Ermentrout B.** Type I membranes, phase resetting curves, and synchrony. *Neural Comput* 8: 979–1001, 1996.
276. **Ermentrout B, Kopell N.** Multiple pulse interactions and averaging in systems of coupled neural oscillators. *J Math Biol* 29: 195–217, 1991.
277. **Ermentrout B, Pascal M, Gutkin B.** The effects of spike frequency adaptation and negative feedback on the synchronization of neural oscillators. *Neural Comput* 13: 1285–1310, 2001.
278. **Ermentrout G, Cowan J.** Temporal oscillations in neuronal nets. *J Math Biol* 7: 265–280, 1979.
279. **Ermentrout G, Kleinfeld D.** Traveling electrical waves in cortex: insights from phase dynamics and speculation on a computational role. *Neuron* 29: 33–44, 2001.
280. **Ermentrout G, Kopell N.** Fine structure of neural spiking and synchronization in the presence of conduction delays. *Proc Natl Acad Sci USA* 95: 1259–1264, 1998.
281. **Ermentrout G, Galn R, Urban N.** Reliability, synchrony and noise. *Trends Neurosci* 31: 428–434, 2008.
282. **Ermentrout GB.** Neural networks as spatio-temporal pattern-forming systems. *Rep Prog Phys* 61: 353–430, 1998.
283. **Esser SK, Hill SL, Tononi G.** Sleep homeostasis and cortical synchronization. I. Modeling the effects of synaptic strength on sleep slow waves. *Sleep* 30: 1617–1630, 2007.
284. **Esser SK, Hill S, Tononi G.** Breakdown of effective connectivity during slow wave sleep: investigating the mechanism underlying a cortical gate using large-scale modeling. *J Neurophysiol* 102: 2096–2111, 2009.
285. **Fan J, Byrne J, Worden M, Guise K, McCandliss B, Fossella J, Posner M.** The relation of brain oscillations to attentional networks. *J Neurosci* 27: 6197–6206, 2007.
286. **Farmer SF.** Rhythmicity, synchronization and binding in human and primate motor systems. *J Physiol* 509: 3–14, 1998.
287. **Fell J, Klaver P, Lehnertz K, Grunwald T, Schaller C, Elger CE, Fernández G.** Human memory formation is accompanied by rhinal-hippocampal coupling and decoupling. *Nat Neurosci* 4: 1259–1264, 2001.
288. **Felleman DJ, Van Essen DC.** Distributed hierarchical processing in the primate cerebral cortex. *Cereb Cortex* 1: 1–47, 1991.
289. **Feller MB, Butts DA, Aaron HL, Rokhsar DS, Shatz CJ.** Dynamic processes shape spatiotemporal properties of retinal waves. *Neuron* 19: 293–306, 1997.
290. **Fellous J, Sejnowski T.** Cholinergic induction of oscillations in the hippocampal slice in the slow (0.5–2 Hz), theta (5–12 Hz), gamma (35–70 Hz) bands. *Hippocampus* 10: 187–197, 2000.
291. **Fisahn A, Pike FG, Buhl EH, Paulsen O.** Cholinergic induction of network oscillations at 40 Hz in the hippocampus in vitro. *Nature* 394: 186–189, 1998.
292. **Flint AC, Connors BW.** Two types of network oscillations in neocortex mediated by distinct glutamate receptor subtypes and neuronal populations. *J Neurophysiol* 75: 951–957, 1996.
293. **Foehring R, Lorenzon N, Herron P, Wilson C.** Correlation of physiologically and morphologically identified neuronal types in human association cortex in vitro. *J Neurophysiol* 66: 1825–1837, 1991.
294. **Fontanini A, Katz D.** Behavioral states, network states, and sensory response variability. *J Neurophysiol* 100: 1160–1168, 2008.
295. **Ford J, Krystal J, Mathalon D.** Neural synchrony in schizophrenia: from networks to new treatments. *Schizophr Bull* 33: 848–852, 2007.
296. **Fortune ES, Rose GJ.** Short-term synaptic plasticity contributes to the temporal filtering of electrosensory information. *J Neurosci* 20: 7122–7130, 2000.
297. **Fourcaud-Trocme N, Hansel D, van Vreeswijk C, Brunel N.** How spike generation mechanisms determine the neuronal response to fluctuating inputs. *J Neurosci* 23: 11628–11640, 2003.
298. **Fransén E, Alonso AA, Dickson CT, Magistretti J, Hasselmo ME.** Ionic mechanisms in the generation of subthreshold oscillations and action potential clustering in entorhinal layer II stellate neurons. *Hippocampus* 14: 368–384, 2004.
299. **Freeman JA, Nicholson C.** Experimental optimization of current source-density technique for anuran cerebellum. *J Neurophysiol* 38: 369–382, 1975.
300. **Freeman W.** Relations between unit activity and evoked potentials in prepyriform cortex of cats. *J Neurophysiol* 31: 337–348, 1968.
301. **Freeman W.** Spatial properties of an EEG event in the olfactory bulb and cortex. *Electroencephalogr Clin Neurophysiol* 44: 586–605, 1978.
302. **Freeman W, Barrie J.** Analysis of spatial patterns of phase in neocortical gamma EEGs in rabbit. *J Neurophysiol* 84: 1266–1278, 2000.
303. **Freeman WJ.** *Mass Action in the Nervous System*. New York: Academic, 1975.
304. **Freund T, Antal M.** GABA-containing neurons in the septum control inhibitory interneurons in the hippocampus. *Nature* 336: 170–173, 1988.
305. **Freund T, Buzski G.** Interneurons of the hippocampus. *Hippocampus* 6: 347–470, 1996.
306. **Friedman D, Strowbridge B.** Both electrical and chemical synapses mediate fast network oscillations in the olfactory bulb. *J Neurophysiol* 89: 2601–2610, 2003.
307. **Friedman-Hill S, Maldonado P, Gray C.** Dynamics of striate cortical activity in the alert macaque. I. Incidence and stimulus-dependence of gamma-band neuronal oscillations. *Cereb Cortex* 10: 1105–1116, 2000.
308. **Friedrich R, Laurent G.** Dynamic optimization of odor representations by slow temporal patterning of mitral cell activity. *Science* 291: 889–894, 2001.
309. **Frien A, Eckhorn R, Bauer R, Woelbern T, Kehr H.** Stimulus-specific fast oscillations at zero phase between visual areas V1 and V2 of awake monkey. *Neuroreport* 5: 2273–2277, 1994.
310. **Fries P.** A mechanism for cognitive dynamics: neuronal communication through neuronal coherence. *Trends Cogn Sci* 9: 474–480, 2005.
311. **Fries P.** Neuronal gamma-band synchronization as a fundamental process in cortical computation. *Annu Rev Neurosci* 32: 209–224, 2009.
312. **Fries P, Reynolds J, Rorie A, Desimone R.** Modulation of oscillatory neuronal synchronization by selective visual attention. *Science* 291: 1560–1563, 2001.
313. **Fries P, Nikolic´ D, Singer W.** The gamma cycle. *Trends Neurosci* 30: 309–316, 2007.
314. **Fries P, Scheeringa R, Oostenveld R.** Finding gamma. *Neuron 5* 8: 303–305, 2008.
315. **Fries P, Womelsdorf T, Oostenveld R, Desimone R.** The effects of visual stimulation and selective visual attention on rhythmic neuronal synchronization in macaque area V4. *J Neurosci* 28: 4823–4835, 2008.
316. **Friston K.** Schizophrenia and the disconnection hypothesis. *Acta Psychiatr Scand Suppl* 395: 68–79, 1999.
317. **Frith U.** *Autism: Explaining the Enigma*. Oxford, UK: Blackwell, 1989.
318. **Frolov A, Medvedev A.** Substantiation of the "point approximation" for describing the total electrical activity of the brain with the use of a simulation model. *Biophysics* 31: 304–308, 1986.
319. **Fründ I, Ohl FW, Herrmann CS.** Spike-timing-dependent plasticity leads to gamma band responses in a neural network. *Biol Cybern* 101: 227–240, 2009.
320. **Fuchs EC, Zivkovic AR, Cunningham MO, Middleton S, Lebeau FE, Bannerman DM, Rozov A, Whittington MA, Traub RD, Rawlins JN, Monyer H.** Recruitment of parvalbumin-positive interneurons determines hippocampal function and associated behavior. *Neuron* 53: 591–604, 2007.
321. **Fuhrmann G, Markram H, Tsodyks M.** Spike frequency adaptation and neocortical rhythms. *J Neurophysiol* 88: 761–770, 2002.
322. **Fukuda T, Kosaka T, Singer W, Galuske R.** Gap junctions among dendrites of cortical GABAergic neurons establish a dense and widespread intercolumnar network. *J Neurosci* 26: 3434–3443, 2006.
323. **Funahashi S, Bruce CJ, Goldman-Rakic PS.** Mnemonic coding of visual space in the monkey's dorsolateral prefrontal cortex. *J Neurophysiol* 61: 331–349, 1989.

324. **Fuster JM.** *The Prefrontal Cortex* (4th ed.). New York: Academic, 2008.
325. **Gagliardi R (Editor).** *Introduction to Communications Engineering* (2nd ed.). New York: Wiley, 1988.
326. **Gahwiler B, Brown D.** Functional innervation of cultured hippocampal neurones by cholinergic afferents from co-cultured septal explants. *Nature* 313: 577–579, 1985.
327. **Gail A, Brinksmeyer HJ, Eckhorn R.** Perception-related modulations of local field potential power and coherence in primary visual cortex of awake monkey during binocular rivalry. *Cereb Cortex* 14: 300–313, 2004.
328. **Galambos R, Makeig S, Talmachoff P.** A 40-Hz auditory potential recorded from the human scalp. *Proc Natl Acad Sci USA* 78: 2643–2647, 1981.
329. **Galán R, Fourcaud-Trocm N, Ermentrout G, Urban N.** Correlation-induced synchronization of oscillations in olfactory bulb neurons. *J Neurosci* 26: 3646–3655, 2006.
330. **Galán R, Ermentrout G, Urban N.** Stochastic dynamics of uncoupled neural oscillators: Fokker-Planck studies with the finite element method. *Phys Rev E Stat Nonlin Soft Matter Phys* 76: 056110, 2007.
331. **Galarreta M, Hestrin S.** A network of fast-spiking cells in the neocortex connected by electrical synapses. *Nature* 402: 72–75, 1999.
332. **Galarreta M, Hestrin S.** Spike transmission and synchrony detection in networks of GABAergic interneurons. *Science* 292: 2295–2299, 2001.
333. **Galarreta M, Hestrin S.** Electrical and chemical synapses among parvalbumin fast-spiking GABAergic interneurons in adult mouse neocortex. *Proc Natl Acad Sci USA* 99: 12438–12443, 2002.
334. **Gao B, Hornung J, Fritschy J.** Identification of distinct $GABA_A$-receptor subtypes in cholinergic and parvalbumin-positive neurons of the rat and marmoset medial septum-diagonal band complex. *Neuroscience* 65: 101–117, 1995.
335. **Garaschuk O, Milos RI, Konnerth A.** Targeted bulk-loading of fluorescent indicators for two-photon brain imaging in vivo. *Nat Protoc* 1: 380–386, 2006.
336. **Garrity A, Pearlson G, McKiernan K, Lloyd D, Kiehl K, Calhoun V.** Aberrant "default mode" functional connectivity in schizophrenia. *Am J Psychiatry* 164: 450–457, 2007.
337. **Gaspard P, Wang XJ.** Noise, chaos and (ε, τ)-entropy per unit time. *Phys Rep* 235: 321–373, 1993.
338. **Gasparini S, Magee JC.** State-dependent dendritic computation in hippocampal CA1 pyramidal neurons. *J Neurosci* 26: 2088–2100, 2006.
339. **Gawne TJ, Richmond BJ.** How independent are the messages carried by adjacent inferior temporal cortical neurons? *J Neurosci* 13: 2758–2771, 1993.
340. **Gaztelu J, Buño W.** Septo-hippocampal relationships during EEG theta rhythm. *Electroencephalogr Clin Neurophysiol* 54: 375–387, 1982.
341. **Geisler C.** *The Interplay Between Intrinsic Cell Properties and Synaptic Dynamics in the Generation of Oscillations in Cortical Network Models* (PhD dissertation). Waltham, MA: Brandeis University, 2004.
342. **Geisler C, Brunel N, Wang XJ.** Contributions of intrinsic membrane dynamics to fast network oscillations with irregular neuronal discharges. *J Neurophysiol* 94: 4344–4361, 2005.
343. **Geisler C, Robbe D, Zugaro M, Sirota A, Buzski G.** Hippocampal place cell assemblies are speed-controlled oscillators. *Proc Natl Acad Sci USA* 104: 8149–8154, 2007.
344. **Gerstner W, Kempter R, van Hemmen J, Wagner H.** A neuronal learning rule for sub-millisecond temporal coding. *Nature* 383: 76–81, 1996.
345. **Gerstner W, van Hemmen L, Cowan J.** What matters in neuronal locking? *Neural Computat* 8: 1653–1676, 1996.
346. **Geschwind DH, Levitt P.** Autism spectrum disorders: developmental disconnection syndromes. *Curr Opin Neurobiol* 17: 103–111, 2007.
347. **Getting PA.** Emerging principles governing the operation of neural networks. *Annu Rev Neurosci* 12: 185–204, 1989.
348. **Gevins A, Smith M, McEvoy L, Yu D.** High-resolution EEG mapping of cortical activation related to working memory: effects of task difficulty, type of processing, and practice. *Cereb Cortex* 7: 374–385, 1997.
349. **Ghazanfar A, Chandrasekaran C, Logothetis N.** Interactions between the superior temporal sulcus and auditory cortex mediate dynamic face/voice integration in rhesus monkeys. *J Neurosci* 28: 4457–4469, 2008.
350. **Gibson J, Beierlein M, Connors B.** Two networks of electrically coupled inhibitory neurons in neocortex. *Nature* 402: 75–79, 1999.
351. **Gibson J, Beierlein M, Connors B.** Functional properties of electrical synapses between inhibitory interneurons of neocortical layer 4. *J Neurophysiol* 93: 467–480, 2005.
352. **Gilbert C, Wiesel T.** Functional organization of the visual cortex. *Prog Brain Res* 58: 209–218, 1983.
353. **Gilbert CD.** Circuitry, architecture, and functional dynamics of visual cortex. *Cereb Cortex* 3: 373–386, 1993.
354. **Gillies M, Traub R, LeBeau F, Davies C, Gloveli T, Buhl E, Whittington M.** A model of atropine-resistant theta oscillations in rat hippocampal area CA1. *J Physiol* 543: 779–793, 2002.
355. **Giocomo LM, Hasselmo ME.** Computation by oscillations: implications of experimental data for theoretical models of grid cells. *Hippocampus* 18: 1186–1199, 2008.
356. **Giocomo LM, Hasselmo ME.** Knock-out of HCN1 subunit flattens dorsal-ventral frequency gradient of medial entorhinal neurons in adult mice. *J Neurosci* 29: 7625–7630, 2009.
357. **Giocomo LM, Zilli EA, Fransn E, Hasselmo ME.** Temporal frequency of subthreshold oscillations scales with entorhinal grid cell field spacing. *Science* 315: 1719–1722, 2007.
358. **Gireesh E, Plenz D.** Neuronal avalanches organize as nested theta- and beta/gamma-oscillations during development of cortical layer 2/3. *Proc Natl Acad Sci USA* 105: 7576–7581, 2008.
359. **Glass LW, Mackey MC.** *From Clocks to Chaos*. Princeton, NJ: Princeton Univ. Press, 1988.
360. **Gnadt JW, Andersen RA.** Memory related motor planning activity in posterior parietal cortex of macaque. *Exp Brain Res* 70: 216–220, 1988.
361. **Goense J, Logothetis N.** Neurophysiology of the BOLD fMRI signal in awake monkeys. *Curr Biol* 18: 631–640, 2008.
362. **Goldberg J, Deister C, Wilson C.** Response properties and synchronization of rhythmically firing dendritic neurons. *J Neurophysiol* 97: 208–219, 2007.
363. **Goldman-Rakic PS.** Working memory dysfunction in schizophrenia. *J Neuropsychol Clin Neurosci* 6: 348–357, 1994.
364. **Goldman-Rakic PS.** Cellular basis of working memory. *Neuron* 14: 477–485, 1995.
365. **Golomb D, Ermentrout G.** Continuous and lurching traveling pulses in neuronal networks with delay and spatially decaying connectivity. *Proc Natl Acad Sci USA* 96: 13480–13485, 1999.
366. **Golomb D, Hansel D.** The number of synaptic inputs and the synchrony of large sparse neuronal networks. *Neural Computation* 12: 1095–139, 2000.
367. **Golomb D, Rinzel J.** Clustering in globally coupled inhibitory neurons. *Physica D* 72: 259–282, 1994.
368. **Golomb D, Wang XJ, Rinzel J.** Propagation of spindle waves in a thalamic slice model. *J Neurophysiol* 75: 750–769, 1996.
369. **Golomb D, Yue C, Yaari Y.** Contribution of persistent Na^+ current and M-type K^+ current to somatic bursting in CA1 pyramidal cells: combined experimental and modeling study. *J Neurophysiol* 96: 1912–1926, 2006.
370. **Goutagny R, Jackson J, Williams S.** Self-generated theta oscillations in the hippocampus. *Nat Neurosci* 12: 1491–1493, 2009.
371. **Gratton G, Coles M, Sirevaag E, Eriksen C, Donchin E.** Investigating causal relations by econometric models and cross-spectral methods. *Econometrics* 37: 424–438, 1969.
372. **Gray CM.** Synchronous oscillations in neuronal systems: mechanisms and functions. *J Comput Neurosci* 1: 11–38, 1994.
373. **Gray CM, McCormick DA.** Chattering cells: superficial pyramidal neurons contributing to the generation of synchronous oscillations in the visual cortex. *Science* 274: 109–113, 1996.
374. **Gray CM, Singer W.** Stimulus-specific neuronal oscillations in orientation columns of cat visual cortex. *Proc Natl Acad Sci USA* 86: 1698–1702, 1989.

375. **Gray CM, Viana Di Prisco G.** Stimulus-dependent neuronal oscillations and local synchronization in striate cortex of the alert cat. *J Neurosci* 17: 3239–3253, 1997.
376. **Gray CM, König P, Engel A, Singer W.** Oscillatory responses in cat visual cortex exhibit inter-columnar synchronization which reflects global stimulus properties. *Nature* 338: 334–337, 1989.
377. **Gray CM, Engel A, König P, Singer W.** Stimulus-dependent neuronal oscillations in cat visual cortex: receptive field properties and feature dependence. *Eur J Neurosci* 2: 607–619, 1990.
378. **Gray CM, Engel A, König P, Singer W.** Synchronization of oscillatory neuronal responses in cat striate cortex: temporal properties. *Vis Neurosci* 8: 337–347, 1992.
379. **Green M.** What are the functional consequences of neurocognitive deficits in schizophrenia? *Am J Psychiatry* 153: 321–330, 1996.
380. **Greenberg DS, Houweling AR, Kerr JN.** Population imaging of ongoing neuronal activity in the visual cortex of awake rats. *Nat Neurosci* 11: 749–751, 2008.
381. **Gregoriou GG, Gotts SJ, Zhou H, Desimone R.** High-frequency, long-range coupling between prefrontal and visual cortex during attention. *Science* 324: 1207–1210, 2009.
382. **Grice SJ, Spratling MW, Karmiloff-Smith A, Halit H, Csibra G, de Haan M, Johnson MH.** Disordered visual processing and oscillatory brain activity in autism and Williams syndrome. *Neuroreport* 12: 2697–2700, 2001.
383. **Grinvald A, Lieke E, Frostig R, Hildesheim R.** Cortical point-spread function and long-range lateral interactions revealed by real-time optical imaging of macaque monkey primary visual cortex. *J Neurosci* 14: 2545–2568, 1994.
384. **Gritti I, Mainville L, Jones B.** Codistribution of GABA- with acetylcholine-synthesizing neurons in the basal forebrain of the rat. *J Comp Neurol* 329: 438–457, 1993.
385. **Gross J, Schmitz F, Schnitzler I, Kessler K, Shapiro K, Hommel B, Schnitzler A.** Modulation of long-range neural synchrony reflects temporal limitations of visual attention in humans. *Proc Natl Acad Sci USA* 101: 13050–13055, 2004.
386. **Gross J, Schnitzler A, Timmermann L, Ploner M.** Gamma oscillations in human primary somatosensory cortex reflect pain perception. *PLoS Biol* 5: e133, 2007.
387. **Grossberg S, Versace M.** Spikes, synchrony, and attentive learning by laminar thalamocortical circuits. *Brain Res* 1218: 278–312, 2008.
388. **Gruber T, Mller M, Keil A, Elbert T.** Selective visual-spatial attention alters induced gamma band responses in the human EEG. *Clin Neurophysiol* 110: 2074–2085, 1999.
389. **Grunze HC, Rainnie DG, Hasselmo ME, Barkai E, Hearn EF, McCarley RW, Greene RW.** NMDA-dependent modulation of CA1 local circuit inhibition. *J Neurosci* 16: 2034–2043, 1996.
390. **Guderian S, Schott BH, Richardson-Klavehn A, Düzel E.** Medial temporal theta state before an event predicts episodic encoding success in humans. *Proc Natl Acad Sci USA* 106: 5365–5370, 2009.
391. **Guillery RW, Sherman SM.** Thalamic relay functions and their role in corticocortical communication: generalizations from the visual system. *Neuron* 33: 163–175, 2002.
392. **Gur M, Snodderly D.** High response reliability of neurons in primary visual cortex (V1) of alert, trained monkeys. *Cereb Cortex* 16: 888–895, 2006.
393. **Gusnard DA, Raichle ME, Raichle ME.** Searching for a baseline: functional imaging and the resting human brain. *Nat Rev Neurosci* 2: 685–694, 2001.
394. **Gutfreund Y, Yarom Y, Segev I.** Subthreshold oscillations and resonant frequency in guinea-pig cortical neurons: physiology and modelling. *J Physiol* 483: 621–640, 1995.
395. **Gutkin B, Ermentrout G, Reyes A.** Phase-response curves give the responses of neurons to transient inputs. *J Neurophysiol* 94: 1623–1635, 2005.
396. **Haas JS, White JA.** Frequency selectivity of layer II stellate cells in the medial entorhinal cortex. *J Neurophysiol* 88: 2422–2429, 2002.
397. **Haas JS, Dorval AD, White JA.** Contributions of Ih to feature selectivity in layer II stellate cells of the entorhinal cortex. *J Comput Neurosci* 22: 161–171, 2007.
398. **Haenschel C, Uhlhaas P, Singer W.** Synchronous oscillatory activity and working memory in schizophrenia. *Pharmacopsychiatry* 40: S54–S61, 2007.
399. **Haenschel C, Bittner RA, Waltz J, Haertling F, Wibral M, Singer W, Linden DE, Rodriguez E.** Cortical oscillatory activity is critical for working memory as revealed by deficits in early-onset schizophrenia. *J Neurosci* 29: 9481–9489, 2009.
400. **Hafting T, Fyhn M, Molden S, Moser MB, Moser EI.** Microstructure of a spatial map in the entorhinal cortex. *Nature* 436: 801–806, 2005.
401. **Hafting T, Fyhn M, Bonnevie T, Moser M, Moser E.** Hippocampus-independent phase precession in entorhinal grid cells. *Nature* 453: 1248–1252, 2008.
402. **Hagmann P, Cammoun L, Gigandet X, Meuli R, Honey C, Wedeen V, Sporns O.** Mapping the structural core of human cerebral cortex. *PLoS Biol.* 6: e159, 2008.
403. **Hahn T, Sakmann B, Mehta M.** Phase-locking of hippocampal interneurons' membrane potential to neocortical up-down states. *Nat Neurosci* 9: 1359–1361, 2006.
404. **Haider B, McCormick DA.** Rapid neocortical dynamics: cellular and network mechanisms. *Neuron* 62: 171–189, 2009.
405. **Haider B, Duque A, Hasenstaub AR, McCormick DA.** Neocortical network activity in vivo is generated through a dynamic balance of excitation and inhibition. *J Neurosci* 26: 4535–4545, 2006.
406. **Hajós M, Hoffmann W, Orbán G, Kiss T, Erdi P.** Modulation of septo-hippocampal theta activity by $GABA_A$ receptors: an experimental and computational approach. *Neuroscience* 126: 599–610, 2004.
407. **Hájos N, Paulsen O.** Network mechanisms of gamma oscillations in the CA3 region of the hippocampus. *Neural Netw* 22: 1113–1119, 2009.
408. **Hájos N, Pálhalmi J, Mann E, Németh B, Paulsen O, Freund T.** Spike timing of distinct types of GABAergic interneuron during hippocampal gamma oscillations in vitro. *J Neurosci* 24: 9127–9137, 2004.
409. **Hamzei-Sichani F, Kamasawa N, Janssen W, Yasumura T, Davidson K, Hof P, Wearne S, Stewart M, Young S, Whittington M, Rash J, Traub R.** Gap junctions on hippocampal mossy fiber axons demonstrated by thin-section electron microscopy and freeze fracture replica immunogold labeling. *Proc Natl Acad Sci USA* 104: 12548–12553, 2007.
410. **Han F, Caporale N, Dan Y.** Reverberation of recent visual experience in spontaneous cortical waves. *Neuron* 60: 321–327, 2008.
411. **Han X, Qian X, Bernstein JG, Zhou HH, Franzesi GT, Stern P, Bronson RT, Graybiel AM, Desimone R, Boyden ES.** Millisecond-timescale optical control of neural dynamics in the nonhuman primate brain. *Neuron* 62: 191–198, 2009.
412. **Hangya B, Borhegyi Z, Szilgyi N, Freund TF, Varga V.** GABAergic neurons of the medial septum lead the hippocampal network during theta activity. *J Neurosci* 29: 8094–8102, 2009.
413. **Hansel D, Mato G.** Existence and stability of persistent states in large neuronal networks. *Phys Rev Lett* 86: 4175–4178, 2001.
414. **Hansel D, Mato G.** Asynchronous states and the emergence of synchrony in large networks of interacting excitatory and inhibitory neurons. *Neural Comput* 15: 1–56, 2003.
415. **Hansel D, Mato G, Meunier C.** Synchrony in excitatory neural networks. *Neural Comp* 7: 307–337, 1995.
416. **Happé F, Frith U.** The weak coherence account: detail-focused cognitive style in autism spectrum disorders. *J Autism Dev Disord* 36: 5–25, 2006.
417. **Happé FG, Booth RD.** The power of the positive: revisiting weak coherence in autism spectrum disorders. *Q J Exp Psychol* 61: 50–63, 2008.
418. **Harris KD, Henze DA, Hirase H, Leinekugel X, Dragoi G, Czurkó A, Buzsáki G.** Spike train dynamics predicts theta-related phase precession in hippocampal pyramidal cells. *Nature* 417: 738–741, 2002.
419. **Harris KD, Csicsvari J, Hirase H, Dragoi G, Buzski G.** Organization of cell assemblies in the hippocampus. *Nature* 424: 552–556, 2003.

420. **Harsch A, Robinson H.** Postsynaptic variability of firing in rat cortical neurons: the roles of input synchronization and synaptic NMDA receptor conductance. *J Neurosci* 20: 6181–6192, 2000.
421. **Hartwich K, Pollak T, Klausberger T.** Distinct firing patterns of identified basket and dendrite-targeting interneurons in the prefrontal cortex during hippocampal theta and local spindle oscillations. *J Neurosci* 29: 9563–9574, 2009.
422. **Harvey CD, Collman F, Dombeck DA, Tank DW.** Intracellular dynamics of hippocampal place cells during virtual navigation. *Nature* 461: 941–946, 2009.
423. **Hasenstaub A, Shu Y, Haider B, Kraushaar U, Duque A, McCormick D.** Inhibitory postsynaptic potentials carry synchronized frequency information in active cortical networks. *Neuron* 47: 423–435, 2005.
424. **Hasselmo M, Bodelón C, Wyble B.** A proposed function for hippocampal theta rhythm: separate phases of encoding and retrieval enhance reversal of prior learning. *Neural Comput* 14: 793–817, 2002.
425. **Hasselmo ME.** What is the function of hippocampal theta rhythm? Linking behavioral data to phasic properties of field potential and unit recording data. *Hippocampus* 15: 936–949, 2005.
426. **Hasselmo ME, Brandon MP, Yoshida M, Giocomo LM, Heys JG, Fransen E, Newman EL, Zilli EA.** A phase code for memory could arise from circuit mechanisms in entorhinal cortex. *Neural Netw* 22: 1129–1138, 2009.
427. **Hauck M, Lorenz J, Engel A.** Attention to painful stimulation enhances gamma-band activity and synchronization in human sensorimotor cortex. *J Neurosci* 27: 9270–9277, 2007.
428. **He B, Shulman G, Snyder A, Corbetta M.** The role of impaired neuronal communication in neurological disorders. *Curr Opin Neurol* 20: 655–660, 2007.
429. **He Y, Chen Z, Gong G, Evans A.** Neuronal networks in Alzheimer disease. *Neuroscientist* 15: 333–350, 2009.
430. **Heggelund P, Albus K.** Response variability and orientation discrimination of single cells in striate cortex of cat. *Exp Brain Res* 32: 197–211, 1978.
431. **Henrie JA, Shapley R.** LFP power spectra in V1 cortex: the graded effect of stimulus contrast. *J Neurophysiol* 94: 479–490, 2005.
432. **Herrmann CS, Fründ I, Lenz D.** Human gamma-band activity: a review on cognitive and behavioral correlates and network models. *Neurosci Biobehav Rev* 2009.
433. **Hertz J.** Cross-correlations in high-conductance states of a model cortical network. *Neural Comput* 22: 427–447, 2010.
434. **Hestrin S, Galarreta M.** Electrical synapses define networks of neocortical GABAergic neurons. *Trends Neurosci* 28: 304–309, 2005.
435. **Higgs MH, Spain WJ.** Conditional bursting enhances resonant firing in neocortical layer 2–3 pyramidal neurons. *J Neurosci* 29: 1285–1299, 2009.
436. **Hilgetag CC, Burns GA, O'Neill MA, Scannell JW, Young MP.** Anatomical connectivity defines the organization of clusters of cortical areas in the macaque monkey and the cat. *Philos Trans R Soc Lond B Biol Sci* 355: 91–110, 2000.
437. **Hodgkin AL, Huxley AF.** A quantitative description of membrane current and its application to conductance and excitation in nerve. *J Physiol* 117: 500, 1952.
438. **Hoffman R, McGlashan T.** Reduced corticocortical connectivity can induce speech perception pathology and hallucinated "voices." *Schizophr Res* 30: 137–141, 1998.
439. **Hoffman R, Varanko M, McGlashan T, Hampson M.** Auditory hallucinations, network connectivity, and schizophrenia. *Behav Brain Sci* 27: 860–861, 2005.
440. **Holcman D, Tsodyks M.** The emergence of Up and Down states in cortical networks. *PLoS Comput Biol* 2: e23, 2006.
441. **Hopfield J.** Odor space and olfactory processing: collective algorithms and neural implementation. *Proc Natl Acad Sci USA* 96: 12506–12511, 1999.
442. **Hormuzdi SG, Pais I, LeBeau FE, Towers SK, Rozov A, Buhl EH, Whittington MA, Monyer H.** Impaired electrical signaling disrupts gamma frequency oscillations in connexin 36-deficient mice. *Neuron* 31: 487–495, 2001.
443. **Horowitz JM.** Evoked activity of single units and neural populations in the hippocampus of the cat. *Electroencephalogr Clin Neurophysiol* 32: 227–240, 1972.
444. **Howard M, Rizzuto D, Caplan J, Madsen J, Lisman J, Aschenbrenner-Scheibe R, Schulze-Bonhage A, Kahana M.** Gamma oscillations correlate with working memory load in humans. *Cereb Cortex* 13: 1369–1374, 2003.
445. **Hu H, Vervaeke K, Storm J.** Two forms of electrical resonance at theta frequencies, generated by M-current, h-current and persistent Na^+ current in rat hippocampal pyramidal cells. *J Physiol* 545: 783–805, 2002.
446. **Hu H, Vervaeke K, Graham LJ, Storm JF.** Complementary theta resonance filtering by two spatially segregated mechanisms in CA1 hippocampal pyramidal neurons. *J Neurosci* 29: 14472–14483, 2009.
447. **Huanag NE, Shen Z, Long SR, Wu MC, Shih HH, Zheng Q, Yen NC, Tung CC, Liu HH.** The empirical mode decomposition and the Hilbert spectrum for nonlinear and nonstationary time-series analysis. *Proc R Soc Lond A* 454: 903–995, 1998.
448. **Huang X, Troy WC, Yang Q, Ma H, Laing CR, Schiff SJ, Wu JY.** Spiral waves in disinhibited mammalian neocortex. *J Neurosci* 24: 9897–9902, 2004.
449. **Huber R, Ghilardi MF, Massimini M, Tononi G.** Local sleep and learning. *Nature* 430: 78–81, 2004.
450. **Huerta PT, Lisman JE.** Heightened synaptic plasticity of hippocampal CA1 neurons during a cholinergically induced rhythmic state. *Nature* 364: 723–725, 1993.
451. **Hughes SW, Cope DW, Blethyn KL, Crunelli V.** Cellular mechanisms of the slow (>1 Hz) oscillation in thalamocortical neurons in vitro. *Neuron* 33: 947–958, 2002.
452. **Hummel F, Andres F, Altenmüller E, Dichgans J, Gerloff C.** Inhibitory control of acquired motor programmes in the human brain. *Brain* 125: 404–420, 2002.
453. **Hutcheon B, Yarom Y.** Resonance, oscillation and the intrinsic frequency preferences of neurons. *Trends Neurosci* 23: 216–222, 2000.
454. **Hutcheon B, Miura R, Puil E.** Models of subthreshold membrane resonance in neocortical neurons. *J Neurophysiol* 76: 698–714, 1996.
455. **Hutcheon B, Miura R, Puil E.** Subthreshold membrane resonance in neocortical neurons. *J Neurophysiol* 76: 683–697, 1996.
456. **Huxter J, Burgess N, O'Keefe J.** Independent rate and temporal coding in hippocampal pyramidal cells. *Nature* 425: 828–832, 2003.
457. **Huxter J, Senior T, Allen K, Csicsvari J.** Theta phase-specific codes for two-dimensional position, trajectory and heading in the hippocampus. *Nat Neurosci* 11: 587–594, 2008.
458. **Hyman JM, Zilli EA, Paley AM, Hasselmo ME.** Medial prefrontal cortex cells show dynamic modulation with the hippocampal theta rhythm dependent on behavior. *Hippocampus* 15: 739–749, 2005.
459. **Idiart MAP, Abbott LF.** Propagation of excitation in neural network models. *Network Comp Neural Sys* 4: 285–294, 1993.
460. **Isope P, Dieudonn S, Barbour B.** Temporal organization of activity in the cerebellar cortex: a manifesto for synchrony. *Ann NY Acad Sci* 978: 164–174, 2002.
461. **Ito I, Bazhenov M, Ong C, Raman B, Stopfer M.** Frequency transitions in odor-evoked neural oscillations. *Neuron* 64: 692–706, 2009.
462. **Itskov V, Pastalkova E, Mizuseki K, Buzsaki G, Harris K.** Theta-mediated dynamics of spatial information in hippocampus. *J Neurosci* 28: 5959–5964, 2008.
463. **Izhikevich E.** Resonate-and-fire neurons. *Neural Netw* 14: 883–894, 2001.
464. **Izhikevich E.** Polychronization: computation with spikes. *Neural Comput* 18: 245–282, 2006.
465. **Izhikevich E.** Solving the distal reward problem through linkage of STDP and dopamine signaling. *Cereb Cortex* 17: 2443–2452, 2007.
466. **Izhikevich EM, Desai NS, Walcott EC, Hoppensteadt FC.** Bursts as a unit of neural information: selective communication via resonance. *Trends Neurosci* 26: 161–167, 2003.

467. **Jacobs J, Kahana M, Ekstrom A, Fried I.** Brain oscillations control timing of single-neuron activity in humans. *J Neurosci* 27: 3839–3844, 2007.
468. **Jarvis MR, Mitra PP.** Sampling properties of the spectrum and coherency of sequences of action potentials. *Neural Comput* 13: 717–749, 2001.
469. **Jasper H, Penfield W.** Electrocorticograms in man: effect of voluntary movement upon the electrical activity of the precentral gyrus. *Eur Arch Psychiatry Clin Neurosci* 183: 163–174, 1949.
470. **Jay TM, Witter MP.** Distribution of hippocampal CA1 and subicular efferents in the prefrontal cortex of the rat studied by means of anterograde transport of *Phaseolus vulgaris*-leucoagglutinin. *J Comp Neurol* 313: 574–586, 1991.
471. **Jeewajee A, Barry C, O'Keefe J, Burgess N.** Grid cells and theta as oscillatory interference: electrophysiological data from freely moving rats. *Hippocampus* 18: 1175–1185, 2008.
472. **Jensen O, Colgin L.** Cross-frequency coupling between neuronal oscillations. *Trends Cogn Sci* 11: 267–269, 2007.
473. **Jensen O, Lisman JE.** Position reconstruction from an ensemble of hippocampal place cells: contribution of theta phase coding. *J Neurophysiol* 83: 2602–2609, 2000.
474. **Jensen O, Tesche C.** Frontal theta activity in humans increases with memory load in a working memory task. *Eur J Neurosci* 15: 1395–1399, 2002.
475. **Jensen O, Gelfand J, Kounios J, Lisman JE.** Oscillations in the alpha band (9–12 Hz) increase with memory load during retention in a short-term memory task. *Cereb Cortex* 12: 877–882, 2002.
476. **Jensen O, Kaiser J, Lachaux J.** Human gamma-frequency oscillations associated with attention and memory. *Trends Neurosci* 30: 317–324, 2007.
477. **Jerbi K, Hamam CM, Ossandn T, Dalal SS.** Role of posterior parietal gamma activity in planning prosaccades and antisaccades. *J Neurosci* 28: 13713–13715, 2008.
478. **Ji D, Wilson M.** Coordinated memory replay in the visual cortex and hippocampus during sleep. *Nat Neurosci* 10: 100–107, 2007.
479. **Jinno S, Klausberger T, Marton L, Dalezios Y, Roberts J, Fuentealba P, Bushong E, Henze D, Buzski G, Somogyi P.** Neuronal diversity in GABAergic long-range projections from the hippocampus. *J Neurosci* 27: 8790–8804, 2006.
480. **Joelving F, Compte A, Constantinidis C.** Temporal properties of posterior parietal neuron discharges during working memory and passive viewing. *J Neurophysiol* 97: 2254–2266, 2007.
481. **Johnson SW, Seutin V, North RA.** Burst firing in dopamine neurons induced by *N*-methyl-D-aspartate: role of electrogenic sodium pump. *Science* 258: 665–667, 1992.
482. **Joliot M, Ribary U, Llinás R.** Human oscillatory brain activity near 40 Hz coexists with cognitive temporal binding. *Proc Natl Acad Sci USA* 91: 11748–11751, 1994.
483. **Jones EG.** Thalamic circuitry and thalamocortical synchrony. *Philos Trans R Soc Lond B Biol Sci* 357: 1659–1673, 2002.
484. **Jones MW, Wilson MA.** Theta rhythms coordinate hippocampal-prefrontal interactions in a spatial memory task. *PLoS Biol.* 3: e402, 2005.
485. **Just MA, Cherkassky VL, Keller TA, Minshew NJ.** Cortical activation and synchronization during sentence comprehension in high-functioning autism: evidence of underconnectivity. *Brain* 127: 1811–1821, 2004.
486. **Jutras MJ, Fries P, Buffalo EA.** Gamma-band synchronization in the macaque hippocampus and memory formation. *J Neurosci* 29: 12521–12531, 2009.
487. **Kable JW, Glimcher PW.** The neurobiology of decision: consensus and controversy. *Neuron* 63: 733–745, 2009.
488. **Kahana MJ.** The cognitive correlates of human brain oscillations. *J Neurosci* 26: 1669–1672, 2006.
489. **Kahana MJ, Sekuler R, Caplan JB, Kirschen M, Madsen JR.** Human theta oscillations exhibit task dependence during virtual maze navigation. *Nature* 399: 781–784, 1999.
490. **Kaiser J, Hertrich I, Ackermann H, Mathiak K, Lutzenberger W.** Hearing lips: gamma-band activity during audiovisual speech perception. *Cereb Cortex* 15: 646–653, 2005.
491. **Kaiser M, Hilgetag CC.** Nonoptimal component placement, but short processing paths, due to long-distance projections in neural systems. *PLoS Comput Biol* 2: e95, 2006.
492. **Kamondi A, Acsady L, Wang XJ, Buzsaki G.** Theta oscillations in somata and dendrites of hippocampal pyramidal cells in vivo: activity-dependent phase-precession of action potentials. *Hippocampus* 8: 244–261, 1998.
493. **Kana RK, Keller TA, Cherkassky VL, Minshew NJ, Just MA.** Atypical frontal-posterior synchronization of Theory of Mind regions in autism during mental state attribution. *Social Neurosci* 4: 135–152, 2009.
494. **Kandel ER, Spencer WA.** Electrophysiology of hippocampal neurons. II. After-potentials and repetitive firing. *J Neurophysiol* 24: 243–259, 1961.
495. **Kara P, Reinagel P, Reid R.** Low response variability in simultaneously recorded retinal, thalamic, cortical neurons. *Neuron* 27: 635–646, 2000.
496. **Kashiwadani H, Sasaki YF, Uchida N, Mori K.** Synchronized oscillatory discharges of mitral/tufted cells with different molecular receptive ranges in the rabbit olfactory bulb. *J Neurophysiol* 82: 1786–1792, 1999.
497. **Kass R, Ventura V.** A spike-train probability model. *Neural Comput* 13: 1713–1720, 2001.
498. **Katzner S, Nauhaus I, Benucci A, Bonin V, Ringach DL, Carandini M.** Local origin of field potentials in visual cortex. *Neuron* 61: 35–41, 2009.
499. **Kawaguchi Y, Kubota Y.** Correlation of physiological subgroupings of nonpyramidal cells with parvalbumin- and calbindinD28k-immunoreactive neurons in layer V of rat frontal cortex. *J Neurophysiol* 70: 387–396, 1993.
500. **Kawaguchi Y, Kubota Y.** GABAergic cell subtypes and their synaptic connections in rat frontal cortex. *Cereb Cortex* 7: 476–486, 1997.
501. **Kay LM.** Two species of gamma oscillations in the olfactory bulb: dependence on behavioral state and synaptic interactions. *J Integr Neurosci* 2: 31–44, 2003.
502. **Kay LM, Freeman WJ.** Bidirectional processing in the olfactory-limbic axis during olfactory behavior. *Behav Neurosci* 112: 541–553, 1998.
503. **Kay LM, Beshel J, Brea J, Martin C, Rojas-Líbano D, Kopell N.** Olfactory oscillations: the what, how and what for. *Trends Neurosci* 32: 207–214, 2009.
504. **Kayser C, Montemurro MA, Logothetis NK, Panzeri S.** Spike-phase coding boosts and stabilizes information carried by spatial and temporal spike patterns. *Neuron* 61: 597–608, 2009.
505. **Kempter R, Gerstner W, van Hemmen J.** Hebbian learning and spiking neurons. *Phys Rev E* 59: 4498–4515, 1999.
506. **Kepecs A, Wang XJ, Lisman J.** Bursting neurons signal input slope. *J Neurosci* 22: 9053–9062, 2002.
507. **Khawaja FA, Tsui JM, Pack CC.** Pattern motion selectivity of spiking outputs and local field potentials in macaque visual cortex. *J Neurosci* 29: 13702–13709, 2009.
508. **Kilpatrick ZP, Bressloff PC.** Spatially structured oscillations in a two-dimensional excitatory neuronal network with synaptic depression. *J Comput Neurosci* 28: 193–209, 2010.
509. **King C, Recce M, O'Keefe J.** The rhythmicity of cells of the medial septum/diagonal band of Broca in the awake freely moving rat: relationships with behaviour and hippocampal theta. *Eur J Neurosci* 10: 464–477, 1998.
510. **Kitano K, Fukai T.** Variability vs. synchronicity of neuronal activity in local cortical network models with different wiring topologies. *J Comput Neurosci* 23: 237–250, 2007.
511. **Klausberger T, Somogyi P.** Neuronal diversity and temporal dynamics: the unity of hippocampal circuit operations. *Science* 321: 53–57, 2008.
512. **Klausberger T, Magill P, Márton L, Roberts J, Cobden P, Buzsáki G, Somogyi P.** Brain-state- and cell-type-specific firing of hippocampal interneurons in vivo. *Nature* 421: 844–848, 2003.
513. **Klausberger T, Mrton L, Baude A, Roberts J, Magill P, Somogyi P.** Spike timing of dendrite-targeting bistratified cells during hippocampal network oscillations in vivo. *Nat Neurosci* 7: 41–47, 2004.
514. **Klausberger T, Marton L, O'Neill J, Huck J, Dalezios Y, Fuentealba P, Suen W, Papp E, Kaneko T, Watanabe M, Csicsvari J, Somogyi P.** Complementary roles of cholecystoki-

nin- and parvalbumin-expressing GABAergic neurons in hippocampal network oscillations. *J Neurosci* 25: 9782–9793, 2005.
515. **Klimesch W.** EEG alpha and theta oscillations reflect cognitive and memory performance: a review and analysis. *Brain Res* 29: 169–195, 1999.
516. **Klimesch W, Doppelmayr M, Schimke H, Ripper B.** Theta synchronization and alpha desynchronization in a memory task. *Psychophysiology* 34: 169–176, 1997.
517. **Klimesch W, Doppelmayr M, Schwaiger J, Auinger P, Winkler T.** "Paradoxical" alpha synchronization in a memory task. *Cogn Brain Res* 7: 493–501, 1999.
518. **Klimesch W, Freunberger R, Sauseng P, Gruber W.** A short review of slow phase synchronization and memory: evidence for control processes in different memory systems? *Brain Res* 1235: 31–44, 2008.
519. **Klink R, Alonso A.** Ionic mechanisms for the subthreshold oscillations and differential electroresponsiveness of medial entorhinal cortex layer II neurons. *J Neurophysiol* 70: 144–157, 1993.
520. **Klostermann F, Nikulin VV, Khn AA, Marzinzik F, Wahl M, Pogosyan A, Kupsch A, Schneider GH, Brown P, Curio G.** Task-related differential dynamics of EEG alpha- and beta-band synchronization in cortico-basal motor structures. *Eur J Neurosci* 25: 1604–1615, 2007.
521. **Koch SP, Werner P, Steinbrink J, Fries P, Obrig H.** Stimulus-induced and state-dependent sustained gamma activity is tightly coupled to the hemodynamic response in humans. *J Neurosci* 29: 13962–13970, 2009.
522. **Kocsis B, Bragin A, Buzsáki G.** Interdependence of multiple theta generators in the hippocampus: a partial coherence analysis. *J Neurosci* 19: 6200–6212, 1999.
523. **Köndgen H, Geisler C, Fusi S, Wang XJ, Lüscher H, Giugliano M.** The dynamical response properties of neocortical neurons to temporally modulated noisy inputs in vitro. *Cereb Cortex* 18: 2086–2097, 2008.
524. **Kopell N, Ermentrout GB.** Symmetry and phaselocking in chains of weakly coupled oscillators. *Comm Pure Appl Math* 39: 623–660, 1986.
525. **Kopell N, Ermentrout GB.** Mechanisms of phase-locking and frequency control in pairs of coupled neural oscillators. In *Handbook on Dynamical Systems*, edited by B. Fielder. New York: Elsevier, 2002, p. 3–54.
526. **Kopell N, LeMasson G.** Rhythmogenesis, amplitude modulation, and multiplexing in a cortical architecture. *Proc Natl Acad Sci USA* 91: 10586–10590, 1994.
527. **Kopell N, Somers D.** Anti-phase solutions in relaxation oscillators coupled through excitatory interactions. *J Math Biol* 33: 261–280, 1995.
528. **Kopell N, Ermentrout G, Whittington M, Traub R.** Gamma rhythms and beta rhythms have different synchronization properties. *Proc Natl Acad Sci USA* 97: 1867–1872, 2000.
529. **Koshino H, Carpenter PA, Minshew NJ, Cherkassky VL, Keller TA, Just MA.** Functional connectivity in an fMRI working memory task in high-functioning autism. *Neuroimage* 24: 810–821, 2005.
530. **Kramer M, Roopun A, Carracedo L, Traub R, Whittington M, Kopell N.** Rhythm generation through period concatenation in rat somatosensory cortex. *PLoS Comput Biol* 4: e1000169, 2008.
531. **Kramis R, Vanderwolf C, Bland B.** Two types of hippocampal rhythmical slow activity in both the rabbit and the rat: relations to behavior and effects of atropine, diethyl ether, urethane, and pentobarbital. *Exp Neurol* 49: 58–85, 1975.
532. **Kreiman G, Hung C, Kraskov A, Quiroga R, Poggio T, DiCarlo J.** Object selectivity of local field potentials and spikes in the macaque inferior temporal cortex. *Neuron* 49: 433–445, 2006.
533. **Kreiter AK, Singer W.** Stimulus dependent synchronization of neuronal responses in the visual cortex of the awake macaque monkey. *J Neurosci* 16: 2381, 1996.
534. **Krishnan GP, Vohs JL, Hetrick WP, Carroll CA, Shekhar A, Bockbrader MA, O'Donnell BF.** Steady state visual evoked potential abnormalities in schizophrenia. *Clin Neurophysiol* 116: 614–624, 2005.
535. **Krystal JH, Karper LP, Seibyl JP, Freeman GK, Delaney R, Bremner JD, Heninger GR, Bowers MB, Charney DS.** Subanesthetic effects of the noncompetitive NMDA antagonist, ketamine, in humans. Psychotomimetic, perceptual, cognitive, and neuroendocrine responses. *Arch Gen Psychiatry* 51: 199–214, 1994.
536. **Kühn AA, Williams D, Kupsch A, Limousin P, Hariz M, Schneider GH, Yarrow K, Brown P.** Event-related beta desynchronization in human subthalamic nucleus correlates with motor performance. *Brain* 127: 735–746, 2004.
537. **Kühn AA, Trottenberg T, Kivi A, Kupsch A, Schneider GH, Brown P.** The relationship between local field potential and neuronal discharge in the subthalamic nucleus of patients with Parkinson's disease. *Exp Neurol* 194: 212–220, 2005.
538. **Kumar A, Schrader S, Aertsen A, Rotter S.** The high-conductance state of cortical networks. *Neural Comput* 20: 1–43, 2008.
539. **Kuramoto Y.** *Chemical Oscillations Waves, Turbulence*. New York: Dover, 2003.
540. **Kwag J, Paulsen O.** The timing of external input controls the sign of plasticity at local synapses. *Nat Neurosci* 12: 1219–1221, 2009.
541. **Kwon J, O'Donnell B, Wallenstein G, Greene R, Hirayasu Y, Nestor P, Hasselmo M, Potts G, Shenton M, McCarley R.** Gamma frequency-range abnormalities to auditory stimulation in schizophrenia. *Arch Gen Psychiatry* 56: 1001–1005, 1999.
542. **Lacaille J, Williams S.** Membrane properties of interneurons in stratum oriens-alveus of the CA1 region of rat hippocampus in vitro. *Neuroscience* 36: 349–359, 1990.
543. **Lachaux J, Rodriguez E, Martinerie J, Varela F.** Measuring phase synchrony in brain signals. *Hum Brain Mapp* 8: 194–208, 1999.
544. **Lagier S, Carleton A, Lledo P.** Interplay between local GABAergic interneurons and relay neurons generates gamma oscillations in the rat olfactory bulb. *J Neurosci* 24: 4382–4392, 2004.
545. **Lagier S, Panzanelli P, Russo R, Nissant A, Bathellier B, Sasso-Pognetto M, Fritschy J, Lledo P.** GABAergic inhibition at dendrodendritic synapses tunes gamma oscillations in the olfactory bulb. *Proc Natl Acad Sci USA* 104: 7259–7264, 2007.
546. **Lago-Fernández L, Huerta R, Corbacho F, Sigüenza J.** Fast response and temporal coherent oscillations in small-world networks. *Phys Rev Lett* 84: 2758–2761, 2000.
547. **Lahtinen H, Palva JM, Sumanen S, Voipio J, Kaila K, Taira T.** Postnatal development of rat hippocampal gamma rhythm in vivo. *J Neurophysiol* 88: 1469–1474, 2002.
548. **Lakatos P, Shah AS, Knuth KH, Ulbert I, Karmos G, Schroeder CE.** An oscillatory hierarchy controlling neuronal excitability and stimulus processing in the auditory cortex. *J Neurophysiol* 94: 1904–1911, 2005.
549. **Lakatos P, Chen C, O'Connell M, Mills A, Schroeder C.** Neuronal oscillations and multisensory interaction in primary auditory cortex. *Neuron* 53: 279–292, 2007.
550. **Lakatos P, Karmos G, Mehta A, Ulbert I, Schroeder C.** Entrainment of neuronal oscillations as a mechanism of attentional selection. *Science* 320: 110–113, 2008.
551. **Lakatos P, O'Connell MN, Barczak A, Mills A, Javitt DC, Schroeder CE.** The leading sense: supramodal control of neurophysiological context by attention. *Neuron* 64: 419–430, 2009.
552. **Lampl I, Yarom Y.** Subthreshold oscillations and resonant behavior: two manifestations of the same mechanism. *Neuroscience* 78: 325–341, 1997.
553. **Lampl I, Reichova I, Ferster D.** Synchronous membrane potential fluctuations in neurons of the cat visual cortex. *Neuron* 22: 361–374, 1999.
554. **Larimer P, Strowbridge BW.** Nonrandom local circuits in the dentate gyrus. *J Neurosci* 28: 12212–12223, 2008.
555. **Laurent G.** Olfactory network dynamics and the coding of multidimensional signals. *Nat Rev Neurosci* 3: 884–895, 2002.
556. **Laurent G, Naraghi M.** Odorant-induced oscillations in the mushroom bodies of the locust. *J Neurosci* 14: 2993–3004, 1994.
557. **Laurent G, Stopfer M, Friedrich R, Rabinovich M, Volkovskii A, Abarbanel H.** Odor encoding as an active, dynamical process: experiments, computation, and theory. *Annu Rev Neurosci* 24: 263–297, 2001.
558. **Lawrie S, Buechel C, Whalley H, Frith C, Friston K, Johnstone E.** Reduced frontotemporal functional connectivity in

schizophrenia associated with auditory hallucinations. *Biol Psychiatry* 51: 1008–1011, 2002.
559. **Le Bon-Jego M, Yuste R.** Persistently active, pacemaker-like neurons in neocortex. *Front Neurosci* 1: 123–129, 2007.
560. **Le Van Quyen M, Bragin A.** Analysis of dynamic brain oscillations: methodological advances. *Trends Neurosci* 30: 365–373, 2007.
561. **Le Van Quyen M, Bragin A, Staba R, Crpon B, Wilson C, Engel J.** Cell type-specific firing during ripple oscillations in the hippocampal formation of humans. *J Neurosci* 28: 6104–6110, 2008.
562. **Lebedev M, Wise S.** Oscillations in the premotor cortex: single-unit activity from awake, behaving monkeys. *Exp Brain Res* 130: 195–215, 2000.
563. **Leblois A, Boraud T, Meissner W, Bergman H, Hansel D.** Competition between feedback loops underlies normal and pathological dynamics in the basal ganglia. *J Neurosci* 26: 3567–3583, 2006.
564. **Leckman JF, Vaccarino FM, Kalanithi PS, Rothenberger A.** Annotation: Tourette syndrome: a relentless drumbeat-driven by misguided brain oscillations. *J Child Psychol Psychiatry* 47: 537–550, 2006.
565. **Lee AK, Wilson MA.** Memory of sequential experience in the hippocampus during slow wave sleep. *Neuron* 36: 1183–1194, 2002.
566. **Lee D.** Coherent oscillations in neuronal activity of the supplementary motor area during a visuomotor task. *J Neurosci* 23: 6798–6809, 2003.
567. **Lee D.** Behavioral context and coherent oscillations in the supplementary motor area. *J Neurosci* 24: 4453–4459, 2004.
568. **Lee D, Port NL, Kruse W, Georgopoulos AP.** Variability and correlated noise in the discharge of neurons in motor and parietal areas of the primate cortex. *J Neurosci* 18: 1161–1170, 1998.
569. **Lee H, Simpson GV, Logothetis NK, Rainer G.** Phase locking of single neuron activity to theta oscillations during working memory in monkey extrastriate visual cortex. *Neuron* 45: 147–156, 2005.
570. **Lee K, Williams L, Breakspear M, Gordon E.** Synchronous gamma activity: a review and contribution to an integrative neuroscience model of schizophrenia. *Brain Res* 41: 57–78, 2003.
571. **Lee M, Chrobak J, Sik A, Wiley R, Buzski G.** Hippocampal theta activity following selective lesion of the septal cholinergic system. *Neuroscience* 62: 1033–1047, 1994.
572. **Lee S, Blake R, Heeger D.** Traveling waves of activity in primary visual cortex during binocular rivalry. *Nat Neurosci* 8: 22–23, 2005.
573. **Lefort S, Tomm C, Floyd Sarria JC, Petersen CC.** The excitatory neuronal network of the C2 barrel column in mouse primary somatosensory cortex. *Neuron* 61: 301–316, 2009.
574. **Lemon N, Turner R.** Conditional spike backpropagation generates burst discharge in a sensory neuron. *J Neurophysiol* 84: 1519–1530, 2000.
575. **Lengyel M, Szatmry Z, Erdi P.** Dynamically detuned oscillations account for the coupled rate and temporal code of place cell firing. *Hippocampus* 13: 700–714, 2003.
576. **Leopold D, Murayama Y, Logothetis N.** Very slow activity fluctuations in monkey visual cortex: implications for functional brain imaging. *Cereb Cortex* 13: 422–433, 2003.
577. **Leung L, Yu H.** Theta-frequency resonance in hippocampal CA1 neurons in vitro demonstrated by sinusoidal current injection. *J Neurophysiol* 79: 1592–1596, 1998.
578. **Leung LS.** Nonlinear feedback model of neuronal populations in hippocampal CAl region. *J Neurophysiol* 47: 845–868, 1982.
579. **Lewis D, Hashimoto T, Volk D.** Cortical inhibitory neurons and schizophrenia. *Nat Rev Neurosci* 6: 312–324, 2005.
580. **Lewis DA, Gonzalez-Burgos G.** Pathophysiologically based treatment interventions in schizophrenia. *Nat Med* 12: 1016–1022, 2006.
581. **Lewis T, Rinzel J.** Self-organized synchronous oscillations in a network of excitable cells coupled by gap junctions. *Network* 11: 299–320, 2000.
582. **Li Q, Clark S, Lewis DV, Wilson WA.** NMDA receptor antagonists disinhibit rat posterior cingulate and retrosplenial cortices: a potential mechanism of neurotoxicity. *J Neurosci* 22: 3070–3080, 2002.
583. **Li YX, Bertram R, Rinzel J.** Modeling *N*-methyl-D-aspartate-induced bursting in dopamine neurons. *Neuroscience* 71: 397–410, 1996.
584. **Li Z, Hopfield J.** Modeling the olfactory bulb and its neural oscillatory processings. *Biol Cybern* 61: 379–392, 1989.
585. **Liang H, Bressler SL, Buffalo EA, Desimone R, Fries P.** Empirical mode decomposition of field potentials from macaque V4 in visual spatial attention. *Biol Cybern* 92: 380–392, 2005.
586. **Lichtman JW, Sanes JR.** Ome sweet ome: what can the genome tell us about the connectome? *Curr Opin Neurobiol* 18: 346–353, 2008.
587. **Light G, Hsu J, Hsieh M, Meyer-Gomes K, Sprock J, Swerdlow N, Braff D.** Gamma band oscillations reveal neural network cortical coherence dysfunction in schizophrenia patients. *Biol Psychiatry* 60: 1231–1240, 2006.
588. **Lin S, Gervasoni D, Nicolelis M.** Fast modulation of prefrontal cortex activity by basal forebrain noncholinergic neuronal ensembles. *J Neurophysiol* 96: 3209–3219, 2006.
589. **Lindner B, Doiron B, Longtin A.** Theory of oscillatory firing induced by spatially correlated noise and delayed inhibitory feedback. *Phys Rev E Stat Nonlin Soft Matter Phys* 72: 061919, 2005.
590. **Lisman J.** Bursts as a unit of neural information: making unreliable synapses reliable. *Trends Neurosci* 20: 38–43, 1997.
591. **Lisman J.** The theta/gamma discrete phase code occuring during the hippocampal phase precession may be a more general brain coding scheme. *Hippocampus* 15: 913–922, 2005.
592. **Lisman J, Buzsáki G.** A neural coding scheme formed by the combined function of gamma and theta oscillations. *Schizophr Bull* 34: 974–980, 2008.
593. **Lisman J, Coyle J, Green R, Javitt D, Benes F, Heckers S, Grace A.** Circuit-based framework for understanding neurotransmitter and risk gene interactions in schizophrenia. *Trends Neurosci* 31: 234–242, 2008.
594. **Lisman JE, Idiart MA.** Storage of 7 ± 2 short-term memories in oscillatory subcycles. *Science* 267: 1512–1515, 1995.
595. **Liu J, Newsome W.** Local field potential in cortical area MT: stimulus tuning and behavioral correlations. *J Neurosci* 26: 7779–7790, 2006.
596. **Liu Y, Liang M, Zhou Y, He Y, Hao Y, Song M, Yu C, Liu H, Liu Z, Jiang T.** Disrupted small-world networks in schizophrenia. *Brain* 131: 945–961, 2008.
597. **Llinás R.** The intrinsic electrophysiological properties of mammalian neurons: insights into central nervous system function. *Science* 242: 1654–1664, 1988.
598. **Llinás R, Ribary U.** Coherent 40-Hz oscillation characterizes dream state in humans. *Proc Natl Acad Sci USA* 90: 2078–2081, 1993.
599. **Llinás R, Yarom Y.** Oscillatory properties of guinea-pig inferior olivary neurones and their pharmacological modulation: an in vitro study. *J Physiol* 376: 163–182, 1986.
600. **Llinás R, Grace A, Yarom Y.** In vitro neurons in mammalian cortical layer 4 exhibit intrinsic oscillatory activity in the 10- to 50-Hz frequency range. *Proc Natl Acad Sci USA* 88: 897–901, 1991.
601. **Llinás RR, Ribary U, Joliot M, Wang XJ.** Content and context in temporal thalamocortical binding. In: *Temporal Coding in the Brain*, edited by G. Buzsáki, R. R. Llinás, and W. Singer. New York: Springer-Verlag, 1994, p. 251–272.
602. **Lodge DJ, Behrens MM, Grace AA.** A loss of parvalbumin-containing interneurons is associated with diminished oscillatory activity in an animal model of schizophrenia. *J Neurosci* 29: 2344–2354, 2009.
603. **Loebel A, Tsodyks M.** Computation by ensemble synchronization in recurrent networks with synaptic depression. *J Comput Neurosci* 13: 111–124, 2002.
604. **Logothetis N, Wandell B.** Interpreting the BOLD signal. *Annu Rev Physiol* 66: 735–769, 2004.
605. **Logothetis NK.** What we can do and what we cannot do with fMRI. *Nature* 453: 869–878, 2008.
606. **Logothetis NK, Pauls J, Augath M, Trinath T, Oeltermann A.** Neurophysiological investigation of the basis of the fMRI signal. *Nature* 412: 150–157, 2001.

607. **Lowry C, Kay L.** Chemical factors determine olfactory system beta oscillations in waking rats. *J Neurophysiol* 98: 394–404, 2007.
608. **Lubenov E, Siapas A.** Decoupling through synchrony in neuronal circuits with propagation delays. *Neuron* 58: 118–131, 2008.
609. **Lubenov EV, Siapas AG.** Hippocampal theta oscillations are travelling waves. *Nature* 459: 534–539, 2009.
610. **Luczak A, Barthó P, Marguet SL, Buzsáki G, Harris KD.** Sequential structure of neocortical spontaneous activity in vivo. *Proc Natl Acad Sci USA* 104: 347–352, 2007.
611. **Lumer E, Edelman G, Tononi G.** Neural dynamics in a model of the thalamocortical system. I. Layers, loops and the emergence of fast synchronous rhythms. *Cereb Cortex* 7: 207–227, 1997.
612. **Lumer E, Edelman G, Tononi G.** Neural dynamics in a model of the thalamocortical system. II. The role of neural synchrony tested through perturbations of spike timing. *Cereb Cortex* 7: 228–236, 1997.
613. **Luo L, Callaway E, Svoboda K.** Genetic dissection of neural circuits. *Neuron* 57: 634–660, 2008.
614. **Lutzenberger W, Ripper B, Busse L, Birbaumer N, Kaiser J.** Dynamics of gamma-band activity during an audiospatial working memory task in humans. *J Neurosci* 22: 5630–5638, 2002.
615. **Luu P, Tucker D, Makeig S.** Frontal midline theta and the error-related negativity: neurophysiological mechanisms of action regulation. *Clin Neurophysiol* 115: 1821–1835, 2004.
616. **Lytton W, Sejnowski T.** Simulations of cortical pyramidal neurons synchronized by inhibitory interneurons. *J Neurophysiol* 66: 1059–1079, 1991.
617. **Mackay WA.** Synchronized neuronal oscillations and their role in motor processes. *Trends Cogn Sci* 1: 176–183, 1997.
618. **MacVicar B, Tse F.** Local neuronal circuitry underlying cholinergic rhythmical slow activity in CA3 area of rat hippocampal slices. *J Physiol* 417: 197–212, 1989.
619. **Madison D, Nicoll R.** Control of the repetitive discharge of rat CA1 pyramidal neurones in vitro. *J Physiol* 354: 319–331, 1984.
620. **Madison D, Lancaster B, Nicoll R.** Voltage clamp analysis of cholinergic action in the hippocampus. *J Neurosci* 7: 733–741, 1987.
621. **Maex R, De Schutter E.** Resonant synchronization in heterogeneous networks of inhibitory neurons. *J Neurosci* 23: 10503–10514, 2003.
622. **Maex R, De Schutter E.** Mechanism of spontaneous and self-sustained oscillations in networks connected through axo-axonal gap junctions. *Eur J Neurosci* 25: 3347–3358, 2007.
623. **Magee J, Hoffman D, Colbert C, Johnston D.** Electrical and calcium signaling in dendrites of hippocampal pyramidal neurons. *Annu Rev Physiol* 60: 327–346, 1998.
624. **Magee JC.** Dendritic hyperpolarization-activated currents modify the integrative properties of hippocampal CA1 pyramidal neurons. *J Neurosci* 18: 7613–7624, 1998.
625. **Magee JC.** Dendritic mechanisms of phase precession in hippocampal CA1 pyramidal neurons. *J Neurophysiol* 86: 528–532, 2001.
626. **Maier J, Neuhoff J, Logothetis N, Ghazanfar A.** Multisensory integration of looming signals by rhesus monkeys. *Neuron* 43: 177–181, 2004.
627. **Maier J, Chandrasekaran C, Ghazanfar A.** Integration of bimodal looming signals through neuronal coherence in the temporal lobe. *Curr Biol* 18: 963–968, 2008.
628. **Maimon G, Assad JA.** Beyond Poisson: increased spike-time regularity across primate parietal cortex. *Neuron* 62: 426–440, 2009.
629. **Mainen Z, Sejnowski T.** Influence of dendritic structure on firing pattern in model neocortical neurons. *Nature* 382: 363–366, 1996.
630. **Maldonado P, Friedman-Hill S, Gray C.** Dynamics of striate cortical activity in the alert macaque. II. Fast time scale synchronization. *Cereb Cortex* 10: 1117–1131, 2000.
631. **Mancilla J, Lewis T, Pinto D, Rinzel J, Connors B.** Synchronization of electrically coupled pairs of inhibitory interneurons in neocortex. *J Neurosci* 27: 2058–2073, 2007.
632. **Mann E, Suckling J, Hajos N, Greenfield S, Paulsen O.** Perisomatic feedback inhibition underlies cholinergically induced fast network oscillations in the rat hippocampus in vitro. *Neuron* 45: 105–117, 2005.
633. **Mann EO, Mody I.** Control of hippocampal gamma oscillation frequency by tonic inhibition and excitation of interneurons. *Nat Neurosci* 2009.
634. **Manning JR, Jacobs J, Fried I, Kahana MJ.** Broadband shifts in local field potential power spectra are correlated with single-neuron spiking in humans. *J Neurosci* 29: 13613–13620, 2009.
635. **Manseau F, Goutagny R, Danik M, Williams S.** The hippocamposeptal pathway generates rhythmic firing of GABAergic neurons in the medial septum and diagonal bands: an investigation using a complete septohippocampal preparation in vitro. *J Neurosci* 28: 4096–4107, 2008.
636. **Mantini D, Perrucci M, Del Gratta C, Romani G, Corbetta M.** Electrophysiological signatures of resting state networks in the human brain. *Proc Natl Acad Sci USA* 104: 13170–13175, 2007.
637. **Manuel M, Meunier C, Donnet M, Zytnicki D.** Resonant or not, two amplification modes of proprioceptive inputs by persistent inward currents in spinal motoneurons. *J Neurosci* 27: 12977–12988, 2007.
638. **Marder E, Calabrese RL.** Principles of rhythmic motor pattern generation. *Physiol Rev* 76: 687–717, 1996.
639. **Marella S, Ermentrout G.** Class-II neurons display a higher degree of stochastic synchronization than class-I neurons. *Phys Rev E Stat NonlinSoft Matter Phys* 77: 041918, 2008.
640. **Margrie T, Schaefer A.** Theta oscillation coupled spike latencies yield computational vigour in a mammalian sensory system. *J Physiol* 546: 363–374, 2003.
641. **Marinazzo D, Kappen H, Gielen S.** Input-driven oscillations in networks with excitatory and inhibitory neurons with dynamic synapses. *Neural Comput* 19: 1739–1765, 2007.
642. **Markowitz D, Collman F, Brody C, Hopfield J, Tank D.** Rate-specific synchrony: using noisy oscillations to detect equally active neurons. *Proc Natl Acad Sci USA* 105: 8422–8427, 2008.
643. **Markram H, Lubke J, Frotscher M, Sakmann B.** Regulation of synaptic efficacy by coincidence of postsynaptic APs and EPSPs. *Science* 275: 213–215, 1997.
644. **Markram H, Wang Y, Tsodyks M.** Differential signaling via the same axon of neocortical pyramidal neurons. *Proc Natl Acad Sci USA* 95: 5323–5328, 1998.
645. **Markram H, Toledo-Rodriguez M, Wang Y, Gupta A, Silberberg G, Wu C.** Interneurons of the neocortical inhibitory system. *Nat Rev Neurosci* 5: 793–807, 2004.
646. **Markram H, Rinaldi T, Markram K.** The intense world syndrome-an alternative hypothesis for autism. *Front Neurosci* 1: 77–96, 2007.
647. **Marshall L, Helgadttir H, Mlle M, Born J.** Boosting slow oscillations during sleep potentiates memory. *Nature* 444: 610–613, 2006.
648. **Martin C, Gervais R, Messaoudi B, Ravel N.** Learning-induced oscillatory activities correlated to odour recognition: a network activity. *Eur J Neurosci* 23: 1801–1810, 2006.
649. **Martinez-Trujillo J, Treue S.** Feature-based attention increases the selectivity of population responses in primate visual cortex. *Curr Biol* 14: 744–751, 2004.
650. **Mason A, Larkman A.** Correlations between morphology and electrophysiology of pyramidal neurons in slices of rat visual cortex. II. Electrophysiology. *J Neurosci* 10: 1415–1428, 1990.
651. **Masquelier T, Hugues E, Deco G, Thorpe SJ.** Oscillations, phase-of-firing coding, and spike timing-dependent plasticity: an efficient learning scheme. *J Neurosci* 29: 13484–13493, 2009.
652. **Massimini M, Huber R, Ferrarelli F, Hill S, Tononi G.** The sleep slow oscillation as a traveling wave. *J Neurosci* 24: 6862–6870, 2004.
653. **Massimini M, Ferrarelli F, Huber R, Esser SK, Singh H, Tononi G.** Breakdown of cortical effective connectivity during sleep. *Science* 309: 2228–2232, 2005.
654. **Massimini M, Ferrarelli F, Esser S, Riedner B, Huber R, Murphy M, Peterson M, Tononi G.** Triggering sleep slow waves by transcranial magnetic stimulation. *Proc Natl Acad Sci USA* 104: 8496–8501, 2007.
655. **Massimini M, Tononi G, Huber R.** Slow waves, synaptic plasticity and information processing: insights from transcranial mag-

netic stimulation and high-density EEG experiments. *Eur J Neurosci* 29: 1761–1770, 2009.
656. **Masuda N, Doiron B.** Gamma oscillations of spiking neural populations enhance signal discrimination. *PLoS Comput Biol* 3: e236, 2007.
657. **Mathewson KE, Gratton G, Fabiani M, Beck DM, Ro T.** To see or not to see: prestimulus alpha phase predicts visual awareness. *J Neurosci* 29: 2725–2732, 2009.
658. **Mato G, Samengo I.** Type I and type II neuron models are selectively driven by differential stimulus features. *Neural Comput* 20: 2418–2440, 2008.
659. **Matveev V, Wang XJ.** Differential short-term synaptic plasticity and transmission of complex spike trains: to depress or to facilitate? *Cereb Cortex* 10: 1143–1153, 2000.
660. **Maurer A, McNaughton B.** Network and intrinsic cellular mechanisms underlying theta phase precession of hippocampal neurons. *Trends Neurosci* 30: 325–333, 2007.
661. **Maurer AP, Cowen SL, Burke SN, Barnes CA, McNaughton BL.** Phase precession in hippocampal interneurons showing strong functional coupling to individual pyramidal cells. *J Neurosci* 26: 13485–13492, 2006.
662. **Mazzoni A, Panzeri S, Logothetis NK, Brunel N.** Encoding of naturalistic stimuli by local field potential spectra in networks of excitatory and inhibitory neurons. *PLoS Comput Biol* 4: e1000239, 2008.
663. **Mazzoni A, Whittingstall K, Brunel N, Logothetis NK, Panzeri S.** Understanding the relationships between spike rate and delta/gamma frequency bands of LFPs and EEGs using a local cortical network model. *Neuroimage* 2009.
664. **McAdams C, Maunsell J.** Effects of attention on the reliability of individual neurons in monkey visual cortex. *Neuron* 23: 765–773, 1999.
665. **McAdams CJ, Maunsell JHR.** Effects of attention on orientation-tuning functions of single neurons in macaque cortical area V4. *J Neurosci* 19: 431–441, 1999.
666. **McBain CJ, Fisahn A.** Interneurons unbound. *Nat Rev Neurosci* 2: 11–23, 2001.
667. **McCarthy MM, Brown EN, Kopell N.** Potential network mechanisms mediating electroencephalographic beta rhythm changes during propofol-induced paradoxical excitation. *J Neurosci* 28: 13488–13504, 2008.
668. **McCormick D, Connors B, Lighthall J, Prince D.** Comparative electrophysiology of pyramidal and sparsely spiny stellate neurons in the neocortex. *J Neurophysiol* 54: 782–806, 1985.
669. **McCormick DA.** Neurotransmitter actions in the thalamus and cerebral cortex and their role in neuromodulation of thalamocortical activity. *Prog Neurobiol* 39: 337–388, 1992.
670. **McLelland D, Paulsen O.** Neuronal oscillations and the rate-to-phase transform: mechanism, model and mutual information. *J Physiol* 587: 769–785, 2009.
671. **McNaughton BL, Morris RGM.** Hippocampal synaptic enhancement and information storage within a distributed memory system. *Trends Neurosci* 10: 408–415, 1987.
672. **Medalla M, Lera P, Feinberg M, Barbas H.** Specificity in inhibitory systems associated with prefrontal pathways to temporal cortex in primates. *Cereb Cortex* 17 *Suppl* 1: i136–150, 2007.
673. **Mehta M, Quirk M, Wilson M.** Experience-dependent asymmetric shape of hippocampal receptive fields. *Neuron* 25: 707–715, 2000.
674. **Mehta M, Lee A, Wilson M.** Role of experience and oscillations in transforming a rate code into a temporal code. *Nature* 417: 741–746, 2002.
675. **Melamed O, Barak O, Silberberg G, Markram H, Tsodyks M.** Slow oscillations in neural networks with facilitating synapses. *J Comput Neurosci* 25: 308–316, 2008.
676. **Melloni L, Schwiedrzik CM, Wibral M, Rodriguez E, Singer W.** Response to: Yuval-Greenberg et al., "Transient Induced Gamma-Band Response in EEG as a Manifestation of Miniature Saccades." Neuron 58: 429–441. *Neuron* 62: 8–10, 2009.
677. **Meltzer J, Zaveri H, Goncharova I, Distasio M, Papademetris X, Spencer S, Spencer D, Constable R.** Effects of working memory load on oscillatory power in human intracranial EEG. *Cereb Cortex* 18: 1843–1855, 2008.
678. **Menon V, Freeman W, Cutillo B, Desmond J, Ward M, Bressler S, Laxer K, Barbaro N, Gevins A.** Spatio-temporal correlations in human gamma band electrocorticograms. *Electroencephalogr Clin Neurophysiol* 98: 89–102, 1996.
679. **Metherate R, Cox CL, Ashe JH.** Cellular bases of neocortical activation: modulation of neural oscillations by the nucleus basalis and endogenous acetylcholine. *J Neurosci* 12: 4701–4711, 1992.
680. **Meyer A, Katona I, Blatow M, Rozov A, Monyer H.** In vivo labeling of parvalbumin-positive interneurons and analysis of electrical coupling in identified neurons. *J Neurosci* 22: 7055–7064, 2002.
681. **Middleton S, Racca C, Cunningham M, Traub R, Monyer H, Knöpfel T, Schofield I, Jenkins A, Whittington M.** High-frequency network oscillations in cerebellar cortex. *Neuron* 58: 763–774, 2008.
682. **Middleton S, Jalics J, Kispersky T, Lebeau FE, Roopun AK, Kopell NJ, Whittington MA, Cunningham MO.** NMDA receptor-dependent switching between different gamma rhythm-generating microcircuits in entorhinal cortex. *Proc Natl Acad Sci USA* 105: 18572–18577, 2008.
683. **Migliore M, Hines M, Shepherd G.** The role of distal dendritic gap junctions in synchronization of mitral cell axonal output. *J Comput Neurosci* 18: 151–161, 2005.
684. **Miller KJ, Zanos S, Fetz EE, den Nijs M, Ojemann JG.** Decoupling the cortical power spectrum reveals real-time representation of individual finger movements in humans. *J Neurosci* 29: 3132–3137, 2009.
685. **Milne E, Scope A, Pascalis O, Buckley D, Makeig S.** Independent component analysis reveals atypical electroencephalographic activity during visual perception in individuals with autism. *Biol Psychiatry* 65: 22–30, 2009.
686. **Milton JG, Chu PH, Cowan JD.** Spiral waves in integrate-and-fire neural network. In: *Advances in Neural Information Processing Systems*, edited by C. L. G. S. J. Hanson and J. D. Cowan. San Mateo, CA: Morgan Kaufmann, 1993, p. 1001–1007.
687. **Mishra J, Martinez A, Sejnowski T, Hillyard S.** Early cross-modal interactions in auditory and visual cortex underlie a sound-induced visual illusion. *J Neurosci* 27: 4120–4131, 2007.
688. **Mitchell J, Sundberg K, Reynolds J.** Differential attention-dependent response modulation across cell classes in macaque visual area V4. *Neuron* 55: 131–141, 2007.
689. **Mitra PP, Pesaran B.** Analysis of dynamic brain imaging data. *Biophys J* 76: 691–708, 1999.
690. **Mitzdorf U.** Current source-density method and application in cat cerebral cortex: investigation of evoked potentials and EEG phenomena. *Physiol Rev* 65: 37–100, 1985.
691. **Mizuseki K, Sirota A, Pastalkova E, Buzski G.** Theta oscillations provide temporal windows for local circuit computation in the entorhinal-hippocampal loop. *Neuron* 64: 267–280, 2009.
692. **Montaron M, Bouyer J, Rougeul A, Buser P.** Ventral mesencephalic tegmentum (VMT) controls electrocortical beta rhythms and associated attentive behaviour in the cat. *Behav Brain Res* 6: 129–145, 1982.
693. **Montemurro MA, Rasch MJ, Murayama Y, Logothetis NK, Panzeri S.** Phase-of-firing coding of natural visual stimuli in primary visual cortex. *Curr Biol* 18: 375–380, 2008.
694. **Montgomery SM, Sirota A, Buzski G.** Theta and gamma coordination of hippocampal networks during waking and rapid eye movement sleep. *J Neurosci* 28: 6731–6741, 2008.
695. **Montgomery SM, Betancur MI, Buzski G.** Behavior-dependent coordination of multiple theta dipoles in the hippocampus. *J Neurosci* 29: 1381–1394, 2009.
696. **Moore C.** Frequency-dependent processing in the vibrissa sensory system. *J Neurophysiol* 91: 2390–2399, 2004.
697. **Moore T.** The neurobiology of visual attention: finding sources. *Curr Opin Neurobiol* 16: 159–165, 2006.
698. **Moran J, Desimone R.** Selective attention gates visual processing in the extrastriate cortex. *Science* 229: 782–784, 1985.
699. **Morgan R, Soltesz I.** Nonrandom connectivity of the epileptic dentate gyrus predicts a major role for neuronal hubs in seizures. *Proc Natl Acad Sci USA* 105: 6179–6184, 2008.

700. **Mori K, Nowycky M, Shepherd G.** Synaptic excitatory and inhibitory interactions at distal dendritic sites on mitral cells in the isolated turtle olfactory bulb. *J Neurosci* 4: 2291–2296, 1984.
701. **Morita K, Kalra R, Aihara K, Robinson H.** Recurrent synaptic input and the timing of gamma-frequency-modulated firing of pyramidal cells during neocortical "UP" states. *J Neurosci* 28: 1871–1881, 2008.
702. **Mormann F, Osterhage H, Andrzejak RG, Weber B, Fernndez G, Fell J, Elger CE, Lehnertz K.** Independent delta/theta rhythms in the human hippocampus and entorhinal cortex. *Front Hum Neurosci* 2: 3, 2008.
703. **Moser EI, Kropff E, Moser MB.** Place cells, grid cells, and the brain's spatial representation system. *Annu Rev Neurosci* 31: 69–89, 2008.
704. **Mukamel R, Gelbard H, Arieli A, Hasson U, Fried I, Malach R.** Coupling between neuronal firing, field potentials, and FMRI in human auditory cortex. *Science* 309: 951–954, 2005.
705. **Mures¸an R, Savin C.** Resonance or integration? Self-sustained dynamics and excitability of neural microcircuits. *J Neurophysiol* 97: 1911–1930, 2007.
706. **Mures¸an R, Jurju¸t O, Moca V, Singer W, Nikolic´ D.** The oscillation score: an efficient method for estimating oscillation strength in neuronal activity. *J Neurophysiol* 99: 1333–1353, 2008.
707. **Murias M, Webb SJ, Greenson J, Dawson G.** Resting state cortical connectivity reflected in EEG coherence in individuals with autism. *Biol Psychiatry* 62: 270–273, 2007.
708. **Murphy BK, Miller KD.** Multiplicative gain changes are induced by excitation or inhibition alone. *J Neurosci* 23: 10040–10051, 2003.
709. **Murphy M, Riedner BA, Huber R, Massimini M, Ferrarelli F, Tononi G.** Source modeling sleep slow waves. *Proc Natl Acad Sci USA* 106: 1608–1613, 2009.
710. **Murray JD.** *Mathematical Biology*. Berlin: Springer-Verlag, 1993.
711. **Murthy V, Fetz E.** Coherent 25- to 35-Hz oscillations in the sensorimotor cortex of awake behaving monkeys. *Proc Natl Acad Sci USA* 89: 5670–5674, 1992.
712. **Murthy V, Fetz E.** Oscillatory activity in sensorimotor cortex of awake monkeys: synchronization of local field potentials and relation to behavior. *J Neurophysiol* 76: 3949–3967, 1996.
713. **Murthy V, Fetz E.** Synchronization of neurons during local field potential oscillations in sensorimotor cortex of awake monkeys. *J Neurophysiol* 76: 3968–3982, 1996.
714. **Nakao H, Arai K, Nagai K, Tsubo Y, Kuramoto Y.** Synchrony of limit-cycle oscillators induced by random external impulses. *PhysRev E Stat Nonlin Soft Matter Phys* 72: 026220, 2005.
715. **Narayanan R, Johnston D.** The h channel mediates location dependence and plasticity of intrinsic phase response in rat hippocampal neurons. *J Neurosci* 28: 5846–5850, 2008.
716. **Nawrot MP, Boucsein C, Rodriguez Molina V, Riehle A, Aertsen A, Rotter S.** Measurement of variability dynamics in cortical spike trains. *J Neurosci Methods* 169: 374–390, 2008.
717. **Nelson M, Pouget P, Nilsen E, Patten C, Schall J.** Review of signal distortion through metal microelectrode recording circuits and filters. *J Neurosci Methods* 169: 141–157, 2008.
718. **Netoff T, Acker C, Bettencourt J, White J.** Beyond two-cell networks: experimental measurement of neuronal responses to multiple synaptic inputs. *J Comput Neurosci* 18: 287–295, 2005.
719. **Netoff T, Banks M, Dorval A, Acker C, Haas J, Kopell N, White J.** Synchronization in hybrid neuronal networks of the hippocampal formation. *J Neurophysiol* 93: 1197–1208, 2005.
720. **Neville K, Haberly L.** Beta and gamma oscillations in the olfactory system of the urethane-anesthetized rat. *J Neurophysiol* 90: 3921–3930, 2003.
721. **Newman ME, Girvan M.** Finding and evaluating community structure in networks. *Phys Rev E Stat Nonlin Soft Matter Phys* 69: 026113, 2004.
722. **Nicholson C, Freeman JA.** Theory of current source-density analysis and determination of conductivity tensor for anuran cerebellum. *J Neurophysiol* 38: 356–368, 1975.
723. **Niebur E, Koch C.** A model for the neuronal implementation of selective visual attention based on temporal correlation among neurons. *J Comput Neurosci* 1: 141–158, 1994.
724. **Niebur E, Koch C, Rosin C.** An oscillation-based model for the neuronal basis of attention. *Vision Res* 33: 2789–2802, 1993.
725. **Niessing J, Ebisch B, Schmidt KE, Niessing M, Singer W, Galuske RAW.** Hemodynamic signals correlate tightly with synchronized gamma oscillations. *Science* 309: 948–951, 2005.
726. **Nikolaev A, Ivanitsky G, Ivanitsky A, Posner M, Abdullaev Y.** Correlation of brain rhythms between frontal and left temporal (Wernicke's) cortical areas during verbal thinking. *Neurosci Lett* 298: 107–110, 2001.
727. **Nir Y, Fisch L, Mukamel R, Gelbard-Sagiv H, Arieli A, Fried I, Malach R.** Coupling between neuronal firing rate, gamma LFP, and BOLD fMRI is related to interneuronal correlations. *Curr Biol* 17: 1275–1285, 2007.
728. **Nirenberg S, Latham P.** Decoding neuronal spike trains: how important are correlations? *Proc Natl Acad Sci USA* 100: 7348–7353, 2003.
729. **Nomura M, Fukai T, Aoyagi T.** Synchrony of fast-spiking interneurons interconnected by GABAergic and electrical synapses. *Neural Comput* 15: 2179–2198, 2003.
730. **Nowak LG, Azouz R, Sanchez-Vives MV, Gray CM, McCormick DA.** Electrophysiological classes of cat primary visual cortical neurons in vivo as revealed by quantitative analyses. *J Neurophysiol* 89: 1541–1566, 2003.
731. **Nowotny T, Huerta R, Rabinovich MI.** Neuronal synchrony: peculiarity and generality. *Chaos* 18: 37–119, 2008.
732. **Nunez P, Srinivasan R, Westdorp A, Wijesinghe R, Tucker D, Silberstein R, Cadusch P.** Coherency EEG. I: Statistics, reference electrode, volume conduction, Laplacians, cortical imaging, and interpretation at multiple scales. *Electroencephalogr Clin Neurophysiol* 103: 499–515, 1997.
733. **Nunez PL, Srinivasan R.** *Electric Fields of the Brain: The Neurophysics of EEG* (2nd ed.). New York: Oxford Univ. Press, 2005.
734. **Nusser Z, Kay L, Laurent G, Homanics G, Mody I.** Disruption of GABA(A) receptors on GABAergic interneurons leads to increased oscillatory power in the olfactory bulb network. *J Neurophysiol* 86: 2823–2833, 2001.
735. **Ohara S, Mima T, Baba K, Ikeda A, Kunieda T, Matsumoto R, Yamamoto J, Matsuhashi M, Nagamine T, Hirasawa K, Hori T, Mihara T, Hashimoto N, Salenius S, Shibasaki H.** Increased synchronization of cortical oscillatory activities between human supplementary motor and primary sensorimotor areas during voluntary movements. *J Neurosci* 21: 9377–9386, 2001.
736. **Ohki K, Chung S, Ch'ng YH, Kara P, Reid RC.** Functional imaging with cellular resolution reveals precise micro-architecture in visual cortex. *Nature* 433: 597–603, 2005.
737. **O'Keefe J, Burgess N.** Dual phase and rate coding in hippocampal place cells: theoretical significance and relationship to entorhinal grid cells. *Hippocampus* 15: 853–866, 2005.
738. **O'Keefe J, Conway DH.** Hippocampal place units in the freely moving rat: why they fire where they fire. *Exp Brain Res* 31: 573–590, 1978.
739. **O'Keefe J, Dostrovsky J.** The hippocampus as a spatial map. Preliminary evidence from unit activity in the freely moving rat. *Exp Brain Res* 34: 171–175, 1971.
740. **O'Keefe J, Recce ML.** Phase relationship between hippocampal place units and the EEG theta rhythm. *Hippocampus* 3: 317–330, 1993.
741. **Onton J, Delorme A, Makeig S.** Frontal midline EEG dynamics during working memory. *Neuroimage* 27: 341–356, 2005.
742. **Oram M, Wiener M, Lestienne R, Richmond B.** Stochastic nature of precisely timed spike patterns in visual system neuronal responses. *J Neurophysiol* 81: 3021–3033, 1999.
743. **Orbach HS, Cohen LB.** Optical monitoring of activity from many areas of the in vitro and in vivo salamander olfactory bulb: a new method for studying functional organization in the vertebrate central nervous system. *J Neurosci* 3: 2251–2262, 1983.
744. **Orbán G, Kiss T, Erdi P.** Intrinsic and synaptic mechanisms determining the timing of neuron population activity during hippocampal theta oscillation. *J Neurophysiol* 96: 2889–2904, 2006.
745. **Orekhova EV, Stroganova TA, Nygren G, Tsetlin MM, Posikera IN, Gillberg C, Elam M.** Excess of high frequency electroencephalogram oscillations in boys with autism. *Biol Psychiatry* 62: 1022–1029, 2007.

746. **Oren I, Mann E, Paulsen O, Hájos N.** Synaptic currents in anatomically identified CA3 neurons during hippocampal gamma oscillations in vitro. *J Neurosci* 26: 9923–9934, 2006.
747. **Paik SB, Kumar T, Glaser DA.** Spontaneous local gamma oscillation selectively enhances neural network responsiveness. *PLoS Comput Biol* 5: e1000342, 2009.
748. **Palva J, Palva S, Kaila K.** Phase synchrony among neuronal oscillations in the human cortex. *J Neurosci* 25: 3962–3972, 2005.
749. **Palva S, Palva JM.** New vistas for alpha-frequency band oscillations. *Trends Neurosci* 30: 150–158, 2007.
750. **Panzeri S, Brunel N, Logothetis NK, Kayser C.** Sensory neural codes using multiplexed temporal scales. *Trends Neurosci* 33: 111–120, 2010.
751. **Paré D, Shink E, Gaudreau H, Destexhe A, Lang EJ.** Impact of spontaneous synaptic activity on the resting properties of cat neocortical pyramidal neurons In vivo. *J Neurophysiol* 79: 1450–1460, 1998.
752. **Parga N, Abbott LF.** Network model of spontaneous activity exhibiting synchronous transitions between up and down States. *Front Neurosci* 1: 57–66, 2007.
753. **Pavlides C, Greenstein YJ, Grudman M, Winson J.** Long-term potentiation in the dentate gyrus is induced preferentially on the positive phase of theta-rhythm. *Brain Res* 439: 383–387, 1988.
754. **Pavlova M, Birbaumer N, Sokolov A.** Attentional modulation of cortical neuromagnetic gamma response to biological movement. *Cereb Cortex* 16: 321–327, 2006.
755. **Pedroarena CM, Pose IE, Yamuy J, Chase MH, Morales FR.** Oscillatory membrane potential activity in the soma of a primary afferent neuron. *J Neurophysiol* 82: 1465–1476, 1999.
756. **Penttonen M, Kamondi A, Acsdy L, Buzski G.** Gamma frequency oscillation in the hippocampus of the rat: intracellular analysis in vivo. *Eur J Neurosci* 10: 718–728, 1998.
757. **Perkel D, Mulloney B.** Motor pattern production in reciprocally inhibitory neurons exhibiting postinhibitory rebound. *Science* 185: 181–183, 1974.
758. **Pervouchine DD, Netoff TI, Rotstein HG, White JA, Cunningham MO, Whittington MA, Kopell NJ.** Low-dimensional maps encoding dynamics in entorhinal cortex and hippocampus. *Neural Comput* 18: 2617–2650, 2006.
759. **Pesaran B, Pezaris JS, Sahani M, Mitra PP, Andersen RA.** Temporal structure in neuronal activity during working memory in marcaque pariental cortex. *Nat Neurosci* 5: 805–811, 2002.
760. **Pesaran B, Nelson M, Andersen R.** Free choice activates a decision circuit between frontal and parietal cortex. *Nature* 453: 406–409, 2008.
761. **Petersen C, Sakmann B.** Functionally independent columns of rat somatosensory barrel cortex revealed with voltage-sensitive dye imaging. *J Neurosci* 21: 8435–8446, 2001.
762. **Petersen C, Grinvald A, Sakmann B.** Spatiotemporal dynamics of sensory responses in layer 2/3 of rat barrel cortex measured in vivo by voltage-sensitive dye imaging combined with whole-cell voltage recordings and neuron reconstructions. *J Neurosci* 23: 1298–1309, 2003.
763. **Petsche H, Stumpf C, Gogolak G.** The significance of the rabbit's septum as a relay station between the midbrain and the hippocampus. I. The control of hippocampus arousal activity by the septum cells. *Electroencephalogr Clin Neurophysiol* 14: 202–211, 1962.
764. **Pettersen KH, Hagen E, Einevoll GT.** Estimation of population firing rates and current source densities from laminar electrode recordings. *J Comput Neurosci* 24: 291–313, 2008.
765. **Pfefferbaum A, Ford JM, Weller BJ, Kopell BS.** ERPs to response production and inhibition. *Electroencephalogr Clin Neurophysiol* 60: 423–434, 1985.
766. **Pfeuty B, Mato G, Golomb D, Hansel D.** Electrical synapses and synchrony: the role of intrinsic currents. *J Neurosci* 23: 6280–6294, 2003.
767. **Pfeuty B, Mato G, Golomb D, Hansel D.** The combined effects of inhibitory and electrical synapses in synchrony. *Neural Comput* 17: 633–670, 2005.
768. **Pfurtscheller G.** Central beta rhythm during sensorimotor activities in man. *Electroencephalogr Clin Neurophysiol* 51: 253–264, 1981.
769. **Pike FG, Goddard RS, Suckling JM, Ganter P, Kasthuri N, Paulsen O.** Distinct frequency preferences of different types of rat hippocampal neurones in response to oscillatory input currents. *J Physiol* 529: 205–213, 2000.
770. **Pikovsky AS, Rosenblum M, Kurths J.** *Synchronization: A Universal Concept in Nonlinear Sciences*. Cambridge, UK: Cambridge Univ. Press, 2001.
771. **Pillow JW, Shlens J, Paninski L, Sher A, Litke AM, Chichilnisky EJ, Simoncelli EP.** Spatio-temporal correlations and visual signalling in a complete neuronal population. *Nature* 454: 995–999, 2008.
772. **Pinsker H.** *Aplysia* bursting neurons as endogenous oscillators. I. Phase-response curves for pulsed inhibitory synaptic input. *J Neurophysiol* 40: 527–543, 1977.
773. **Pinsky P, Rinzel J.** Intrinsic and network rhythmogenesis in a reduced Traub model for CA3 neurons. *J Comput Neurosci* 1: 39–60, 1994.
774. **Pogosyan A, Gaynor LD, Eusebio A, Brown P.** Boosting cortical activity at Beta-band frequencies slows movement in humans. *Curr Biol* 19: 1637–1641, 2009.
775. **Poo C, Isaacson JS.** Odor representations in olfactory cortex: "sparse" coding, global inhibition, and oscillations. *Neuron* 62: 850–861, 2009.
776. **Popa D, Popescu AT, Paré D.** Contrasting activity profile of two distributed cortical networks as a function of attentional demands. *J Neurosci* 29: 1191–1201, 2009.
777. **Popescu AT, Popa D, Paré D.** Coherent gamma oscillations couple the amygdala and striatum during learning. *Nat Neurosci* 12: 801–807, 2009.
778. **Pouille F, Scanziani M.** Enforcement of temporal fidelity in pyramidal cells by somatic feed-forward inhibition. *Science* 293: 1159–1163, 2001.
779. **Poulet JF, Petersen CC.** Internal brain state regulates membrane potential synchrony in barrel cortex of behaving mice. *Nature* 454: 881–885, 2008.
780. **Praamstra P, Kourtis D, Kwok HF, Oostenveld R.** Neurophysiology of implicit timing in serial choice reaction-time performance. *J Neurosci* 26: 5448–5455, 2006.
781. **Prechtl J, Cohen L, Pesaran B, Mitra P, Kleinfeld D.** Visual stimuli induce waves of electrical activity in turtle cortex. *Proc Natl Acad Sci USA* 94: 7621–7626, 1997.
782. **Prescott SA, Ratt S, De Koninck Y, Sejnowski TJ.** Nonlinear interaction between shunting and adaptation controls a switch between integration and coincidence detection in pyramidal neurons. *J Neurosci* 26: 9084–9097, 2006.
783. **Puig M, Ushimaru M, Kawaguchi Y.** Two distinct activity patterns of fast-spiking interneurons during neocortical UP states. *Proc Natl Acad Sci USA* 105: 8428–8433, 2008.
784. **Puil E, Gimbarzevsky B, Miura R.** Quantification of membrane properties of trigeminal root ganglion neurons in guinea pigs. *J Neurophysiol* 55: 995–1016, 1986.
785. **Pulvermüller F, Birbaumer N, Lutzenberger W, Mohr B.** High-frequency brain activity: its possible role in attention, perception and language processing. *Prog Neurobiol* 52: 427–445, 1997.
786. **Quian Quiroga R, Panzeri S.** Extracting information from neuronal populations: information theory and decoding approaches. *Nat Rev Neurosci* 10: 173–185, 2009.
787. **Quill U, Wörgötter F.** Investigations on emergent spatio-temporal neural response characteristics in a small network model. *Biol Cybern* 83: 461–470, 2000.
788. **Rabinovich M, Volkovskii A, Lecanda P, Huerta R, Abarbanel H, Laurent G.** Dynamical encoding by networks of competing neuron groups: winnerless competition. *Phys Rev Lett* 87: 68–102, 2001.
789. **Rabinovich M, Huerta R, Laurent G.** Neuroscience. Transient dynamics for neural processing. *Science* 321: 48–50, 2008.
790. **Raghavachari S, Kahana M, Rizzuto D, Caplan J, Kirschen M, Bourgeois B, Madsen J, Lisman J.** Gating of human theta oscillations by a working memory task. *J Neurosci* 21: 3175–3183, 2001.

791. **Rall W, Shepherd G.** Theoretical reconstruction of field potentials and dendrodendritic synaptic interactions in olfactory bulb. *J Neurophysiol* 31: 884–915, 1968.
792. **Rasch M, Logothetis NK, Kreiman G.** From neurons to circuits: linear estimation of local field potentials. *J Neurosci* 29: 13785–13796, 2009.
793. **Rauch A, La Camera G, Luscher H, Senn W, Fusi S.** Neocortical pyramidal cells respond as integrate-and-fire neurons to in vivo-like input currents. *J Neurophysiol* 90: 1598–1612, 2003.
794. **Rauch A, Rainer G, Logothetis N.** The effect of a serotonin-induced dissociation between spiking and perisynaptic activity on BOLD functional MRI. *Proc Natl Acad Sci USA* 105: 6759–6764, 2008.
795. **Ravel N, Chabaud P, Martin C, Gaveau V, Hugues E, Tallon-Baudry C, Bertrand O, Gervais R.** Olfactory learning modifies the expression of odour-induced oscillatory responses in the gamma (60–90 Hz) and beta (15–40 Hz) bands in the rat olfactory bulb. *Eur J Neurosci* 17: 350–358, 2003.
796. **Ray S, Hsiao S, Crone N, Franaszczuk P, Niebur E.** Effect of stimulus intensity on the spike-local field potential relationship in the secondary somatosensory cortex. *J Neurosci* 28: 7334–7343, 2008.
797. **Ray S, Niebur E, Hsiao S, Sinai A, Crone N.** High-frequency gamma activity (80–150 Hz) is increased in human cortex during selective attention. *Clin Neurophysiol* 119: 116–133, 2008.
798. **Reboreda A, Snchez E, Romero M, Lamas J.** Intrinsic spontaneous activity and subthreshold oscillations in neurones of the rat dorsal column nuclei in culture. *J Physiol* 551: 191–205, 2003.
799. **Remme MW, Lengyel M, Gutkin BS.** The role of ongoing dendritic oscillations in single-neuron dynamics. *PLoS Comput Biol* 5: e1000493, 2009.
800. **Renart A, Song P, Wang XJ.** Robust spatial working memory through homeostatic synaptic scaling in heterogeneous cortical networks. *Neuron* 38: 473–485, 2003.
801. **Renart A, de la Rocha J, Bartho P, Hollender L, Parga N, Reyes A, Harris KD.** The asynchronous state in cortical circuits. *Science* 327: 587–590, 2010.
802. **Reyes A, Fetz E.** Two modes of interspike interval shortening by brief transient depolarizations in cat neocortical neurons. *J Neurophysiol* 69: 1661–1672, 1993.
803. **Reynolds J, Chelazzi L, Desimone R.** Competitive mechanisms subserve attention in macaque areas V2 and V4. *J Neurosci* 19: 1736–1753, 1999.
804. **Ribary U, Ioannides A, Singh K, Hasson R, Bolton J, Lado F, Mogilner A, Llinás R.** Magnetic field tomography of coherent thalamocortical 40-Hz oscillations in humans. *Proc Natl Acad Sci USA* 88: 11037–11041, 1991.
805. **Richardson MJE, Brunel N, Hakim V.** From subthreshold to firing-rate resonance. *J Neurophysiol* 89: 2538–2554, 2003.
806. **Riecke H, Roxin A, Madruga S, Solla S.** Multiple attractors, long chaotic transients, and failure in small-world networks of excitable neurons. *Chaos* 17: 026110, 2007.
807. **Rinaldi T, Kulangara K, Antoniello K, Markram H.** Elevated NMDA receptor levels and enhanced postsynaptic long-term potentiation induced by prenatal exposure to valproic acid. *Proc Natl Acad Sci USA* 104: 13501–13506, 2007.
808. **Rinaldi T, Perrodin C, Markram H.** Hyper-connectivity and hyper-plasticity in the medial prefrontal cortex in the valproic Acid animal model of autism. *Front Neural Circuits* 2: 4, 2008.
809. **Rinaldi T, Silberberg G, Markram H.** Hyperconnectivity of local neocortical microcircuitry induced by prenatal exposure to valproic acid. *Cereb Cortex* 18: 763–770, 2008.
810. **Rinzel J.** A formal classification of bursting mechanisms in excitable systems. In: *Proceedings of the International Congress of Mathematicians*, edited by A. M. Gleason. Providence, RI: American Mathematical Society, 1987, p. 1578–1594.
811. **Rinzel J, Ermentrout GB.** Analysis of neural excitability and oscillations. In: *Methods in Neuronal Modeling: From Synapses to Networks*, edited by C. Koch and I. Segev. Cambridge, MA: MIT Press, 1989, p. 135–169.
812. **Rinzel J, Terman D, Wang XJ, Ermentrout B.** Propagating activity patterns in large-scale inhibitory neuronal networks. *Science* 279: 1351–1355, 1998.
813. **Rippon G, Brock J, Brown C, Boucher J.** Disordered connectivity in the autistic brain: challenges for the "new psychophysiology." *Int J Psychophysiol* 63: 164–172, 2007.
814. **Robinson DA.** The electrical properties of metal microelectrodes. *Proc. IEEE* 56: 1065–1071, 1968.
815. **Robinson PA, Rennie CJ, Wright JJ.** Propagation and stability of waves of electrical activity in the cerebral cortex. *Phys Rev E* 56: 826840, 1997.
816. **Rojas-Líbano D, Kay LM.** Olfactory system gamma oscillations: the physiological dissection of a cognitive neural system. *Cogn Neurodyn* 2: 179–194, 2008.
817. **Roopun A, Middleton S, Cunningham M, LeBeau F, Bibbig A, Whittington M, Traub R.** A beta2-frequency (20–30 Hz) oscillation in nonsynaptic networks of somatosensory cortex. *Proc Natl Acad Sci USA* 103: 15646–15650, 2006.
818. **Roopun A, Cunningham M, Racca C, Alter K, Traub R, Whittington M.** Region-specific changes in gamma and beta2 rhythms in NMDA receptor dysfunction models of schizophrenia. *Schizophr Bull* 34: 962–973, 2008.
819. **Roopun AK, Kramer MA, Carracedo LM, Kaiser M, Davies CH, Traub RD, Kopell NJ, Whittington MA.** Temporal interactions between cortical rhythms. *Front Neurosci* 2: 145–154, 2008.
820. **Ros H, Sachdev RN, Yu Y, Sestan N, McCormick DA.** Neocortical networks entrain neuronal circuits in cerebellar cortex. *J Neurosci* 29: 10309–10320, 2009.
821. **Rotstein H, Pervouchine D, Acker C, Gillies M, White J, Buhl E, Whittington M, Kopell N.** Slow and fast inhibition and an H-current interact to create a theta rhythm in a model of CA1 interneuron network. *J Neurophysiol* 94: 1509–1518, 2005.
822. **Rougeul A, Bouyer J, Dedet L, Debray O.** Fast somato-parietal rhythms during combined focal attention and immobility in baboon and squirrel monkey. *Electroencephalogr Clin Neurophysiol* 46: 310–319, 1979.
823. **Roxin A, Riecke H, Solla S.** Self-sustained activity in a small-world network of excitable neurons. *Phys Rev Lett* 92: 198101, 2004.
824. **Roy A, Steinmetz P, Hsiao S, Johnson K, Niebur E.** Synchrony: a neural correlate of somatosensory attention. *J Neurophysiol* 98: 1645–1661, 2007.
825. **Rubenstein JL, Merzenich MM.** Model of autism: increased ratio of excitation/inhibition in key neural systems. *Genes Brain Behav* 2: 255–267, 2003.
826. **Rubin J, Lee D, Sompolinsky H.** Equilibrium properties of temporally asymmetric Hebbian plasticity. *Phys Rev Lett* 86: 364–367, 2001.
827. **Rubin JE, Hayes JA, Mendenhall JL, Del Negro CA.** Calcium-activated nonspecific cation current and synaptic depression promote network-dependent burst oscillations. *Proc Natl Acad Sci USA* 106: 2939–2944, 2009.
828. **Rubino D, Robbins K, Hatsopoulos N.** Propagating waves mediate information transfer in the motor cortex. *Nat Neurosci* 9: 1549–1557, 2006.
829. **Rubinov M, Knock SA, Stam CJ, Micheloyannis S, Harris AW, Williams LM, Breakspear M.** Small-world properties of nonlinear brain activity in schizophrenia. *Hum Brain Mapp* 30: 403–416, 2009.
830. **Rudolph M, Destexhe A.** A fast-conducting, stochastic integrative mode for neocortical neurons in vivo. *J Neurosci* 23: 2466–2476, 2003.
831. **Rudolph M, Pospischil M, Timofeev I, Destexhe A.** Inhibition determines membrane potential dynamics and controls action potential generation in awake and sleeping cat cortex. *J Neurosci* 27: 5280–5290, 2007.
832. **Rushworth M, Behrens T.** Choice, uncertainty and value in prefrontal and cingulate cortex. *Nat Neurosci* 11: 389–397, 2008.
832a. **Rutishauser U, Ross IB, Mamelak AN, Schuman EM.** Human memory strength is predicted by theta-frequency phase-locking of single neurons. *Nature* 464: 903–907, 2010.
833. **Rye D, Wainer B, Mesulam M, Mufson E, Saper C.** Cortical projections arising from the basal forebrain: a study of cholinergic and noncholinergic components employing combined retrograde tracing and immunohistochemical localization of choline acetyltransferase. *Neuroscience* 13: 627–643, 1984.

834. **Saalmann Y, Pigarev I, Vidyasagar T.** Neural mechanisms of visual attention: how top-down feedback highlights relevant locations. *Science* 316: 1612–1615, 2007.
835. **Sakamoto K, Mushiake H, Saito N, Aihara K, Yano M, Tanji J.** Discharge synchrony during the transition of behavioral goal representations encoded by discharge rates of prefrontal neurons. *Cereb Cortex* 18: 2036–2045, 2008.
836. **Salenius S, Hari R.** Synchronous cortical oscillatory activity during motor action. *Curr Opin Neurobiol* 13: 678–684, 2003.
837. **Salinas E, Sejnowski T.** Impact of correlated synaptic input on output firing rate and variability in simple neuronal models. *J Neurosci* 20: 6193–6209, 2000.
838. **Salinas E, Sejnowski TJ.** Correlated neuronal activity and the flow of neural information. *Nat Rev Neurosci* 2: 539–550, 2001.
839. **Sanchez-Vives M, McCormick DA.** Cellular and network mechanisms of rhythmic recurrent activity in neocortex. *Nature Neurosci* 3: 1027–1034, 2000.
840. **Sanchez-Vives M, Descalzo V, Reig R, Figueroa N, Compte A, Gallego R.** Rhythmic spontaneous activity in the piriform cortex. *Cereb Cortex* 18: 1179–1192, 2008.
841. **Sanchez-Vives MV, Nowak LG, McCormick DA.** Cellular mechanisms of long-lasting adaptation in visual cortical neurons in vitro. *J Neurosci* 20: 4286–4299, 2000.
842. **Sanes J, Donoghue J.** Oscillations in local field potentials of the primate motor cortex during voluntary movement. *Proc Natl Acad Sci USA* 90: 4470–4474, 1993.
843. **Sargolini F, Fyhn M, Hafting T, McNaughton BL, Witter MP, Moser MB, Moser EI.** Conjunctive representation of position, direction, and velocity in entorhinal cortex. *Science* 312: 758–762, 2006.
844. **Sarnthein J, Petsche H, Rappelsberger P, Shaw GL, von Stein A.** Synchronization between prefrontal and posterior association cortex during human working memory. *Proc Natl Acad Sci USA* 95: 7092–7096, 1998.
845. **Sauseng P, Klimesch W, Stadler W, Schabus M, Doppelmayr M, Hanslmayr S, Gruber WR, Birbaumer N.** A shift of visual spatial attention is selectively associated with human EEG alpha activity. *Eur J Neurosci* 22: 2917–2926, 2005.
846. **Sauseng P, Klimesch W, Heise KF, Gruber WR, Holz E, Karim AA, Glennon M, Gerloff C, Birbaumer N, Hummel FC.** Brain oscillatory substrates of visual short-term memory capacity. *Curr Biol* 19: 1846–1852, 2009.
847. **Schaefer A, Angelo K, Spors H, Margrie T.** Neuronal oscillations enhance stimulus discrimination by ensuring action potential precision. *PLoS Biol* 4: e163, 2006.
848. **Schmidt R, Diba K, Leibold C, Schmitz D, Buzski G, Kempter R.** Single-trial phase precession in the hippocampus. *J Neurosci* 29: 13232–13241, 2009.
849. **Schmitz D, Schuchmann S, Fisahn A, Draguhn A, Buhl E, Petrasch-Parwez E, Dermietzel R, Heinemann U, Traub R.** Axo-axonal coupling. *a* novel mechanism for ultrafast neuronal communication. *Neuron* 31: 831–840, 2001.
850. **Schneider G, Havenith MN, Nikoli D.** Spatiotemporal structure in large neuronal networks detected from cross-correlation. *Neural Comput* 18: 2387–2413, 2006.
851. **Schneidman E, Berry M, Segev R, Bialek W.** Weak pairwise correlations imply strongly correlated network states in a neural population. *Nature* 440: 1007–1012, 2006.
852. **Schroeder CE, Lakatos P.** Low-frequency neuronal oscillations as instruments of sensory selection. *Trends Neurosci* 32: 9–18, 2009.
853. **Seamans J, Yang C.** The principal features and mechanisms of dopamine modulation in the prefrontal cortex. *Prog Neurobiol* 74: 1–58, 2004.
854. **Sederberg PB, Schulze-Bonhage A, Madsen JR, Bromfield EB, McCarthy DC, Brandt A, Tully MS, Kahana MJ.** Hippocampal and neocortical gamma oscillations predict memory formation in humans. *Cereb Cortex* 17: 1190–1196, 2007.
855. **Sehatpour P, Molholm S, Schwartz T, Mahoney J, Mehta A, Javitt D, Stanton P, Foxe J.** A human intracranial study of long-range oscillatory coherence across a frontal-occipital-hippocampal brain network during visual object processing. *Proc Natl Acad Sci USA* 105: 4399–4404, 2008.
856. **Selverston A, Moulins M.** Oscillatory neural networks. *Annu Rev Physiol* 47: 29–48, 1985.
857. **Senkowski D, Schneider T, Foxe J, Engel A.** Crossmodal binding through neural coherence: implications for multisensory processing. *Trends Neurosci* 31: 401–409, 2008.
858. **Serafin M, Williams S, Khateb A, Fort P, Muhlethaler M.** Rhythmic firing of medial septum non-cholinergic neurons. *Neuroscience* 75: 671–675, 1996.
859. **Serödio P, Rudy B.** Differential expression of Kv4 K^+ channel subunits mediating subthreshold transient K^+ (A-type) currents in rat brain. *J Neurophysiol* 79: 1081–1091, 1998.
860. **Seung HS.** Reading the book of memory: sparse sampling versus dense mapping of connectomes. *Neuron* 62: 17–29, 2009.
861. **Shadlen M, Movshon J.** Synchrony unbound: a critical evaluation of the temporal binding hypothesis. *Neuron* 24: 67–77, 1999.
862. **Shadlen MN, Newsome WT.** Noise, neural codes and cortical organization. *Curr Opin Neurobiol* 4: 569–579, 1994.
863. **Shadlen MN, Newsome WT.** The variable discharge of cortical neurons: implications for connectivity, computation, and information coding. *J Neurosci* 18: 3870–3896, 1998.
864. **Shafi M, Zhou Y, Quintana J, Chow C, Fuster J, Bodner M.** Variability in neuronal activity in primate cortex during working memory tasks. *Neuroscience* 146: 1082–1108, 2007.
865. **Shapiro ML, Ferbinteanu J.** Relative spike timing in pairs of hippocampal neurons distinguishes the beginning and end of journeys. *Proc Natl Acad Sci USA* 103: 4287–4292, 2006.
866. **Sharp AA, Skinner FK, Marder E.** Mechanisms of oscillation in dynamic clamp constructed two-cell half-center circuits. *J Neurophysiol* 76: 867–883, 1996.
867. **Sherman A, Rinzel J.** Rhythmogenic effects of weak electrotonic coupling in neuronal models. *Proc Natl Acad Sci USA* 89: 2471–2474, 1992.
868. **Shin S, De Schutter E.** Dynamic synchronization of Purkinje cell simple spikes. *J Neurophysiol* 96: 3485–3491, 2006.
869. **Shu Y, Hasenstaub A, McCormick DA.** Turning on and off recurrent balanced cortical activity. *Nature* 423: 288–293, 2003.
870. **Siapas A, Lubenov E, Wilson M.** Prefrontal phase locking to hippocampal theta oscillations. *Neuron* 46: 141–151, 2005.
871. **Siegel M, Körding KP, König P.** Integrating top-down and bottom-up sensory processing by somato-dendritic interactions. *J Comput Neurosci* 8: 161–173, 2000.
872. **Siegel M, Donner TH, Oostenveld R, Fries P, Engel AK.** Neuronal synchronization along the dorsal visual pathway reflects the focus of spatial attention. *Neuron* 60: 709–719, 2008.
873. **Siegel M, Warden MR, Miller EK.** Phase-dependent neuronal coding of objects in short-term memory. *Proc Natl Acad Sci USA* 106: 21341–21346, 2009.
874. **Sik A, Penttonen M, Ylinen A, Buzski G.** Hippocampal CA1 interneurons: an in vivo intracellular labeling study. *J Neurosci* 15: 6651–6665, 1995.
875. **Silva L, Amitai Y, Connors B.** Intrinsic oscillations of neocortex generated by layer 5 pyramidal neurons. *Science* 251: 432–435, 1991.
876. **Singer W.** Neuronal synchrony: a versatile code for the definition of relations? *Neuron* 24: 49–65, 1999.
877. **Singer W, Gray C.** Visual feature integration and the temporal correlation hypothesis. *Annu Rev Neurosci* 18: 555–586, 1995.
878. **Sirota A, Montgomery S, Fujisawa S, Isomura Y, Zugaro M, Buzsáki G.** Entrainment of neocortical neurons and gamma oscillations by the hippocampal theta rhythm. *Neuron* 60: 683–697, 2008.
879. **Sjöström P, Rancz E, Roth A, Häusser M.** Dendritic excitability and synaptic plasticity. *Physiol Rev* 88: 769–840, 2008.
880. **Sjöström PJ, Turrigiano GG, Nelson SB.** Rate, timing, and cooperativity jointly determine cortical synaptic plasticity. *Neuron* 32: 1149–1164, 2001.
881. **Skaggs W, McNaughton B, Wilson M, Barnes C.** Theta phase precession in hippocampal neuronal populations and the compression of temporal sequences. *Hippocampus* 6: 149–172, 1996.
882. **Skinner FK, Kopell N, Marder E.** Mechanisms for oscillation and frequency control in reciprocally inhibitory model neural networks. *J Comput Neurosci* 1: 69–87, 1994.

883. **Snowden R, Treue S, Andersen R.** The response of neurons in areas V1 and MT of the alert rhesus monkey to moving random dot patterns. *Exp Brain Res* 88: 389–400, 1992.
884. **Softky WR, Koch C.** The highly irregular firing of cortical cells is inconsistent with temporal integration of random EPSPs. *J Neurosci* 13: 334–350, 1993.
885. **Sohal VS, Zhang F, Yizhar O, Deisseroth K.** Parvalbumin neurons and gamma rhythms enhance cortical circuit performance. *Nature* 459: 698–702, 2009.
886. **Sokolov A, Lutzenberger W, Pavlova M, Preissl H, Braun C, Birbaumer N.** Gamma-band MEG activity to coherent motion depends on task-driven attention. *Neuroreport* 10: 1997–2000, 1999.
887. **Soltesz I.** *Diversity in the Neuronal Machine*. New York: Oxford Univ. Press, 2005.
888. **Soltesz I, Deschênes M.** Low- and high-frequency membrane potential oscillations during theta activity in CA1 and CA3 pyramidal neurons of the rat hippocampus under ketamine-xylazine anesthesia. *J Neurophysiol* 70: 97–116, 1993.
889. **Somogyi P, Klausberger T.** Defined types of cortical interneurone structure space and spike timing in the hippocampus. *J Physiol* 562: 9–26, 2005.
890. **Sompolinsky H, Golomb D, Kleinfeld D.** Global processing of visual stimuli in a neural network of coupled oscillators. *Proc Natl Acad Sci USA* 87: 7200–7204, 1990.
891. **Song S, Miller KD, Abbott LF.** Competitive hebbian learning through spike-time-dependent synaptic plasticity. *Nat Neurosci* 3: 919–926, 2000.
892. **Song S, Sjöström P, Reigl M, Nelson S, Chklovskii D.** Highly nonrandom features of synaptic connectivity in local cortical circuits. *PLoS Biol* 3: e68, 2005.
893. **Spain W, Schwindt P, Crill W.** Two transient potassium currents in layer V pyramidal neurones from cat sensorimotor cortex. *J Physiol* 434: 591–607, 1991.
894. **Spencer K, Nestor P, Niznikiewicz M, Salisbury D, Shenton M, McCarley R.** Abnormal neural synchrony in schizophrenia. *J Neurosci* 23: 7407–7411, 2003.
895. **Spencer K, Nestor P, Perlmutter R, Niznikiewicz M, Klump M, Frumin M, Shenton M, McCarley R.** Neural synchrony indexes disordered perception and cognition in schizophrenia. *Proc Natl Acad Sci USA* 101: 17288–17293, 2004.
896. **Sporns O, Zwi JD.** The small world of the cerebral cortex. *Neuroinformatics* 2: 145–162, 2004.
897. **Sporns O, Tononi G, Kötter R.** The human connectome: a structural description of the human brain. *PLoS Comput Biol* 1: e42, 2005.
898. **Springer M, Paulsson J.** Biological physics: harmonies from noise. *Nature* 439: 27–28, 2006.
899. **Spruston N.** Pyramidal neurons: dendritic structure and synaptic integration. *Nat Rev Neurosci* 9: 206–221, 2008.
900. **Sripati A, Johnson K.** Dynamic gain changes during attentional modulation. *Neural Comput* 18: 1847–1867, 2006.
901. **Stam CJ, de Haan W, Daffertshofer A, Jones BF, Manshanden I, van Cappellen van Walsum AM, Montez T, Verbunt JP, de Munck JC, van Dijk BW, Berendse HW, Scheltens P.** Graph theoretical analysis of magnetoencephalographic functional connectivity in Alzheimer's disease. *Brain* 132: 213–224, 2009.
902. **Stepanyants A, Hirsch JA, Martinez LM, Kisvárday ZF, Ferecskó AS, Chklovskii DB.** Local potential connectivity in cat primary visual cortex. *Cereb Cortex* 18: 13–28, 2008.
903. **Stephan KE, Friston KJ, Frith CD.** Dysconnection in schizophrenia: from abnormal synaptic plasticity to failures of self-monitoring. *Schizophr Bull* 35: 509–527, 2009.
904. **Steriade M.** Synchronized activities of coupled oscillators in the cerebral cortex and thalamus at different levels of vigilance. *Cereb Cortex* 7: 583–604, 1997.
905. **Steriade M.** Impact of network activities on neuronal properties in corticothalamic systems. *J Neurophysiol* 86: 1–39, 2001.
906. **Steriade M.** *Neuronal Substrates of Sleep and Epilepsy*. New York: Cambridge Univ. Press, 2003.
907. **Steriade M.** Grouping of brain rhythms in corticothalamic systems. *Neuroscience* 137: 1087–1106, 2006.
908. **Steriade M, Llinas R.** The functional states of the thalamus and the associated neuronal interplay. *Physiol Rev* 68: 649–742, 1988.
909. **Steriade M, McCarley RW.** *Brainstem Control of Wakefulness and Sleep*. New York: Plenum, 1990.
910. **Steriade M, Gloor P, Llinás R, Lopes de Silva F, Mesulam M.** Report of IFCN Committee on Basic Mechanisms. *Basic* mechanisms of cerebral rhythmic activities. *Electroencephalogr Clin Neurophysiol* 76: 481–508, 1990.
911. **Steriade M, Niuñez A, Amzica F.** Intracellular analysis of relations between the slow (>1 Hz) neocortical oscillation and other sleep rhythms of the electroencephalogram. *J Neurosci* 13: 3266–3283, 1993.
912. **Steriade M, Niuñez A, Amzica F.** A novel slow (>1 Hz) oscillation of neocortical neurons in vivo: depolarizing and hyperpolarizing components. *J Neurosci* 13: 3252–3265, 1993.
913. **Steriade M, McCormick D, Sejnowski T.** Thalamocortical oscillations in the sleeping and aroused brain. *Science* 262: 679–685, 1993.
914. **Steriade M, Amzica F, Contreras D.** Synchronization of fast (30–40 Hz) spontaneous cortical rhythms during brain activation. *J Neurosci* 16: 392–417, 1996.
915. **Steriade M, Timofeev I, Grenier F.** Natural waking and sleep states: a view from inside neocortical neurons. *J Neurophysiol* 85: 1969–1985, 2001.
916. **Stern EA, Kincaid AE, Wilson CJ.** Spontaneous subthreshold membrane potential fluctuations and action potential variability of rat corticostriatal and striatal neurons in vivo. *J Neurophysiol* 77: 1697–1715, 1997.
917. **Stevens C, Zador A.** Input synchrony and the irregular firing of cortical neurons. *Nat Neurosci* 1: 210–217, 1998.
918. **Stewart M, Fox S.** Do septal neurons pace the hippocampal theta rhythm? *Trends Neurosci* 13: 163–168, 1990.
919. **Stickgold R.** Sleep-dependent memory consolidation. *Nature* 437: 1272–1278, 2005.
920. **Stickgold R, Walker MP.** Sleep-dependent memory consolidation and reconsolidation. *Sleep Med* 8: 331–343, 2007.
921. **Stiefel K, Gutkin B, Sejnowski T.** The effects of cholinergic neuromodulation on neuronal phase-response curves of modeled cortical neurons. *J Comput Neurosci* 26: 289–301, 2009.
922. **Strogatz SH.** *Nonlinear Dynamics and Chaos: With Applications to Physics, Biology, Chemistry and Engineering*. Cambridge, MA: Perseus, 2003.
923. **Stumpf C.** The fast component in the electrical activity of rabbit's hippocampus. *Electroencephalogr Clin Neurophysiol* 18: 477–486, 1965.
924. **Sun W, Dan Y.** Layer-specific network oscillation and spatiotemporal receptive field in the visual cortex. *Proc Natl Acad Sci USA* 106: 17986–17991, 2009.
925. **Swann N, Tandon N, Canolty R, Ellmore TM, McEvoy LK, Dreyer S, DiSano M, Aron AR.** Intracranial EEG reveals a time- and frequency-specific role for the right inferior frontal gyrus and primary motor cortex in stopping initiated responses. *J Neurosci* 29: 12675–12685, 2009.
926. **Symond M, Symond M, Harris A, Gordon E, Williams L.** "Gamma synchrony" in first-episode schizophrenia: a disorder of temporal connectivity? *Am J Psychiatry* 162: 459–465, 2005.
927. **Szücs A, Huerta R, Rabinovich MI, Selverston AI.** Robust microcircuit synchronization by inhibitory connections. *Neuron* 61: 439–453, 2009.
928. **Tabak J, Senn W, O'Donovan MJ, Rinzel J.** Modeling of spontaneous activity in developing spinal cord using activity-dependent depression in an excitatory network. *J Neurosci* 20: 3041–3056, 2000.
929. **Tabak J, O'Donovan MJ, Rinzel J.** Differential control of active and silent phases in relaxation models of neuronal rhythms. *J Comput Neurosci* 21: 307–328, 2006.
930. **Takács V, Freund T, Gulyás A.** Types and synaptic connections of hippocampal inhibitory neurons reciprocally connected with the medial septum. *Eur J Neurosci* 28: 148–164, 2008.
931. **Takehara-Nishiuchi K, McNaughton BL.** Spontaneous changes of neocortical code for associative memory during consolidation. *Science* 322: 960–963, 2008.

932. **Tallon-Baudry C, Bertrand O, Delpuech C, Pernier J.** Stimulus specificity of phase-locked and non-phase-locked 40 Hz visual responses in human. *J Neurosci* 16: 4240–4249, 1996.
933. **Tallon-Baudry C, Bertrand O, Fischer C.** Oscillatory synchrony between human extrastriate areas during visual short-term memory maintenance. *J Neurosci* 21: RC177, 2001.
934. **Tamás G, Szabadics J, Lörincz A, Somogyi P.** Input and frequency-specific entrainment of postsynaptic firing by IPSPs of perisomatic or dendritic origin. *Eur J Neurosci* 20: 2681–2690, 2004.
935. **Tanifuji M, Sugiyama T, Murase K.** Horizontal propagation of excitation in rat visual cortical slices revealed by optical imaging. *Science* 266: 1057–1059, 1994.
936. **Tateno T, Robinson H.** Phase resetting curves and oscillatory stability in interneurons of rat somatosensory cortex. *Biophys J* 92: 683–695, 2007.
937. **Tateno T, Harsch A, Robinson HPC.** Threshold firing frequency-current relationships of neurons in rat somatosensory cortex: type 1 and type 2 dynamics. *J Neurophysiol* 92: 2283–2294, 2004.
938. **Taylor K, Mandon S, Freiwald WA, Kreiter AK.** Coherent oscillatory activity in monkey area v4 predicts successful allocation of attention. *Cereb Cortex* 15: 1424–1437, 2005.
939. **Tegnér J, Compte A, Wang XJ.** The dynamical stability of reverberatory neural circuits. *Biol Cybern* 87: 471–481, 2002.
940. **Teramae J, Tanaka D.** Robustness of the noise-induced phase synchronization in a general class of limit cycle oscillators. *Phys Rev Lett* 93: 204103, 2004.
941. **Thivierge JP, Cisek P.** Nonperiodic synchronization in heterogeneous networks of spiking neurons. *J Neurosci* 28: 7968–7978, 2008.
942. **Thomson A.** Presynaptic frequency- and pattern-dependent filtering. *J Comput Neurosci* 15: 159–202, 2003.
943. **Thomson A, Lamy C.** Functional maps of neocortical local circuitry. *Frontiers Neurosci* 1:1: 19–42, 2007.
944. **Thomson A, West D.** Presynaptic frequency filtering in the gamma frequency band: dual intracellular recordings in slices of adult rat and cat neocortex. *Cereb Cortex* 13: 136–143, 2003.
945. **Thurley K, Leibold C, Gundlfinger A, Schmitz D, Kempter R.** Phase precession through synaptic facilitation. *Neural Comput* 20: 1285–1324, 2008.
946. **Thut G, Nietzel A, Brandt SA, Pascual-Leone A.** Alpha-band electroencephalographic activity over occipital cortex indexes visuospatial attention bias and predicts visual target detection. *J Neurosci* 26: 9494–9502, 2006.
947. **Tiesinga P, José J.** Robust gamma oscillations in networks of inhibitory hippocampal interneurons. *Network* 11: 1–23, 2000.
948. **Tiesinga P, Sejnowski T.** Rapid temporal modulation of synchrony by competition in cortical interneuron networks. *Neural Comput* 16: 251–275, 2004.
949. **Tiesinga P, Sejnowski TJ.** Cortical enlightenment: are attentional gamma oscillations driven by ING or PING? *Neuron* 63: 727–732, 2009.
950. **Tiesinga P, Fellous J, Salinas E, Jos J, Sejnowski T.** Inhibitory synchrony as a mechanism for attentional gain modulation. *J Physiol* 98: 296–314, 2004.
951. **Tiesinga P, Fellous J, Sejnowski T.** Regulation of spike timing in visual cortical circuits. *Nat Rev Neurosci* 9: 97–107, 2008.
952. **Tiitinen H, Sinkkonen J, Reinikainen K, Alho K, Lavikainen J, Ntnen R.** Selective attention enhances the auditory 40-Hz transient response in humans. *Nature* 364: 59–60, 1993.
953. **Tillmann C, Wibral M, Leweke M, Kohler A, Singer W, Koethe D, Kranaster L, Maurer K, Uhlhaas PJ.** High-frequency gamma-band oscillations during perceptual organisation in chronic and first-episode schizophrenia patients. *Soc Neurosci Abstr* 38: 54.2, 2008.
954. **Timofeev I, Grenier F, Steriade M.** Disfacilitation and active inhibition in the neocortex during the natural sleep-wake cycle: an intracellular study. *Proc Natl Acad Sci USA* 98: 1924–1929, 2001.
955. **Tognoli E, Kelso JA.** Brain coordination dynamics: true and false faces of phase synchrony and metastability. *Prog Neurobiol* 87: 31–40, 2009.
956. **Tohidi V, Nadim F.** Membrane resonance in bursting pacemaker neurons of an oscillatory network is correlated with network frequency. *J Neurosci* 29: 6427–6435, 2009.
957. **Tolhurst D, Movshon J, Dean A.** The statistical reliability of signals in single neurons in cat and monkey visual cortex. *Vision Res* 23: 775–785, 1983.
958. **Tomko G, Crapper D.** Neuronal variability: non-stationary responses to identical visual stimuli. *Brain Res* 79: 405–418, 1974.
959. **Tononi G, Cirelli C.** Sleep function and synaptic homeostasis. *Sleep Med Rev* 10: 49–62, 2006.
960. **Tort AB, Kramer MA, Thorn C, Gibson DJ, Kubota Y, Graybiel AM, Kopell NJ.** Dynamic cross-frequency couplings of local field potential oscillations in rat striatum and hippocampus during performance of a T-maze task. *Proc Natl Acad Sci USA* 105: 20517–20522, 2008.
961. **Tort AB, Komorowski RW, Manns JR, Kopell NJ, Eichenbaum H.** Theta-gamma coupling increases during the learning of item-context associations. *Proc Natl Acad Sci USA* 2009.
962. **Tóth K, Borhegyi Z, Freund T.** Postsynaptic targets of GABAergic hippocampal neurons in the medial septum-diagonal band of broca complex. *J Neurosci* 13: 3712–3724, 1993.
963. **Tóth K, Freund T, Miles R.** Disinhibition of rat hippocampal pyramidal cells by GABAergic afferents from the septum. *J Physiol* 500: 463–474, 1997.
964. **Traub R, Wong R.** Cellular mechanism of neuronal synchronization in epilepsy. *Science* 216: 745–747, 1982.
965. **Traub R, Miles R, Buzski G.** Computer simulation of carbachol-driven rhythmic population oscillations in the CA3 region of the in vitro rat hippocampus. *J Physiol* 451: 653–672, 1992.
966. **Traub R, Kopell N, Bibbig A, Buhl E, LeBeau F, Whittington M.** Gap junctions between interneuron dendrites can enhance synchrony of gamma oscillations in distributed networks. *J Neurosci* 21: 9478–9486, 2001.
967. **Traub R, Bibbig A, LeBeau F, Buhl E, Whittington M.** Cellular mechanisms of neuronal population oscillations in the hippocampus in vitro. *Annu Rev Neurosci* 27: 247–278, 2004.
968. **Traub RD, Miles R.** *Neuronal Networks of the Hippocampus*. Cambridge, UK: Cambridge Univ. Press, 1991.
969. **Traub RD, Miles R, Wong RKS.** Model of the origin of rhythmic population oscillations in the hippocampal slice. *Science* 243: 1319–1325, 1989.
970. **Traub RD, Whittington MA, Collins SB, Buzsáki G, Jefferys JGR.** Analysis of gamma rythms in the rat hippocampus in vitro and in vivo. *J Physiol* 493: 471–484, 1996.
971. **Traub RD, Schmitz D, Jefferys JGR, Draguhn A.** High-frequency population oscillations are predicted to occur in hippocampal pyramidal neuronal networks interconnected by axo-axonal gap junctions. *Neuroscience* 92: 407–426, 1999.
972. **Traub RD, Buhl EH, Gloveli T, Whittington MA.** Fast rhythmic bursting can be induced in layer 2/3 cortical neurons by enhancing persistent Na^+ conductance or by blocking BK channels. *J Neurophysiol* 89: 909–921, 2003.
973. **Treue S, Martínez Trujillo JC.** Feature-based attention influences motion processing gain in macaque visual cortex. *Nature* 399: 575–579, 1999.
974. **Treue S, Maunsell J.** Attentional modulation of visual motion processing in cortical areas MT and MST. *Nature* 382: 539–541, 1996.
975. **Trujillo LT, Peterson MA, Kaszniak AW, Allen JJ.** EEG phase synchrony differences across visual perception conditions may depend on recording and analysis methods. *Clin Neurophysiol* 116: 172–189, 2005.
976. **Tsodyks M, Skaggs W, Sejnowski T, McNaughton B.** Paradoxical effects of external modulation of inhibitory interneurons. *J Neurosci* 17: 4382–4388, 1997.
977. **Tsodyks MV, Skaggs WE, Sejnowski TJ, McNaughton BL.** Population dynamics and theta rhythm phase precession of hippocampal place cell firing: a spiking neuron model. *Hippocampus* 6: 271–280, 1996.
978. **Tsubo Y, Takada M, Reyes A, Fukai T.** Layer and frequency dependencies of phase response properties of pyramidal neurons in rat motor cortex. *Eur J Neurosci* 25: 3429–3441, 2007.

979. **Tsujimoto S, Genovesio A, Wise SP.** Transient neuronal correlations underlying goal selection and maintenance in prefrontal cortex. *Cereb Cortex* 18: 2748–2761, 2008.
980. **Tsujimoto T, Shimazu H, Isomura Y.** Direct recording of theta oscillations in primate prefrontal and anterior cingulate cortices. *J Neurophysiol* 95: 2987–3000, 2006.
981. **Tsujimoto T, Shimazu H, Isomura Y, Sasaki K.** Theta oscillations in primate prefrontal and anterior cingulate cortices in forewarned reaction time tasks. *J Neurophysiol* 103: 827–843, 2010.
982. **Tukker J, Fuentealba P, Hartwich K, Somogyi P, Klausberger T.** Cell type-specific tuning of hippocampal interneuron firing during gamma oscillations in vivo. *J Neurosci* 27: 8184–8189, 2007.
983. **Tuladhar AM, ter Huurne N, Schoffelen JM, Maris E, Oostenveld R, Jensen O.** Parieto-occipital sources account for the increase in alpha activity with working memory load. *Hum Brain Mapp* 28: 785–792, 2007.
984. **Turner R, Maler L, Deerinck T, Levinson S, Ellisman M.** TTX-sensitive dendritic sodium channels underlie oscillatory discharge in a vertebrate sensory neuron. *J Neurosci* 14: 6453–6471, 1994.
985. **Turner R, Lemon N, Doiron B, Rashid A, Morales E, Longtin A, Maler L, Dunn R.** Oscillatory burst discharge generated through conditional backpropagation of dendritic spikes. *J Physiol* 96: 517–530, 2002.
986. **Uhlhaas P, Singer W.** Neural synchrony in brain disorders: relevance for cognitive dysfunctions and pathophysiology. *Neuron* 52: 155–168, 2006.
987. **Uhlhaas P, Haenschel C, Nikolic´ D, Singer W.** The role of oscillations and synchrony in cortical networks and their putative relevance for the pathophysiology of schizophrenia. *Schizophr Bull* 34: 927–943, 2008.
988. **Uhlhaas PJ, Singer W.** Abnormal neural oscillations and synchrony in schizophrenia. *Nat Rev Neurosci* 11: 100–113, 2010.
989. **Uhlhaas PJ, Pipa G, Lima B, Melloni L, Neuenschwander S, Nikolic´ D, Singer W.** Neural synchrony in cortical networks: history, concept and current status. *Front Integr Neurosci* 3: 17, 2009.
990. **Ujfalussy B, Kiss T, Orbn G, Hoffmann W, Erdi P, Hajs M.** Pharmacological and computational analysis of alpha-subunit preferential GABA(A) positive allosteric modulators on the rat septo-hippocampal activity. *Neuropharmacology* 52: 733–743, 2007.
991. **Ulrich D.** Dendritic resonance in rat neocortical pyramidal cells. *J Neurophysiol* 87: 2753–2759, 2002.
992. **Usrey W, Reid R.** Synchronous activity in the visual system. *Annu Rev Physiol* 61: 435–456, 1999.
993. **Valencia M, Pastor MA, Fernández-Seara MA, Artieda J, Martinerie J, Chavez M.** Complex modular structure of large-scale brain networks. *Chaos* 19: 23–119, 2009.
994. **Van Der Werf J, Jensen O, Fries P, Medendorp W.** Gamma-band activity in human posterior parietal cortex encodes the motor goal during delayed prosaccades and antisaccades. *J Neurosci* 28: 8397–8405, 2008.
995. **Van Dijk H, Schoffelen JM, Oostenveld R, Jensen O.** Prestimulus oscillatory activity in the alpha band predicts visual discrimination ability. *J Neurosci* 28: 1816–1823, 2008.
996. **Van Dijk KR, Hedden T, Venkataraman A, Evans KC, Lazar SW, Buckner RL.** Intrinsic functional connectivity as a tool for human connectomics: theory, properties, and optimization. *J Neurophysiol* 103: 297–321, 2010.
997. **Van Rossum M, Turrigiano G, Nelson S.** Fast propagation of firing rates through layered networks of noisy neurons. *J Neurosci* 22: 1956–1966, 2002.
998. **Van Vreeswijk C.** Partial synchronization in populations of pulse-coupled oscillators. *Phys. Rev. E* 54: 5522–5537, 1996.
999. **Van Vreeswijk C, Hansel D.** Patterns of synchrony in neural networks with spike adaptation. *Neural Comput* 13: 959–992, 2001.
1000. **Van Vreeswijk C, Abbott L, Ermentrout GB.** When inhibition not excitation synchronizes neural firing. *J Comput Neurosci* 1: 313–321, 1994.
1001. **Van Wijk BC, Daffertshofer A, Roach N, Praamstra P.** A role of beta oscillatory synchrony in biasing response competition? *Cereb Cortex* 19: 1294–1302, 2009.
1002. **Vanderwolf C.** Hippocampal electrical activity and voluntary movement in the rat. *Electroencephalogr Clin Neurophysiol* 26: 407–418, 1969.
1003. **Vanderwolf C, Zibrowski E.** Pyriform cortex beta-waves: odor-specific sensitization following repeated olfactory stimulation. *Brain Res* 892: 301–308, 2001.
1004. **Varela F, Lachaux J, Rodriguez E, Martinerie J.** The brainweb: phase synchronization and large-scale integration. *Nat Rev Neurosci* 2: 229–239, 2001.
1005. **Varga V, Hangya B, Krnitz K, Ludnyi A, Zemankovics R, Katona I, Shigemoto R, Freund T, Borhegyi Z.** The presence of pacemaker HCN channels identifies theta rhythmic GABAergic neurons in the medial septum. *J Physiol* 586: 3893–3915, 2008.
1006. **Vertes R, Kocsis B.** Brainstem-diencephalo-septohippocampal systems controlling the theta rhythm of the hippocampus. *Neuroscience* 81: 893–926, 1997.
1007. **Vicente R, Gollo LL, Mirasso CR, Fischer I, Pipa G.** Dynamical relaying can yield zero time lag neuronal synchrony despite long conduction delays. *Proc Natl Acad Sci USA* 105: 17157–17162, 2008.
1008. **Vida I, Bartos M, Jonas P.** Shunting inhibition improves robustness of gamma oscillations in hippocampal interneuron networks by homogenizing firing rates. *Neuron* 49: 107–117, 2006.
1009. **Vierling-Claassen D, Siekmeier P, Stufflebeam S, Kopell N.** Modeling GABA alterations in schizophrenia: a link between impaired inhibition and altered gamma and beta range auditory entrainment. *J Neurophysiol* 99: 2656–2671, 2008.
1010. **Villalobos ME, Mizuno A, Dahl BC, Kemmotsu N, Mller RA.** Reduced functional connectivity between V1 and inferior frontal cortex associated with visuomotor performance in autism. *Neuroimage* 25: 916–925, 2005.
1011. **Vinck M, Lima B, Womelsdorf T, Oostenveld R, Singer W, Neuenschwander S, Fries P.** Gamma-phase shifting in awake monkey visual cortex. *J Neurosci* 30: 1250–1257, 2010.
1012. **Vinogradova O.** Expression, control, and probable functional significance of the neuronal theta-rhythm. *Prog Neurobiol* 45: 523–583, 1995.
1013. **Viswanathan A, Freeman R.** Neurometabolic coupling in cerebral cortex reflects synaptic more than spiking activity. *Nat Neurosci* 10: 1308–1312, 2007.
1014. **Vogels R, Spileers W, Orban G.** The response variability of striate cortical neurons in the behaving monkey. *Exp Brain Res* 77: 432–436, 1989.
1015. **Vogels TP, Abbott LF.** Gating multiple signals through detailed balance of excitation and inhibition in spiking networks. *Nat Neurosci* 12: 483–491, 2009.
1016. **Vogels TP, Rajan K, Abbott LF.** Neural network dynamics. *Annu Rev Neurosci* 28: 357–376, 2005.
1017. **Von Stein A, Sarnthein J.** Different frequencies for different scales of cortical integration: from local gamma to long range alpha/theta synchronization. *Int J Psychophysiol* 38: 301–313, 2000.
1018. **Von Stein A, Chiang C, König P.** Top-down processing mediated by interareal synchronization. *Proc Natl Acad Sci USA* 97: 14748–14753, 2000.
1019. **Vyazovskiy VV, Cirelli C, Pfister-Genskow M, Faraguna U, Tononi G.** Molecular and electrophysiological evidence for net synaptic potentiation in wake and depression in sleep. *Nat Neurosci* 11: 200–208, 2008.
1020. **Walker MP, Stickgold R.** Sleep, memory, and plasticity. *Annu Rev Psychol* 57: 139–166, 2006.
1021. **Wallenstein G, Hasselmo M.** GABAergic modulation of hippocampal population activity: sequence learning, place field development, and the phase precession effect. *J Neurophysiol* 78: 393–408, 1997.
1022. **Wang C, Ulbert I, Schomer DL, Marinkovic K, Halgren E.** Responses of human anterior cingulate cortex microdomains to error detection, conflict monitoring, stimulus-response mapping, familiarity, and orienting. *J Neurosci* 25: 604–613, 2005.

1023. **Wang H, Stradtman GG, Wang XJ, Gao WJ.** A specialized NMDA receptor function in layer 5 recurrent microcircuitry of the adult rat prefrontal cortex. *Proc Natl Acad Sci USA* 105: 16791–16796, 2008.
1024. **Wang HX, Gao WJ.** Cell type-specific development of NMDA receptors in the interneurons of rat prefrontal cortex. *Neuropsychopharmacology* 34: 2028–2040, 2009.
1025. **Wang XJ.** Ionic basis for intrinsic 40 Hz neuronal oscillations. *Neuroreport* 5: 221–224, 1993.
1026. **Wang XJ.** Multiple dynamical modes of thalamic relay neurons: rhythmic bursting and intermittent phase-locking. *Neuroscience* 59: 21–31, 1994.
1027. **Wang XJ.** Calcium coding and adaptive temporal computation in cortical pyramidal neurons. *J Neurophysiol* 79: 1549–1566, 1998.
1028. **Wang XJ.** Fast burst firing and short-term synaptic plasticity: a model of neocortical chattering neurons. *Neuroscience* 89: 347–362, 1999.
1029. **Wang XJ.** Synaptic basis of cortical persistent activity: the importance of NMDA receptors to working memory. *J Neurosci* 19: 9587–9603, 1999.
1030. **Wang XJ.** Synaptic reverberation underlying mnemonic persistent activity. *Trends Neurosci* 24: 455–463, 2001.
1031. **Wang XJ.** Pacemaker neurons for the theta rhythm and their synchronization in the septohippocampal reciprocal loop. *J Neurophysiol* 87: 889–900, 2002.
1032. **Wang XJ.** Probabilistic decision making by slow reverberation in cortical circuits. *Neuron* 36: 955–968, 2002.
1033. **Wang XJ.** Toward a prefrontal microcircuit model for cognitive deficits in schizophrenia. *Pharmacopsychiatry* 39 *Suppl* 1: 80–87, 2006.
1034. **Wang XJ.** Decision making in recurrent neuronal circuits. *Neuron* 60: 215–234, 2008.
1035. **Wang XJ, Buzsáki G.** Gamma oscillation by synaptic inhibition in a hippocampal interneuronal network model. *J Neurosci* 16: 6402–6413, 1996.
1036. **Wang XJ, Rinzel J.** Alternating and synchronous rhythms in reciprocally inhibitory model neurons. *Neural Computat* 4: 84–97, 1992.
1037. **Wang XJ, Rinzel J.** Spindle rhythmicity in the reticularis thalami nucleus: synchronization among mutually inhibitory neurons. *Neuroscience* 53: 899–904, 1993.
1038. **Wang XJ, Rinzel J.** Oscillatory and bursting properties of neurons. In: *Handbook of Brain Theory and Neural Networks*, edited by M. Arbib. Cambridge, MA: MIT Press, 1995, p. 686–691.
1039. **Wang XJ, Rinzel J, Rogawski MA.** A model of the T-type calcium current and the low-threshold spike in thalamic neurons. *J Neurophysiol* 66: 839–850, 1991.
1040. **Wang XJ, Golomb D, Rinzel J.** Emergent spindle oscillations and intermittent burst firing in a thalamic model: specific neuronal mechanisms. *Proc Natl Acad Sci USA* 92: 5577–5581, 1995.
1041. **Wang XJ, Liu Y, Sanchez-Vives MV, McCormick DA.** Adaptation and temporal decorrelation by single neurons in the primary visual cortex. *J Neurophysiol* 89: 3279–3293, 2003.
1042. **Watts D, Strogatz S.** Collective dynamics of "small-world" networks. *Nature* 393: 440–442, 1998.
1043. **Wehr M, Laurent G.** Odour encoding by temporal sequences of firing in oscillating neural assemblies. *Nature* 384: 162–166, 1996.
1044. **Weimann J, Marder E.** Switching neurons are integral members of multiple oscillatory networks. *Curr Biol* 4: 896–902, 1994.
1045. **Wespatat V, Tennigkeit F, Singer W.** Phase sensitivity of synaptic modifications in oscillating cells of rat visual cortex. *J Neurosci* 24: 9067–9075, 2004.
1046. **White J, Budde T, Kay A.** A bifurcation analysis of neuronal subthreshold oscillations. *Biophys J* 69: 1203–1217, 1995.
1047. **White J, Klink R, Alonso A, Kay A.** Noise from voltage-gated ion channels may influence neuronal dynamics in the entorhinal cortex. *J Neurophysiol* 80: 262–269, 1998.
1048. **White J, Rubinstein J, Kay A.** Channel noise in neurons. *Trends Neurosci* 23: 131–137, 2000.
1049. **White JA, Chow CC, Soto-Trevio C, Kopell N.** Synchronization and oscillatory dynamics in heterogeneous, mutually inhibited neurons. *J Comput Neurosci* 5: 5–16, 1998.
1050. **White JA, Banks MI, Pearce RA, Kopell NJ.** Networks of interneurons with fast and slow gamma-aminobutyric acid type A ($GABA_A$) kinetics provide substrate for mixed gamma-theta rhythm. *Proc Natl Acad Sci USA* 97: 8128–8133, 2000.
1051. **Whittingstall K, Logothetis NK.** Frequency-band coupling in surface EEG reflects spiking activity in monkey visual cortex. *Neuron* 64: 281–289, 2009.
1052. **Whittington M, Traub R, Faulkner H, Stanford I, Jefferys J.** Recurrent excitatory postsynaptic potentials induced by synchronized fast cortical oscillations. *Proc Natl Acad Sci USA* 94: 12198–12203, 1997.
1053. **Whittington MA, Traub RD, Jefferys JGR.** Synchronized oscillations in interneuron networks driven by metabotropic glutamate receptor activation. *Nature* 373: 612–615, 1995.
1054. **Whittington MA, Traub RD, Kopell N, Ermentrout B, Buhl EH.** Inhibition-based rhythms: experimental and mathematical observations on network dynamics. *Int J Psychophysiol* 38: 315–336, 2000.
1055. **Wierzynski CM, Lubenov EV, Gu M, Siapas AG.** State-dependent spike-timing relationships between hippocampal and prefrontal circuits during sleep. *Neuron* 61: 587–596, 2009.
1056. **Wilbur W, Rinzel J.** A theoretical basis for large coefficient of variation and bimodality in neuronal interspike interval distributions. *J Theor Biol* 105: 345–368, 1983.
1057. **Williams J, Kauer J.** Properties of carbachol-induced oscillatory activity in rat hippocampus. *J Neurophysiol* 78: 2631–2640, 1997.
1058. **Williams S, Stuart G.** Mechanisms and consequences of action potential burst firing in rat neocortical pyramidal neurons. *J Physiol* 521: 467–482, 1999.
1059. **Williamson P.** Are anticorrelated networks in the brain relevant to schizophrenia? *Schizophr Bull* 33: 994–1003, 2007.
1060. **Wilson HR, Cowan JD.** Excitatory and inhibitory interactions in localized populations of model neurons. *Biophys J* 12: 1–24, 1972.
1061. **Wilson HR, Cowan JD.** A mathematical theory of the functional dynamics of cortical and thalamic nervous tissue. *Kybernetik* 13: 55–80, 1973.
1062. **Wilson M, Bower J.** Cortical oscillations and temporal interactions in a computer simulation of piriform cortex. *J Neurophysiol* 67: 981–995, 1992.
1063. **Wilson T, Hernandez O, Asherin R, Teale P, Reite M, Rojas D.** Cortical gamma generators suggest abnormal auditory circuitry in early-onset psychosis. *Cereb Cortex* 18: 371–378, 2008.
1064. **Wilson TW, Rojas DC, Reite ML, Teale PD, Rogers SJ.** Children and adolescents with autism exhibit reduced MEG steady-state gamma responses. *Biol Psychiatry* 62: 192–197, 2007.
1065. **Winfree AT.** *The Geometry of Biological Time*. New York: Springer-Verlag, 2001.
1066. **Witham C, Wang M, Baker S.** Cells in somatosensory areas show synchrony with beta oscillations in monkey motor cortex. *Eur J Neurosci* 26: 2677–2686, 2007.
1067. **Woloszyn L.** Could frequency-specific coupling between single-cell activity and the local field potential underlie memory encoding in the hippocampus? *J Neurosci* 30: 417–419, 2010.
1068. **Womelsdorf T, Fries P.** The role of neuronal synchronization in selective attention. *Curr Opin Neurobiol* 17: 154–160, 2007.
1069. **Womelsdorf T, Fries P, Mitra PP, Desimone R.** Gamma-band synchronization in visual cortex predicts speed of change detection. *Nature* 439: 733–736, 2006.
1069a. **Womelsdorf T, Johnston K, Vinck M, Everling S.** Theta-activity in anterior cingulate cortex predicts task rules and their adjustments following errors. *Proc Natl Acad Sci USA* 107: 5248–5753, 2010.
1070. **Womelsdorf T, Schoffelen J, Oostenveld R, Singer W, Desimone R, Engel A, Fries P.** Modulation of neuronal interactions through neuronal synchronization. *Science* 316: 1609–1612, 2007.
1071. **Wong KF, Wang XJ.** A recurrent network mechanism of time integration in perceptual decisions. *J Neurosci* 26: 1314–1328, 2006.
1072. **Wong R, Prince D.** Participation of calcium spikes during intrinsic burst firing in hippocampal neurons. *Brain Res* 159: 385–390, 1978.
1073. **Worden MS, Foxe JJ, Wang N, Simpson GV.** Anticipatory biasing of visuospatial attention indexed by retinotopically spe-

cific alpha-band electroencephalography increases over occipital cortex. *J Neurosci* 20: RC63, 2000.
1074. **Wróbel A, Ghazaryan A, Bekisz M, Bogdan W, Kamin´ski J.** Two streams of attention-dependent beta activity in the striate recipient zone of cat's lateral posterior-pulvinar complex. *J Neurosci* 27: 2230–2240, 2007.
1075. **Wu J, Guan L, Tsau Y.** Propagating activation during oscillations and evoked responses in neocortical slices. *J Neurosci* 19: 5005–5015, 1999.
1076. **Wu J, Huang X, Zhang C.** Propagating waves of activity in the neocortex: what they are, what they do. *Neuroscientist* 14: 487–502, 2008.
1077. **Wyart V, Sergent C.** The phase of ongoing EEG oscillations uncovers the fine temporal structure of conscious perception. *J Neurosci* 29: 12839–12841, 2009.
1078. **Xing D, Yeh CI, Shapley RM.** Spatial spread of the local field potential and its laminar variation in visual cortex. *J Neurosci* 29: 11540–11549, 2009.
1079. **Xu W, Huang X, Takagaki K, Wu J.** Compression and reflection of visually evoked cortical waves. *Neuron* 55: 119–129, 2007.
1080. **Yamaguchi Y, Aota Y, McNaughton B, Lipa P.** Bimodality of theta phase precession in hippocampal place cells in freely running rats. *J Neurophysiol* 87: 2629–2642, 2002.
1081. **Yamaguchi Y, Sato N, Wagatsuma H, Wu Z, Molter C, Aota Y.** A unified view of theta-phase coding in the entorhinal-hippocampal system. *Curr Opin Neurobiol* 17: 197–204, 2007.
1082. **Yang JW, Hanganu-Opatz IL, Sun JJ, Luhmann HJ.** Three patterns of oscillatory activity differentially synchronize developing neocortical networks in vivo. *J Neurosci* 29: 9011–9025, 2009.
1083. **Ylinen A, Soltész I, Bragin A, Penttonen M, Sik A, Buzsáki G.** Intracellular correlates of hippocampal theta rhythm in identified pyramidal cells, granule cells, and basket cells. *Hippocampus* 5: 78–90, 1995.
1084. **Young CK, Eggermont JJ.** Coupling of mesoscopic brain oscillations: recent advances in analytical and theoretical perspectives. *Prog Neurobiol* 89: 61–78, 2009.
1085. **Yu S, Huang D, Singer W, Nikolic D.** A small world of neuronal synchrony. *Cereb Cortex* 18: 2891–2901, 2008.
1086. **Yuste R, MacLean J, Smith J, Lansner A.** The cortex as a central pattern generator. *Nat Rev Neurosci* 6: 477–483, 2005.
1087. **Yuval-Greenberg S, Deouell L.** What you see is not (always) what you hear: induced gamma band responses reflect cross-modal interactions in familiar object recognition. *J Neurosci* 27: 1090–1096, 2007.
1088. **Yuval-Greenberg S, Tomer O, Keren A, Nelken I, Deouell L.** Transient induced gamma-band response in EEG as a manifestation of miniature saccades. *Neuron* 58: 429–441, 2008.
1089. **Yuval-Greenberg S, Tomer O, Keren A, Nelken I, Deouell L.** Response to Letter: Melloni et al., "Transient induced gamma-band response in EEG as a manifestation of miniature saccades." *Neuron* 62: 10–12, 2009.
1090. **Zaehle T, Fründ I, Schadow J, Thärig S, Schoenfeld MA, Herrmann CS.** Inter- and intra-individual covariations of hemodynamic and oscillatory gamma responses in the human cortex. *Front Hum Neurosci* 3: 8, 2009.
1091. **Zeitler M, Fries P, Gielen S.** Assessing neuronal coherence with single-unit, multi-unit, local field potentials. *Neural Comput* 18: 2256–2281, 2006.
1092. **Zeitler M, Fries P, Gielen S.** Biased competition through variations in amplitude of gamma-oscillations. *J Comput Neurosci* 25: 89–107, 2008.
1093. **Zhang LI, Tao HW, Holt CE, Harris WA, Poo MM.** A critical window for cooperation and competition among developing retinotectal synapses. *Nature* 395: 37–44, 1998.
1094. **Zhang Y, Chen Y, Bressler SL, Ding M.** Response preparation and inhibition: the role of the cortical sensorimotor beta rhythm. *Neuroscience* 156: 238–246, 2008.
1095. **Zhigulin V.** Dynamical motifs: building blocks of complex dynamics in sparsely connected random networks. *Phys Rev Lett* 92: 238–701, 2004.
1096. **Zilli EA, Yoshida M, Tahvildari B, Giocomo LM, Hasselmo ME.** Evaluation of the oscillatory interference model of grid cell firing through analysis and measured period variance of some biological oscillators. *PLoS Comput Biol* 5: e1000573, 2009.
1097. **Zohary E, Shadlen MN, Newsome WT.** Correlated neuronal discharge rate and its implications for psychophysical performance. *Nature* 370: 140–143, 1994.
1098. **Zucker RS, Regehr WG.** Short-term synaptic plasticity. *Annu Rev Physiol* 64: 355–405, 2002.
1099. **Zugaro M, Monconduit L, Buzsáki G.** Spike phase precession persists after transient intrahippocampal perturbation. *Nat Neurosci* 8: 67–71, 2005.